HIGHWAY RESEARCH RECORD

Number 104

Surface Treatments, Bituminous Mixtures and Pavements

9 Reports

Presented at the
44th ANNUAL MEETING
January 11-15, 1965

SUBJECT CLASSIFICATION

31 Bituminous Materials and Mixes
33 Construction
25 Pavement Design
26 Pavement Performance
40 Maintenance, General

HIGHWAY RESEARCH BOARD
of the
Division of Engineering and Industrial Research
National Academy of Sciences—National Research Council
Washington, D. C.
1965

Department of Materials and Construction

R. L. Peyton, Chairman
Assistant State Highway Engineer
State Highway Commission of Kansas, Topeka

BITUMINOUS DIVISION

William H. Goetz, Chairman
Joint Highway Research Project
Purdue University, Lafayette, Indiana

COMMITTEE ON CHARACTERISTICS OF BITUMINOUS MATERIALS AND MEANS FOR THEIR EVALUATION

(As of December 31, 1964)

J. York Welborn, Chairman
U. S. Bureau of Public Roads, Washington, D. C.

Stephen H. Alexander, Research Center, Monsanto Company, St. Louis, Missouri
Edwin J. Barth, Asphalt Consultant, New York, New York
John H. Barton, Director, Chemical and Bituminous Laboratories, Missouri State Highway Department, Jefferson City
James V. Evans, Marketing Technical Service Department, American Oil Company, Chicago, Illinois
J. H. Goshorn, Managing Engineer, The Asphalt Institute, Columbus, Ohio
W. H. Gotolski, Department of Civil Engineering, Pennsylvania State University, University Park
F. C. Gzemski, The Atlantic Refining Company, Research and Development Department, Philadelphia, Pennsylvania
W. J. Halstead, Chemical Engineer, Materials Research Division, U. S. Bureau of Public Roads, Washington, D. C.
James H. Havens, Director of Research, Kentucky Department of Highways, Lexington
Arnold J. Hoiberg, Assistant Director, The Flintkote Company, Whippany, New Jersey
Robert E. Meskill, Standard Oil Company (New Jersey), New York, New York
W. G. O'Harra, Engineer of Materials, Arizona State Highway Department, Phoenix
Vytautas P. Puzinauskas, Associate Research Engineer, The Asphalt Institute, University of Maryland, College Park
J. C. Reed, Supervising Engineer, Testing Laboratory, Bureau of Testing and Materials, New Jersey State Highway Department, Trenton
E. O. Rhodes, Pittsburgh, Pennsylvania
F. S. Rostler, Director of Research, Materials R and D Division, Woodward, Clyde, Sherard and Associates, Oakland, California
R. J. Schmidt, California Research Corporation, Richmond
H. E. Schweyer, Department of Chemical Engineering, University of Florida, Gainesville
D. E. Stevens, California Crude Oil Sales Company, San Francisco
E. G. Swanson, Staff Materials Engineer, Colorado Department of Highways, Denver
Edmund Thelen, Manager, Colloids and Polymers Laboratory, Franklin Institute, Philadelphia, Pennsylvania
R. N. Traxler, Texas Transportation Institute, Texas A and M University, College Station
W. B. Warden, President, Miller-Warden Associates, Raleigh, North Carolina
L. E. Wood, Department of Civil Engineering, Purdue University, Lafayette, Indiana

COMMITTEE ON BITUMINOUS SURFACE TREATMENTS

(As of December 31, 1964)

Moreland Herrin, Chairman
Department of Civil Engineering
University of Illinois, Urbana

D. W. Anderson, Assistant Research Engineer, South Dakota Department of Highways, Pierre
E. W. Bauman, Managing Director, National Slag Association, Washington, D. C.
J. E. Bell, Assistant to Engineering Director, National Crushed Stone Association, Washington, D. C.
C. W. Chaffin, Supervising Chemical Engineer, Materials and Tests Division, Texas Highway Department, Austin
Robert A. Crawford, Assistant Research Engineer, South Dakota Department of Highways, Pierre
Leslie B. Crowley, Senior Directorate of Civil Engineering, Headquarters U. S. Air Force, Washington, D. C.
John B. Dunbar, District Engineer, The Asphalt Institute, Montgomery, Alabama
Bob M. Gallaway, Research Engineer, Civil Engineering Department, Texas Transportation Institute, Texas A and M University, College Station
David C. Mahone, Highway Research Engineer, Virginia Council of Highway Investigation and Research, Charlottesville
Phillip L. Melville, Civil Engineering Branch, Engineering Division, Military Construction, Office, Chief of Engineers, Department of the Army, Washington, D. C.
William H. Mills, Consulting Engineer, Atlanta, Georgia
J. W. Reppel, Engineer of Maintenance, Ohio Department of Highways, Columbus
James M. Rice, Highway Research Engineer, Division of Physical Research, U. S. Bureau of Public Roads, Washington, D. C.
Ernest Zube, Supervising Materials and Research Engineer, California Division of Highways, Sacramento

COMMITTEE ON MECHANICAL PROPERTIES OF BITUMINOUS PAVING MIXTURES

(As of December 31, 1964)

Lloyd F. Rader, Chairman
Department of Civil Engineering
University of Wisconsin, Madison

Harry C. Bower, American Bitumuls and Asphalt Company, Baltimore, Maryland
T. W. Cavanaugh, Engineer of Materials, Connecticut State Highway Department, Portland
A. B. Cornthwaite, Division Managing Engineer, Eastern Division, The Asphalt Institute, Washington, D. C.
Ladis H. Csanyi, In Charge, Bituminous Research Laboratory, Iowa State University, Ames
Joseph F. Goode, Highway Physical Research Engineer, Physical Research Branch, U. S. Bureau of Public Roads, Washington, D. C.
Hyoungkey Hong, Assistant Professor of Civil Engineering, Marquette University, Milwaukee, Wisconsin
Donald I. Inghram, Senior Engineer of Physical Tests, Nebraska Department of Roads, Lincoln
Rudolf A. Jimenez, Associate Research Engineer, Texas Transportation Institute, Texas A and M University, College Station
Bernard F. Kallas, The Asphalt Institute, University of Maryland, College Park
W. H. Larsen, Chief, Bituminous Section, U. S. Army Engineer Waterways Experiment Station, Corps of Engineers, Vicksburg, Mississippi
Kamran Majidzadeh, Department of Civil Engineering, University of Florida, Gainesville

Phillip L. Melville, Civil Engineering Branch, Engineering Division, Military Construction, Office, Chief of Engineers, Department of the Army, Washington, D. C.
Fred Moavenzadeh, Associate Professor of Civil Engineering, Ohio State University, Columbus
Carl L. Monismith, University of California, Berkeley
O. A. Philippi, Supervising Engineer, Texas Highway Department, Austin
C. K. Preus, Materials and Research Engineer, Minnesota Department of Highways, St. Paul
James H. Schaub, Head, Department of Civil Engineering, West Virginia University, Morgantown
J. E. Stephens, Professor of Civil Engineering, University of Connecticut, Storrs
B. A. Vallerga, Director of Engineering, Materials Research and Development, Oakland, California
Ellis G. Williams, District Engineer, The Aaphalt Institute, Louisville, Kentucky
Ernest Zube, Supervising Materials and Research Engineer, California Division of Highways, Sacramento
George H. Zuehlke, Materials Tests Engineer, State Highway Commission of Wisconsin, Madison

Foreword

Brunstrum et al. attempt to evaluate quantitatively the material and construction variables that contribute to plastic deformation of asphalt-concrete pavements. The variables studied included initial consistency and temperature susceptibility of asphalt, amount of asphalt and aggregate fines, compaction, and temperature of pavement. The effect of the variables was determined by measuring rutting after simulated traffic on a laboratory test track. A rut-depth equation was developed showing the relative contribution of the properties to performance under the conditions of testing.

This paper should be of interest to materials engineers and researchers who are concerned with making and evaluating asphalt paving mixtures. The authors suggest that the rut depth may be used to study the changes in surface profile that occur in pavements in service.

The next three papers, related to bituminous surface treatments, should be of interest to materials engineers, and construction and maintenance engineers will also find it interesting. Two of the papers are related to factors that influence the design and performance of seal coats and surface treatments, while the other paper is related to the design of slurry seal mixtures.

The development of a tenacity test for measuring aggregate retention in surface treatments is reported by Schweyer and Gartner. The strength of the bituminous bond between the aggregate and the underlying surface is determined for various consistencies and amounts of asphalt, amount and type of aggregates, and other variables.

Another new test method is reported by Harper, Jimenez, and Gallaway. The test apparatus was developed for evaluating the performance (abrasion) of slurry seals in the laboratory. The primary objective was to determine the effect of mineral filler and residual asphalt content on slurry seal mixtures and to develop a method of designing this type of mixture. The resulting design equation for predicting optimum residual asphalt content was determined to be valid by other tests.

Saner and Herrin have studied the volume of voids in a one-size surface treatment aggregate, since the fundamental concept used in the design of surface treatments is that the quantity of bituminous material needed is determined as the amount required to fill the voids between the aggregates to an optimum depth. The actual volume of voids between the aggregates was measured (not theoretically calculated). Among the factors studied, the most important appear to be the shape of the aggregate and the depth to which the voids within the aggregates will be filled.

Although great advances have been made in highway technology, little effort has been spent in improving the design and construction of thin bituminous surface treatments. Papers such as these are advancing the knowledge in this field and someday the life of these surfaces may be considerably extended.

The remaining papers give information concerning current research in the field of mechanical properties of bituminous paving mixtures. The scope is rather broad, covering topics of theoretical interest as well as of a practical nature. These papers should be of interest to materials and design engineers and paving technologists who are concerned with design of bituminous paving mixtures and their properties.

Hewitt analyzes flexible paving mixtures by a theoretical design procedure based on shear strength and describes instrumentation and test procedures for the testing of paving mixtures in flexure, tension, unconfined compression, and triaxial compression. Variables include asphalt content, asphalt viscosity, flake asphalt-penetration grade asphalt blends, asphalt-polyethylene blends, Viadon binder, and asbestos fibers in the mixture. The paving mixtures tested are analyzed for suitability to resist compressive stresses in the pavement and the practical application of this procedure to design is shown.

Moavenzadeh and Sendze report on the effect of the degree of aging on the creep and relaxation behavior of sand-asphalt mixes. The materials include Ottawa sand and silica fillers. The rate of creep generally decreases with aging. Maximum relaxation load increases with aging. Semilogarithmic relations are developed.

Pagen and Ku present the results of constant-load compressive tests on cylindrical test specimens to show the effects of asphalt viscosity on the rheological properties of bituminous concrete for a wide range of experimental loads and temperatures. Using a standard creep testing program, the instantaneous elastic, retarded elastic, and plastic deformations are recorded and analyzed. Cyclic repetition of loading and unloading are also studied. Correlations between asphalt viscosity and rheological strength moduli of the bituminous mixes are developed for different loading times and temperatures. The application of the linear viscoelastic theory and the time-temperature superposition concept are rigorously investigated.

Zube and Cechetini report on a research study conducted on the causes and effects of expansion and contraction of asphalt concrete mixes containing aggregates ranging from nonabsorptive to highly absorptive. Those specimens containing highly absorptive aggregates, when exposed to atmospheric conditions, absorb moisture from the air and may expand considerably. When subjected to drying, these expanded specimens contract, causing transverse cracking. Data show that expansion is affected by type of mineral filler and asphalt content of the mix.

The paper by Ruth and Schaub deals with the development of a bituminous mixture design procedure using West Virginia aggregate and gradation and the gyratory testing machine in an effort to reproduce designs which have given good service.

Contents

Relation of Asphalt Pavement Variables To Performance

L. C. BRUNSTRUM, L. E. OTT, A. W. SISKO, T. L. SPEER and R. A. WILKE, Research and Development Department, American Oil Company, Whiting, Indiana; and
J. V. EVANS, Marketing Technical Service Department, American Oil Company, Chicago, Illinois

Plastic deformation in asphalt pavements determines the contribution of two important factors, slope variance and rut depth, in the AASHO serviceability equation. Previous research on a laboratory test track showed the dependence of plastic deformation on the viscosity of the asphalt under pavement conditions. This research has now been extended to determine, on 66 pavements, the effect of pavement variables such as asphalt content, fines content and compaction. Factors affecting asphalt viscosity (temperature susceptibility, mixing at high temperature, and aging in the pavements) were also studied.

The contributions and interactions of pavement and asphalt variables were combined in a single equation by means of least squares multiple regression, enabling comparison of the relative effects of common variations in these properties. Results are illustrated by a bar chart. Charts presented relate actual deformation to that predicted by the regression equation. The basic form of the equation should now be tested with data from actual roads in service.

•IF THE many factors determining the performance of flexible pavements are not rigidly controlled, roads can undergo changes in thickness and surface profile that, in time, adversely affect the riding quality (1). These changes are the result of plastic deformation and are evident in the development of slope variances along the road and shallow depressions across the road (2). The rate of deformation changes as the bituminous layers compact and as the mechanical properties of the constituents change.

To minimize plastic deformation, a variety of criteria (e.g., asphalt content, aggregate gradation, specific gravity, voids, asphalt grade, thin film oven tests (TFOT), and compressive stabilities of several sorts) are used during design and construction. Collectively, these diverse criteria insure optimum performance. It would be advantageous if the contribution of all factors relating directly to pavement performance could be expressed in common units that would provide means for comparing the relative importance of each factor.

In previous research (phase 1), plastic deformation was studied in terms of the rut depths developed in experimental pavements on a laboratory test track (3). This study showed the significance of asphalt viscosity in the rutting process and led to the equation, $R = k\eta^{-n}$, where R is rate of rutting, η is asphalt viscosity, and k and n are constants. The data strongly indicated that pavement characteristics such as asphalt content and compaction influenced these constants. Thus, if the contribution of composition and construction variables could be quantitatively determined, k and n might be used to characterize a pavement or serve as a basis for design. In addition, these

Paper sponsored by Committee on Characteristics of Bituminous Materials and Means for Their Evaluation.

constants could provide the desired means for comparing the relative effects of the variables.

Research has been continued in this area to determine the effect of viscosity grading at 140 F and of pavement composition and construction. Two series of pavements (phase 2 and phase 3), comprising about 50 individual pavements, were made with 13 asphalts from eight crude sources. Pavements were subjected to many wheel passes, simulating severe traffic conditions, on the laboratory test track.

EXPERIMENTAL CONSIDERATIONS

All pavements had the same basic design (similar to that of a dense-graded Illinois I-11 specification). In phase 2, pavement composition was constant, but all the asphalts were used. In phase 3, a single asphalt was used throughout, but pavement composition was varied somewhat more than would normally occur in the construction of actual roads. Pavement design and construction and track equipment were substantially as described in phase 1 (3).

Asphalts

The asphalts included domestic and foreign crude sources and were made by several manufacturing methods. All were commercial paving materials but were blended in the laboratory to be in the midpoint of the viscosity study ranges proposed by the Asphalt Institute. As indicated in Table 1, all four grades were represented, although most were either AC-10 or AC-20 grade. Temperature susceptibility was judged by

TABLE 1

ASPHALT CHARACTERISTICS

Asphalt No.	Asphalt Source	Asph. Inst. Study Grade	Original Viscosity 140 F Posises	Original Viscosity 275 F Centistokes	TFOT Ratio (140 F)	Walther Slope (140-275 F)	Penetration at 77 F	Sp. Gr. at 60 F	Flash COC
1	A	5	530	183	2.9	3.68	108	1.025	500
2	B	10	1,300	377	3.1	3.43	128	1.035	465
3	C	10	1,330	324	2.4	3.57	82	1.017	620
4	D	10	1,400	325	2.7	3.58	85	1.013	595
5	E	10	1,360	304	2.8	3.62	81	1.036	590
6	F	10	1,370	392	2.2	3.41	105	0.999	640
7	G	10	1,420	352	2.7	3.52	83	1.015	615
8	A	20	2,650	339	2.8	3.78	37	1.044	520
9	H	20	2,020	402	4.6	3.55	82	1.019	620
10	E	20	2,590	432	2.8	3.57	51	1.041	660
11	F	20	2,610	498	2.4	3.49	72	0.998	625
12	B	40	4,440	671	3.5	3.43	56	1.045	480
13	F	40	4,540	645	3.2	3.50	53	0.999	680

TABLE 2

AVERAGE AGGREGATE GRADATION

Series	Passing Sieve (%) ¾ In.	½ In.	No. 4	No. 10	No. 40	No. 80	No. 200	Fines
(a) Surface								
Design	-	0	36	20	22	7	6	9
Phase 2	-	0	33.9	21.2	22.3	10.2	4.7	7.7
Phase 3	-	0	32.4	22.6	20.2	7.4	8.6	8.8
(b) Binder								
Design	0	25	45	45	30	30	30	30
Phase 2	0	20.7	38.0	10.3	17.5	10.5	1.7	1.3
Phase 3	0	24.1	33.7	10.9	16.5	12.5	1.5	0.8

TABLE 3

PAVEMENT CHARACTERISTICS, PHASE 2

Pavement No.	Asphalt No.	% Asphalt		% Fines, Surface	Mix Ratio
		Surface	Binder		
(a) Pavements Tested at 150 F					
108	10	4.68	4.87	8.4	4.63
109	5	5.19	4.50	6.5	2.97
110	3	4.82	4.73	7.9	2.56
111	8	4.85	4.76	8.3	4.68
112	4	4.86	4.95	8.4	3.33
113	11	5.16	4.45	7.4	3.06
114	2	4.82	5.05	6.7	3.31
115	7	4.86	4.70	8.6	3.01
117	6	4.78	4.84	6.7	4.04
118	1	5.25	5.05	7.7	2.51
119	12	4.57	4.82	7.4	3.51
120	13	4.61	4.65	6.7	4.21
121	1	5.07	5.10	7.5	2.00
122	5	4.66	5.09	8.2	2.44
123	13	5.38	4.34	5.9	2.38
124	9	5.01	4.74	7.1	3.02
(b) Pavements Tested at 110 F					
125	5	4.97	4.66	6.5	2.44
126	5	5.01	4.72	8.0	2.38
127	6	4.96	4.90	6.8	1.97
128	4	5.20	4.90	7.7	2.98
129	3	5.20	4.70	8.2	2.53
130	7	4.80	4.60	6.6	2.25
131	2	4.98	4.69	6.4	2.67
132	11	5.35	4.76	7.3	2.17
133	10	5.04	4.80	7.8	2.74
134	8	4.80	4.80	7.4	3.72
135	13	4.83	4.60	6.7	2.86
136	13	4.66	4.72	7.2	3.44
137	12	4.67	4.50	6.3	3.20
138	9	4.72	4.70	6.8	3.27
139	5	5.00	5.07	7.2	2.48
140	1	4.70	4.80	7.7	2.35

TABLE 4

EXTREMES OF MAJOR VARIABLES IN PAVEMENTS

Variable	Base Case (%)	Max. (%)	Min. (%)
Asphalt in surface	4.75	6.63	3.81
Asphalt in binder	4.95	6.33	4.37
Fines in surface	8.6	11.7	6.6

Walther slopes between 140 and 275 F. The TFOT ratio (see Appendix) was less than 5 in all cases. Penetration, flash, and gravity relate the asphalts to existing practice.

Pavements

The basic design was by Marshall criteria; optimum asphalt content was 4.75 percent.

The phase 2 series consisted of 32 pavements made with asphalts representing all four grades of the study specification. Average aggregate gradation is given in Table 2. Asphalt content of the surface course averaged 4.92 ± 0.38 percent, and that of the binder 4.76 ± 0.33 percent, as indicated in Table 3. The 32 pavements were subjected to several million wheel passes with 16 pavements at 150 F and 16 at 110 F. Replication was provided in pavements containing asphalts 1, 5 and 13; asphalt 5 was replicated at both temperatures.

The phase 3 series consisted of 16 pavements made with asphalt 11. To gain pronounced response in performance, asphalt and fines contents of the surface course were varied above and below the base case, which was the design of phase 2. Because variable amounts of constituents adhere to the pug mill, composition was determined by extraction of the pavements. Extremes of the major variables, none of which occurred in the same pavement, are given in Table 4. Aggregate gradation was similar to phase 2 and is also given in Table 2. Compaction was done at two levels, one normal and one somewhat below normal.

The number of batches at each level was selected from several statistical designs based on the experience of phase 2 and was chosen to provide the optimum opportunity to test the major variables with the 16 track positions available. Replication of the base case provided an opportunity to check possible technique variations from the earlier phases.

Testing in the laboratory track was done at three temperatures in three cycles, the orders being 80, 125, and 100 F; 100, 125, and 80 F; and 80, 125, and 100 F. At each temperature, rut depth was measured at three or four intervals. Duration of the test at each temperature depended on attaining a measurable increase in rut depth. Temperature variation in the pavements was ±1 F all around the track, as measured with four dial thermometers in each pavement.

Determination of Viscosity in Pavement

The viscosity of either the original asphalt or the TFOT residue, measured at the temperature of the track test, was used in $R = k\eta^{-n}$. Either viscosity provides useful

TABLE 5

PAVEMENT CHARACTERISTICS, PHASE 3

Pavement No.	% Asphalt		% Fines, Surface	Mix Ratio	Age Ratio
	Surface	Binder			
147	5.85	4.98	9.7	1.50	1.31
148	5.90	4.58	9.1	1.52	1.29
149	3.81	4.75	10.3	3.47	4.48
150	5.51	4.45	11.7	1.83	1.65
151	4.67	4.72	7.7	2.50	3.17
152	4.79	4.72	7.4	2.58	2.36
153	4.65	4.75	7.5	2.99	2.98
154	4.72	4.69	7.2	2.79	3.38
155	6.63	6.00	9.8	1.16	1.41
156	4.47	6.33	7.4	2.51	3.82
157	4.28	4.37	7.8	3.49	3.30
158	5.80	5.99	7.8	1.58	1.43
159	4.00	4.65	9.4	3.96	5.50
160	5.80	4.58	6.6	1.65	1.51
161	4.11	4.38	6.8	3.72	3.05
162	6.11	6.19	7.8	1.38	1.27
163	3.94	6.22	8.7	5.67	2.98

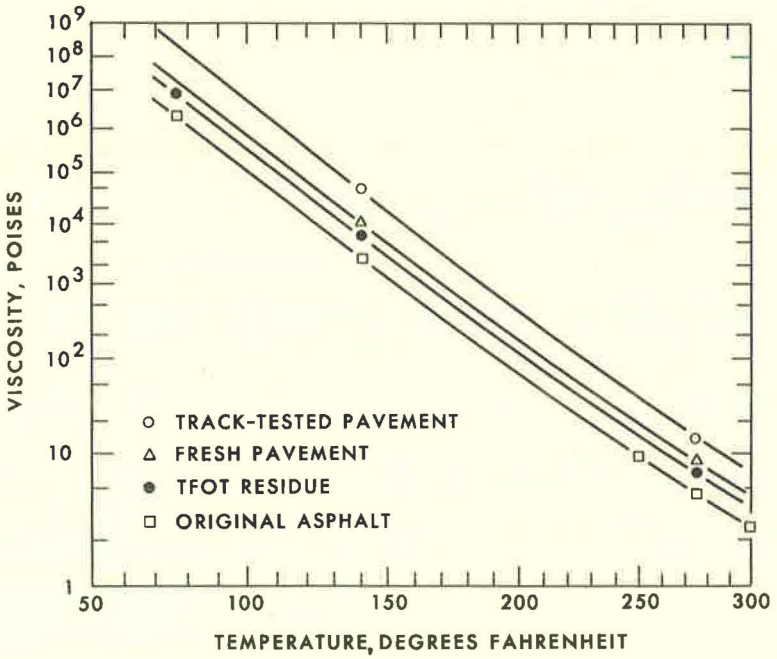

Figure 1. Determination of viscosity in pavement 149.

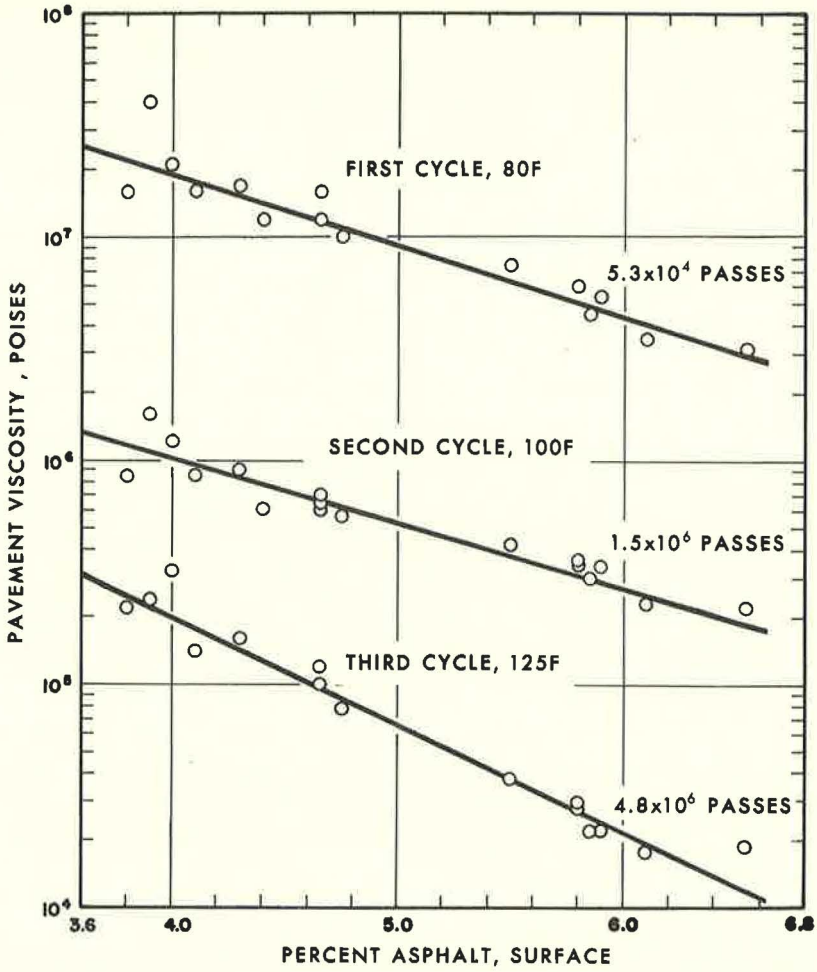

Figure 2. Viscosity of asphalt in pavement.

correlations, but that of the asphalt in the pavement at the temperature and time of the test should provide the best correlation.

The viscosity of an asphalt increases during mixing by a factor called the mix ratio, which is determined by the nature of the asphalt, the mixing time and temperature, and the composition of the pavement. Mix ratios are given in Table 3. Viscosity continues to increase over that in the fresh pavement by a time-dependent factor known as the age ratio. The value given in Table 5 reflects the change that occurred near the end of each test. Some pavements rutted faster than others and were removed from the track before the end of the experiment.

The method of determining viscosity in the pavement is illustrated in Figure 1 by the data on pavement 149. The original viscosity of each asphalt was determined at 77, 140, 250, 275, and 300 F and plotted on the viscosity-temperature chart. Viscosities of the TFOT residues were determined at 77, 140, and 275 F. The plotted data are generally parallel to the original curves. Asphalts extracted from fresh pavements were measured at 140 and 275 F and extrapolated parallel to the original and TFOT curves. Finally, asphalts extracted from tested pavements were measured at 140 and 275 F and similarly extrapolated. For a given temperature level, viscosities were interpolated

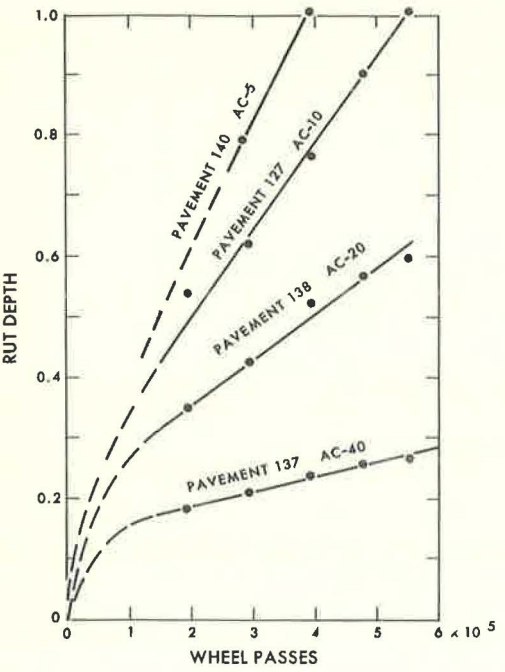

Figure 3. Determination of rut rate.

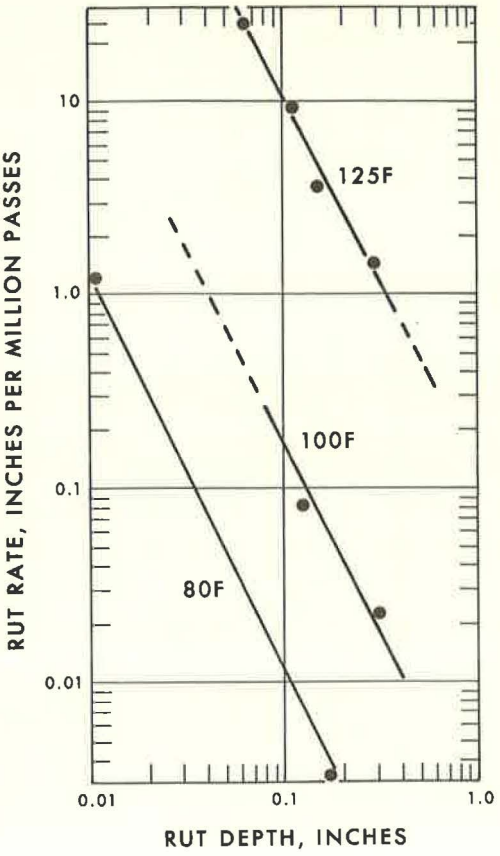

Figure 4. Dependence of rut rate on depth.

linearly between the curves for the fresh pavement and the tested pavement, using the number of wheel passes between the two pavement conditions as the criterion.

Although phase 3 pavements were made with the same asphalt, the viscosities in the pavements differ considerably as a result of testing conditions and asphalt content (Fig. 2). Low asphalt content decreases the asphalt film thickness on the aggregate particles, resulting in higher viscosities and, therefore, higher mix and age ratios.

Determination of Rut Rate

A detailed description of rut measurement has been given (3). Briefly, the track is shut down at intervals and a profilometer with 60 places for a dial indicator is located over each pavement by means of fixed bench marks. The average maximum difference in transverse profiles is taken as the rut depth. Depth is plotted against wheel passes and the rate is calculated in inches per million wheel passes.

The phase 2 pavements were tested at two temperatures and the rate of rutting was determined graphically. Four of the 32 curves obtained are reproduced in Figure 3. Rutting is relatively rapid during the early passes, probably due to compaction and reorientation of the surface particles. The rate soon reduces to a nearly constant level. Correlations between rut rate and viscosity in phase 2 make use of this level. The rate continues to reduce in tests of longer duration; similar rates have been reported for actual roads (1). High rates ended phase 2 too early to determine the full shape of the curves. Also, the need for more frequent rut measurements at the initial stage was indicated.

In phase 3, more attention was given to initial rutting. As in phase 2, plots of rut depth vs wheel passes were prepared. These were not smooth curves but consisted of segments of varying slope, a segment for each temperature in each cycle. Plots of log R vs log D showed a marked dependence of rate on depth as shown in Figure 4 for pave-

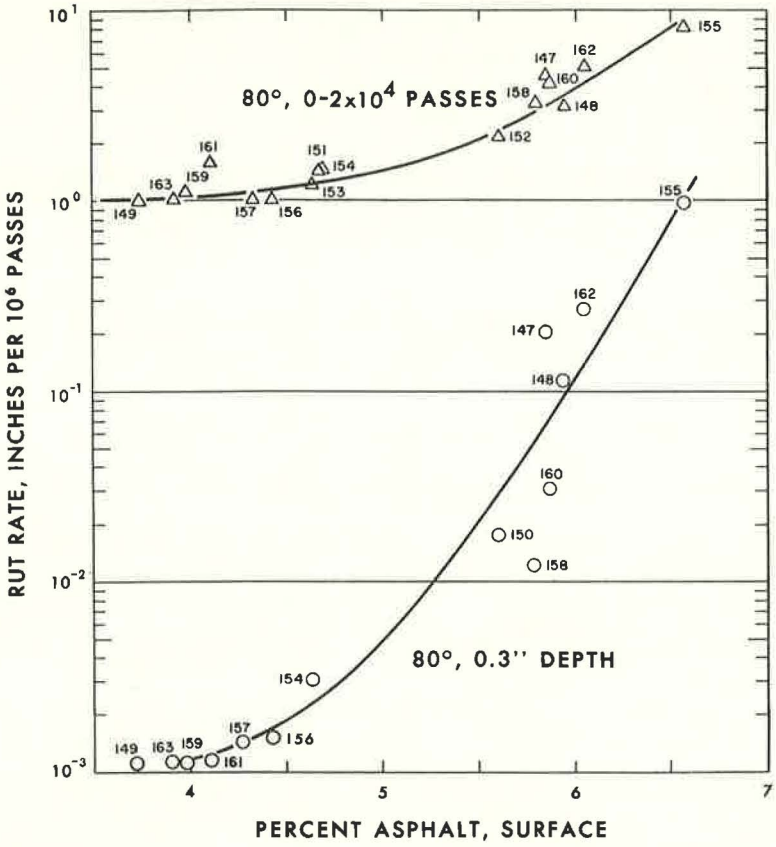

Figure 5. Dependence of rut rate on asphalt content.

ment 149. Similar plots for all pavements showed that the data form a family of parallel straight lines with temperature as a parameter. The family of plots was used to compare the 16 pavements at fixed rut depths and temperatures. A correlation between rut depth and wheel passes was developed from the two plots: $R = dD/dP$ from the depth vs wheel pass plots, and $R = h/D^g$ from the rate vs depth plots.

Equating and integrating these plots yields the following equation:

$$D = \left[(g + 1)\ hP \right]^{\frac{1}{g+1}} \qquad (1)$$

where g an h are constants. This equation can be used to reconstruct continuous rut depth-wheel pass curves for each pavement and temperature.

The effect of asphalt content and rut depth is emphasized in Figure 5. The upper curve shows the rate, calculated by the method used in phases 1 and 2, for all pavements during the first cycle on the test track at 80 F. The rates are averages for the first 20,000 passes, during which time the depths became different for each pavement. These initial rates are high, and the apparent effect of the 2.8 percent difference in asphalt content is only tenfold. The lower curve takes cognizance of the effect of rut depth on rate; rate decreases with rut depth much more rapidly for pavements with low asphalt content. By the time each pavement had reached a depth of 0.3 in., the better pavements rut about 1,000 times less than the poorest pavement (155). The two curves show that the most meaningful comparison between pavements must be made at the same rut depth.

REGRESSION ANALYSIS

Other variables affecting the performance of pavements are fines in the surface, asphalt content in the binder, and compaction. No single figure can show the effect of all the variables, much less the interactions between the variables. To resolve these complex actions and interactions, the data were subjected to regression analysis. Data from the two phases were separately analyzed by linear least squares regression. The same model form was used for both phases, but additional terms were used in the models for phase 3 because of the emphasis on pavement variables.

Phase 2 Regression

The data are most conveniently handled as plots of log R vs log η. An adequate regression equation includes both asphalt viscosity in the fresh pavement and asphalt content:

$$\log R = -0.13 - 0.62 \log (\eta \times 10^{-3}) + 0.28 A \qquad (2)$$

It applies at the average rut depths encountered in phase 2, i. e., from zero to approximately 0.5 in.

Observations on phase 2 pavements were adjusted to a common value of A = 5 percent by means of Figure 6, which is a graphical solution to Eq. 2. At the intersection of R and A, for example, R = 9 and A = 5.2, one can follow the viscosity parameter to A = 5 and read R = 7.8. The figure can also be used to predict R for pavements of known η and A. For example, if A is 5.4 percent and η at some temperature is 4×10^4, R is 2.5 in./million wheel passes.

Data adjusted in this way for phase 2 are shown in Figure 7. Deviations from the central line represent minor differences in percent fines, percent asphalt in the binder, and residual errors. At each test temperature, separation of the pavements by grade is evident. Source of the asphalt is of little or no importance except insofar as it determines the viscosity-temperature slope, m. Because 150 F is nearer to the temperature at which the asphalts were graded (140 F) than is 110 F, the data tend to spread more at the lower temperature.

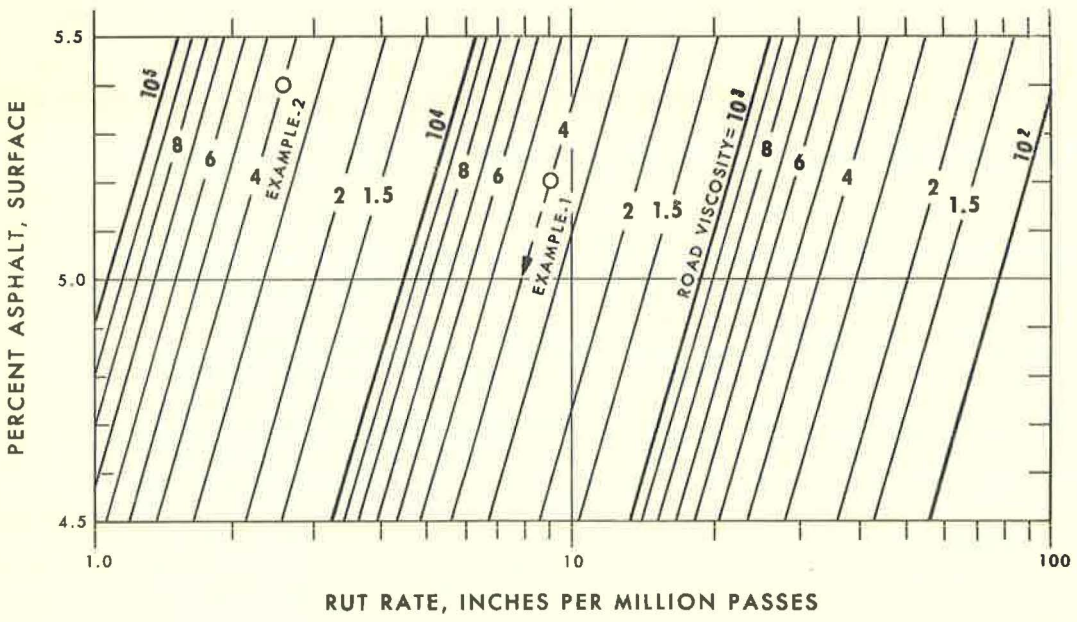

Figure 6. Determining rut rate from η and A, phase 2.

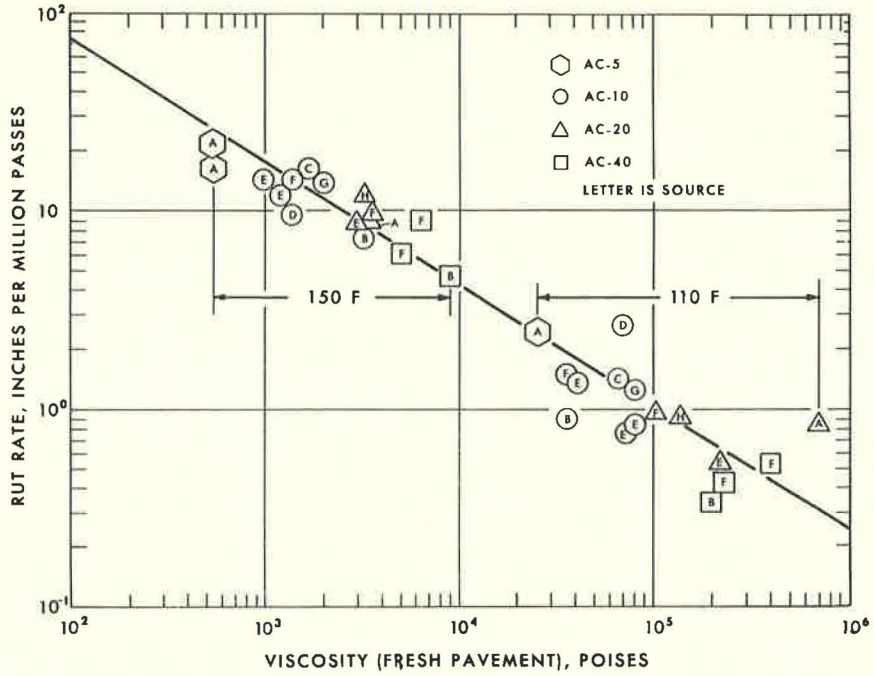

Figure 7. Effect of viscosity on rut rate.

Phase 3 Regression

The results can be expressed in several ways: rut depth vs wheel passes (Eq. 3), wheel passes vs selected rut depths (Eq. 4), or rate of rutting vs viscosity (Eq. 5):

$$D = \left[(1 - B_1)\ 10^{B_0} P \left(\eta \times 10^{-5}\right)^{B_2 + B_3 \log (\eta \times 10^{-5})}\right]^{\frac{1}{1 - B_1}} \quad (3)$$

$$P = \frac{D^{1-B_1}}{1 - B_1}\left[10^{B_0}\left(\eta \times 10^{-5}\right)^{B_2 + B_3 \log (\eta \times 10^{-5})}\right]^{-1} \quad (4)$$

$$R = \frac{dD}{dP} = 10^{B_0} D^{B_1}\left(\eta \times 10^{-5}\right)^{B_2 + B_3 \log (\eta \times 10^{-5})} \quad (5)$$

where

$B_0 = -0.515 + 0.914\,(A - 5) + 0.322\,(F - 8.5) - 0.086\,C - 0.1578\,(F - 8.5)\,C$;

$B_1 = -1.719 + 0.209\,(A - 5) + 0.235\,(F - 8.5) - 0.001C - 0.20\,(F - 8.5)\,C$;

$B_2 = -1.149 + 0.143\,(A - 5)$;

$B_3 = -0.0135 - 0.143\,(A - 5)$;

C = +1 for normal compaction, -1 for less than normal; and

η = pavement viscosity at the time of measuring D.

Eq. 3 is preferred because these measurements are made on actual roads and because rut depth is a significant factor in the AASHO serviceability index. The equation is conveniently expressed graphically as plots of log D vs log P with the other variables as parameters, as shown in Figure 8 for the case of normal compaction at 7.0 percent F.

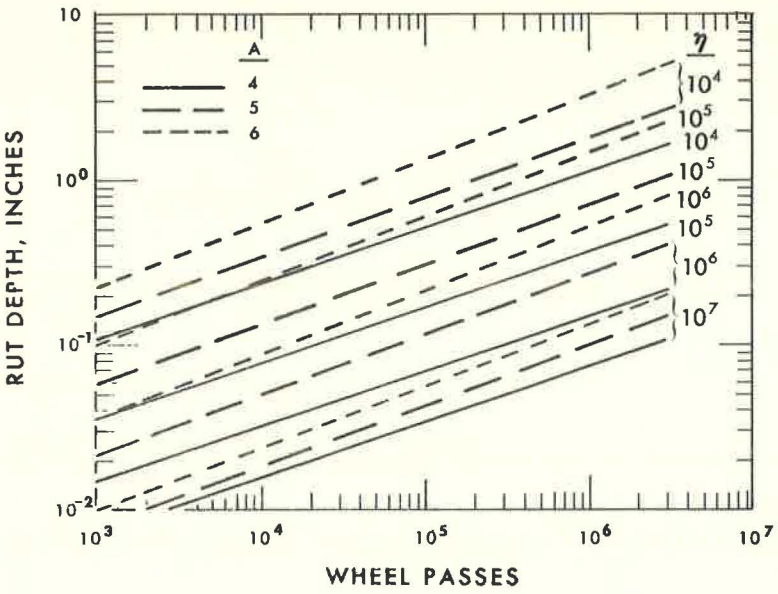

Figure 8. Effect of pavement variables on rut depth.

For a particular pavement, Eq. 3 reduces to

$$D = KP^N \tag{6}$$

where K and N are constants; this equation is similar to Eq. 1. Thus, all of the data may be expressed by this simplified equation and a table relating composition variables to values of K and N. Table 6 lists such values for whole numbers of A, F and η.

The value of K for any value of A and η may be determined from Figure 9. For example, K = 0.5 at A = 5.2, F = 9, and $\eta = 6 \times 10^5$. The corresponding value of N (which does not vary with η) is determined from the equation

$$N = 0.212 + 0.030A + 0.005(F - 7) = 0.378 \tag{7}$$

Observed vs Calculated Rut Rates

The utility of the phase 3 regression equation for predicting plastic deformation from pavement design was judged by comparing the calculated and observed rut rates from all three phases. In each case, the observed rates were compared with the rates calculated by means of the phase 3 equation. The comparison for phase 3 is shown in Figure 10, where the points cluster around the 45° line of perfect correlation through five decades of rut rate. The fit to the central line is good, considering this wide range in rates and the difficulties in making precise observations on so complicated a system.

Comparisons for the earlier phases are shown in Figure 11. The bias in case of phase 1 may be caused by temperature measurement and control and other track technique improvements incorporated in phase 3. Individual pavement thermometers were not used in phases 1 and 2. The comparisons also require considerable extrapolation of phase 3 data with regard to pavement viscosity. Despite these variations, the phase 3 equations adequately predict plastic deformation.

Relative Effect of Pavement Variables

The relative effect of pavement variables may be judged using Eq. 3. Important pavement composition variables include A and F. Pavement temperature is a major

TABLE 6

VALUES OF CONSTANTS FOR NORMAL COMPACTION

Viscosity (poises)	A	4		5		6	
	F	K	N	K	N	K	N
10^4	7	1.110	0.335	1.835	0.361	3.285	0.390
	9	1.430	0.343	2.441	0.370	4.547	0.401
	11	1.866	0.352	3.300	0.380	6.412	0.413
10^5	7	0.370	0.335	0.715	0.361	1.532	0.390
	9	0.464	0.343	0.928	0.370	2.076	0.401
	11	0.589	0.352	1.221	0.380	2.862	0.413
10^6	7	0.151	0.335	0.272	0.361	0.540	0.390
	9	0.185	0.343	0.344	0.370	0.710	0.401
	11	0.230	0.352	0.442	0.380	0.948	0.413
10^7	7	0.075	0.335	0.101	0.361	0.143	0.390
	9	0.091	0.343	0.125	0.370	0.182	0.401
	11	0.110	0.352	0.156	0.380	0.233	0.413

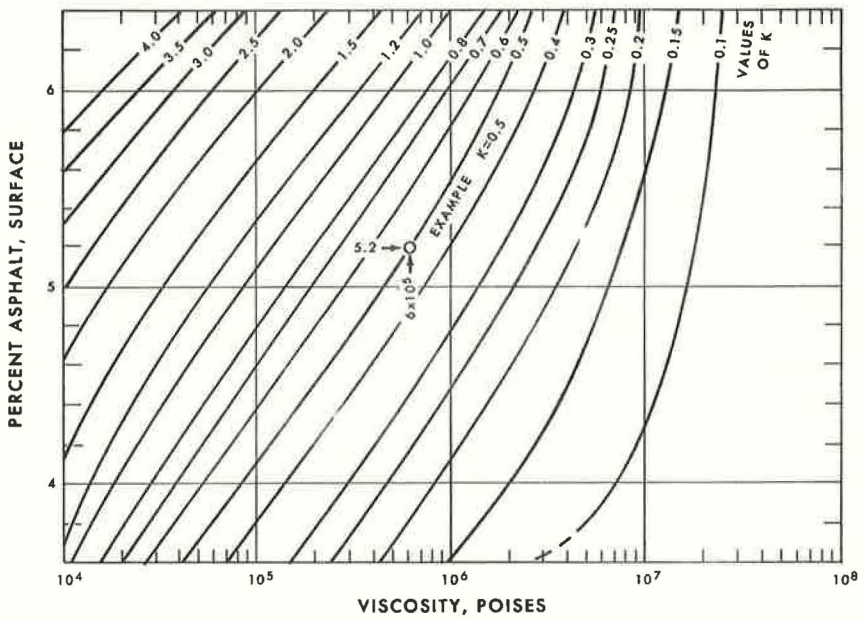

Figure 9. Determining K from A and η (for F = 9, C = +1).

variable in rutting performance. Asphalt properties affecting road viscosity and, consequently, rutting performance include the original viscosity level or grade, a measure of temperature susceptibility (m), mix ratio, and age ratio. Ruts are not as deep for pavements using viscosity graded asphalts when (a) A, F, or pavement temperature are decreased; and (b) compactive effort, mix and age ratios, m, or original asphalt viscosity level are increased.

Since there is a relation between mix and age ratios and asphalt content, the effect of asphalt content is magnified by its additional effect on road viscosity.

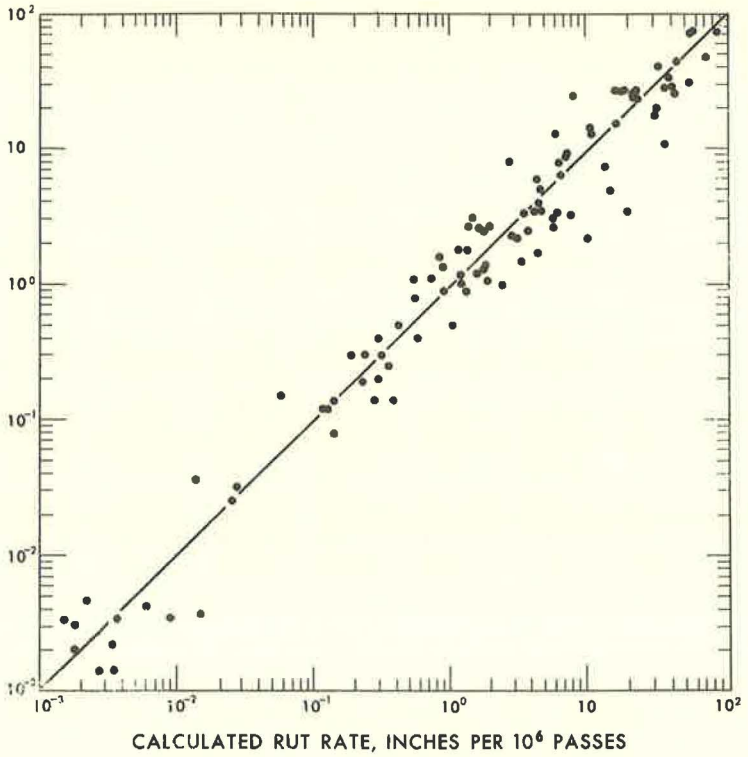

Figure 10. Observed vs calculated rut rate.

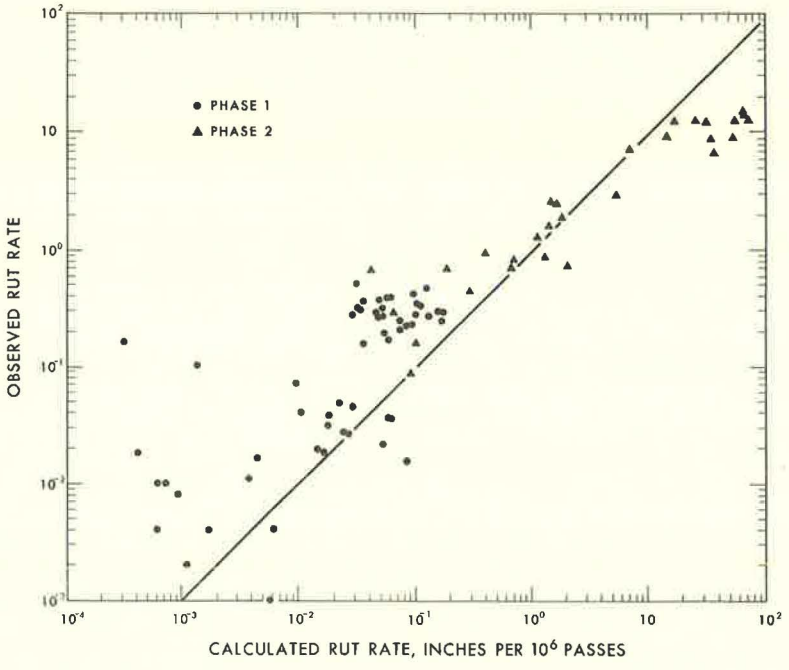

Figure 11. Observed vs calculated rut rate.

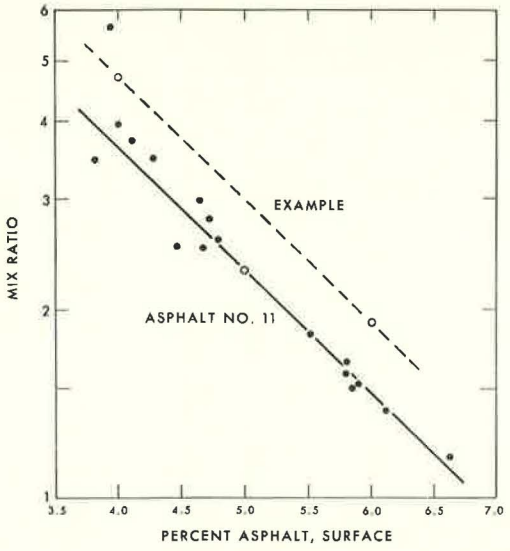

Figure 12. Dependence of mix ratio on asphalt content.

For asphalt 11, the experimental relationship between mix ratio and A is log (mix ratio) = 1.345 - 0.196 A, as shown by the solid line in Figure 12. At A = 5 the mix ratio is 2.3, which agrees well with the TFOT ratio of 2.4. It was assumed that for other asphalts the relationship is parallel, as shown by the dotted line for an asphalt of mix ratio of 3 at A = 5. Here the equation is log (mix ratio) = 1.455 - 0.196 A, which leads to mix ratios of 4.7 at A = 4 and 1.9 at A = 6.

Road viscosity for an average AC-10 asphalt (1,250 poises at 140 F) with a mix ratio of 3.0, age ratio of 3.0, A of 5, and slope of 3.5 at a pavement temperature of 100 F would be 5×10^5 poises, as shown in Figure 13. Lines are also shown for asphalts with slopes of 3 and 4. Applying the mix ratios for A = 4 and 6 leads to viscosities of 16×10^5 and 1.7×10^5, respectively.

Using viscosities so derived, the relative effect of the pavement variables may be judged by the example given in Table 7. The constants for the typical cases, shown at the top of the variables columns, are K = 0.465 and N = 0.370, where K is numerically equal to the rut depth at a million wheel passes. This is equivalent to a rut depth of ½ in. at about 1 ¼ million wheel passes. The values of K and N are the result of varying each property separately (except for asphalt content of which mix ratio and age ratio are a function as determined by experiment). For example, if all the

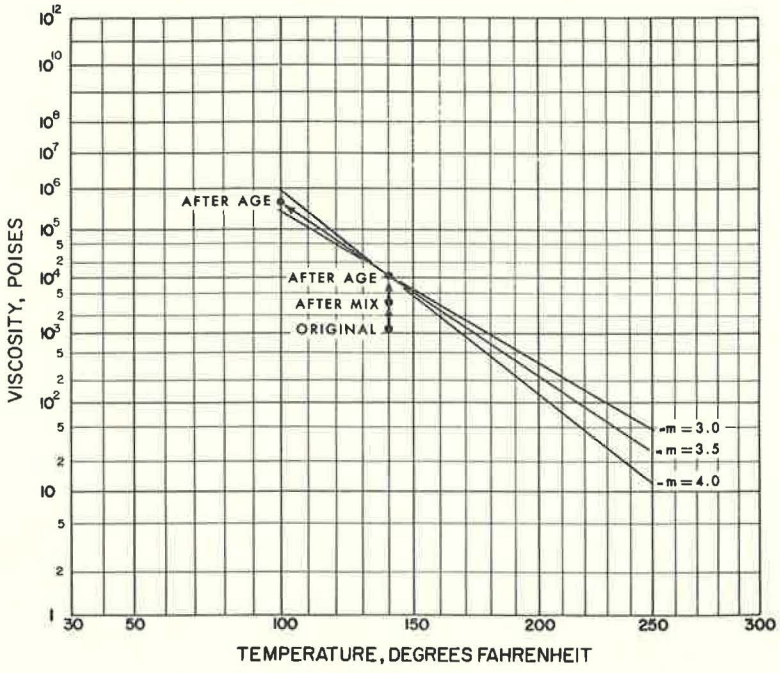

Figure 13. Dependence of road viscosity on asphalt characteristics.

TABLE 7

RELATIVE EFFECT OF PAVEMENT CHARACTERISTICS

% Asphalt, Surface	% Fines, Surface	Temp. (°F)	Grade	Walther Slope	Mix Ratio	Age Ratio	η (poises $\times 10^{-5}$)	K	N	P to 0.5-In. D
5[a]	9[a]	100[a]	10[a]	3.5[a]	3[a]	3[a]	5.0	0.465	0.370	1.25
4	-	-	-	-	4.8	4.8	16.0	0.158	0.344	14.6
5	-	-	-	-	3.0	3.0	5.0	0.465	0.370	1.25
6	-	-	-	-	1.9	1.9	1.7	1.665	0.401	0.050
-	7	-	-	-	-	-	5.0	0.365	0.361	2.41
-	9	-	-	-	-	-	5.0	0.465	0.370	1.25
-	11	-	-	-	-	-	5.0	0.601	0.380	0.62
-	-	80	-	-	-	-	50.0	0.170	0.370	18.5
-	-	100	-	-	-	-	5.0	0.465	0.370	1.25
-	-	120	-	-	-	-	0.7	1.080	0.370	0.125
-	-	-	20	-	-	-	13.0	0.307	0.370	3.70
-	-	-	10	-	-	-	5.0	0.465	0.370	1.25
-	-	-	5	-	-	-	2.0	0.690	0.370	0.43
-	-	-	-	4	-	-	10.0	0.345	0.370	2.74
-	-	-	-	3.5	-	-	5.0	0.465	0.370	1.25
-	-	-	-	3	-	-	3.0	0.580	0.370	0.68
-	-	-	-	-	4.5	4.5	15.0	0.291	0.370	4.30
-	-	-	-	-	3.0	3.0	5.0	0.465	0.370	1.25
-	-	-	-	-	1.5	1.5	0.9	0.973	0.370	0.165
4	7	-	-	-	4.8	4.8	16.0	0.130	0.335	55.8
6	11	-	-	-	1.9	1.9	1.7	2.200	0.447	0.036
-	-	-	20	4	4.5	4.5	80.0	0.140	0.370	31.2
-	-	-	5	3	1.5	1.5	0.23	1.730	0.370	0.034

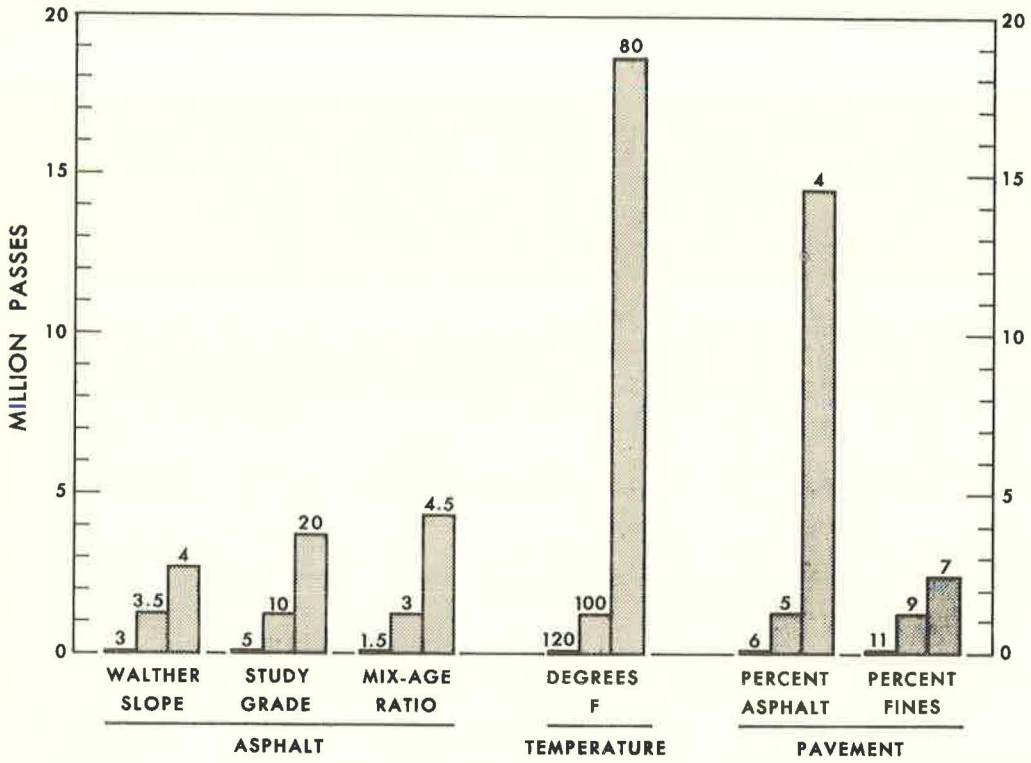

Figure 14. Effect of variables on performance.

properties except asphalt content in the surface course are held at the typical value and A is varied from 4 to 6 percent, K would vary from 0.158 to 1.66; or if the temperature for the typical case is varied from 80 to 120 F, K would vary from 0.17 to 1.08.

The relative effect of the variables can also be expressed as wheel passes to a given rut depth, as in Figure 14, where the typical case is shown at the top of the center bars. Varying one property at a time clearly shows that temperature and asphalt content overshadow the effects of asphalt properties.

The effect of simultaneously varying the pavement parameters A and F compared with simultaneously varying the asphalt parameters is shown at the bottom of Table 7. Possible variations in pavement job-mix parameters for a single construction project introduce greater variations in performance than do asphalt parameters, even when the range is from the center of the AC-5 to the center of the AC-20 grade with values of m and mix ratio selected to encompass the national range of available paving asphalts.

CONCLUSION

The rut depth equation is of practical significance because it quantitatively relates the contribution and interactions of pavement properties to performance. These contributions can be calculated as precisely as current measurement techniques permit, and can make more meaningful mix design feasible. Although the term rut depth has been used, the general phenomenon studied in these experiments has been plastic deformation of pavements. The functional relationships in the rut depth equation should be applicable to the study of changes in surface profile which originate in actual roads under traffic.

The results are sufficiently encouraging to justify further studies on the contributions of aggregate type and gradation and of pavement compaction. Should these also prove successful, it would be reasonable to extend the study to mix design and possibly to structural design. Experiments on actual roads should now be made to verify the relationships found on the laboratory test track.

ACKNOWLEDGMENT

The authors are grateful to Dr. J. W. Gorman for assistance with the statistical design and development of regression equations.

REFERENCES

1. Lee, A. R., and Croney, D. Proc. 1st Conf. Australian Road Research Board, Vol. 1, pp. 622-643, 1962.
2. The AASHO Road Test: Report 5—Pavement Research. Highway Research Board Spec. Rept. 61-E, 1962.
3. Speer, T. L., Brunstrum, L. C., Sisko, A. W., Ott, L. E., and Evans, J. V. Proc. AAPT, Vol. 32, p. 236, 1963.

Appendix

GLOSSARY

Symbols

A = weight percent asphalt in surface course;
B = constant in regression equations;
C = compactive effort;
D = rut depth (in.);
F = weight percent fines, < 200 mesh, in surface course;
K = intercept in log D vs log P plots;
N = slope in log D vs log P plots;

P = wheel passes (million);
R = rut rate (in./million wheel passes);
g = slope in log R vs log D plots;
h = intercept in log R vs log D plots;
k = intercept in log R vs log η plots;
m = slope in walther plots;
n = slope in log R vs log η plots; and
η = asphalt viscosity (poises).

Terms

TFOT ratio—ratio of viscosity of TFOT residue to viscosity of original asphalt, both at 140 F;
Mix ratio—ratio of asphalt viscosity just after mix plant operation to original viscosity, both at 140 F; and
Age ratio—ratio of viscosity after aging in track to viscosity after mix plant operation, both at 140 F.

Discussion

C. R. FOSTER, National Bituminous Concrete Assoc. —This paper has been prepared in the usual excellent manner that characterizes papers from American Oil Company's Research and Development Department and I have no comments on the data contained in the paper or the analysis made of the data. I do think, however, that a comment on the applicability of these findings to real pavements is in order.

In this paper the variables are evaluated in terms of rut depth under traffic. The manner of presentation and references to the AASHO serviceability index imply that a small rut depth, or rather a slow rate of development of rut depth, is desirable. Figure 14 summarizes the effect of the variables in terms of passes required to produce 0.5-in. rut. Applying these findings to real pavements would dictate using: (a) the hardest grade of asphalt available; (b) the asphalt that hardens most in the mixing cycle and fastest on the road; (c) the least asphalt content; and (d) the least filler content. I believe a, b, and c would lead to short lived, raveling pavements.

It hardly seems necessary to remind ourselves that in real performance on the road, rich pavements flush and lean pavements ravel and that our desire is to "put in all the asphalt that traffic will bear." I believe the data would be far more meaningful if information was presented on passes required to produce flushing, and if rut depth analysis was made only of pavements that were not flushed.

L. C. BRUNSTRUM, L. E. OTT, A. W. SISKO, T. L. SPEER, R. A. WILKE, and J. V. EVANS, Closure—The authors appreciate Mr. Foster's perceptive comments concerning pavement design and selection of the most meaningful pavement response. We were exploring the relative effects of variations from optimum Marshall design in terms of resistance of the pavement to plastic deformation. Certainly, there is no substitute for good design in producing durable roads. Furthermore, such a design does not require the hardest grade of asphalt, asphalts that harden rapidly, and low asphalt content. But optimum design may not always be achieved and our experimental design was intended to extend the variables beyond the narrow range of optimum design.

Responses other than plastic deformation were observed during the course of the work, including flushing, densification, aggregate reorientation and asphalt migration. A general correlation between plastic deformation and flushing was noted. However, plastic deformation was considered the primary variable because it appears in the

AASHO equation for serviceability index and because it is measurable. The onset and progress of plastic deformation can be precisely measured on the test track and on actual roads. We have not, as yet, developed means to follow flushing or densification on the track. The rutting vs passes curves (Fig. 3) apparently are determined by two rates: an initial portion controlled primarily by densification or other realignment of the aggregate and asphalt, and a straight-line portion controlled by asphalt viscosity. More detailed studies of the initial portion might be rewarding.

Mr. Foster has alluded to applicability of the findings to real roads. The authors, too, realize the need to test the applicability of the relationships to real roads and encouraged such tests in the conclusion.

A Study of Tenacity of Aggregates in Surface Treatments

H. E. SCHWEYER and WILLIAM GARTNER, JR.
Respectively, Department of Chemical Engineering, University of Florida; and Division of Research, Florida State Road Department

A study was made to develop a tenacity test for measuring chip retention in surface treatment. A laboratory procedure is described for forming a monolithic structure on the surface of a simulated roadbed made up on a metal panel. The aggregate chips were encapsulated on the surface so that the entire mass could be pulled away from the roadbed and the strength of the bond between the aggregate and the roadbed determined.

To keep experimental work to a minimum the number of variables studied have been limited to aggregate and asphalt spread quantity, the type, size and size distribution of the aggregate, and consistency of the asphalt. Results cover a number of these variables but are not a complete survey of all of them. To reduce variability of results, test procedures were standardized carefully and enough samples were tested so that statistical methods could be used with confidence. Additional variables studied by statistical techniques include: (a) effect of moisture and dust in the aggregate, (b) different operators, and (c) the effect of aging before testing.

•MINERAL SURFACE TREATMENT of roads for either the construction of new pavements or the repair and improvement of old roads is a relatively simple and effective operation. However, many variables affect the actual construction of this type of surface and introduce considerable variability in the final results, for example, by causing whip off of the aggregate or chips applied to the surface. Equally important is the consideration that excessive use of aggregate is uneconomical and adds to the cost of the treatment.

This research investigates factors that might be most important in determining the economic and technical utilization of surface treatments with aggregates applied to asphalts to provide a satisfactory road surface. Only preliminary laboratory research which can be correlated with field performance is considered.

A considerable amount of work has been reported on mineral surface treatments, and a review of surface treatments was made by Herrin, Majidzadeh and Marek (4) which includes an annotated bibliography, an additional supplemental list of references, and a comprehensive compilation of selected design procedures proposed by other investigators.

Another comprehensive report has been given by McLeod (5); however, much of this report is concerned with field practices rather than laboratory procedures. The most extensive work found on laboratory study of surface treatments was that of Benson and Gallaway (2). This report discusses experimental equipment used for and results of the study of chip retention. Many variables were studied and a selected bibliography is included.

Another pertinent reference is a paper by Nevitt (6) which discusses seal coat aggregates generally and, in particular, particle size gradation effects and bitumen

Paper sponsored by Committee on Bituminous Surface Treatments.

requirements. A bibliography is also included. A number of the variables involved in chip retention are also considered in a report by Hank and Brown (3).

A review of the material available indicated that it would be desirable to study chip retention with the particular combinations of asphalt and aggregate components used in Florida. A design procedure following the proposed procedure of Benson (1) using the Kearby embedment vs mat thickness diagram was utilized for consideration of the asphalt and aggregate spread quantities. In addition, the studies also utilized the standard practice in Florida for these quantities, although they were at the low end of the specifications.

Herrin et al. (4) point out that there are a number of variables that must be considered in a test for evaluation of chip retention in surface treatment. Among the most important aggregate properties are type, size distribution, mean size, percent voids, surface texture, surface condition (dusty, damp), surface charge, and aggregate spread quantity. Their list of important asphalt properties includes penetration or consistency, source or type, asphalt cutbacks, asphalt emulsion, bitumen spread quantity, and embedment.

Because of the range of variables that could be investigated, only a limited number could be selected for this particular study. Those selected will be discussed in more detail later. A single slag aggregate and an asphalt cement of about 150 penetration were primarily used for the study.

The three main objectives in developing a tenacity test for chip retention were (a) to provide a test section of optimum size for laboratory work that would be useful in a simple rapid test, yet would be of proper sensitivity and indicative of actual service conditions; (b) to develop a rapid curing formulation that would adhere to the aggregate to provide a physical bond so that the aggregate could be pulled from the surface; and (c) to design a suitable arrangement whereby the force required to separate the aggregate from the asphalt could be measured with the proper degree of sensitivity.

PRELIMINARY EXPLORATORY STUDIES

To attain the objectives listed in the preceding section, considerable exploratory work was conducted to establish a procedure and an apparatus that would meet the requirements. The two principal goals of the exploratory study were to establish a technique for preparing a suitable and representative miniature roadbed and to evaluate various types of bonding agents to determine what types could best be used.

Design of Mineral Surface Roadbed

As a first approach to the selection of a roadbed, a 6.125- by 5.125-in. aluminum plate was made with shoulders to retain the asphalt applied in the center. The asphalt was laid on the plate and spread uniformly by maintaining a level surface and warming the plate, without overheating, in an oven. After cooling, the aggregate was spread by hand shaking as uniformly as possible on the asphalt surface and the prepared surface was covered with a 1-in. thick rubber mat and subjected to a pressure of 15 psi in a hydraulic press. The excess aggregate was removed by turning the plate upside down without jarring. Approximately 85 percent of the spread quantity was retained. Thus, there was a 15 percent excess above the experimentally observed spread quantity obtained by hand spreading. This result corresponds approximately with those obtained by Benson and Gallaway. After pressing the aggregate into the roadbed, a circular metal form was pressed into the surface by a rotary motion with sideways displacement of aggregate where necessary to embed the form into the asphalt. This form then constituted a mold into which some type of a bonding agent could be cast to form a monolithic structure with the aggregate after the bonding agent had set. For the first experiments, 3-oz penetration tins were used as molds, as shown in Figure 1.

Figure 1 also demonstrates the manner in which the pulling arrangement for the first experiments was accomplished. A nail through the tin was attached by a hook to a chain which was, in turn, attached to the loading head of the testing machine. This arrangement permitted a vertical pullout of the bonded aggregate, and tests were made under a variety of conditions.

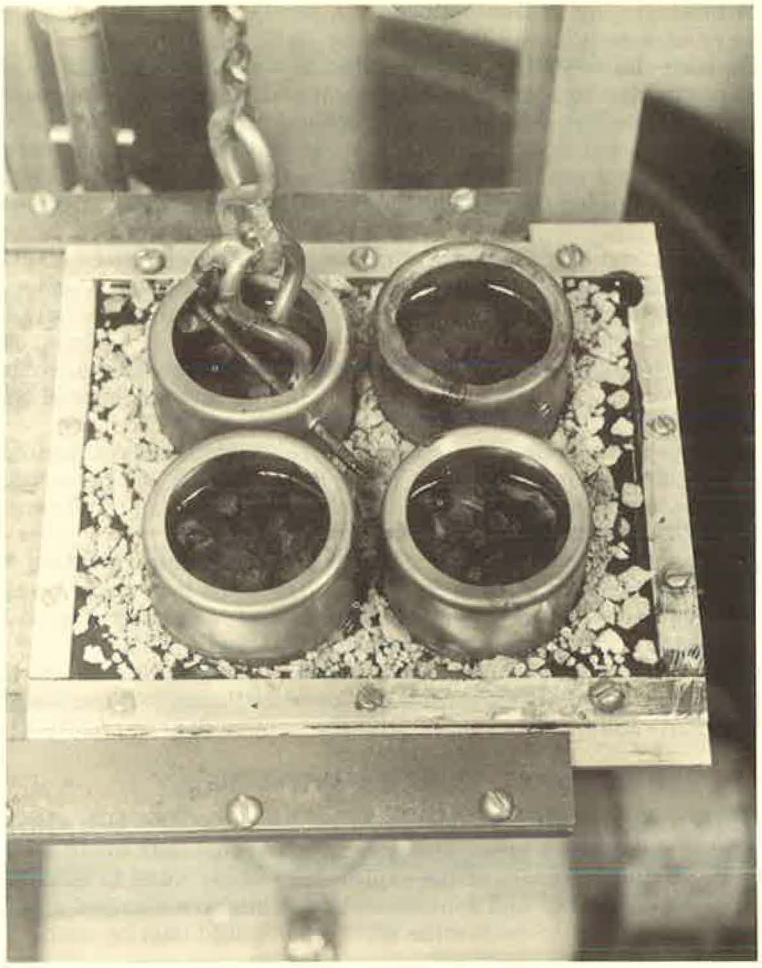

Figure 1. First experimental mold arrangements for tenacity tests.

There was great variability in this test arrangement, and, therefore, arrangements were made to change the designs of the mold and the test plate. As a matter of record, the experiments reported here used a Scott tensile tester, which consists of a cross-head moving at a constant speed against an increasing load. This machine was selected because of its availability and because a rather high sensitivity was desired. However, this type of test machine causes certain difficulties in analyzing the data, since failures at different values probably do not occur under similar conditions of deformation. In general, failure occurred in these tests by a single rapid pullout at some indicated load where the surface parted, as shown in Figure 2.

To reduce the variability of the test, the design of the mold was changed by increasing its diameter and also by substituting a solid bar for the chain in the linkage between the mold and the loading head on the Scott testing machine. The new mold, shown in Figure 3, was used in all studies following preliminary exploration work with different bonding agents. The mold is essentially 4 in. in diameter. The solid bar linkage was free to move for proper alignment and is shown in Figure 4. The use of mold with the test linkage on a small roadbed, similar to that used previously, is shown in Figure 5. After these experiments, a roadbed surface was used which could accommodate three molds at one time (Fig. 6). Since a number of these test plates was available, at least 27 test specimens could be set up when the statistical analysis was

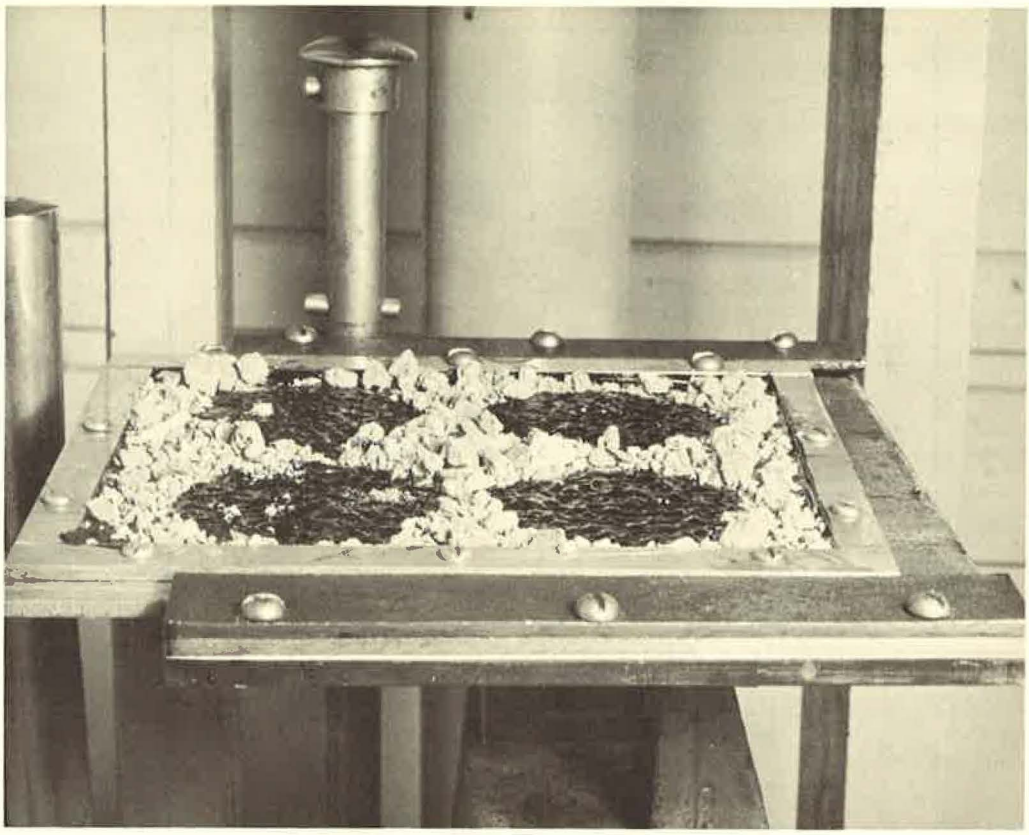

Figure 2. Illustration of nature of surface after pullout.

made for variability. However, certain defective tests, either because of improper preparation or improper assembly of the testing head, made it impossible to have 27 results in every case. The minimum number of tests run was 24. For some experiments, 51 samples were used. A few tests with limited quantities of materials were made.

Selection of a Bonding Agent

The preliminary experiments on this test were made using an epoxy resin formulation which set rapidly through the formation of a solid polymer by a heat-accelerated process. Since this heat is self-generated in the setting process, its effect on the relationship of the asphalt to the aggregate posed problems. A curing time of less than 2 hr was desired so that the samples could be tested within a reasonable time after being prepared. However, the exothermic reaction heat was too great and the bonding agent had too short a pot life, requiring a new batch for each mold poured. Shell Epon 815 with 5 percent ethylenediamine and 5 and 10 percent curing agent U gave about the same results but required 4 days to cure sufficiently. Because of these results, the epoxy type resin bonding agent was discarded.

A second type of polymeric bonding agent made up of polyesters was next considered for study. These materials set to solid polymers by the use of free radical forming catalysts, but their curing has a disadvantage where surfaces are exposed to oxygen. The internal curing occurring below the surface of the tenacity test molds proceeds independently and is not affected. This resin proved interesting and for a time it was thought that a satisfactory formulation could be perfected with these materials. After

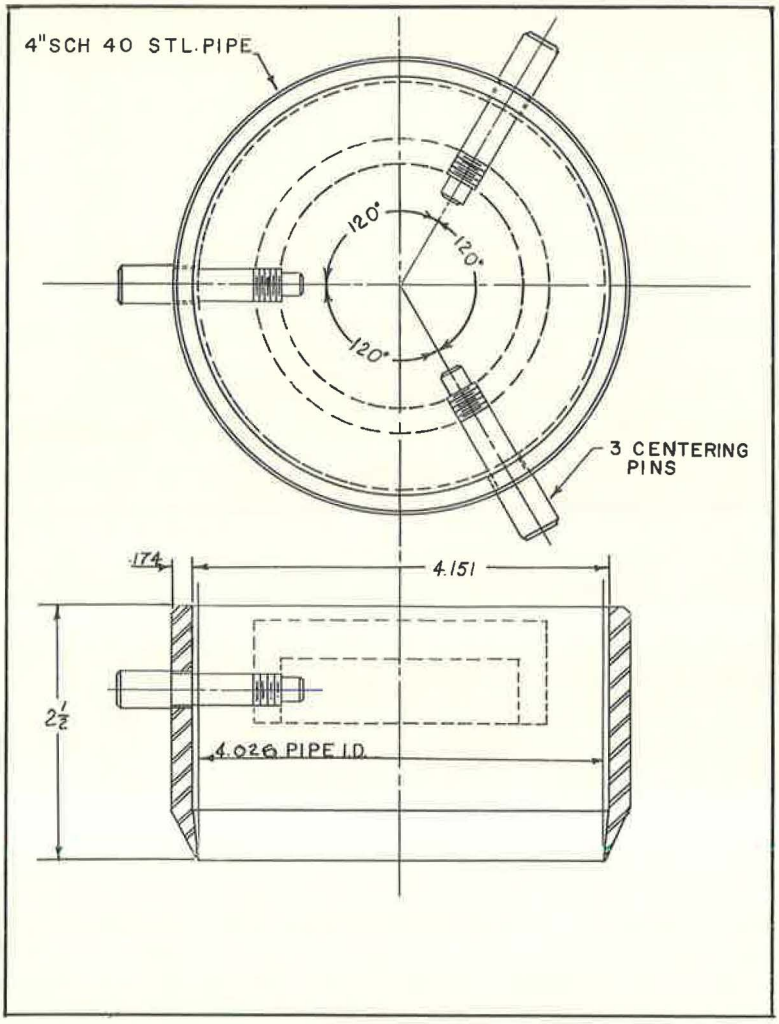

Figure 3. Large mold for tenacity test.

making various trials, a Celanese MR-62-CL polyester resin with a 3 percent cobalt accelerator (Nuodex) and 3 percent MC-1 catalyst paste (benzoyl peroxide) formulation was developed. This starts to set within 15 min and produces a satisfactory setting agent within a short time. Accordingly, a considerable amount of experimentation was carried out using this particular type of formulation. For these experiments, various spread quantities of asphalt and a slag aggregate and a Miami limestone aggregate were used. These tests were carried out concomitantly with the studies on the roadbed and small molds. Figure 1 shows the transparency of the resin and how it covers the aggregate.

Further experimental work with the polyester resins indicated that they also had certain disadvantages, principally the displacement of the asphalt from the baseplate by preferential wetting of the baseplate and a rather high shrinkage factor, resulting in some cases in the mold pulling from the baseplate without carrying the complete bonded structure with it. For these reasons, this type of bonding agent was also discarded.

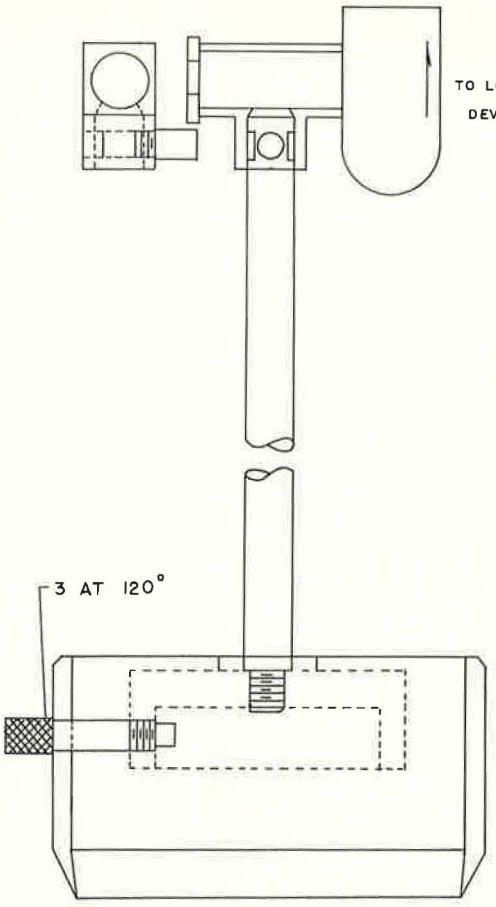

Figure 4. Linkage for attaching tenacity test mold to loading head.

Following the experiments with the organic-type bonding agents, it was decided to try an inorganic type such as Hydrocal (U.S. Gypsum Co.). This agent sets in a relatively rapid time and is quite simple to handle. Accordingly, after satisfactory preliminary experiments, this material was used throughout the remainder of the work done on the tenacity test. The details of the preparation of the Hydrocal are given in the Appendix. The enlarged test plate, together with three molds, is shown in Figure 6 after the Hydrocal has been added and the samples have set.

On completion of these exploratory experiments, it was thought that the test had some merit as a measure of the strength of the bond between the asphalt and the aggregate as typifying a mineral surface roadbed. Accordingly, a more elaborate experimental program was undertaken to obtain certain quantitative information regarding the test data.

EXPERIMENTAL WORK

The test procedure is described in the Appendix. Essentially, the procedure consisted of adding an excess of asphalt to the preheated test plate and then removing the excess with a doctor blade, leaving the desired asphalt spread quantity on the test plate. As mentioned before, the aggregate was then spread on the cooled asphalt by hand as uniformly as possible and the mixture was compressed in a hydraulic press with a rubber mat on top of the aggregate. The excess aggregate was removed and molds were pressed in position on the compacted roadbed. During this step, no attempt was made to move the aggregate; if a large aggregate was in the way, it was broken since the molds were placed on the roadbed under pressure. The Hydrocal slurry was then prepared, poured into the molds, and permitted to harden in a constant temperature room at 73 F. All tests at ambient temperature ranges were made at 73 F. However, other tests (reported later) were made with the test machine placed in a constant temperature room large enough to permit a man to work. These tests were made at temperatures up to 140 F.

Materials Used

The two asphalt cements used for most of these tests were Florida AC-15 materials, commercially supplied, which met AASHO specification M20 for the 150 to 200 penetration grade. One (S59-16) had a penetration of 168 and a viscosity at 77 F of 0.33 megastokes. A second sample (S62-9) of AC-15 was required because the initial supply was exhausted. This sample had a penetration of 150 and a viscosity at 77 F of 0.32 megastokes. In addition, for one set of results four other asphaltic materials of differing viscosities were studied. Data on these materials are given in Table 1.

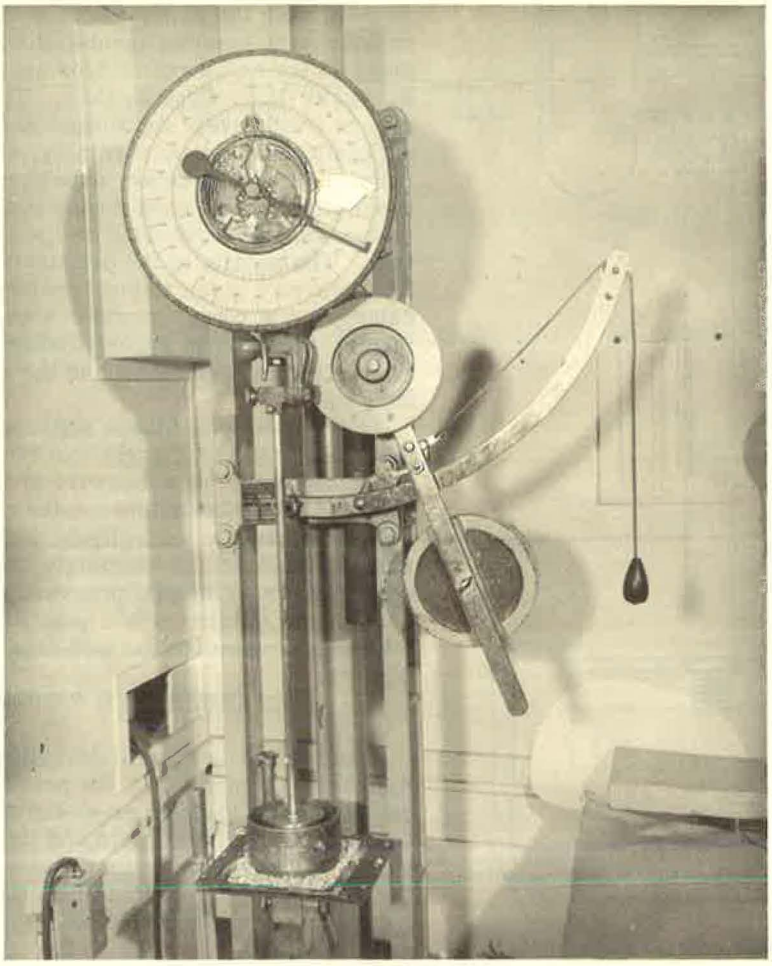

Figure 5. Assembly of test equipment with 4-in. mold.

Two base aggregates were used in this study, a slag (S62-1) and a Miami limestone (S59-19), both meeting the specifications of the Florida State Road Department for grade No. 16 modified aggregate. The gradation of this aggregate is as follows:

Passing ½-in. sieve, 100 percent;
Passing ⅜-in. sieve, 90 to 100 percent;
Passing No. 4 sieve, 30 to 60 percent;
Passing No. 10 sieve, 0 to 10 percent; and
Passing No. 16 sieve, 0 to 5 percent.

Certain other aggregates were used in the studies of the effect of size distribution, but these were derived from the slag No. 16 mentioned previously. The aggregate spread quantity applied to the samples was 20 percent greater than the spread quantity designated by the Florida State Road Manual. After pressing the aggregate under a rubber mat at a pressure of 15 psi, excess was removed from the surface by a wrist-snapping action. The mold was then placed on the roadbed. The plate, asphalt, and aggregate were weighed separately after each component had been added to record the amounts. In general, most of the studies reported in this paper refer to an

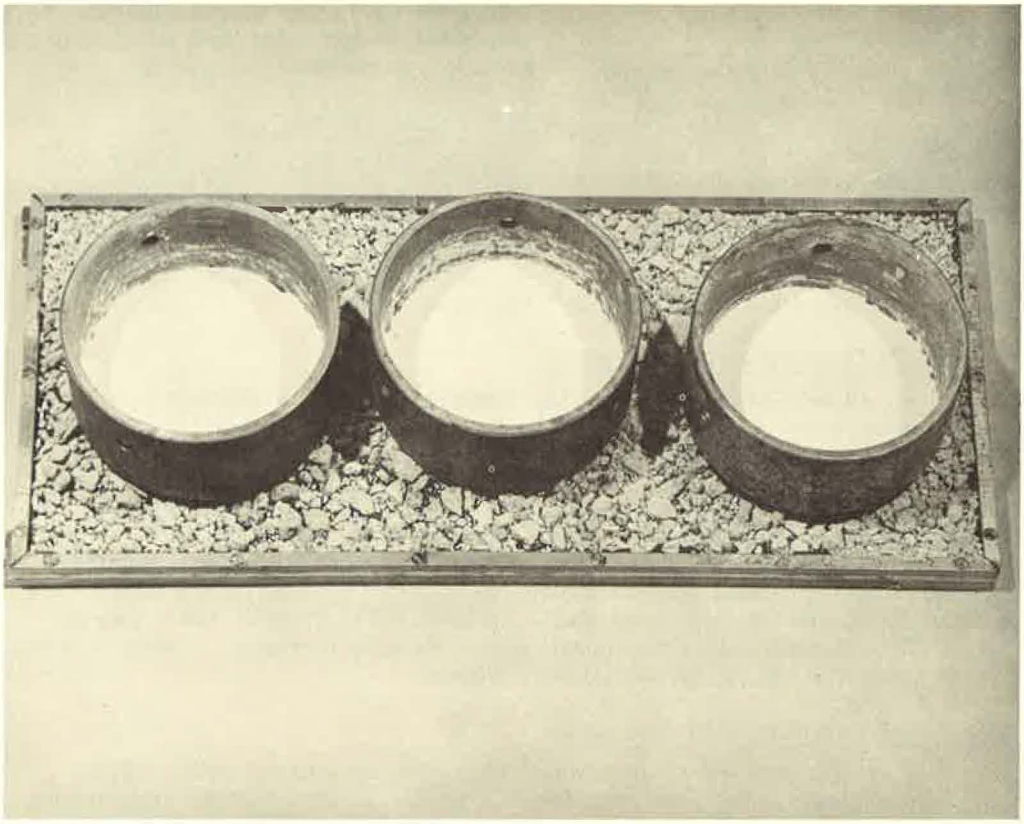

Figure 6. Samples on test plate preparatory to measuring tenacity.

asphalt spread quantity of 0.12 gal/sq yd. However, some studies were made at different spread quantities. Generally, the aggregate quantity was 0.10 cu ft/sq yd.

Testing Procedures

After the samples had been prepared and the Hydrocal poured, the assembly was allowed to set for about 1 to 1½ hr. These samples were aged at 73 F, as mentioned before. The Scott tensile tester was employed to measure the pullout force using a linear speed of 11.3 in./min on the pulling head. The total force is measured on the instrument and coverted to pounds per square inch, based on the area of the mold. The results for the experimental program are given in the form of tables and figures, but many of the details have been omitted to conserve space.

RESULTS

Effect of Asphalt Spread Quantity

The influence of the spread quantity of asphalt when increased from 0.12 to 0.30 gal/sq yd is indicated by the frequency polygons shown in Figures 7 and 8. A statistical analysis of the results for these figures is given in Table 2.

Considering the individual aggregates, the results show an increase in tenacity of approximately 5 to 10 percent for an increase of 2½ times the spread quantity of asphalt. This effect is of about the same order of magnitude as has been noted for certain field tests for Florida asphalt cements of the type used in this study. The statistical analysis indicated that only once out of 100 times would the larger tenacity

TABLE 1

ASPHALT PENETRATION AND VISCOSITY DATA

Asphalt	Penetration, 77 F (100g/5 sec)	Viscosity, 77 F (megastokes)
Gulf Coast naphthenic (S119)	Soft	0.0027
East Central Texas resid. (S120)	235	0.11
East Texas asphalt (S117)	174	0.27
Florida AC-8 (S60-17)	92	1.0

values for the higher spread quantities be attributed to chance for both the slag aggregate and the Miami limestone.

Effect of Aggregate Type

Additional study of the data in Table 2 at the same asphalt spread quantities for the two aggregates when based on asphalt spread quantities of 0.12 and 0.30 gal/sq yd indicates that there is no appreciable difference for the results obtained by either aggregate.

Influence of Size Distribution of Aggregate

The slag No. 16 (S62-1) used in these experiments was separated into a coarse and fine fraction using a No. 4 Tyler sieve (0.185-in. opening). These two fractions were compared with the tenacity results for the whole aggregate (Fig. 9, Table 3).

The data for the fine fraction are similar to those for the whole material. The null hypothesis that they are from the same populations cannot be rejected at the 0.01 probability level. However, a study of the results for the coarse fraction shows a somewhat lower value for the tenacity test. At a spread quantity of 0.12 gal/sq yd, the tenacity value for the fine and whole fractions are about 21 percent higher than for the values using the coarse fraction of the slag. As indicated in Table 3, there was an increase in the tenacity value as the asphalt spread quantity increased. Other data in Table 3 are given to complete the statistical analysis.

Influence of Moisture Content of Aggregate

A series of experiments were run in which the aggregate was wet with water to various degrees. When completely wet, the slag aggregate used in these experiments was found to carry about 12.5 percent water. By partially drying some of the wet aggregate, it was possible to obtain more or less uniform moisture contents for the

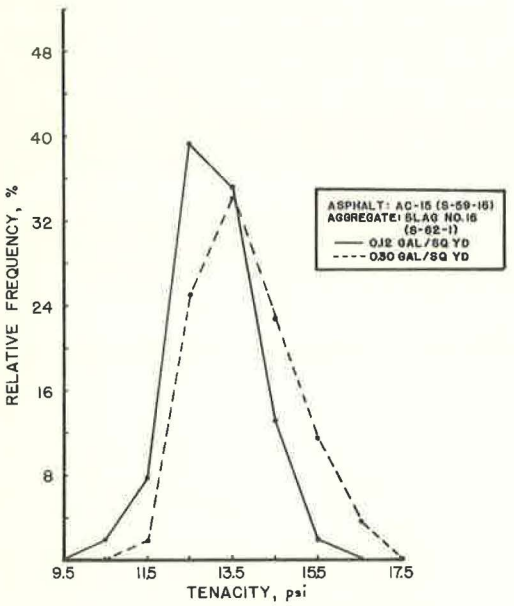

Figure 7. Effect of asphalt spread quantity on tenacity test for slag.

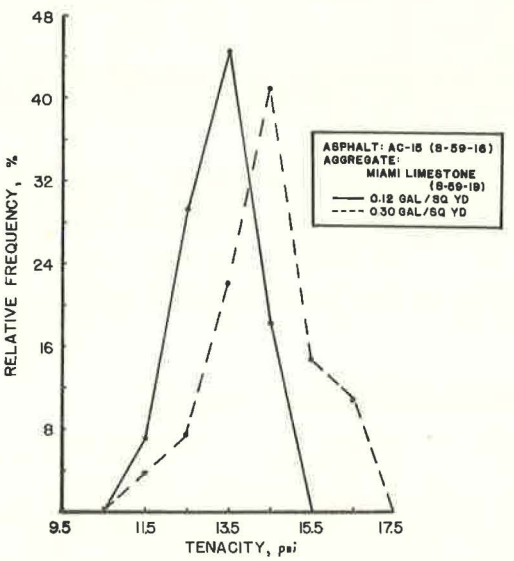

Figure 8. Effect of asphalt spread quantity on tenacity test for Miami limestone.

TABLE 2

EFFECT OF ASPHALT SPREAD QUANTITY (AC-15)

Measurement	Slag No. 16 (S62-1)		Miami Limestone No. 16 (S59-19)	
	0.12 Gal/Sq Yd	0.30 Gal/Sq Yd	0.12 Gal/Sq Yd	0.30 Gal/Sq Yd
No. of samples	51	52	27	27
Mean tenacity value at 73 F, psi	13.1	13.9	13.2	14.4
Std. dev., psi	0.88	1.21	0.89	1.27
Coeff. of variation, percent	6.72	8.71	6.75	8.80
95 percent confidence limits for mean	12.8 13.4	13.5 14.2	12.8 13.5	13.9 14.9
Mean aggregate weight per plate, gm[a]	220	262	269	310

[a]Reported here as a matter of interest to show effect of spread quantity.

aggregate at different levels, as indicated in Table 4. The statistical results, shown in Figure 10, indicate that a partially wet aggregate did not greatly influence the results, although when the aggregate was completely wet there was an appreciable change in the tenacity value.

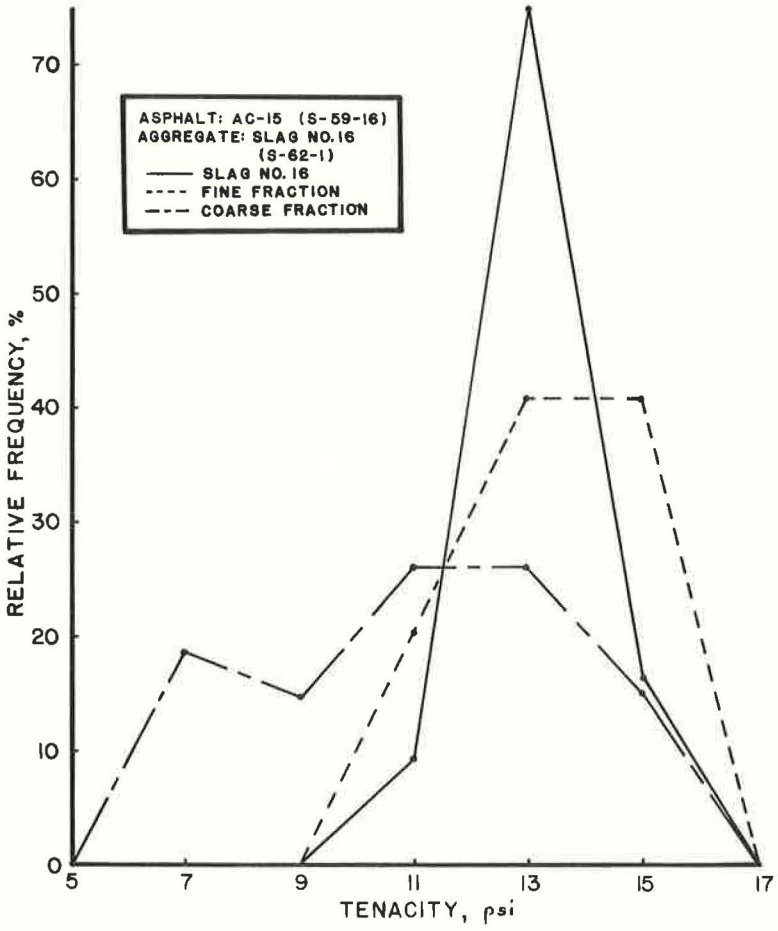

Figure 9. Effect of aggregate size distribution.

TABLE 3

EFFECT OF AGGREGATE SIZE DISTRIBUTION[a]

Measurement	S62-1 Whole	R62-23 Fine	R62-24 Coarse	R62-24 Coarse
No. of samples	51	27	27	17[b]
Mean tenacity value at 73 F, psi	13.1	13.3	10.9	12.8
Std. dev., psi	0.88	1.71	2.74	0.97
Coeff. of variation	6.72	12.8	25.1	7.58
95 percent confidence limits for mean, psi	12.8	12.9	9.8	12.3
	13.4	13.7	12.0	13.3
Mean aggregate weight per plate, gm	220	165	286	305

[a]Asphalt AC-15 (S59-16) at 0.12 gal/sq yd.
[b]These data are for an asphalt spread quantity of 0.30 gal/sq yd; the number of samples is low because the supply of this fraction of the aggregate was exhausted.

Influence of Dust in Aggregate

It was also considered desirable to test the effect of a high dust content in the slag on the tenacity value. Some of the slag No. 16 (S62-1) was ground overnight in a ball mill and that portion of the ground material which passed through a No. 200 sieve was used as a dusting agent. Certain preliminary experiments using dust without any aggregate gave a very large variability in results with tenacity values ranging from 6.2 to 16.7 psi. A study of the surfaces indicated that there was a partial and variable bond with the dust, asphalt, and Hydrocal. This would cause the variance obtained and would not be similar to the separation of the mineral from the asphalt. Certain tests were also made in which an aggregate dust combination was used, but here again there was considerable variation in the results because a uniform dusting of the aggregate could not be obtained with the small quantities involved in the mixing. One other set of experiments was carried out in which the surface was first covered with the dust, the excess removed, and the aggregate applied to the surface. This procedure resulted in a very definite lowering (approximately 33 percent) in the tenacity value. Here it is expected that the presence of dust interfered with any coherent bond between the mineral aggregate and the asphalt component.

TABLE 4

EFFECT OF MOISTURE CONTENT OF AGGREGATE ON TENACITY VALUE[a]

Measurement	Oven Dry	4.08% Moist.	8.5% Moist.	12.5% Moist.
No. of samples	27	27	27	26
Mean tenacity value at 73 F, psi	12.5	11.9	11.7	4.85
Std. dev., psi	1.48	1.22	1.73	1.00
Coeff. of variation, percent	11.8	10.3	14.9	20.6
95 percent confidence limits for mean, psi	13.1	12.4	12.4	5.3
	11.9	11.4	10.9	4.4

[a]Asphalt AC-15 (S62-9), 0.12 gal/sq yd; aggregate, slag No. 16 (S62-1).

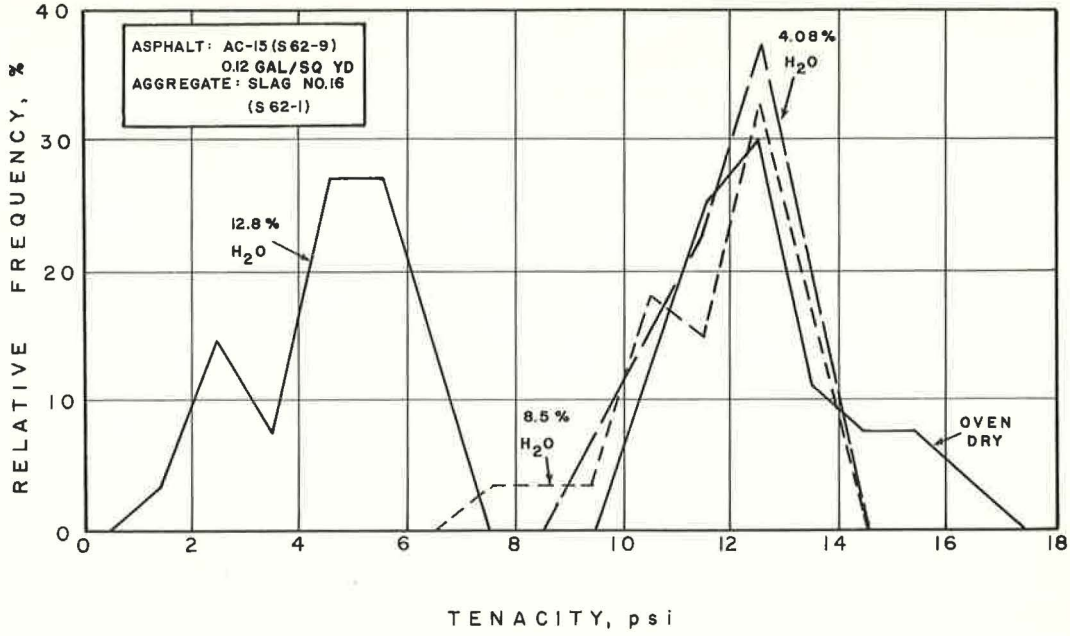

Figure 10. Effect of moisture content of slag aggregate.

Effect of Viscosity of Asphalt

During this investigation, it seemed apparent that the viscosity of the asphalt had a considerable influence on the value of the tenacity measurement. Accordingly, it was considered desirable to investigate exactly how this viscosity might influence the results. Tests were run at temperatures up to 140 F and results showed a rapid decrease in the tenacity value (Fig. 11). All tests above 73 F were performed in a special constant temperature room in which the operator actually aged the samples and performed the measurements at the test temperature (92, 104, 122, and 140 F). The

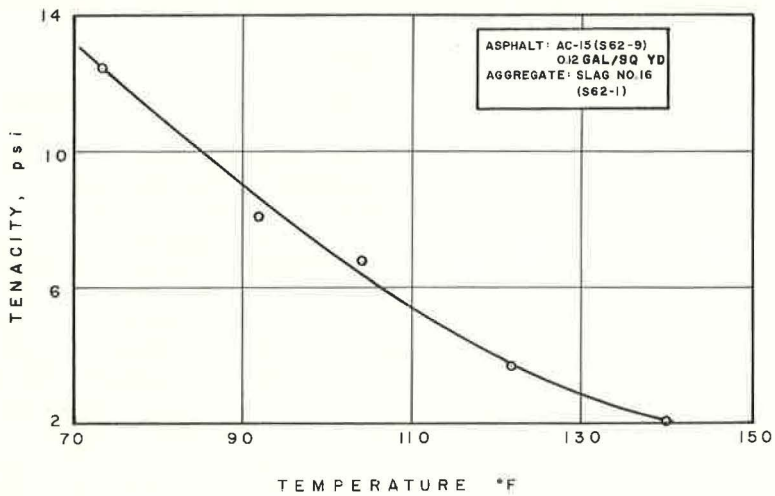

Figure 11. Influence of test temperature on tenacity value.

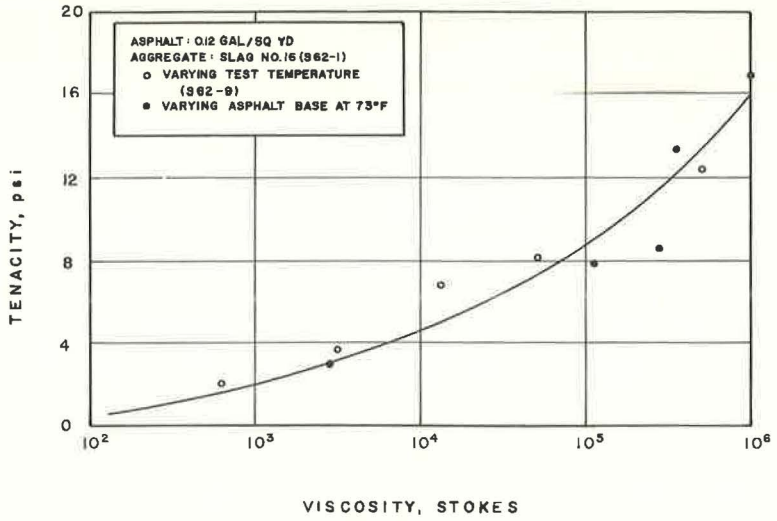

Figure 12. Relation between tenacity and viscosity for several asphalt-aggregate systems.

operator was able to remain in the room at 140 F for the time necessary to perform the test because the humidity in the room was very low. In each of these cases, at least 24 samples were run at each temperature.

The results indicated that the viscosity of the asphalt greatly influenced the tenacity value; accordingly, a chart was made up, as shown in Figure 12, in which the tenacity values at different temperatures are plotted against the viscosity of the asphalt AC-15 (S62-9) at the same temperatures. In addition, as indicated by the solid dots, data were also included for some additional asphalt base materials having a different range of viscosity from the AC-15 used in most of the work reported here. These different asphaltic materials ranged from a soft fluid Gulf Coast naphthenic residuum to a Florida AC-8 asphalt cement. The line drawn in Figure 12 represents an estimated smooth curve through all of the data that were available. The viscosity data at different temperatures for the asphalt cement AC-15 used in most of the experiments were obtained by plotting experimental data on the standard ASTM viscosity chart and reading off the values at the temperatures used for the tenacity test measurement.

TABLE 5

EFFECT OF AGING ON TENACITY[a]

Measurement	Roadbed Age			
	2 Hr	22½ Hr	92 Hr	170 Hr
No. of samples	27	9	9	9
Mean tenacity at 73 F, psi	12.5	16.3	19.4	20.1
Std. dev., psi	1.48	1.7	0.58	1.6
Coeff. of variation, percent	11.8	10.7	3.0	10.1

[a]Asphalt S62-9, 0.12 gal/sq yd; aggregate, slag No. 16 (S62-1).

Influence of Aging

There was some indication that the test values were affected by the length of time between the preparation and the testing of the samples. This phenomenon was not totally unexpected since it is well known that there is an aging effect on asphalt in many physical tests because of the colloidal nature of the asphalt which sets after it has once been melted. Apparently this effect has also shown up in this tenacity test. To obtain quantitative data on the influence of aging, certain experiments were run as indicated in Table 5.

Samples aged up to 170 hr displayed a steady increase in the tenacity value which, when plotted against the log of time,

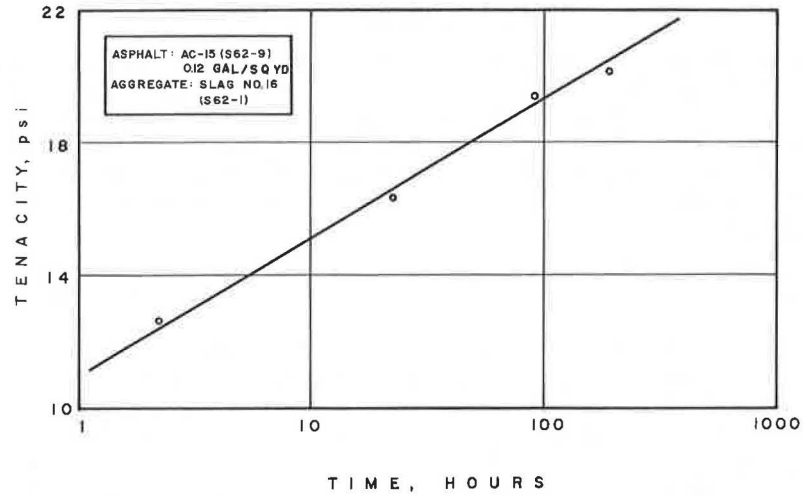

Figure 13. Change in tenacity value with aging of samples.

showed essentially a straight line (Fig. 13). For these samples, as indicated in Table 5, the number of samples was somewhat limited because the quantity of materials was limited. However, the trend is significant and is perhaps one of the most important results obtained in this study. If the correct relationship between time and tenacity value is a semilog plot as shown, the tenacity value increases with aging at a rate which decreases as an inverse function of time.

Variance for Two Operators

A brief survey was made of the effect of using two different operators for performance of the tenacity test. The results are given in Table 6. The data in the table include results for a new sample for AC-15 (S62-9) which is compared with the results obtained on the AC-15 used for the earlier work. As noted earlier, the viscosity of the asphalt had an appreciable effect on the results and, therefore, any variation in the viscosity of the asphalt for a given asphalt cement specification would be expected to affect the tenacity value. The range of data shown for S62-9 with two operators was from 12.5 to 13.9 psi, which is considered an acceptable agreement. Refinements of the test procedure probably could reduce this difference, but no further work was done in this direction.

TABLE 6

COMPARISON OF DATA BY TWO OPERATORS[a]

Measurement	Asphalt S59-16, Operator A	Asphalt S62-9	
		Operator A	Operator B
No. of samples	51	27	50
Viscosity at 77 F, megastokes	0.33	0.32	0.32
Mean tenacity at 73 F, psi	13.1	12.5	13.9
Std. dev., psi	0.88	1.48	2.34
Coeff. of variation, percent	6.7	11.8	16.8
95 percent confidence limits for mean, psi	12.8	11.9	13.4
	13.4	13.1	14.5

[a]Asphalt AC-15, 0.12 gal/sq yd; aggregate, slag No. 16 (S62-1).

CONCLUSIONS

The studies conducted on the tenacity of aggregate according to the procedures used in this research have resulted in the following conclusions and inferences. Not all of the data have been reported here, but the major points are covered and indicate some of the problems involved in developing a laboratory test suitable for evaluating mineral surface treatments with respect to the tenacity with which the aggregate is held. In general, these conclusions confirm the work of Benson and Gallaway (2) whose evaluations were made by a different procedure.

1. The tenacity test as developed appears to give a quantitative measure of the retention force holding the aggregate, but the data are subject to a relatively high variance.
2. There is a complex interrelationship among the variables influencing the tenacity with which the aggregate is held; any of these may be a critical factor in a particular evaluation. Based on the results for Miami limestone and slag, which are somewhat different in surface characteristics, it appears that the type of aggregate is not too critical a factor.
3. A moisture content below a certain threshold value of approximately 8 percent did not appear too critical, but since this was based on slag No. 16, such a generalization should be used with caution.
4. A generalized relationship among tenacity and viscosity, where the viscosity is altered either by changing the temperature or by changing the asphalt, has been shown based on the results for a single aggregate.
5. The variance for the tenacity test as now run shows a high value with different operators, although it is believed that this could be reduced by refinements of the test procedure.
6. A definite relationship between the tenacity value and the aging of the samples before testing was indicated. It was shown that even for short periods of time there was an appreciable effect on the tenacity value. This might be one of the most important considerations in reducing whipoff and one of the most important conclusions of this research. Thus by prohibiting traffic for somewhat longer periods during general surface-treatment operation, it might be possible to reduce the whipoff if the results of this research can be translated into field performance.

REFERENCES

1. Benson, F.J. Seal Coats and Surface Treatments. Purdue Eng. Ext. Dept., 44th Ann. Road Sch. Proc. Bull. No. 95, 1958.
2. Benson, F.J., and Gallaway, B.M. Retention of Cover Stone by Asphalt Treatments. Texas A and M Univ., Texas Eng. and Exp. Sta. Bull. No. 133, 1953.
3. Hank, R.J., and Brown, M. Aggregate Retention Studies of Seal Coats. Proc. AAPT, Vol. 18, p. 261, 1949.
4. Herrin, M., Majidzadeh, K., and Marek, C. Surface Treatments—Summary of Existing Literature. Univ. of Illinois, Illinois Coop. Highway Res. Prog., Ser. NP-2, 1963.
5. McLeod, N.W. Basic Principles for the Design and Construction of Seal Coats and Surface Treatments with Cutback Asphalts and Asphalt Cements. Proc. AAPT, Vol. 29, Suppl., 1960.
6. Nevitt, H.G. Aggregate for Seal Coating. Proc. AAPT, Vol. 20, p. 343, 1951.

Appendix

TEST PROCEDURE

This is an abbreviated statement of the test procedure used in obtaining the results reported in the paper. To conserve space, not all of the details of the procedure have been included.

Test Equipment

A simulated roadbed of $\frac{1}{8}$-in. thick aluminum plate is made, having the dimensions of 15.5 by 6.23 in. A steel form surrounding the edges of the roadbed has steps corresponding to specific spread quantities of asphalt, assuming that the asphalt has a density of unity. These steps are used as guides for a doctor blade so that the proper amount of asphalt is retained on the roadbed. The roadbed will take three molds approximately 4 in. in diameter with an inside cross-sectional area of 12.8 sq in.

Preparation of Roadbed

The clean tared test plate is heated to about 375 F, and sufficient asphalt to provide 30 percent excess of the desired spread quantity is heated to about 300 F and poured on the plate. The plate is manipulated to spread the asphalt uniformly over the surface and then the assembly is permitted to cool. When the plate is cooled to about 110 F, a heated doctor blade is used to wipe off the excess quantity of asphalt so that the desired spread quantity remains on the plate. The plate and asphalt are weighed and the weight of asphalt is recorded.

While the asphalt is still warm, a properly dried quantity of aggregate sufficient to give a 20 percent excess over the desired spread quantity is spread over the asphalt surface. After cooling, a 1-in. thick foam rubber mat is placed on the aggregate and the entire assembly pressed at about 15 psi. Excess aggregate is shaken off by a wrist-snapping action and the plate is again weighed to determine the amount of aggregate retained. Four-inch molds are then arranged down the center line of the plate and pressed into the roadbed by means of a press.

Preparation of Bonding Material

Hydrocal A-11 or B-11 quick-setting cement (U.S. Gypsum Co.) is used as a bonding agent to bind the aggregate to the molds. The material is prepared by thoroughly mixing 125 gm of cement and 67 ml of water for each mold to be prepared and pouring the slurry into the mold. The aggregate should be completely covered. The completed roadbeds are placed at a desired test temperature and allowed to stand for about 1.5 hr.

Test Conditions

The normal testing of the tenacity was carried out at a temperature of 73 F, using a Scott tensile tester with a pulling head speed of 11.3 in./min. In most cases, the tenacity test used an asphalt spread quantity of 0.12 gal/sq yd and an aggregate spread quantity of 0.10 cu ft/sq yd which are the minimum spread quantities specified by the Florida State Road Department for this type of treatment with the aggregate used.

In general, three plates of nine molds were run in one group and three of these groups were run in 1 day to give a total of 27 test values, provided none of the mold and bonding setups were defective. Twenty-seven values were considered sufficient for a statistical analysis.

Comments

The desired spread quantity of approximately 0.10 cu ft/sq yd was sought in these experiments, but it turned out the actual value was about 10 percent less as reported in some of the tables.

The spread quantity of asphalt, theoretically, is the amount filling the spaces between the aggregate particles up to a thickness or embedment t. The total voids

volume, therefore, is A·t, where A is the total area over which the aggregate is spread.

As shown in Figure 14, the Kearby embedment chart indicates the fraction of total embedment that should be used for an average mat thickness t in inches. This is a design chart to determine the amount of asphalt to be used for aggregates of different sizes, since the size of the aggregate determines the average mat thickness t. The average mat thickness is computed from Eq. 2, which follows, or from some physical measurement of the average particle size of the aggregates.

The following information relates the embedment and the amount of asphalt that should be used for a given operation.

1. Embedment is that fraction of the average mat thickness that should be filled with asphalt or bitumen. This is determined empirically as a function of the average mat thickness t using the chart in Figure 14.
2. Spread quantity of aggregate, S:

$$S = S'/D_L, \text{ cu ft/sq yd} \quad (1)$$

where S' is spread quantity (lb_m/sq yd) and D_L is loose-packed density (lb_m/cu ft).

3. Average mat thickness, t:

$$t = 1.33S = 1.33S'/D_L, \text{ in.} \quad (2)$$

also sometimes given as $t = \sum G_f d_f/100$ in. where G_f is percent of mean size d_f from sieve analysis.

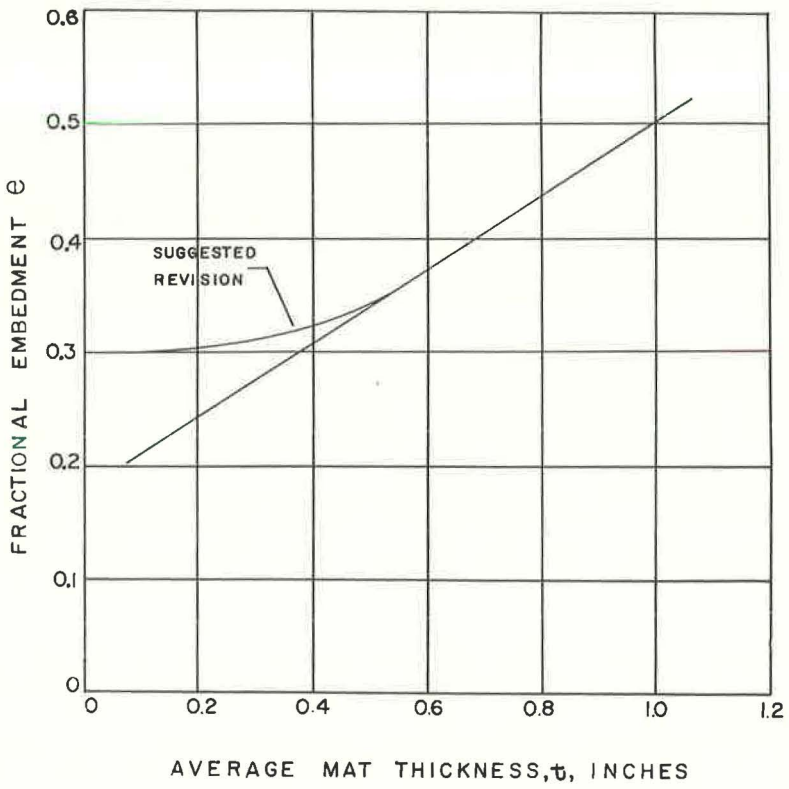

Figure 14. Kearby embedment chart (2).

4. Spread quantity of bitumen or asphalt B:

$$B = 5.60etV = 5.60et\,(1-D_L/D_A),\ \text{gal/sq yd} \quad (3)$$

where V is total void space in the loose-packed aggregate, e is fractional embedment, and D_A is apparent density of aggregate equal to 62.4 times its specific gravity (lb_m/cu ft).

5. Material weight for area A (sq yd):

$$wt = Bp_bA = \text{lb of bitumen} \quad (4)$$

$$wt = Sp_aA = \text{lb of aggregate} \quad (5)$$

where p_b is lb/gal for bitumen and p_a is lb/cu ft for aggregate randomly packed.

Effects of Mineral Fillers in Slurry Seal Mixtures

WILLIAM J. HARPER, RUDOLF A. JIMENEZ and BOB M. GALLAWAY
Respectively, Assistant Research Engineer, Associate Research Engineer, and Research Engineer, Texas Transportation Institute, Texas A&M University

Slurry seal coats have become useful in maintenance operations during the past few years; however, technology has lagged construction knowledge. Present specifications for slurry seals generally constitute an empirical proportioning of components rather than a design. The primary objectives of this research were (a) to determine the effect of mineral filler (a common additive) and residual asphalt content on the slurry seal mixture, (b) to evaluate a new slurry seal testing machine, and (c) to develop a method of design.

A method was for developed estimating the optimum emulsion content so that filler effects could be studied at the same level of design. Operating and testing procedures were carefully evaluated for applicability, and the variables of this testing procedure were standardized for the ensuing slurry seal research program. The objectives were evaluated from the test results and from visual inspections of the specimens. The test variables, abrasion, shoving and relative thickness, were correlated with a visual rating system. The data show that: (a) abrasion is the best measure to consider when evaluating a slurry seal mixture; (b) limestone dust and cement were better fillers for use with Rockdale slag aggregate; (c) cement and fly ash were more suitable with concrete sand mixtures; and (d) the design equation for predicting the optimum residual asphalt content was valid for slurry seal mixtures when tested in the Young wet track abrasion device.

•A SLURRY SEAL is a mixture of fine aggregate, emulsified asphalt, and water. Initially, the consistency of the mixture is low so that it can be spread easily in thin layers on the surface of an existing pavement or on a prepared base. Slurry seal mixtures of proper consistency are pourable, free flowing, and self-leveling. After placing, the water evaporates causing the emulsion to break, and the remaining mixture is a relatively durable, skid-resistant coating resembling asphaltic concrete in appearance.

A slurry seal coat has excellent sealing properties because of its low initial consistency. This sealing property was first utilized extensively for roadway work by the County of Los Angeles, Calif., in 1955, although the use of slurry seals had been known since the 1930's (1). Since then, a great interest has developed, and slurry seal coats have become useful in maintenance operations.

However, slurry seal technology has lagged behind construction; hence, the need for a rational design procedure and evaluation method has become paramount. Present specifications for slurry seals are based on the experience of the construction engineer and constitute an empirical proportioning of the components rather than a design. The current practice among engineers and contractors is to prepare a mixture in accordance with these specifications, using local materials. In many cases, a mineral filler, usually portland cement, is added to "improve" the slurry seal mixture.

Since experience has been the basis for the design of slurry seals, a primary purpose of this research was to determine the effect of mineral fillers on the mixture, and a secondary objective was to evaluate a method of slurry seal design.

Paper sponsored by Committee on Bituminous Surface Treatments.

The general approach was to develop a method for estimating the optimum emulsion content so that the filler effect could be studied at the same level of design. Accordingly, a method of testing was adopted. Operating and testing procedures were carefully evaluated to determine if the tests were applicable to this study, and the variables of this testing procedure were standardized for the ensuing slurry seal research program. The objectives were evaluated from the test results and from visual inspections of the specimens.

SLURRY SEAL CONSTRUCTION

Purpose

The primary purposes of a slurry seal are to rejuvenate old and weathered asphaltic pavements, to fill cracks and small depressions, and to prevent moisture and air from entering the pavement (1). Slurry seal was used as a crack filler in the 1930's, and this property is still useful. As an illustration of the relative effectiveness of slurry seal coats, Zube (2) shows that they can reduce the water infiltration of pavements from 750 to 25 ml/min for a given area.

It has also been observed that a seal coat of this type will completely fill cracks in the pavement, whereas in a conventional chip seal coat, the aggregate will often bridge the cracks (3). In the same manner, small depressions and pop-outs will be filled and leveled.

Applications

Streets and Highways. —Slurry seal coats are used on streets and highways for the purposes discussed. In general, slurry seals are applied to existing pavements of asphaltic concrete or to surface treatments. They have also been applied to portland cement concrete pavements to improve the skid resistance and riding qualities of the surface. A slurry seal coat does not increase or improve the strength of the pavement structure.

Slurry seals have been used for street maintenance in Las Vegas, N. M. A continuous-type mixer was employed for this project, and the slurry seal coat was placed at the rate of 2,000 sq yd/hr. The slurry seal mixture contained 1 to 2 percent portland cement, 10 percent water, and 18 percent emulsion, based on the weight of dry aggregate (4).

The application rate for slurry seals used for street and highway work usually varies from 3 to 15 lb/sq yd depending on the thickness desired and the intented purpose of the coat.

Airport Runways. —One of the major problems in resurfacing an airport runway or apron is the time factor. Many large commercial and military installations cannot make costly shutdowns for normal resurfacing maintenance. Slurry seals have been used effectively in these instances because large areas can be resurfaced in relatively short periods of time. Another advantage is that no loose stones remain on the runway and shoulders to be picked up by jet engines.

The application rate for airports will generally be a little heavier than for streets and highways, probably about 10 to 14 lb/sq yd. But here again, the desired thickness and type of application are the controlling factors. When anionic emulsions are used, the greater thicknesses will increase the curing time; therefore, cationic emulsions are recommended for use in airport construction.

Parking Lots. —Slurry seal coats have been widely used on parking lots because of the speed and economy of the operation. The rate of application for these surfaces will usually be the same as that for streets and highways.

New Construction. —The slurry seal coat is generally considered to be a maintenance measure to resurface older pavements; however, it has been applied directly to the prepared base of new construction projects. A 3-year-old city street of this type was inspected in Waco, Texas, and was found to be in good condition.

Slurry seals, when used in this manner, are spread in one or more applications depending on the thickness desired; however, if more than one application is to be made, the first must be properly cured before any succeeding layer is placed.

Bridge Decks. —Concrete bridge decks have been paved with slurry seal coats to protect the concrete from de-icing chemicals used during the winter months. This covering is usually applied in the northern regions where these chemicals are used extensively. One of the major advantages of slurry seal for this purpose is that the thin application will not increase the dead load on the bridge or raise the grade line appreciably; hence, the effective height of the curbs will remain the same. Also, successive applications can be placed at the required maintenance intervals that will level the wheelpath without increasing the thickness of cover.

Rumble Strips. —Thicker applications of slurry seal have been used experimentally in the form of rumble strips and for the protection and delineation of highway transitions and medians. This is a mixture of coarse aggregate (½ in.) in a matrix of slurry seal; it can be formed and placed in a manner similar to that of portland cement concrete. Experimental strips have been placed with thicknesses up to ¾ in.

Color. —Although they are still in the experimental stage, colored slurry seals have been successfully placed. These applications have been on small test strips, parking lots, and driveways. Colored slurry seals have a potential in the field of traffic engineering as a type of lane delineation at interchanges.

These slurry seals are made with emulsified resins instead of asphalt, which accounts for their slower development. At the present time, the cost of a colored slurry is approximately 5 or 6 times that of a conventional slurry seal coat.

Methods of Placement

Slurry seals are mixed for placement on the roadway by the batch and continuous feed methods. When processed by the batch method, the mixture is usually made in transit-mix trucks enroute to the jobsite. After mixing, the slurry seal in placed by pouring the mixture in a spreader box pulled by the truck.

The spreader box is approximately 10 ft wide and 8 ft long with an adjustable gate near the end. Placement of the slurry seal proceeds as the spreader box moves forward. The mixture flows under the gate at the predetermined lane width and is struck off to the specified thickness by a squeegee attached to the box. The consistency of the slurry seal mixture at the time of placement should be such that it will flow in a wave approximately 2 ft in front of the strike-off squeegee (1).

The quantities for a typical batch of slurry seal are 25 gal of water and 47 gal of emulsion for each ton of dry aggregate (1). However, the quantities will vary with the nature of the aggregate and the desired consistency of the mixture.

The continuous feed mixer may be one of several patented devices. These are usually self-propelled units with storage bins for the emulsion, water and aggregate. The raw materials are fed continuously into the mixer, and the slurry seal mixture is discharged into an attached spreader box similar to the one already described.

Slurry seals may also be placed manually. In this case, the slurry mixture is spread by a hand squeegee in areas that are inaccessible to the spreader box. Slurry seal is also mixed in small mortar mixers and hand placed for patching operations.

Problems in Slurry Seal Construction

The problems associated with slurry seal coat construction lie in the general areas of mixing and placing. In mixing the slurry seal, the aggregates may ball or the emulsion may break. Segregation, streaking, and surface preparation are the primary considerations when placing the slurry seal.

Mixing Problems. —The mixing time of the slurry seal mixture is important because, during mixing, the emulsion must coat the aggregate particles and the desired consistency must be achieved. However, if the mixing time is too long, the excessive rolling and tumbling of the mixture will cause an early break of the emulsion (1). When this happens, the mixture will retain the brown emulsion color but will have a consistency similar to that of stiff concrete. The slurry seal mixture cannot be placed in this condition, and the addition of more water will not improve the consistency.

Other factors causing the emulsion to break in the mixer are the amount of fines or mineral fillers and the chemical activity of these powders. Large amounts of mineral powders and particularly powders with high chemical activity should be avoided.

A different problem related to mixing of slurry seals occurs when dry fines or mineral powders come into contact with the emulsion. Occasionally, there is a tendency for these powders to form balls or lumps, which may reach the size of baseballs. These balls are coated with emulsion on the outside, but when broken open consist of dry uncoated aggregate. Balling can be eliminated by blending the dust and mineral fillers with the aggregate before it is introduced into the mixer (5). Another preventive measure is to wet the aggregates before they are mixed with the emulsion; however, if too much water is added initially, the resulting slurry seal will have a very low consistency and cannot be properly placed and manipulated.

Placing Problems. —The surface of the existing pavement must be carefully prepared before the slurry seal is placed. This is done by thoroughly cleaning and wetting the old surface, thus assuring a good bond of the slurry seal coat. The existing surface is wet immediately ahead of the sealing operation with a fog spray of water, or a diluted emulsion tack coat may be used if the old surface is particularly absorptive (3, 5).

Another problem is placing the slurry mixture is segregation of the aggregate, which will result in loss of adhesion. If the mixture is too fluid, the larger, heavier aggregate will segregate or settle, leaving the smaller particles and emulsion in the upper levels of the exposed surface. Since the larger aggregate will not have enough binder, the seal coat will lose its adhesion and will fail. Segregation of the aggregate and emulsion can be controlled by using a well-graded aggregate and controlling the water and, thereby, the consistency (1). Usually the gradation can be improved by the addition of a mineral filler to the aggregate; however, this will vary with local aggregates and conditions.

Still another problem in the placement of slurry seal mixtures is the streaking of the seal coat surface by oversized aggregates. If the diameter of any aggregate is larger than the depth of the seal coat, it will be caught under the strike-off squeegee and leave a long streak in the surface. This can be prevented by screening the aggregate before it enters the mixer (1).

PREVIOUS DESIGN METHODS

Existing Specifications

In general, the design of slurry seal mixtures is an art. The present design methods are based on the experience of engineers and contractors and on the performance of existing slurry seal coats. Since conditions and materials vary with time and locality, a number of general specifications have resulted from these experience methods.

The Asphalt Institute enumerates the design requirements as aggregate gradation, emulsion content, and consistency of the mixture; however, the design is regulated to comply with the consistency requirement (6). For example, this specification gives a range of emulsion content of 20 to 25 percent by weight of the dry aggregate and a water content of 10 to 15 percent. The water content of the mixture should include the water in the emulsion and in the aggregates. The specification also recommends that trial batches of the slurry seal mixture be made with the materials to be used on the job to insure that the proper proportions and consistency have been maintained. The aggregate gradation recommended in this specification is given in Table 1.

TABLE 1

SPECIFICATIONS FOR AGGREGATE GRADATION

U. S. Std. Sieve Sizes	% Passing		
	Asphalt Inst.	Amer. Bitumuls	TTI[a]
3/8 in.	100	100	100
No. 4	100	100	85-100
No. 8	100	80-100	65-90
No. 16	55-85	50-90	45-70
No. 30	35-60	30-60	30-50
No. 50	20-45	20-45	18-30
No. 100	10-30	10-25	10-20
No. 200	5-15	5-15	5-15

[a]General application.

Field Adjustments

The final emulsion content of the slurry seal mixture is selected from the trial mixtures; however, since this selection is generally the result of limited tests, the

mixture may be adjusted by the project engineer for unusual conditions encountered in the field. The emulsion content may be increased if the mixture appears to be dry and porous, that is, if the slurry seal contains an insufficient quantity of residual asphalt.

The consistency of a slurry seal mixture is estimated in the laboratory, but it is controlled by field adjustments. The basic method of controlling the consistency is the addition of water to the mixture, but if too much water is added the consistency will be low and segregation may occur. The consistency of a slurry mixture is difficult to measure because the available methods seem inadequate. Some of the methods considered for possible use were slump test, penetration test, and flow devices. Subsequently, the consistency of the slurry seal mixture is not determined, but the workability of the mixture is controlled in the field by experienced operators and in the laboratory by the feel of the mixture.

Workability is controlled in the field by regulating the water content of the mixture. The workability may be improved in some cases by the addition of 1 or 2 percent mineral filler. Normally, portland cement is used for this purpose because of its availability. However, caution should be observed when adding these fillers because they may cause the emulsion to break in the mixer or produce a dry mixture.

Difficulties Resulting from Improper Design

The most important factor in the design or proportioning of a slurry seal mixture is the selection of the proper emulsion content for the particular aggregate involved. If too much emulsion is used, the resulting seal coat will be sticky and will bleed; if too little emulsion is provided, the pavement will ravel and wear excessively. These same difficulties arise in some cases where the correct amount of emulsion was used initially, but the existing surface absorbed the asphalt, resulting in a low residual asphalt content in the slurry seal.

Another design factor to consider in preventing difficulties is that of gradation. Mixtures low in fines or material passing the No. 200 sieve will generally segregate and result in raveling and excessive wear, whereas those with excessive material passing the No. 200 sieve will be brittle and develop shrinkage cracks as the water evaporates from the mixture (5). The aggregates used for slurry seal mixtures must be free of clay and other deleterious materials. Most specifications require a minimum value of 40 for the sand equivalent test. The aggregate should consist of sharp angular particles to provide a skid-resistant surface.

Objectives of Proposed Research

The development of a rational design procedure for the optimum emulsion content of a slurry seal mixture is an important need in slurry seal technology. This research will attempt to develop such a design method so that the results of this study, including abrasion, shoving, and relative thickness of the specimen, can be examined at the same level of design.

Once the design method for optimum emulsion content had been established, the evaluation of the type and amount of mineral filler was made for each of the two aggregates used in this study. These aggregates were Rockdale slag aggregate and a concrete sand; the mineral fillers studied were Rockdale fly ash, portland cement, and limestone dust.

NEW DESIGN METHOD

Basis of Design

The design procedure developed in this thesis was conceived by Jimenez and is known as the Surface Area Method for Design of Slurry Seal Mixtures. This method is based on the amount of asphalt cement required to coat the aggregate particles to a specified film thickness, and the amount of asphalt necessary to satisfy the absorptive characteristics of the aggregate. (The asphalt cement in the voids of the mixture was not considered, except indirectly by use of the film thickness.) Absorption of asphalt by the existing pavement is another factor influencing the asphalt content, but it does not

enter into these calculations. The pavement absorption is corrected in the field as previously described.

The amount of asphalt to meet the film thickness requirement was calculated from the surface area of the aggregate which was determined in accordance with the California centrifuge kerosene equivalent (CKE) (7). The correct gradation was computed from a combination of the aggregate and the amount of the mineral filler under consideration. Using this gradation and the factors from the CKE test, the surface area was computed in units of square feet per pound of dry aggregate. The surface area thus determined was corrected for the specific gravity of the material in much the same manner as in the original CKE test. For the purpose of this design method, the calculated surface area was corrected by the ratio of the apparent specific gravity of the material in question to 2.65 as follows:

$$\text{Corr. SA} = \text{SA} \times \frac{\text{SG}}{2.65} \quad (1)$$

where

Corr. SA = corrected surface area, sq ft/lb;
SA = computed surface area, sq ft/lb; and
SG = apparent specific gravity of the aggregate.

The value of 2.65 was chosen as a basis for correction because it represents a good average for most fine aggregates.

The asphalt film thickness used in this procedure is one of the principal design variables. The design equation is presented so that the user may substitute into the equation a film thickness based on his own experience. A film thickness of 8μ was chosen for use in this research because it resulted in computed asphalt contents that correlated very closely to asphalt contents used with good results in field mixtures of nearly the same aggregate combination. The selection of this value for film thickness was also influenced by the fact that slurry seals may be considered as a form of asphaltic concrete, and data (8) have shown that 8μ is a reasonable film thickness for asphaltic concrete.

Another important design consideration is the absorptive characteristics of the aggregate. The absorption of the aggregate may be determined by the CKE test, the ASTM test for water absorption, or in any other suitable manner, but the absorption for the liquid used must be correlated to the absorption of asphalt by the same type of aggregate. The CKE test (7) was used to determine the aggregate absorption in this research, and the procedure is outlined in that test method. The amount of asphalt absorbed is assumed to be the same amount as the kerosene retained by the aggregate.

Since the design factors have been established, the residual asphalt content can be computed. The residual asphalt is the amount of asphalt cement remaining after the emulsion has broken and the water has evaporated. The equation for predicting the optimum residual asphalt content is as follows:

$$\text{RA} = 0.0002047 \times \text{SG}_\text{A} \times \text{t} \times \text{Corr. SA} + \frac{\text{KA}}{100} \quad (2)$$

where

RA = residual asphalt, lb/lb dry aggregate;
SG_A = specific gravity of residual asphalt;
t = film thickness, μ;
Corr. SA = corrected surface area, sq ft/lb dry aggregate; and
KA = kerosene absorption, percent.

An example of this computation and a typical data sheet are shown in the Appendix.

The equation coefficient consists of the conversion factors for the units of the components of the equation. The coefficient used in this research was 0.000209, based on

a specific gravity of the residual asphalt of 1.02. The value of specific gravity was assumed at the beginning of the project, and all of the emulsion contents were calculated using this assumption. At the conclusion of the slurry seal testing program, the actual specific gravity of the residual asphalt was found to be 1.03. It was determined that this variation in specific gravity would not significantly affect the optimum emulsion content.

The equation will yield an estimate of the designed optimum residual asphalt content in pounds per pound of dry aggregate, or this may be taken on a percentage basis as the percent residual asphalt of the dry aggregate. If the amount of residual asphalt in the emulsion to be used is known, 67.0 percent in this case, the emulsion content in percent can be easily calculated as a percent of the dry weight of the aggregate.

Testing Device

After the design of the slurry seal mixture has been completed, specimens must be made and tested so that the design can be evaluated and compared to others that have been field proven. The purpose of the testing device for this research was to compare the optimum emulsion content with other amounts and to compare the type and amount of mineral fillers at these emulsion contents.

The testing device for slurry seals was developed by Young Brothers of Waco, Texas, and is called the Young wet track abrasion device (Fig. 1). The apparatus is constructed so that the testing head is mounted on an inclined axis. When the machine is in operation, the testing head rotates and imparts a gyratory shearing action to the surface of the specimen. In addition, it creates a sucking or lifting effect similar to that of a tire rolling on the surface of the pavement.

The testing head is a hard rubber (durometer value of 50) annulus approximately 2 in. high with an outside diameter of 3⅞ in. and an inside diameter of 1⅜ in. The head is held by a steel positioning jacket so that it may be raised or lowered on the inclined shaft. For the purpose of this research, the head was located so that its speed of rotation was 6.6 rpm.

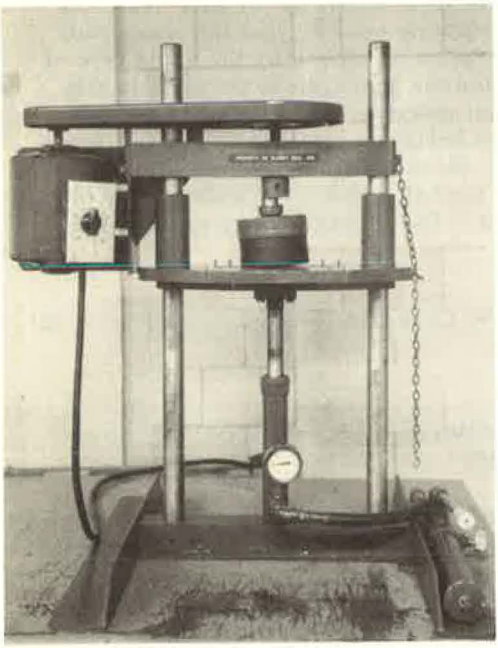

Figure 1. Young wet track abrasion device.

Testing Procedure

Operating and testing procedures for the Young wet track abrasion device, developed by Slurry Seal, Inc., were analyzed to determine their applicability to this research and the extent to which they should be adopted. The test variables examined were time, temperature, pressure, and specimen thickness. The study of these variables was conducted before the method for numerical evaluation of the tested specimens was finalized; therefore, the evaluation was made from a visual examination of the specimens on completion of these tests, and this rating of specimens was based on the experience of the operator.

Condition of Test. —To establish a standard condition of testing, the specimens were soaked in water and then tested under water. It was believed that testing under water would be the worst condition imposed on a slurry seal and would also help keep the surface of the specimen free of any abraded material. Since the specimens were tested in a water bath, the temperature could be more easily controlled.

Temperature. —The temperature at which the test is conducted has a very definite influence on the results of the experiment. A series of tests was conducted at various temperatures using a slurry seal mixture field proven by 4 years of good performance. The effects of temperature were determined by testing 6-in. diameter specimens at 56, 75, 100, and 135 F while holding the other test variables constant. The slurry seal mixture used for these experiments was a combination of 70 percent Rockdale slag aggregate and 30 percent field sand at an estimated optimum residual asphalt content of 10.7 percent. In fact, this slurry seal mixture was used as a standard for the test procedure study.

The test specimens at 100 and 135 F were slightly abraded, and a considerable amount of material was displaced from under the testing head and shoved outward and upward at the outer edge of the tested surface. This behavior will hereafter be termed shoving. At the lower temperatures, there was no evidence of shoving or abrasion in the tested area. Since the two lower temperatures were considered reasonable choices for test controls, the 75 F temperature was selected because of the ease with which it could be maintained and because it agrees closely with temperatures used in other asphalt testing procedures.

Pressure. —The wet track abrasion device is constructed so that a hydraulic jacking system holds the specimen against the testing head during the test, and a pressure gage is used to determine the pressure on the jack. This gage pressure was used to control the pressure on the specimen. Tests performed at gage pressures of 150 and 200 psi revealed that there was essentially no difference in the resistance of the specimen to pressure. Since the procedure recommended by Slurry Seal, Inc., uses a gage pressure of 150 psi, this value was used for the research.

The average pressure on the specimen was calculated by the basic principles of fluid mechanics in which

$$P_1 \times A_1 = P_2 \times A_2 \qquad (3)$$

where

P_1 = pressure on jack, psi;
A_1 = area of ram, sq in.;
P_2 = pressure on specimen, psi; and
A_2 = contact area of the specimen, sq in.

The gage pressure was a known value of 150 psi and the diameter of the hydraulic jacking ram was 1 in. The contact area of the specimen was calculated as a sector of an annulus after the central angle had been determined. Thus, substituting these known quantities into Eq. 3 yields an average pressure on the specimen of 25.6 psi.

If a triangular pressure distribution is assumed, the maximum pressure will occur at the outer edge of the tested area. Such a pressure distribution did not exist, but the assumption was made to determine the relative magnitude of the maximum pressure. Hence, the pressure at the outer edge of the tested area was calculated to be approximately 38 psi.

Time. —The duration of the test was similarly studied with the emphasis placed on the length of time required to test the specimen. Time trials of 5, 10, and 15 min were employed using the standard mixture and at the temperature and pressure determined. A profile of the specimen surface was determined before and after the test, and the decrease in height and amount of shoving were obtained from these measurements. These calculations indicated that the thickness of the tested area decreased with time. An appreciable amount of shoving was not detected in the 5- and 10-min specimens, but was evident in the 15-min determinations. The greatest decrease in thickness and shoving occurred in the 15-min specimen, and it was concluded that the time should be shorter. The only difference in the 5- and 10-min specimens was the thickness of the tested area. It was felt that the 5-min duration was too short; consequently, the 10-min test period was selected.

Specimen Thickness. —The thickness of slurry seals commonly used in the field varies with the intended purpose, but the maximum is approximately ¼ in. The thick-

nesses considered in this study were 1/8, 3/16, and 1/4 in. Thickness experiments were conducted using the standard mixture with varying conditions of time, temperature and pressure. When these test variables were evaluated and compared at the proposed thicknesses, it was felt that the 3/16-in. specimen would be more suitable as a basis of evaluation than either the 1/8- or 1/4-in. specimens. Moreover, the 3/16-in. thickness is representative of the thicknesses currently used in construction.

Selection of Test Procedure. —The result of the foregoing studies was that the basic procedure outlined by the developers was found applicable to this research. The only additional test control included in the final testing procedure was temperature.

The original specimen size was modified to eliminate the edge effects of the testing head on the slurry seal sample. The specimens used in this study were 6 in. in diameter, whereas the original specimens were 4 in. in diameter. The specimen thickness was increased from 1/8 to 3/16 in. as previously described.

The testing procedures and specimen size adopted for this research are believed to insure adequate and efficient testing of the slurry seal mixture. Summarizing, the slurry seal specimens were 6 in. in diameter and 3/16 in. thick. They were tested in a water bath at 75 ± 5 F at a gage pressure of 150 psi for 10 min in the Young wet track abrasion device.

Another factor influencing the selection of these variables was the possibility of future field correlation. Since the developers have field data on slurry seals tested in a similar manner by this machine, these data may be used for comparison with this research.

MATERIALS

Aggregate

The aggregates used for slurry seal mixtures are usually controlled by specifications based on good field performance. The aggregate gradation recommended by the Asphalt Institute Specification ST-3 (previously discussed) and the gradation limits proposed by American Bitumuls and Asphalt Co. as reported by Kari and Coyne (5) are indicated in Table 1 (6). The gradation suggested by Kari is based on the results obtained from actual construction projects. The gradation recommended by the Texas Transportation Institute (TTI) is based on the maximum density curves derived by Fuller and Thompson (9).

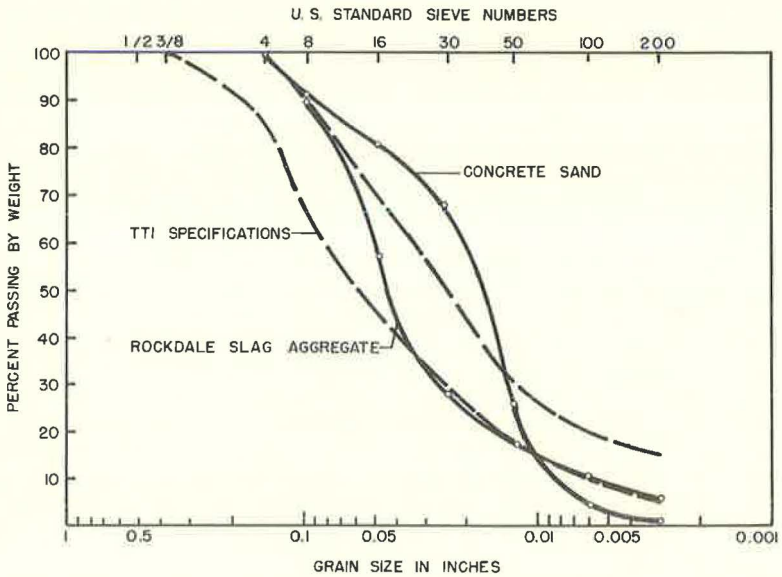

Figure 2. Aggregate gradation.

The maximum density curve was modified in consideration of workability by Jimenez, in accordance with experience gained from field studies.

The aggregates used in this study were Rockdale slag aggregate and a concrete sand. The Rockdale slag aggregate, produced at Sandow near Rockdale, Texas, is a by-product of the lignite burned at the plant as a power source. The specific gravity of this aggregate is 2.90, and the gradation is shown in Figure 2. The concrete sand was from the vicinity of Hearne, Texas. The specific gravity of this material was found to be 2.67, and its gradation is also shown in Figure 2. It appears from these graphs that the Rockdale slag aggregate, for all practical purposes, is within the previously recommended gradation limits, whereas the concrete sand is not. The Rockdale slag aggregate has not been used in the field as a complete aggregate for slurry seal mixtures; however, it appears to be satisfactory for this purpose.

The concrete sand requires an alteration of the particle size distribution before it will meet the recommended gradation. For the purpose of this research, the gradation of the concrete sand was changed to make it identical to the gradation of the slag aggregate. This was done so that the mixtures made from these aggregates could be compared on the basis of particle shape and surface texture, and the effect of asphalt content on these mixtures could be determined when the particle size distribution was held constant.

Mineral Fillers

A primary objective of this study was to evaluate the effect of three mineral fillers in slurry seal mixtures. A specification for mineral fillers, designated by the American Society for Testing Materials (ASTM) as D242-57T, was followed:

Passing No. 30 (590 μ) sieve, 100 percent;
Passing No. 50 (297 μ) sieve, 95-100 percent;
Passing No. 100 (149 μ) sieve, 90-100 percent; and
Passing No. 200 (74 μ) sieve, 70-100 percent.

The three mineral fillers used in this study were Rockdale fly ash, portland cement, and limestone dust with apparent specific gravities of 2.57, 3.03, and 2.74, respec-

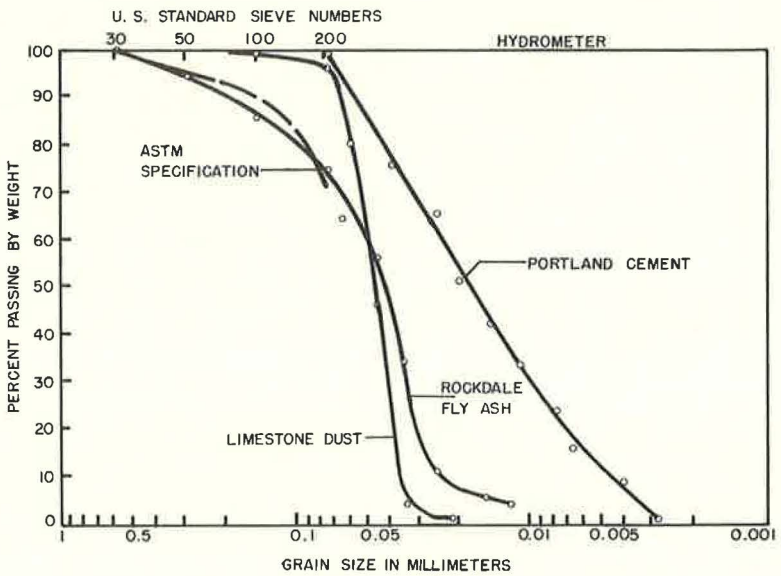

Figure 3. Mineral filler gradation.

TABLE 2

EMULSION CHARACTERISTICS[a]

Test Type	Laboratory Test	Manu. Spec.	
		Min.	Max.
Emulsion:			
Viscosity, Saybolt Furol	—	—	—
50 ml at 25 C (77 F) (sec)	87	30	100
Residual asphalt (%)	67.0	60	—
Settlement, 5 days	—	—	3.0
Demulsibility in 50 ml of 0.10N $CaCl_2$ (%)	—	—	1.0
Sieve test (%)	—	—	0.10
Miscibility in water, appreciable coagulation in 2 hr	—	—	none
Cement mixing test (%)	—	—	2.0
Residual asphalt:			
Specific gravity, 25/25 C (77/77 F)	1.034	—	—
Penetration, 100 g, 5 sec, 25 C (77 F)	80	—	—
Ductility, 5 cm/min, 25 C (77 F)	150+	—	—
Viscosity, 25 C (77 F), megapoises at $S_R = 5 \times 10^{-2}$/sec	1.8	—	—
Soluble in CCl_4	—	98	—
Ash	—	—	1.5

[a]American Petrofina SS-1h.

TABLE 3

EMULSION VISCOSITY BY THE BROOKFIELD VISCOMETER

Spindle No. 2 Speed (rpm)	Brookfield Viscosity (centipoises)[a]
2	2,500
4	1,590
10	828
20	596

[a]At 25 C or 77 F.

tively. The Rockdale fly ash was also a by-product of the burned lignite described previously. The portland cement was a Type I cement obtained locally, and the limestone dust from Pontiac, Ill., was used in the rehabilitation of the AASHO test road in Ottawa. The grain size distribution of each filler is shown in Figure 3. The particle size distribution for the filler passing the No. 200 sieve was determined by a hydrometer analysis. The fly ash is slightly outside the specification limits, whereas the portland cement and limestone dust are well within the specifications.

Portland cement and limestone dust are commonly used in field mixtures as mineral fillers, and it is believed that fly ash can also be used effectively when locally available. The cement and limestone dust are commercially available in almost any locality.

Emulsion

Slurry seal mixtures are commonly made with anionic emulsions, either Type SS-1 or SS-1h. The emulsion used in this research was American Petrofina Type SS-1h produced from a Talco, Texas, field crude. The physical characteristics of the emulsion and residual asphalt are indicated in Table 2. The viscosity of the emulsion was also determined by the Brookfield viscometer using spindle No. 2. The values of viscosity and viscometer speed are given in Table 3.

PREPARATION AND TESTING OF SPECIMENS

Experimental Design

This investigation was conducted with slurry seal mixtures containing combinations of the two aggregates and three mineral fillers at five different emulsion contents. Duplicate test specimens were made for each mixture. A total of 140 specimens were prepared. Mixtures were first prepared using each of the two aggregates with no mineral filler and at the selected emulsion contents. Similarly, mixtures were made containing 2 and 4 percent (by total weight of dry aggregate) mineral filler. These filler contents were selected because 1 or 2 percent is commonly used in the field whereas 4 percent is probably the maximum amount that can be used economically.

The emulsion content of each mixture was based on a specified residual asphalt content. After the optimum residual asphalt content was estimated, the others were chosen at 2 and 4 percent above and below the estimated optimum. These values were selected because this range would include most of the values currently in use, and it was also felt that the sensitivity of the testing device might not detect differences much smaller than 2 percent.

Blending Procedure

Once the number of specimens and the emulsion and filler contents had been selected, the constituents of the mixture were proportioned. A 1,000-gm batch of dry aggregate and mineral filler was prepared for each set of specimens. This mixture was then wetted with a small portion of the mixing water to prevent balling of the fines and breaking of the emulsion. The water added to the aggregate was measured so that it could be included in the total water content of the slurry seal mixture.

The emulsion for one batch was weighed into the mixing bowl which was then transferred to the mixer. The aggregate was added to the emulsion along with enough water to give the mixture the proper consistency. The total mixing time was 2 min, and the constituents were added during the first minute of operation. The total amount of water required was controlled by the operator who judged the consistency of the mixture by experience. Normally, the water content of the slurry seal mixture was about 10 percent by weight of the dry aggregate.

The mixer used for this study was a Hobart C-10 food mixer. A mechanical mixer was preferred over manual methods because it was believed that more uniform results could be obtained and it approached field mixing conditions.

Some difficulty was occasionally encountered. The emulsion would break in the mixer, and the resulting slurry seal mixture had a very stiff consistency. This was particularly evident in the mixtures of concrete sand with fly ash and cement. No trouble was encountered in any of the mixtures containing Rockdale slag aggregate.

Molding Procedure

After the constituents were mixed, they were cast as circular specimens on 7 sq in. steel plates. These plates were thin (approximately 0.05 in.) and were primarily used to facilitate the handling, testing, and removal of the slurry seal specimens.

The specimens were cast using thin steel rings as molds. These molds had an inside diameter of 6 in. and a depth of $^{3}/_{16}$ in. The slurry seal mixture was placed in the mold, and the top was struck off flush to obtain the desired thickness. The molding ring was then removed, and the finished specimen was cured in an oven at 140 F for 24 hr until it reached a constant weight.

Testing Procedure

The cured specimens were tested in the Young wet track abrasion device within 48 hr after removal from the oven. The normal procedure requires the specimens to be tested within 24 hr, but the time was extended to 48 hr because of the large number of specimens.

The testing procedure included compacting the specimens in the abrasion device at normal room temperature, about 75 F. The compaction was accomplished using the

TABLE 4

COMPACTION OF SLURRY SEAL BY TRAFFIC

Time	Density (gm/cu cm)		Voids[a] (%)	
	t = 1/8 In.	t = 3/16 In.	t = 1/8 In.	t = 3/16 In.
Init.	1.48	1.46	36.8	37.6
1 day	2.12	2.12	9.4	8.6
1 wk	2.19	2.21	6.4	5.6
1 mo	2.22	2.25	5.1	3.8
2 mo	2.23	2.26	4.7	3.4

[a]Based on computed maximum theoretical specific gravity of 2.34.

standard procedures described previously; however, the surface of the specimen was protected from the testing head by a steel plate during the compaction process, and the specimen was not compacted under water. Compaction is necessary because a newly placed slurry seal has an extremely high void content. Traffic will compact the mixture in most instances as indicated in Table 4, but areas subjected to high surface shears, such as turning movements, are likely to be torn before adequate traffic compaction can be achieved.

After compaction, the specimens were measured for density and soaked in a water bath at the test temperature for at least 30 min. The testing sequence was such that the maximum soaking period was approximately 1 hr.

On completion of the minimum soaking period, the specimens were tested in the abrasion device under the standard conditions. Observations were made throughout the test to determine if excessive abrasive action occurred. When this was the case, the time that disintegration began was noted as well as the time the specimen had abraded to its full depth.

At the conclusion of the test, the specimen was dried in a 140 F oven to a constant weight, and the unit weight and final surface profile were determined. At this time, the specimens were also rated visually for abrasion, shoving, and relative thickness. From these and other measurements described in the next section, the necessary factors were obtained to evaluate the slurry seal mixture.

MEASUREMENTS AND CALCULATIONS

Measurements

Presently, the most common method of determining the quality of a slurry seal coat is by field inspection or by visual examination of a specimen. Kari and Coyne (5) developed a method whereby slurry seal specimens are tested and a wear value is obtained. This is currently the only method available for numerically rating a slurry seal mixture; however, one of the objectives of this research is to establish a better method for rating a slurry seal mixture. The necessary measurements and calculations to rate the slurry seal mixture are presented in the following paragraphs.

Density. —The density of the test specimens was determined initially after compaction and finally at the conclusion of the test. Both the initial and final densities are required to compute the density of the material in the abraded portion of the specimen. This computation is based on the fact that the density after testing is calculated from the final weight divided by the volume after test. This volume has two components: the volume of the unabraded portion and that of the abraded portion. The volume of the unabraded portion may be calculated from the initial conditions if it is assumed that this volume was unchanged by the test. Thus, all of the conditions are known except the volume of the abraded portion of the specimen. Since the volume of the abraded portion can be calculated, the only other factor needed to compute the density of this portion of the specimen is the weight of the material in the tested section. This weight was calculated from the initial condition of thickness, area, and density; however, it was assumed that the only weight change was due to the abrasion of the machine. Hence, the weight of material in the abraded portion is the initial weight of this portion less the abrasion. With these factors known, the bulk specific gravity (SG_t) of the tested portion of the specimen was computed.

Thickness. —The thickness of the test specimen was determined initially when the compaction process was completed. The measurements were made with a dial gage mounted on a stand so that the gage could be positioned horizontally and vertically over the specimen. The measurements were made from a fixed reference, and the thickness was obtained by subtracting the thickness of the steel plate. The initial measurements

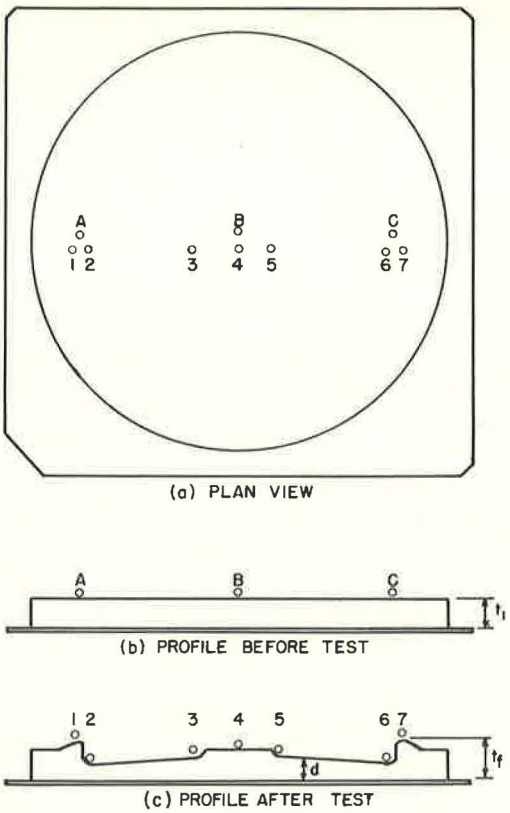

Figure 4. Sketch of typical specimen.

were made on a diameter of the specimen with the thickness determined at the center and 1 in. from each edge. These are shown in Figures 4a and 4b as measurements A, B, and C. The average of these depths was taken as the initial thickness, t_i.

The final measurements were made on the same diameter at locations numbered 1 to 7, and these are shown in Figures 4a and 4c. Measurements at locations 1 and 7 were made at the outer rim of the abraded portion of the specimen where the greatest amount of shoving was present. The average of these measurements was the final thickness, t_f. The measurement at location 4 was not used in this study. Measurements at locations 2, 3, 5, and 6 were taken inside the tested portion as indicated in the figure. The average depth of the specimen at these locations was indicated by the distance, d.

All of these thickness measurements were made at locations that were, in the opinion of the operator, representative of the surface of the specimen. The thickness at each location was the average of several readings taken in the immediate vicinity of that location.

Calculations

Shoving. —The shoving behavior has been described previously. This characteristic is measured by the increase in thickness at the outer edge of the tested surface as a percentage of the original thickness. The computation of the shoving characteristic is

$$S = \frac{t_f - t_i}{t_i} \times 100 \qquad (4)$$

where

S = shoving, percent,
t_f = final thickness, average of 1 and 7, in., and
t_i = initial thickness, average of A, B, and C, in.

Shoving was observed in nearly all of the specimens tested, although it was significantly greater in some of the specimens. The shoving feature is discussed in the following chapter.

Relative Thickness. —The relative thickness, T_R, of a slurry seal specimen is defined as the ratio of final to initial thickness of the test specimen caused by the action of the abrasion device. The volume of the portion of the specimen under abrasion will usually be reduced, and a depressed area of the general shape shown in Figure 4c will be formed. However, this not always the situation because the depressed section did not occur on all specimens. In some samples the abrasive action of the testing head was so great that all of the material in the tested area was worn away, and in other samples there was no compaction or wear at all. Hence, evaluation of the relative thickness must consider the wear on the specimen.

The relative thickness was determined considering the average final depth as a percentage of the initial thickness. This calculation is shown by

$$T_R = (d/t_i) \times 100 \quad (5)$$

where

T_R = relative thickness, percent;
d = final thickness, average of 2, 3, 5, and 6, in.; and
t_i = initial thickness, average of A, B, and C, in.

Abrasion. —The wear or material loss of the slurry seal specimen will be termed the abrasion. This feature is measured as the percent weight loss of the material in the tested portion of the specimen. The weight loss was found by the difference in dry weights as determined in the density measurements made before and after testing. The weight of the material in the abraded portion of the specimen is a function of the area of the annulus (tested area), the initial thickness, and the initial density. The calculation is

$$W_A = 168.8 \times t_i \times SG_i \quad (6)$$

where

W_A = weight of mixture in area to be abraded, gm; and
SG_i = initial specific gravity of specimen.

This calculation is based on the assumption that the area under the testing head remains constant throughout the test. Using this value, the abrasion computation is

$$A = \frac{W_i - W_f}{W_A} \times 100 \quad (7)$$

where

A = abrasion, percent;
W_i = initial weight of specimen, gm;
W_f = final weight of specimen, gm; and
W_A = weight of mixture in area to be abraded, gm.

It is believed that this characteristic is the most important for the purpose of evaluating any slurry seal mixture. The range of abrasion values for this study was from 0 to more than 100 percent. The values greater than 100 arose from the fact that for cases where abrasion was appreciable, the testing head vigorously attacked the outer edge of the abraded area. When this was the case, the previous assumption is no longer valid, but a slurry seal mixture in this condition would not be considered for field use. Therefore, the slurry seal may be rated visually as unacceptable.

ANALYSIS OF DATA

Effects of Filler Content

As outlined previously, slurry seal specimens were made and tested using Rockdale slag aggregate and a concrete sand with 0, 2, and 4 percent Rockdale fly ash, portland cement, and limestone dust. The effects considered were abrasion, shoving, and relative thickness as discussed in the section on the preparation and testing of specimens. The density of the specimens was also studied to obtain a better understanding of the specimens and their behavior during the test; however, the density was not considered a test variable.

A statistical evaluation in the form of an analysis of variance (AOV) was made for each of the test variables including density. The analysis of variance was arranged as

a two-way classification with two observations per combination. All tests were evaluated at the 5 percent significance level, and the two classifications were filler content as columns and residual asphalt content as rows. The AOV disclosed that in many cases there was interaction between the filler content and asphalt content. This indicates that the effects cannot be separated because they are not independent. In addition, the AOV often showed no effects of filler or residual asphalt content on the results; however, the data revealed that there were effects. Further examination of the data showed the variance within the combinations was greater than the variance between the groups; therefore, no effects were indicated by the AOV. Additional information obtained from the statistical analysis was the indication of filler and/or residual asphalt content effects.

The computations of the test measurements and the analysis of variance were made using the IBM 709 computer.

In addition to the statistical analysis, a visual rating system was established so that the slurry seal specimens could be rated as they were tested. Typical specimens were photographed and are included here to provide a basis of comparison for the potential users of this system. The slurry seal specimen with less than 1 percent abrasion, little or no shoving, and a high relative thickness (85 to 100 percent) was rated as excellent (Fig. 5). Specimens with 2 to 5 percent abrasion, little shoving and a medium relative thickness (60 to 85 percent) were classified as good (Fig. 6). If the specimen

Figure 5. Slurry seal test specimen—excellent: A = < 1 percent, S = < 10 percent, T_R = 85-100 percent.

Figure 6. Slurry seal test specimen—good: A = 2-5 percent, S = 10-15 percent, T_R = 70-85 percent.

Figure 7. Slurry seal test specimen—fair: A = 5-10 percent, S = 10-15 percent, T_R = 65- 80 percent.

Figure 8. Slurry seal test specimen—unsatisfactory: A = > 10 percent, S = > 15 percent, T_R cannot be determined.

was fair (Fig. 7), the abrasion was less than 10 percent, some shoving was noticed, and the relative thickness ranged from 65 to 80 percent. Specimens with more than 10 percent abrasion were rated as unsatisfactory (Fig. 8). This rating system was used as the best judge of the slurry seal specimen at the time of testing, and it could possibly be correlated to field performance. An abrasion value of 10 percent is approximately the same as a wear value of 70 gm/sq ft as reported by Kari (5).

The shoving of specimens was termed noticeable if a slight hump could be felt by passing the hand over the outer rim of the abraded annulus. Shoving values of less than 10 percent could not be detected by the hand, whereas values above 10 percent could be felt. For the purpose of this rating system, shoving values up to 15 percent are not considered excessive. When abrasion was not excessive, the relative thickness was estimated by the observer for the visual rating of the specimens. The range of values for the classification has been discussed previously.

Rockdale Slag Aggregate. —The data indicated that the abrasion was slightly increased in the Rockdale slag aggregate mixtures with the addition of mineral filler even though the asphalt content was adjusted for the addition of filler. Mixtures containing fly ash abraded more than those with cement or limestone dust; however, the abrasion did not increase to the extent that the samples were unacceptable by the visual rating system. The maximum abrasion, with the exception of one set of fly ash specimens, was approximately 5 percent which was rated as good to fair by the visual method. In most cases, the weight loss was not increased above the 1 percent abrasion level by the addition of mineral filler. Also, the density of specimens containing filler was generally less than that of specimens with no filler. This reduction in density might have been caused by a fluffing effect of the filler. The data indicate that abrasion was slightly greater in the less dense samples.

Summarizing, the weight loss increased as the filler content increased; however, the abrasion of the cement specimens seemed to reach a maximum value at the 2 percent level and to decrease slightly as the filler content was increased to 4 percent.

The shoving of Rockdale slag aggregate mixtures was improved by the addition of mineral filler in all cases tested, although higher percentages of filler were usually required to accomplish this result. Fly ash was the only filler used that appreciably reduced the shoving at 2 percent filler content. However, the shoving for all these mixtures was not considered excessive when rated by visual methods. The maximum shoving was approximately 16 percent in the Rockdale slag aggregate specimens with no filler, and the minimum amount was about 1 percent in the specimens containing fly ash and cement.

The relative thickness of the specimens tested was slightly decreased by the addition of mineral filler, but this reduction was generally less than 5 percent. Therefore, for all practical purposes, the relative thickness of the specimens was unaltered. The relative thickness ranged from 69.8 to 74.9 percent, with the lowest value occuring in the cement specimens and the highest in the specimens containing no filler. All of these were rated as fair by the visual rating system as shown in Figure 7.

Concrete Sand. —The data show that abrasion of the sand mixtures was not significantly improved by the addition of mineral filler if the proper amount of asphalt was used. The AOV showed that interaction between the filler content and residual asphalt content was present for all filler types. The only case where the addition of filler appeared to improve the abrasion characteristics was in the +2 percent of optimum residual asphalt mixtures; however, this apparent improvement was created by an excessive amount of abrasion in one of the specimens of the sand mixture with no filler. The abrasion of specimens made with limestone dust seemed to increase with larger amounts of filler as was the case in the slag mixtures, but again, this increase was relatively small. All of the specimens prepared at the optimum asphalt content were rated as fair to excellent by the visual rating system; however, those prepared at asphalt contents below optimum were abraded excessively and were rated unsuitable for use in slurry seal coats.

The effect of mineral filler on abrasion for specimens at optimum residual asphalt content can be seen in Figure 9. The abrasion of the specimens in these tests ranged from almost 0 to 125 percent.

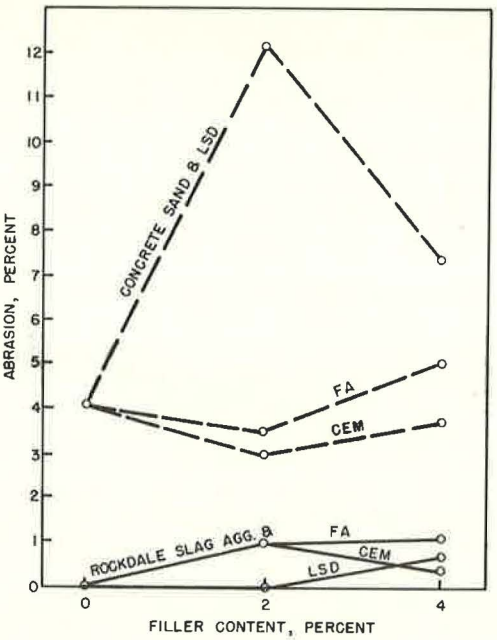

Figure 9. Effect of mineral filler on abrasion at optimum residual asphalt content.

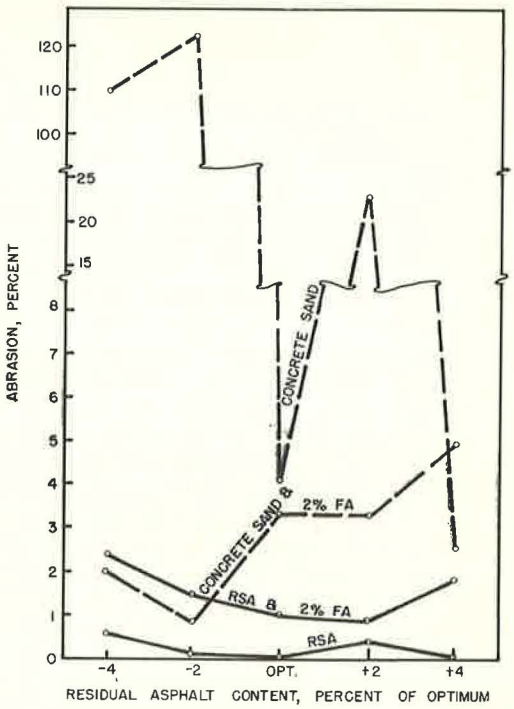

Figure 10. Effect of asphalt content on abrasion.

Shoving of the test specimens generally increased with the addition of fly ash and cement, but there was essentially no effect on the specimens with the addition of limestone dust. In the fly ash specimens, an increase from 2 to 4 percent filler did not affect the shoving for any particular residual asphalt content, whereas increasing the cement content by the same amount generally increased the shoving. The range of shoving values was from approximately 0 to 29 percent in the case of specimens prepared with fly ash.

The relative thickness of the specimens could not be evaluated for the sand mixtures because there was excessive abrasion of the samples. The reduction in thickness due to the action of the testing device cannot be separated from the reduction caused by excessive wear on the specimen; therefore, when the abrasion is high, for instance in excess of 10 percent, the relative thickness is meaningless.

Effects of Asphalt Content

The residual asphalt content was an important factor in the behavior of the test specimens. In every case, the residual asphalt content had an effect on the variable under consideration. In the following paragraphs, these effects are discussed for each of the aggregates tested.

Rockdale Slag Aggregate. —The data indicate the abrasion of the test specimens decreases as the residual asphalt content increases from -4 percent of optimum to optimum. If the residual asphalt content is increased to +2 percent of optimum, the abrasion also increases; however, further increases in asphalt content will not necessarily increase the abrasion. In the specimens containing cement and limestone dust, the abrasion at +4 percent of optimum residual asphalt content was approximately the same as the +2 percent value; however, the fly ash specimens indicated a slight decrease in abrasion at the +4 percent asphalt level. The effect of asphalt content on abrasion is shown in Figure 10 for Rockdale slag aggregate with no filler and with 2 percent Rockdale fly ash.

The shoving of the test specimens followed the same trend as the abrasion. The maximum amount of shoving occurred at -4 percent of optimum residual asphalt content, and the minimum values were at the optimum. The shoving then increased with increasing asphalt content to the +2 percent level with a slight drop at +4 percent residual asphalt content.

The relative thickness of the specimens generally increased with increasing residual asphalt content with the greatest thickness occurring at -2 percent of the optimum asphalt content; however, the peak value of relative thickness for the specimens containing fly ash occurred at optimum residual asphalt content. The relative thickness then decreased with increasing amounts of asphalt.

Concrete Sand. —The residual asphalt content was the primary factor in determining the suitability of the concrete sand for use in slurry seal mixtures. When the proper amount of asphalt was used, excessive abrasion was minimized, and the mixtures were usually acceptable. The data revealed that the abrasion was substantially decreased as the residual asphalt content was increased to the optimum amount; however, the abrasion was also affected by the type and amount of filler in the mixture. The specimens prepared with fly ash did not exhibit abrasion values in excess of 5 percent at asphalt contents below optimum, and the abrasion was decreased as the asphalt content was increased to optimum and above. As the residual asphalt was increased to +2 and +4 percent of the optimum amount, the abrasion for all practical purposes remained about the same; however, there was some fluctuation in the values with various types and amounts of filler. The specimens containing no filler were abraded excessively at +2 percent of optimum asphalt content, but the wear was back to an acceptable level when this asphalt content was increased to +4 percent of optimum. These observations were confirmed by the AOV which indicated that interaction was present between the filler content and the residual asphalt content. An example of the effect of asphalt content on abrasion is shown in Figure 10. The data indicate a range of abrasion values from 0.2 percent at +4 percent of optimum asphalt content to 125.6 percent at the -4 percent level. These specimens were classified as excellent to poor by the visual rating system.

The shoving of the test specimens varied considerably but the data seemed to indicate that shoving was high at the lower asphalt contents and decreased as the amount of asphalt was increased. Consequently, the lower asphalt contents should be avoided when preparing slurry seal mixtures with this aggregate.

The relative thickness could not be evaluated because of the excessive abrasion of the specimens at the lower asphalt contents.

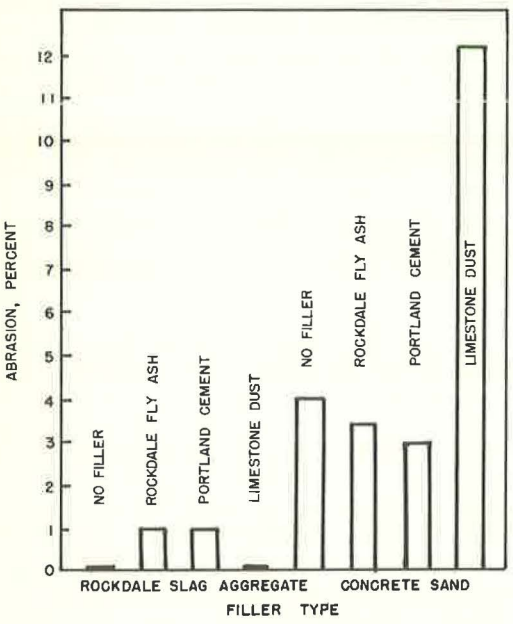

Figure 11. Effect of filler type on abrasion at optimum residual asphalt content and 2 percent filler content.

Effects of Filler Type

An analysis of variance was made for each of the aggregates at fixed filler contents to determine the effects of the filler type. The comparison was made at 2 and 4 percent filler contents for Rockdale slag aggregate and concrete sand with the filler type (fly ash, cement and limestone dust) as the columns and residual asphalt content as the rows.

Rockdale Slag Aggregate and 2 Percent Filler. —The AOV indicates that abrasion was less for limestone dust mixtures than

for the other fillers, and that cement was generally more effective than fly ash in reducing the abrasion. An example of the effect of filler type on abrasion for 2 percent filler content and at the optimum residual asphalt content is shown in Figure 11. The abrasion for these mixtures ranged from 0 to 5 percent, and all were classified as good to excellent by the visual rating system.

Rockdale Slag Aggregate and 4 Percent Filler. —The data showed that as the filler content was increased to 4 percent, the cement tended to become the more effective filler in reducing abrasion, and the limestone dust continued to give good performance. Although the specimens containing fly ash showed the most abrasion, they were still acceptable by the visual rating system. The abrasion for this group of specimens ranged from 0 to 12.3 percent. This maximum abrasion value occurred in the fly ash specimens at the +2 percent of optimum residual asphalt content. These specimens received a rating of excellent in the visual classification, and there appeared to have been very little material loss. However, even if these high values were disregarded in the analysis, the results would not change significantly.

Concrete Sand and 2 Percent Filler. —The data indicate that specimens made with fly ash will reduce the abrasion considerably more than either cement of limestone dust for lower (less than optimum) residual asphalt contents; however, the cement becomes more effective at optimum asphalt content and above. The limestone dust appeared to be the least effective in reducing abrasion for this particular aggregate. The abrasion ranged from 0.8 percent to 75.3 percent.

Concrete Sand and 4 Percent Filler. —When the filler content is increased to the 4 percent level, the indication is that cement is foremost in producing a low abrasion level. The fly ash was also effective in reducing the weight loss; however, the specimens made with limestone dust showed a greater amount of wear. The range of abrasion values for these specimens was from 0.2 to 107.6 percent.

Effect of Particle Shape and Texture

The original gradation of the concrete sand was changed by separation and recombination so that it would be the same as the gradation of the Rockdale slag aggregate. This was done so that the aggregates could be compared to determine the effect of particle shape and texture. The Rockdale slag aggregate has an angular particle shape and is rough textured, whereas the concrete sand has rounded smooth-textured particles.

The comparison was made by rearranging the data so that an analysis of variance could be made to test for differences in the aggregates. This was accomplished by using a two-way classification with the aggregate type as the columns and residual asphalt content as the rows. The AOV was made for the aggregates with no mineral filler, for the aggregates of each filler content, and for each type of filler.

The data revealed that for all types and amounts of mineral filler and for all except two of the 70 asphalt contents tested, the abrasion in the Rockdale slag aggregate specimens was less than that of the concrete sand. This seems to indicate that the more angular and textured particles make better slurry seals than the rounded smooth-textured particles.

SUMMARY AND CONCLUSIONS

Mixture Design

The results of the test conducted with the Young wet track abrasion device seem to verify the design equation (Eq. 2). The predicted optimum residual asphalt contents occurred, for the most part, at or near the minimum values of specimen abrasion. The predicted optimum asphalt content nearly always resulted in a good mixture (by visual rating system) suitable for use in slurry seal coat construction. However, the proper aggregate gradation is essential in obtaining good mixtures.

Test Variables

The data indicated that abrasion was the best measure of the slurry seal performance in the laboratory. The relative thickness and, to some extent, the density of the tested

portion of the specimens are dependent on the amount of abrasion; when this weight loss is excessively high, these effects cannot be separated. The shoving did not seem to follow any particular trend or pattern that would influence the suitability of a slurry mixture. However, these effects should be measured and reviewed to obtain a better understanding of the mixtures.

Type and Amount of Mineral Filler

Mineral fillers are used in slurry seal mixtures to improve the gradation and workability of the mixture. This research indicated that when mineral fillers are used for this purpose in Rockdale slag aggregate or concrete sand slurry seals, the effectiveness of the mixture may be reduced by an increase in the abrasion of the slurry seal coat. However, this increase in abrasion may be very slight, and the qualities gained may offset the increased wear. It was also found that some fillers will produce less wear than others, and the data show that limestone dust and cement are the best of the fillers tested for use with Rockdale slag aggregate in slurry seal mixtures, whereas cement and fly ash are better suited for mixtures of concrete sand. In addition, the amount of filler did not significantly affect the abrasion values of properly designed slurry seal; therefore, the amount of filler will be governed by economy and the intended purpose.

Asphalt Content

As pointed out in discussing the design method, if the residual asphalt content is estimated by Eq. 2, the slurry seal mixture will give good performance when tested in the Young wet track abrasion device. It may be generally stated that a properly designed slurry seal will give good service irrespective of the amount and type of mineral filler.

ACKNOWLEDGMENTS

Gratitude is expressed to Slurry Seal, Inc., the Aluminum Co. of America, Texas Power and Light Co., and the Texas Transportation Institute for the equipment, materials, and funds that made this research possible.

REFERENCES

1. The Design, Mixing, Application, and Cost of Emulsified Asphalt Slurry Seal Coats. Western Construction, Vol. 31, No. 2, pp. 21-23, Feb. 1956.
2. Zube, E. Studies on Water Permeability of Asphaltic Concrete Pavements. Proc. 4th Ann. Highway Conf., Univ. of the Pacific, Mar. 1961.
3. Nelson, M. L. Slurry Seal—Where and How to Use It. Western Construction, Vol. 32, No. 2, pp. 25-27, Feb. 1957.
4. Lab Test Control Las Vegas Slurry Seal. Street Eng., Vol. 9, No. 5, pp. 20-24, May 1963.
5. Kari, W. J., and Coyne, L. D. Emulsified Asphalt Slurry Seal Coats. Proc. AAPT, Vol. 33, pp. 502-537, 1964.
6. Asphalt Surface Treatments and Asphalt Penetration Macadam. Asphalt Inst., Ser. No. 13 (MS-13), pp. 127, 154-159, Mar. 1964.
7. Method of Testing for Centrifuge Kerosene Equivalent Including K Factor. Materials Manual of Testing and Control Procedures, California Div. of Highways, Vol. 1, Sect. 303-B, 1963.
8. Gallaway, B. M. Laboratory and Field Densities of Hot-Mix Asphaltic Concrete in Texas. Highway Research Board Bull. 251, pp. 12-17, 1960.
9. Fuller, W. B., and Thompson, S. E. The Laws of Proportioning Concrete. Trans. ASCE, Vol. 59, pp. 67-143, 1907.

Appendix

EXAMPLE DATA SHEETS AND CALCULATIONS

Surface Area

Sieve Size	Surface Area Factor	X	Total %/100 Passing	=	Surface Area
Max.	2		1.00		2.00
#4	2		0.991		1.98
#8	4		0.893		3.57
#16	8		0.568		4.54
#30	14		0.275		3.85
#50	30		0.177		5.31
#100	60		0.103		6.18
#200	160		0.059		9.44

Total Area = 36.87 sq ft/lb

Absorption

	A	B	AVG.
Tare + dry sample, gm.	407.0	407.1	
Tare, gm.	307.0	307.1	
Tare + wet sample, gm.	411.6	411.8	
% Kerosene Ret. (C.K.E.)	4.6	4.7	4.65

Note: See California test method #303B

SLURRY SEAL DATA SHEET

Kerosene absorption 4.65 % Film thickness, t 8 microns

Surface Area 36.87 ft^2/lb App. Specific Gravity 2.90

Corrected Surface Area = SA x $\frac{2.65}{\text{app. SG}}$

= $\frac{36.87}{} \times \frac{2.65}{2.90} = \frac{33.8}{}$ ft^2/lb

Asphalt for Surface Area/lb Aggr.

= 0.0002047 x SG_A x t x corr. SA

= 0.0002047 x 1.03 x 8 x 33.8 = 0.0570 lb

Asphalt for absorption/lb Aggr. = Kerosene Absorption ÷ 100

= 4.65 ÷ 100 0.0465 lb

Total Residual Asphalt/lb Aggr. 0.1035 lb

Amount of asphalt in given emulsion = 67 % by wt.

Emulsion/lb Aggr. = $\frac{\text{total Residual Asphalt}}{\text{Asphalt in Emulsion}} = \frac{0.1035}{0.67} = 0.154$ lb

Remarks (evaluation): _____

_____

_____

_____

_____

Discussion

W. H. CAMPEN, Omaha Testing Laboratories, Omaha, Neb. —On the whole, this paper is very good. It enumerates many good points relative to the use, design and construction of slurry seals.

The use of the surface area as a criterion for design is sound. However, the assumption that slurry seal mixtures should have the same film thickness as similar hot-mixed hot-laid mixtures is questionable. In my opinion, slurry seal mixtures should be much richer in asphalt than hot ones. More specifically, slurry seal mixtures should have film thicknesses about 50 percent greater than hot ones. Based on many years of experience in both the laboratory and the field, I have come to the conclusion that a film thickness of about 6μ is adequate for hot asphaltic concrete mixtures having maximum sizes of about 0.2 in. and higher. Therefore, I would recommend a minimum of 9μ for slurry seal mixtures.

My experience has shown that lean slurry seal mixtures are brittle and either fail to adhere to the treated surfaces or abrade easily. For this reason, I prefer the richer ones, even if they tend to shove a little.

WILLIAM J. HARPER, RUDOLF A. JIMENEZ, and BOB M. GALLAWAY, Closure—The authors thank Mr. Campen for his discussion of this paper. However, we would like to remind Mr. Campen that the film thickness in the design equation is not specified; hence, the user of this method may substitute a film thickness based on his own experience or use our value of 8μ.

The computed residual asphalt content is based on both film thickness and absorption requirements. For example, in the illustration in the Appendix of the paper, the amount of asphalt required for absorption is 0.0465 lb/lb of aggregate and that for effective film thickness is 0.0570 lb/lb of aggregate. The total amount of residual asphalt for this example is 0.1035 lb/lb of aggregate. Using this amount and a corrected surface area of 33.8 sq ft/lb of aggregate, the ratio of asphalt to aggregate surface area obtained is 14.5μ. Although this value may appear to be high, it is necessary for coating the usual existing pavement surface. In view of this, it appears that we are in accord with Mr. Campen in that slurry seals should be richer in asphalt than asphaltic concrete.

The film thickness of 8μ used in this study was based on experience, substantiated by field performance of existing slurry seals in Texas.

Voids in One-Size Surface Treatment Aggregates

JOHN L. SANER and MORELAND HERRIN
Respectively, Graduate Research Assistant and Professor of Civil Engineering, University of Illinois

A fundamental concept used in the design of surface treatments is that the quantity of bituminous material needed is determined as the amount required to fill the voids between the aggregates to an optimum depth. This study was performed to determine the influence of aggregate characteristics on the void space in a one-size surface treatment aggregate. The laboratory investigation was conducted by spreading the aggregate one layer thick in a flat bottom pan and pouring known volumes of water into the container between the aggregate. By measuring the depth of the water and the volume of the voids, the percent voids could be computed.

The volume of the voids did not vary in direct proportion with the depth within the aggregate, as is assumed in current design methods. In general, the more rounded aggregates, such as the gravels, had a smaller volume of voids than the more angular crushed stone. In some instances, the difference in the percent voids produced by a change in shape of the aggregate was quite large. Regardless of the shape of the aggregate, the smaller aggregates had greater percent voids than the larger aggregates. The aggregate particles, when placed with their least dimension in a vertical direction, had less voids than when in random arrangement.

•IN DESIGNING surface treatments, perhaps the most important quantity to be computed is the amount of bituminous material that must be sprayed on the roadbed. In most of the existing design methods, this quantity is determined as the amount required to fill the voids between the aggregates to an optimum depth (Fig. 1). This fundamental concept was first stated by Hanson in 1935 (2). It is so simple and logical that it is used by most of the other design methods. Since there is a direct relationship between the voids space and the amount of bituminous material needed, this investigation has been performed to determine the influence of various aggregate characteristics on the void space in one-size surface treatment aggregates. Indirectly, this study should indicate which aggregate factors influence the amount of bitumen needed in a surface treatment construction.

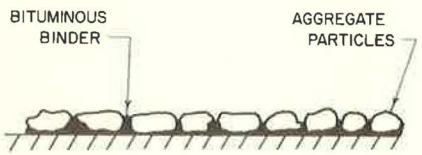

Figure 1. Cross-section of surface treatment.

VOIDS AS USED IN EXISTING METHODS OF DESIGNING SURFACE TREATMENTS

In his early investigations, Hanson (2) observed that the aggregate particles, when first dropped on the asphalt surface, are oriented in random directions; i. e.,

Paper sponsored by Committee on Bituminous Surface Treatments.

some are on edge, some are vertical, and others lie on their largest side. Hanson reported that the aggregates in this state had approximately 50 percent voids. After rolling and even under traffic loads, the aggregates tended to reorient themselves so that they presented their least dimension in the vartical direction. Under these conditions, Hanson reported, the voids between the aggregates were approximately 20 percent. Hanson and McLeod (6) indicate that this void volume is independent of the size of the cover aggregate, e.g., ¼, ½, or ¾ in. Thus, it is thought by some investigators that the volume of voids in the surface treatment aggregate is only related to the position or orientation of the aggregate and is not influenced by the size or type of the aggregate.

Other investigators believe that the percentage of voids between the aggregate varies with the character or shape and surface texture of the aggregate. McLeod and engineers in Australia indirectly consider the shape by varying the amount of bituminous material needed to fill the aggregate voids to an optimum amount according to the type of aggregate (6). Other investigators, (1, 4, 5), indirectly consider the shape by determining the volume of the voids to be filled with bituminous materials directly by first placing aggregate in a large cylinder. Benson (1) and Kearby (4) weighed the aggregates and computed the percent voids by using the specific gravity of the aggregate. Mackintosh (5), on the other hand, measured the volume between the aggregate particles in the cylinder by determining the quantity of water needed to fill the voids. In both cases, the assumption is made that the aggregate in the one-stone thick layer will have the same arrangement and voids on the road surface as it will have in the cylinder. This assumption is probably not true. Benson (1) even acknowledges that this assumption is incorrect, but he uses it nevertheless.

No design method considers that the volume of voids may vary other than linearly with depth. For example, it is considered that, if a ¾-in. aggregate (with 24 percent voids) is to be filled with bituminous material to one-half its depth, the volume of the voids to be filled would be ½ x 24 = 12 percent. In other words, in design, it has always been assumed that the voids vary directly with the depth in the aggregate.

In summary, some investigators think that the percent voids in a layer of aggregate one stone thick is a constant value for all aggregates and is only related to the orientation of the aggregate. Other investigators think that the percent voids is related to the shape and, possibly, to the size of the aggregate. No design method, however, considers that the voids may vary with depth within the aggregate.

A number of aggregate characteristics, therefore, could possibly influence the volume of voids, but only the following factors were investigated in this study: (a) depth in the aggregate layer, (b) maximum size of the aggregate, (c) particle arrangement, and (d) shape of the aggregate. In addition, it should be noted that the investigation is limited only to one-size surface treatment aggregates.

PROCEDURE

The procedure used to determine the volume of the voids in the aggregate layer was relatively simple. After the aggregate was washed, it was allowed to soak completely immersed in water for at least 12 hr. Just before testing, the aggregate was dried until it was in a saturated surface dry condition. This soaking and drying was done to account for the absorbent powers of the aggregate. The aggregate was then spread one layer thick in a flat bottom container. Care was taken to place the aggregate, by hand, in the desired particle orientation.

Measured volumes of water were then poured into the container and allowed to flow into the void spaces between the aggregate particles. The depth of this known volume of water was measured. Depth measurements were made at regular intervals of water volume, starting at the lowest possible depth of water up to the point at which the aggregate layer was completely immersed. Data were verified by repeating this procedure, including a resoaking and drying of the aggregate.

With the depth, the volume of water in the pan at that depth, and the surface area of the bottom of the pan known, the percentage voids could be calculated by the following simple computation:

$$\text{Percent voids} = \frac{\text{Volume of water at depth d}}{\text{Area of bottom of pan} \times \text{depth d}} \times 100$$

This method of computing percentage voids should not be confused with other methods. It is the percentage voids in the aggregate layer below the surface of the water, not a percentage of the total voids in the aggregate layer nor a percentage of the total volume of the whole aggregate layer. This particular method of defining percent voids was chosen because of its simplicity and because the total volume or the total depth of the aggregate layer cannot be defined exactly due to variations in aggregate particle size.

Not only are the data presented in terms of percent voids, but also as volume of voids in gallons per square yard. This was done in specific instances to present the data in a manner that is more useful for illustrating points.

EQUIPMENT

The equipment used for testing was very simple in design. The pan was constructed of $\frac{3}{8}$-in. thick aluminum and was approximately 5 in. deep and 3 ft square. The bottom of the pan was flat and so rigid that no deflection took place. The instrument used for depth measurement was a standard penetrometer normally used in bituminous material testing. The penetrometer was removed from its base and the vertical rod on which it is raised and lowered was clamped with a C-clamp into one corner of the pan at a location where a few particles of aggregate had been removed. (Because of the large size of the test pan, the removal of the few aggregate particles had little effect on the results.) First the needle was gently lowered until it was just touching the bottom of the pan. After the dial was set at zero, the needle was raised and relowered until the point was just touching the surface of the water. This point could be seen relatively easily by looking at a light reflection on the surface of the water. The dial was then adjusted and measurements of the depth were taken and recorded in 0.1-mm increments. Each depth measurement was repeated to insure against errors.

CALIBRATION OF TEST EQUIPMENT

A micrometer was used to check the penetrometer's accuracy in measuring distances. The needle movement was measured by the dial and with the micrometer through various distances all starting with zero, as in the testing procedure. The penetrometer was found very accurate in its readings.

Proof was needed that this method of investigation did measure the volume of the voids and that some unknown factor did not create a significant error. A procedure was needed by which the percentage of voids could not only be measured, but also computed by simple geometry. For this purpose, polished aluminum spheres of $\frac{5}{8}$-in. diameter were used as aggregate. The spheres were placed in the pan in a single layer with a close-packed arrangement. Void data given in Table 1 were then obtained by the procedure previously outlined. A plot of the theoretical and experimental data is shown in Figure 2. This figure reveals that the measured values of percent voids, at depths below that at which the minimum percentage of voids occurs, were about 3 to 4 percent greater than the theoretical values. At depths above the minimum, the measured values were about 3 percent lower than the theoretical ones. At the depth of minimum percent voids and above the depth of the spheres themselves (i.e., when the spheres were completely covered with water), the experimental data agreed very closely with the theoretical calculations.

A definite phenomenon caused the deviation of the experimental from the theoretical results at some depths, although there was a close agreement at others. At depths below which the minimum percent voids occurred, $\frac{3}{4}$ of the diameter of the perfect spheres, the water was clearly observed to be drawn up around the spheres by means of surface tension, causing a concave upward surface on the water between adjoining spheres. Since the depth measurements were taken at a location where one sphere had been removed and the water was not drawn up as much, the measured depth was less than the average water depth in the pan. This lower depth, caused by a smaller drawing up where the sphere was missing, is produced in much the same way that

water rises in a tube due to capillary action. The smaller the diameter of tube, the higher the capillary rise will be. The percentage voids computed was therefore too large. Above the depth at which the minimum voids occurred, an opposite effect was clearly observed. The water was held down around the spheres by surface tension, causing a concave downward surface on the water between spheres. This caused the depth at the location where the depth measurement was taken to be slightly greater than the average water depth in the pan. This larger measured depth caused the computed percentage of voids to be smaller than the theoretical. At the depth at which the minimum percent voids occurred, the effect of the surface tension was negligible and there was essentially no drawing up nor holding down of the water between adjacent spheres. Therefore, exact readings of depth were taken and the computed percent voids compared very closely with the theoretical. Also, at depths of water above the top of the spheres, when the spheres were completely immersed, the surface tension did not have any effect between the adjacent spheres, and the experimental data compared closely with the theoretical.

TABLE 1

CALIBRATION OF EQUIPMENT[a]

Trial 1		Trial 2		Trial 3	
Depth (in.)	Voids (%)	Depth (in.)	Voids (%)	Depth (in.)	Voids (%)
0.197	64.2	0.205	60.8	0.181	68.8
0.327	40.5	0.331	40.3	0.323	41.4
0.437	32.4	0.437	32.7	0.437	32.7
0.504	30.1	0.484	31.8	0.484	31.8
0.535	30.4	0.563	31.3	0.547	32.1
0.563	30.9	0.598	33.2	0.597	33.4
0.579	32.0	0.634	34.9	0.614	36.0
0.598	32.9	0.638	37.7	0.650	37.3
0.634	34.7	0.650	41.2	0.665	40.2
0.646	37.6	0.657	44.2	0.657	44.2
0.650	40.8	0.689	45.5	0.689	45.5
0.661	43.6	0.709	47.7	0.728	46.2
0.685	45.5	-	-	-	-
0.705	47.5	-	-	-	-

[a]Using 5/8-in. diameter spheres in close-packed arrangement.

The data taken on the aggregate samples might be assumed to be similarly incorrect. This is not believed to be true, because the effect caused by the surface tension of the water was not observed when the aggregates were tested. This phe-

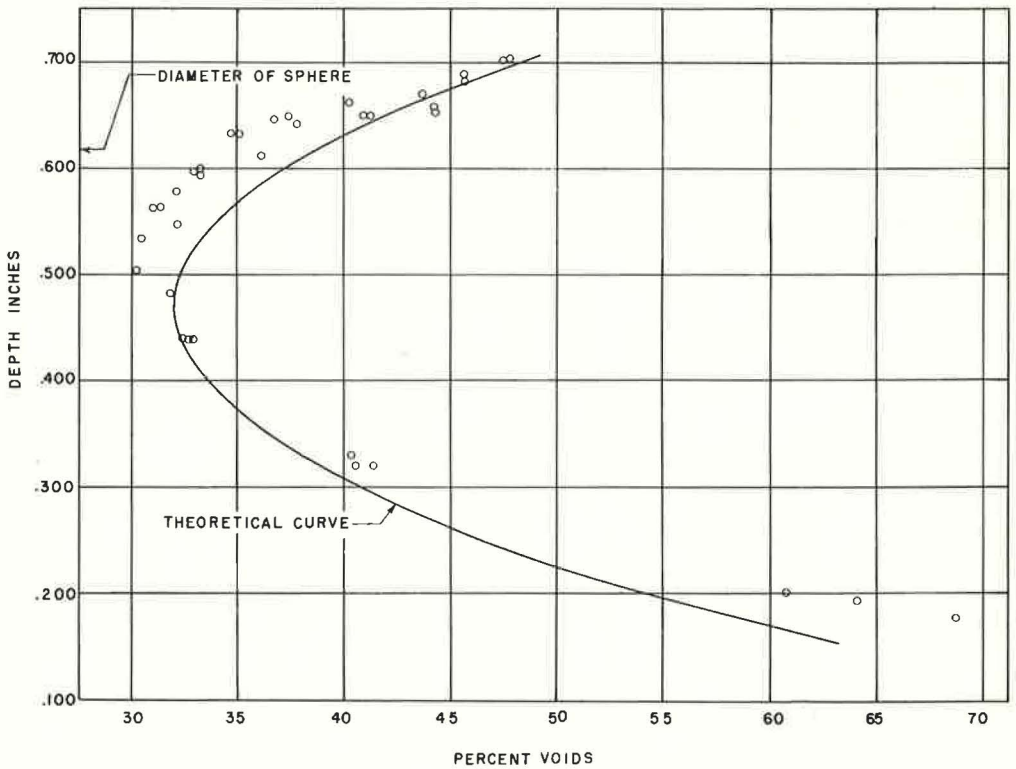

Figure 2. Calibration of equipment, 5/8-in. diameter spheres, close-packed arrangement.

nomenon of drawing up and holding down of the water by the polished aluminum spheres did not take place with the aggregate because the latter does not have the uniformity of shape nor the exceptional smoothness of surface usually necessary for this type of effect to take place. The measurements of depth taken with the various samples of aggregates should be very close to the average depth in the pan. Therefore, the computed values of percent voids in this investigation should compare very well with the actual percent voids in the aggregate layer.

AGGREGATES USED

In the investigation it was desired to determine what effect aggregate types and sizes had on the volume of the voids in an aggregate layer. A wide variety of types and sizes of aggregates were obtained. Seven different shapes of aggregates, ranging from crushed stone to rounded gravel, were used and are listed in Table 2. All of these aggregate samples were one size; i. e., they were materials retained between two sieves in a standard arrangement of sieves. The sizes used were ½ to ¾ in., ⅜ to ½ in., ¼ to ⅜ in., and No. 4 to ⅜ in. Because sieving does not allow a perfect sizing of aggregates of equal size, one size, as used here, does not mean a perfect uniformity of size. There was some variation in size within these aggregate samples. Table 2 gives other data pertaining to the aggregate, which are explained in the next section.

VARIATION IN PERCENT VOIDS WITH DEPTH WITHIN AGGREGATE LAYER

When the test procedure was being developed, questions arose as to what depth in the aggregate layer the percent voids measurement should be made, and if the percent voids at some particular depth would give an adequate parameter for describing the aggregate sample. To answer these questions, measurements were taken in intervals from the smallest possible depth to a point up to and a little beyond where the aggregate layer was completely immersed.

Figures 3 and 4 show how the percent voids and volume of voids varied with depth in the aggregate layer. Although the aggregate used in this example was a crushed limestone of ½- to ¾-in. size, the results presented here are typical of those obtained from other sizes and types of aggregates.

The data presented in Figure 3 indicate that the percent voids varies with depth and has a minimum value that occurs at a depth slightly above one-half the maximum size of the aggregate (⅜ in.). Figure 4 shows that the plot of volume of voids vs depth is a smooth curve with the top and bottom parts of the curves approaching straight lines. If the volume of voids varies linearly with the depth within the aggregate layer, this curve should be a straight line. However, the relationship is not linear and, thus, the

TABLE 2

AGGREGATE TYPES AND PARAMETERS

Symbol	Type	Size	Parameters		
			Intersection Depth (in.)	Intersection Vol (gal/sq ft)	Min. Void (%)
No. 61	Gravel	½ - ¾ in.	0.443	0.972	41.6
No. 178	Crushed stone	½ - ¾ in.	0.479	1.076	48.3
75-25[a]	Mixture Nos. 61 and 178	½ - ¾ in.	0.457	0.881	36.0
50-50[a]	Mixture Nos. 61 and 178	½ - ¾ in.	0.440	0.880	42.8
No. 178 (a)[b]	Crushed stone[b]	½ - ¾ in.	0.428	1.030	47.4
75-25	Mixture Nos. 61 and 178	⅜ - ½ in.	0.311	0.684	49.2
50-50	Mixture Nos. 61 and 178	⅜ - ½ in.	0.313	0.693	45.4
No. 61	Gravel	⅜ - ½ in.	0.376	0.827	45.2
No. 178	Crushed stone	⅜ - ½ in.	0.343	0.750	50.8
MC(a)[c]	Mine chat[c]	⅜ - ½ in.	0.354	0.861	50.2
Cr. Gr.	Crushed gravel	⅜ - ½ in.	0.317	0.817	50.8
No. 61	Gravel	No. 4-⅜ in.	-	-	48.0
No. 178	Crushed stone	¼-⅜ in.	-	-	54.3

[a]Mixture (by weight) 75 percent No. 61 and 25 percent No. 178.

[b]Crushed stone No. 178 is stone as received from plant; No. 178 (a) is stone No. 178 sorted to contain more cubical particles.

[c]Mine chat sorted to contain more cubical particles.

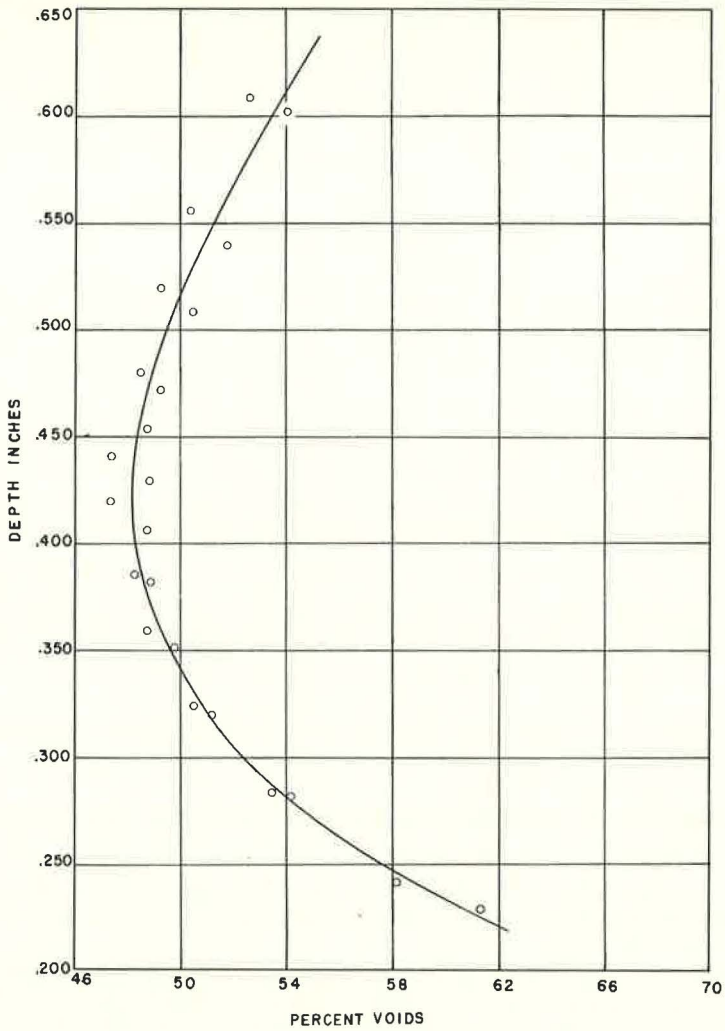

Figure 3. Variation in percent voids with depth, crushed stone No. 178, ½- to ¾-in. size.

volume of voids does not vary in direct proportion with depth. This is a major difference from what has been assumed in many current methods for designing surface treatments.

The variations in percent voids and volume of voids with depth were studied to determine if some value could be used as a parameter in describing the aggregate. Three aggregate parameters were investigated. From the curve of percent voids vs depth, the minimum value of percent voids was used as one parameter. From the curve of volume of voids vs depth, two other parameters were determined by the following method. The straight portions of the curve were extended until they intersected as shown in Figure 4. The coordinates of this intersection were then used separately as parameters; i.e., one parameter is the volume of voids at this intersection and the other is the corresponding depth. The values of these parameters for the various aggregates are given in Table 2. The use of these parameters is more fully explained in the discussion of the variation in percent voids with shape.

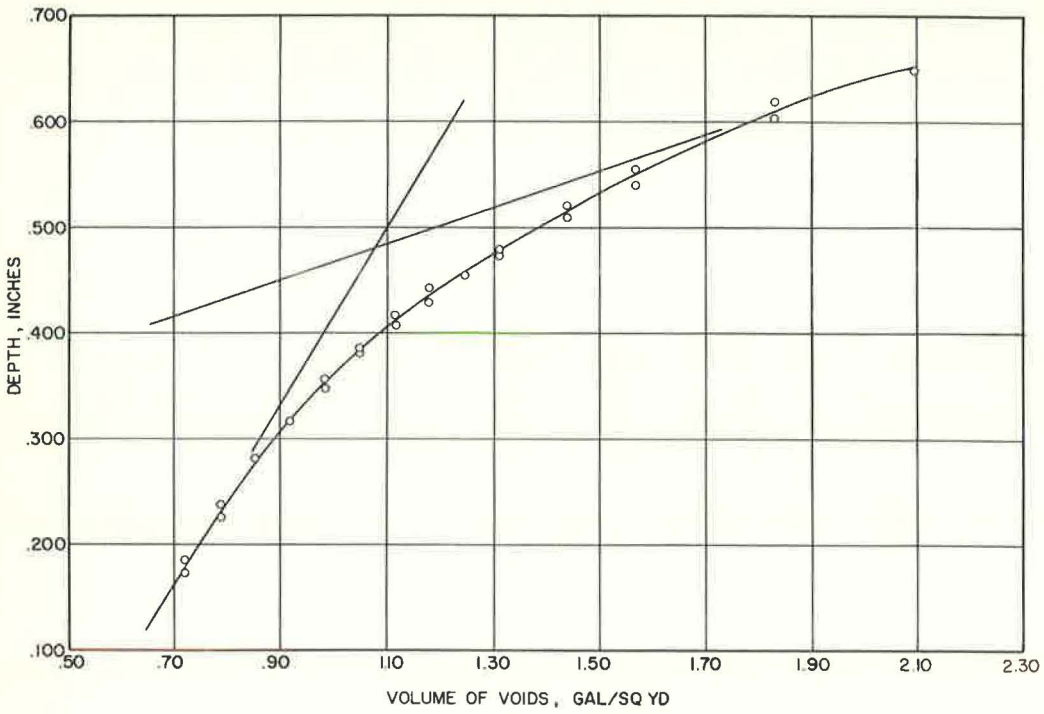

Figure 4. Variation in volume voids with depth, crushed stone No. 178, ½- to ¾-in. size.

VARIATION IN PERCENT VOIDS WITH SIZE OF AGGREGATE

Tests were performed on two types of aggregates at three different sizes of each type: ½ to ¾ in., ⅜ to ½ in., and No. 4 to ⅜ in. The aggregate types used were an angular crushed stone and a rounded gravel. The results of this series of tests are shown in Figures 5 and 6.

Regardless of the type, the smallest size aggregates had greater minimum percent voids than the largest sizes. This difference is quite significant, in some instances as great as 8 percent. Also, a comparison of Figures 5 and 6 indicates that the shapes of these curves are similar. A difference in aggregate type does not seem to have any effect on this phenomenon of increasing voids with decreasing size of aggregate, except perhaps on the magnitude of the increase.

VARIATION IN PERCENT VOIDS WITH PARTICLE ARRANGEMENT

We should first define aggregate particle arrangement. Hanson (2) observed that aggregate particles, when first spread on the asphalt surface in a surface treatment construction, will be oriented in various directions. In other words, there will be a random arrangement of the particles. Hanson also observed that after the surface treatment had been compacted by rolling and by traffic, the aggregate particles were all oriented with their least dimension in a vertical direction. These two particle arrangements, the random arrangement and the least dimension arrangement, were used in this study.

To study the effect of arrangement, tests were performed on three aggregate samples. The samples were a ½- to ¾-in. crushed stone (type a), a ⅜- to ½-in. and a No. 4 to ⅜-in. gravel. Each sample was tested with the aggregate in both arrangements. The least dimension arrangement was carefully prepared by hand placing and orientating every aggregate particle in the pan so the least dimension was in the vertical direction. The random arrangement was prepared by sprinkling handfuls of the aggregate from a small

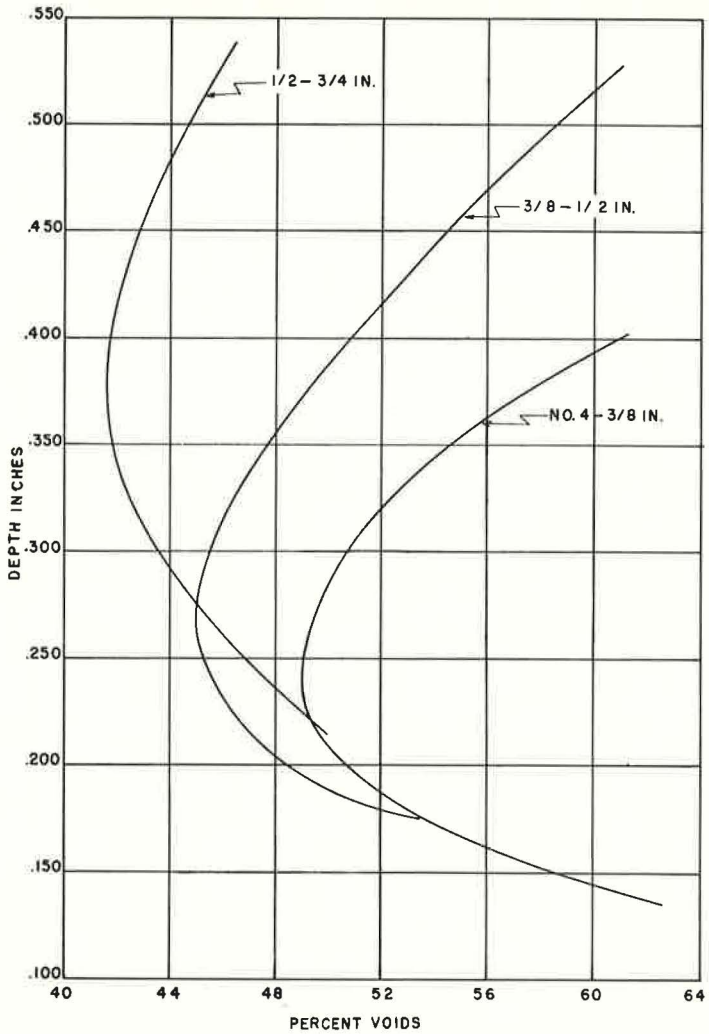

Figure 5. Variation in percent voids with depth for three sizes of gravel No. 61.

height onto the surface of the pan. In both arrangements, care was taken to keep the layer of the aggregate one particle thick.

The results obtained from these series of tests, shown in Figures 7, 8 and 9, indicate that arrangement has some effect on the percentage voids, but regardless of the type or size of aggregate, this effect is relatively small. In the random arrangement, the minimum percent voids is only approximately 4 percent greater than the minimum voids in the aggregate with the least dimension arrangement.

The decrease in the percentage of voids is considerably less than the percentage decrease often attributed to particle reorientation in actual construction. The decrease in percent voids that takes place when a surface treatment is compacted by rolling in the field may not be caused primarily by particle reorientation, but by some unknown factor, possibly resulting from a breakdown or degradation of the aggregate. This investigation was limited, however, to one-size aggregate and no definite statement can be made concerning the effect of aggregate gradation on the percentage voids. This is an area needing further investigation and study.

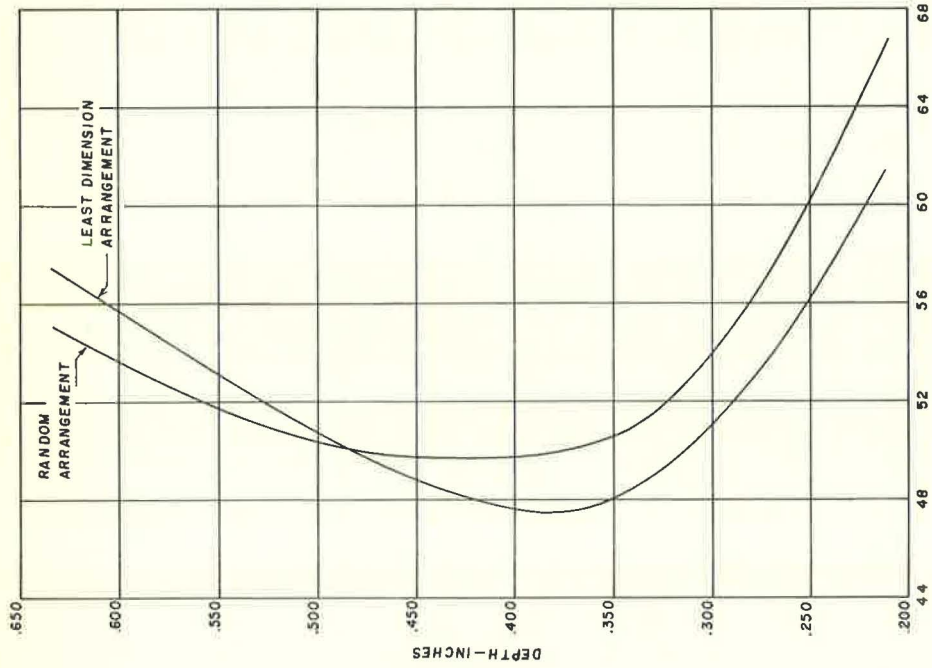

Figure 7. Variation in percent voids with depth for two different particle arrangements, crushed stone No. 178 (a), ½- to ¾-in. size.

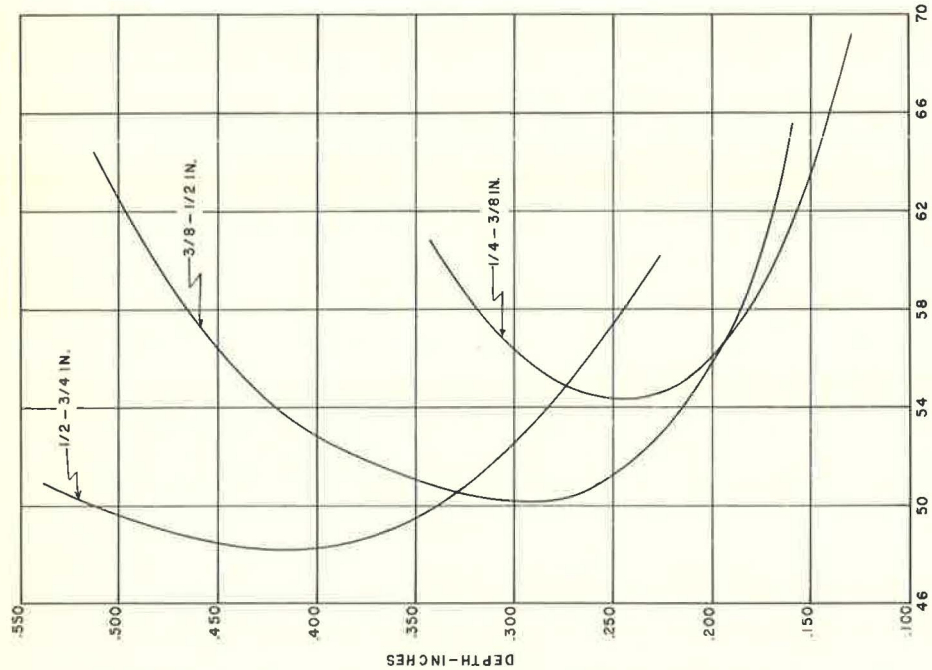

Figure 6. Variation in percent voids with depth for three sizes of crushed stone No. 178.

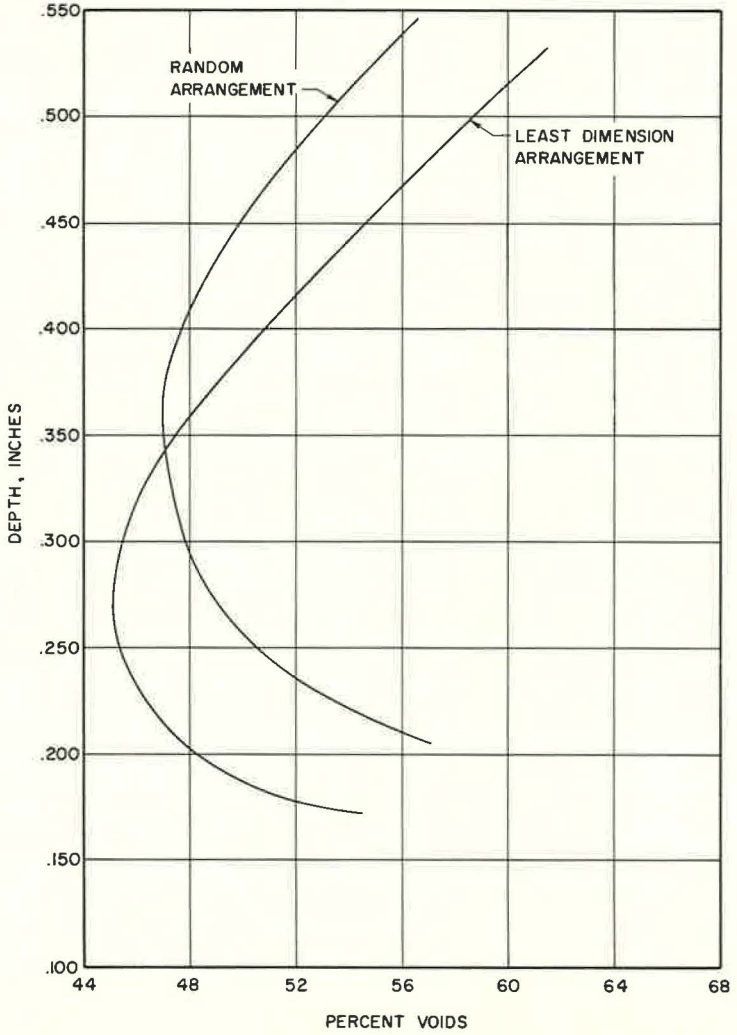

Figure 8. Variation in percent voids with depth for two different particle arrangements, gravel No. 61, $\frac{3}{8}$- to $\frac{1}{2}$-in. size.

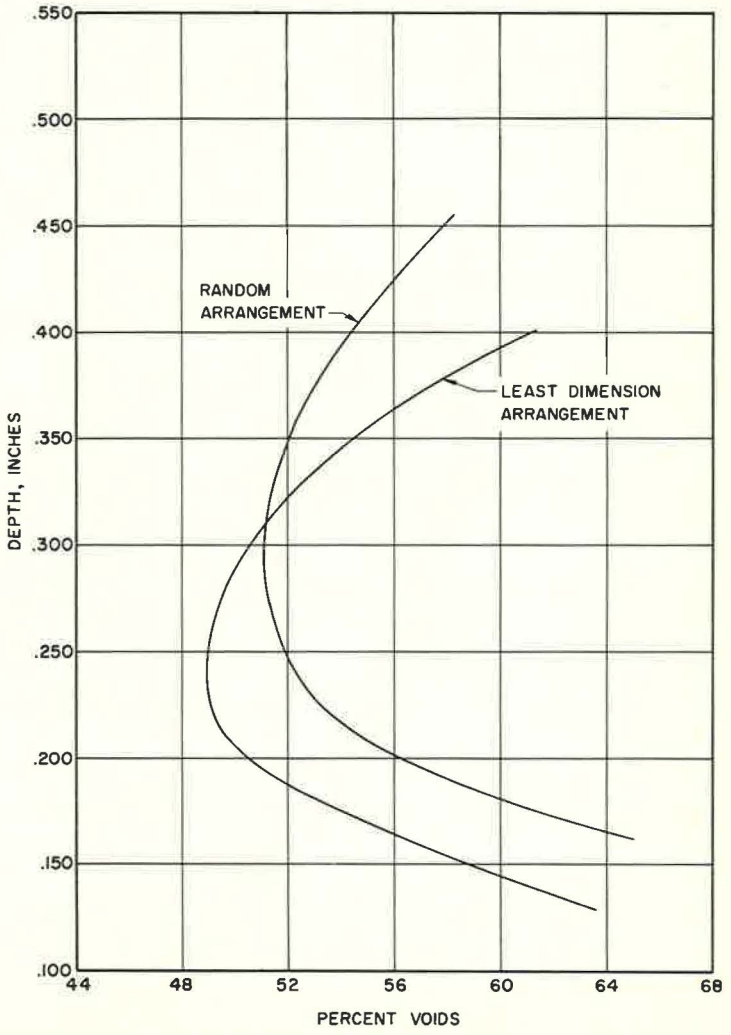

Figure 9. Variation in percent voids with depth for two different particle arrangements, gravel No. 61, No. 4 to $\frac{3}{8}$- in.size.

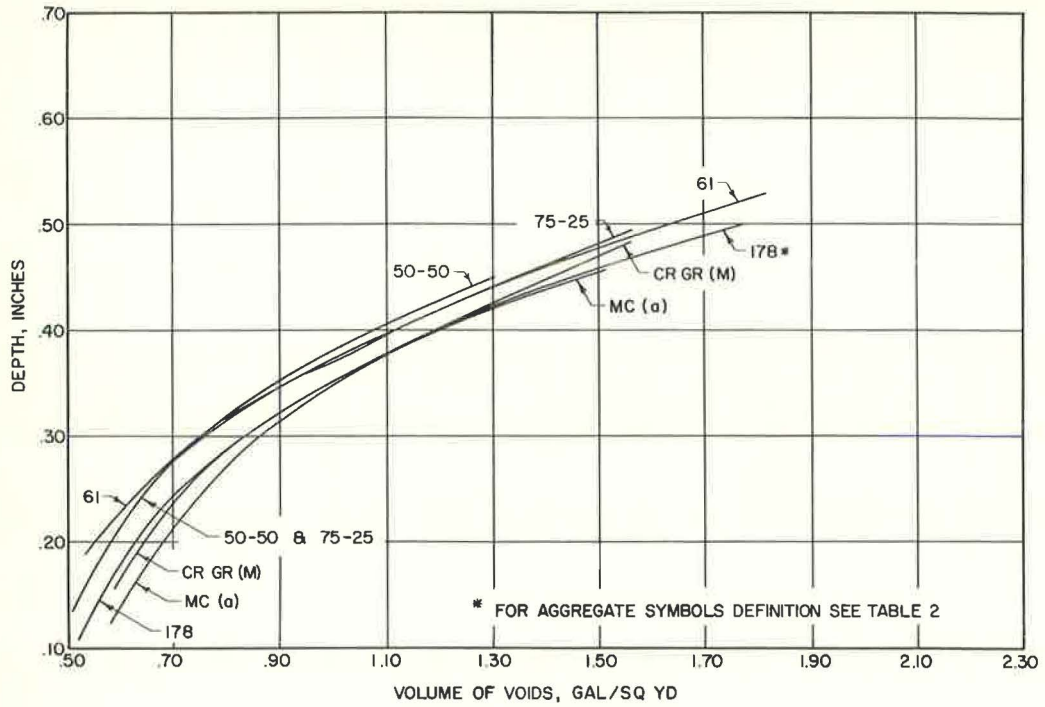

Figure 10. Variation in volume voids with depth for different aggregate types, $\frac{1}{2}$- to $\frac{3}{4}$-in. size.

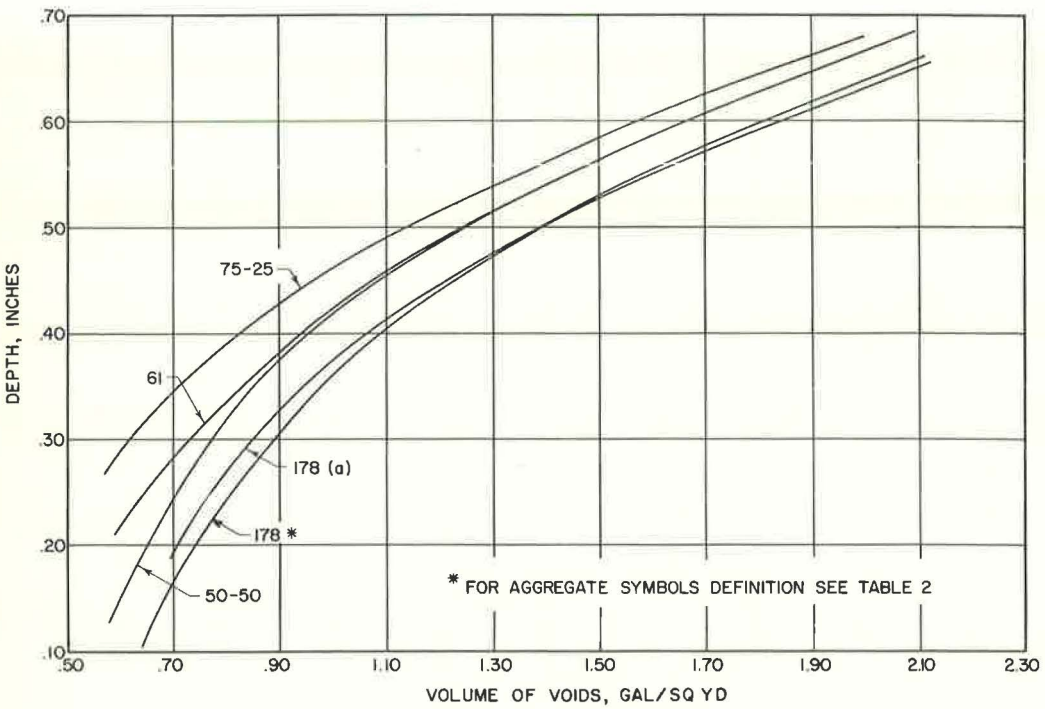

Figure 11. Variation in volume voids with depth for different aggregate types, $\frac{1}{2}$- to $\frac{3}{4}$-in. size.

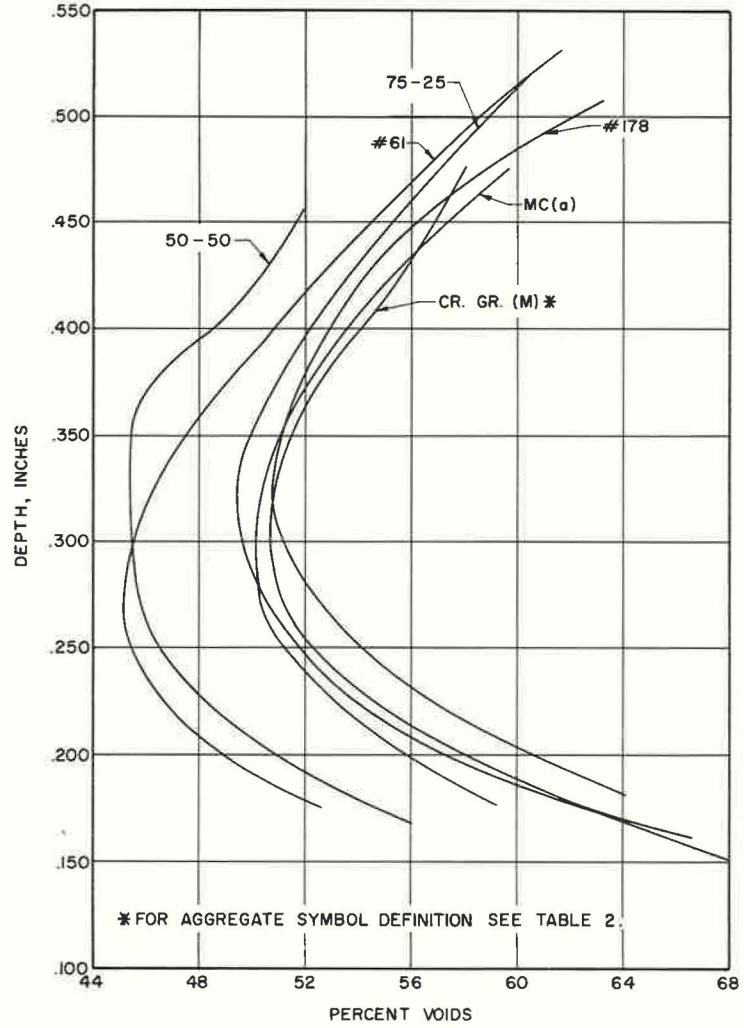

Figure 12. Variation in percent voids with depth for different aggregate types, $^{3}/_{8}$- to $^{1}/_{2}$-in. size.

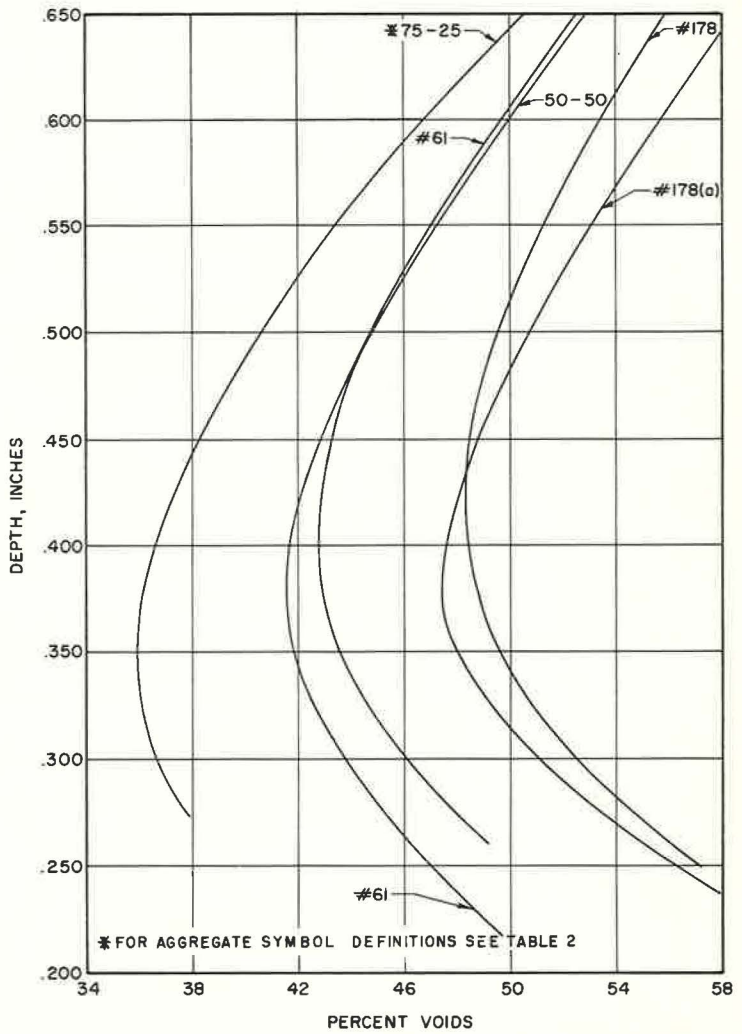

Figure 13. Variation in percent voids with depth for different aggregate types, $^{1}/_{2}$- to $^{3}/_{4}$-in. size.

VARIATION IN PERCENT VOIDS WITH SHAPE

Two questions need to be answered: Is the shape of the aggregate a significant factor in determining the quantity of voids for surface treatment design? If it is significant, how can the shape be accounted for in determining the amount of void space?

Some believe that differences in shape have little effect on the amount of void space in an aggregate layer. The data collected in this experiment indicated that this is not

TABLE 3

AGGREGATE SHAPE FACTORS

Aggregate		Shape Factor			
Symbol	Size (in.)	Compacted Voids (%)	Loose Voids (%)	Particle Index	Flakiness Index (%)
75-25	1/2-3/4	39.5	48.0	12.4	6.42
50-50	1/2-3/4	40.7	50.1	14.0	7.75
No. 61	1/2-3/4	37.9	46.5	12.2	7.60
No. 178	1/2-3/4	43.4	52.3	17.4	5.97
No. 178(a)	1/2-3/4	42.8	50.8	13.4	-
75-25	3/8-1/2	-	-	13.6	10.10
50-50	3/8-1/2	42.0	51.2	15.0	10.04
No. 61	3/8-1/2	40.6	47.8	13.7	7.67
No. 178	3/8-1/2	43.8	52.6	18.4	8.64
MC(a)	3/8-1/2	41.8	48.2	-	-
Cr Gr(M)	3/8-1/2	40.6	48.4	-	-

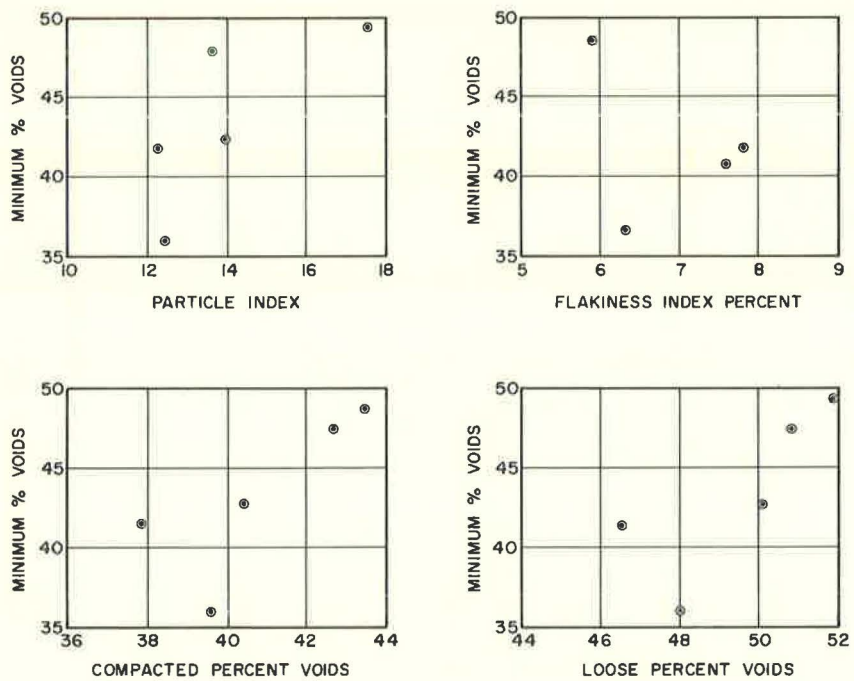

Figure 14. Variation of shape factors with minimum percent voids, 1/2- to 3/4-in. size.

true because a significant difference was found. This difference is illustrated in Figures 10 and 11 which show the variation of the volume of voids, in gallons per square yard, with depth, in inches, for aggregate samples of $\frac{3}{8}$- to $\frac{1}{2}$-in. and $\frac{1}{2}$- to $\frac{3}{4}$-in. size, respectively. The various curves in each figure represent aggregates of different shapes. In the $\frac{1}{2}$- to $\frac{3}{4}$-in. aggregate (Fig. 10), the difference between the greatest and the smallest value of volume of voids for the different aggregate samples was about 0.27 gal/sq yd. In the $\frac{3}{8}$- to $\frac{1}{2}$-in. aggregate, the difference was about 0.12 gal/sq yd. These are very significant differences in the amount of void space in an aggregate layer and, therefore, the shape of the aggregate should be considered in determining the quantity of voids.

In examining Figures 10 and 11, the range of values for the volume of voids may seem to be high when compared to values used in actual construction. The volume of voids ranges from values of 0.50 gal/sq yd to 2.10 gal/sq yd. These data are for a one-size aggregate and would most likely not be as high if the aggregate were a less uniform size or a graded aggregate. Also, the upper limit of the values of volume of voids may appear to be extremely high. Again, it must be realized that these data were obtained when the aggregate layer was completely immersed, and that by this method of investigation, when depths used are greater than the maximum size of the aggregate, there will be large values of volume of voids measured.

The data presented in Figures 10 and 11 are also presented in Figures 12 and 13 in terms of percent voids. A definite difference in the percentage of voids for the different aggregate shapes can be noted. The difference between the upper and lower values of minimum percent voids for the $\frac{1}{2}$- to $\frac{3}{4}$-in. aggregate samples was about 12 percent, whereas for the $\frac{3}{8}$- to $\frac{1}{2}$-in. aggregate samples the difference was about 6 percent.

Figures 10, 11, 12 and 13 show a general trend of the variation in voids with shape. The percentage voids in the crushed stone was approximately 6 percent greater than in the gravel. In other words, the more rounded aggregates, such as the gravels, have a smaller percentage of volume of voids than the more angular crushed stone aggregate.

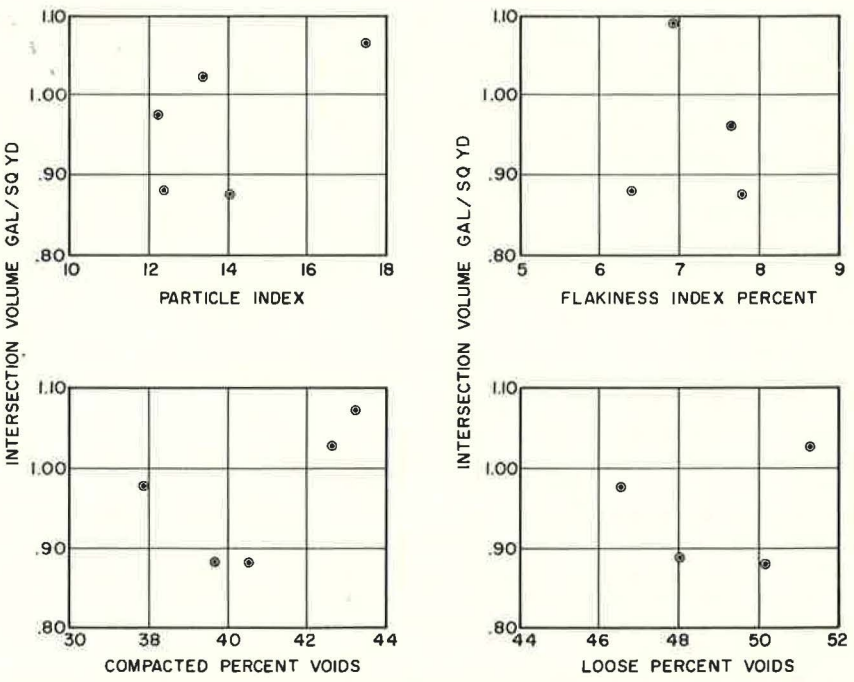

Figure 15. Variation of shape factors with intersection volume, $\frac{1}{2}$- to $\frac{3}{4}$-in. size.

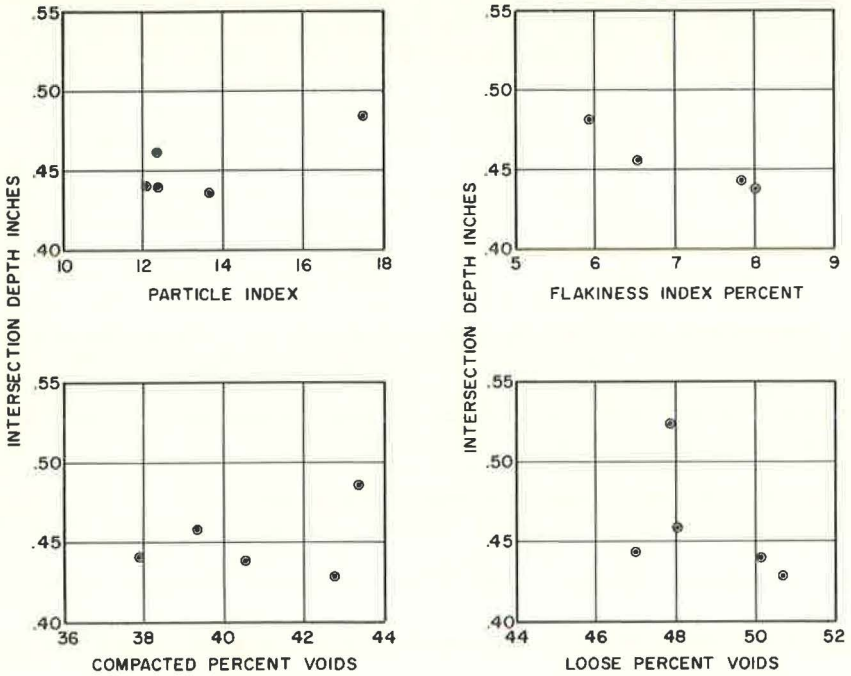

Figure 16. Variation of shape factors with intersection depth, ½- to ¾-in. size.

An attempt was made in this investigation to determine a method that would compensate for aggregate shape in determining the volume of voids in an aggregate layer. This was done by attempting to correlate aggregate parameters with some shape factor. The parameters are the minimum percent voids and the intersection coordinates previously defined in the section on variation in percent voids with depth within the aggregate layer. The intention was to correlate the parameters with some easily obtainable shape factors so that these shape factors could be used in design to account for the differences in the volume of voids produced by various aggregate shapes.

The shape factors used were particle index, flakiness index, compacted percent voids and loose percent voids. The particle index of an aggregate is determined by a test developed by Huang (3). The test to determine the particle index is fairly time consuming and tedious, but has been used with fairly good results for soil-aggregate mixtures. The flakiness index is a British standard test developed by the County Roads Board of Victoria, Australia (British Standards Institution 812). It is a numerical index used primarily to determine the average least dimension of an aggregate, but it does take shape somewhat into account. The compacted and loose percent voids are simply the percent voids in the aggregate when it is placed in a 1/10-cu ft cylinder in its densest and loosest state. The numerical values of these four shape factors for the various types of aggregate are given in Table 3.

The relationships between these four shape factors and the three aggregate parameters of minimum percent voids, intersection volume, and intersection depth are shown in Figures 14, 15 and 16, respectively, for ½- to ¾-in. aggregates. Data for aggregate of other sizes are similar to the data presented in these figures. None of these plots indicate that a logical relationship exists between the aggregate parameters and shape factors which could be used in a design method. Apparently none of these aggregate shape factors can adequately differentiate between the change in voids produced by different aggregate shapes.

Although no relationship was found in this investigation that would account for the variation in shape in determining the volume of voids, it is believed that the shape of

the aggregate must be considered in surface treatment design. If no significant relationship can be found utilizing aggregate shape factors, it may be desirable to utilize a direct measurement of the void space. Some design methods already utilize a direct measurement of void space by measuring the voids in the aggregate when placed in a hollow cylinder (1, 5). These methods do not give a true measurement of the void space because the aggregate in a surface treatment is in a single layer and not in a closely packed arrangement as it is when placed in the cylinder. Procedures similar to the one developed in this study could possibly be used to measure directly the volume of the voids in a single layer with some adaptation of the equipment for field use. Direct measurement could then possibly account for shape and differences in aggregates.

SUMMARY AND CONCLUSIONS

From the analysis of the data the following conclusions can be drawn concerning the influence of various factors on the void space in a one-size, one-particle thick, aggregate layer.

1. Contrary to the assumption made in many current procedures for designing surface treatments, the volume of voids does not vary linearly with depth within the aggregate layer. The relationship is curvilinear and varies with different aggregates.
2. The percent voids vary with aggregate size; as the aggregate size is decreased, the percent voids are increased.
3. The volume of voids tends to decrease as the particles are reoriented from a random placement to a position with their least dimension in a vertical direction. The decrease in volume is relatively small.
4. Aggregate samples of different shapes have significant differences in percent voids. This difference can be as much as 6 percent if the aggregate shape is changed from a rounded gravel to an angular crushed stone.
5. There is apparently no relationship between the aggregate parameters developed and used in this study and any of the following aggregate shape factors: particle index, flakiness index, voids in the compacted state or voids in the loose state. It seems that none of these aggregate shape factors can adequately differentiate between the change in voids produced by different aggregate shapes.
6. A suitable shape factor needs to be developed for design purposes that will tend to relate the volume of the voids to the shape of the aggregate. If this development is not possible, a direct measurement of the void space may be necessary.

ACKNOWLEDGMENTS

The research for this paper was conducted as part of the Illinois Cooperative Highway Research Project No. IHR-75, Basic Properties of Seal Coats and Surface Treatments. This project is conducted by the Engineering Experiment Station of the University of Illinois, in cooperation with the Division of Highways of the State of Illinois and the U. S. Bureau of Public Roads.

REFERENCES

1. Benson, F. J. Seal Coats and Surface Treatments. Proc. 44th Ann. Road Sch., Purdue Univ., Eng. Ext. Dept., Ser. No. 95, p. 73, Apr. 1958.
2. Hanson, F. M. Bituminous Surface Treatments of Rural Highways. Proc. New Zealand Soc. of Civ. Eng., Vol. 21, p. 89, 1934-1935.
3. Huang, Eugene Y. A Test for Evaluating the Geometric Characteristics of Coarse Aggregate Particles. Proc. ASTM, Vol. 62, 1962.
4. Kearby, J. P. Test and Theories on Penetration Surfaces. Highway Research Board Proc., Vol. 32, pp. 232-237, 1953.
5. Mackintosh, C. S. Rates of Spread and Spray in Bituminous Surface Dressing of Roads. Civ. Eng. of South Africa, Vol. 3, No. 10, p. 183, 1961.
6. McLeod, Norman W. Basic Principles for the Design and Construction of Seal Coats and Surface Treatments With Cutback Asphalts and Asphalt Cements. Proc. AAPT, Vol. 29, Suppl., 1960.

Discussion

RICHARD L. DAVIS, Technical Representative, Koppers Co., Inc., Tar and Chemical Div. —The authors are to be congratulated on writing a paper about voids in surface treatment aggregates. Although a tremendous amount of surface treatment work is done each year, the principles of good design for surface treatment construction are not very well understood. The measurement of the voids or space in surface treatment aggregates available for binder deserves study. The authors' finding that aggregate shape factors now in use cannot adequately differentiate between the change in voids produced by different aggregate shapes is very interesting.

The authors point out that the volume of voids does not vary linearly with depth within the aggregate layer for one-size aggregate, and they mention that it is usually assumed that the voids vary linearly with depth in most surface treatment design methods. Most surface treatment design methods, and specifically Hanson's design method, are concerned with the estimation of the voids or space in the mineral aggregate which will be available for bituminous material when the surface treatment has reached equilibrium under the compaction of traffic, rather than with the original void space. The voids in the mineral aggregate at equilibrium with traffic, although related to the original voids in the mineral aggregate, also depend on several other variables. Two of these are (a) the extent to which the aggregate voids are reduced when the aggregate particles are forced down into the old surface, and (b) the extent to which the aggregate voids are reduced when the aggregate particles are broken or degraded under the action of traffic.

Inasmuch as these two variables usually reduce the voids in a one-size aggregate to less than half the original value, and the contribution of each variable depends on a number of factors such as the resistance of the underlying surface to indentation and the resistance of the stone to degradation, the originators of surface treatment design methods have used a linear relationship in their design methods as is often done in complex situations when the true relationship is not very well understood.

The authors also state that voids increase as the aggregate size is decreased. Having had some experience with the method used by the authors to determine voids in the aggregate and being aware of the increasing difficulty of keeping the aggregate particles close together as the size of the particles become smaller, I can understand that greater void space was found with decrease in particle size. However, since the findings of many other investigators indicate that there is no change in void space with size of aggregate particles, it would appear desirable that the authors check their findings carefully for some explanation of the difference between their results and those of others.

This writer hopes that the authors will continue their work and that a practical, effective method of designing surface treatments will result.

JOHN L. SANER and MORELAND HERRIN, Closure—The discussion by R. L. Davis is sincerely appreciated. The authors will attempt to clarify the questions arising from this discussion. Mr. Davis points out that Hanson's design method is concerned with the void space in the mineral aggregate which will be available for bituminous material when the surface treatment has reached equilibrium under the compaction of traffic, rather than with the original void space. The authors agree that this concept is correct. The authors further agree that the reduction in voids is also due to other variables such as aggregate particle embedment and aggregate degradation. All that the authors were trying to point out in the paper is that only a small part of the reduction is due to particle reorientation from a random arrangement to a least dimension arrangement.

Mr. Davis also doubts the evidence obtained by the authors that the percent voids increases with decreasing aggregate size. He attributes this to the increasing difficulty of keeping the aggregate particles closer together as the size of the aggregate particles becomes smaller. The authors, in testing, did not notice this increasing difficulty. Even if this were true, would this not take place in the actual surface treatment?

Another factor that may have influenced test results, and one that had bothered the authors, was the effect of the surface tension of the water. It had been assumed from observing the water during testing that this effect was negligible because the of the random shape, random size, and surface texture of the aggregate particles. It was decided to check this assumption by testing an aggregate sample with a solution containing a wetting agent. The wetting agent used for this purpose was a 0.1 percent solution of detergent which reduced the surface tension to approximately one-tenth of its original value. The results obtained in testing the aggregate with the solution differ little from those obtained when testing with the water. This serves to prove that the authors' assumption of the negligible effect of surface tension is correct.

Analysis of Flexible Paving Mixtures by Theoretical Design Procedure Based on Shear Strength

WILLIAM L. HEWITT, Associate Professor of Civil Engineering, Cornell University

Instrumentation for the preparation and testing of flexible paving mixtures in flexure, tension, and triaxial compression is described. The influence of test temperature and rate of loading on asphalt concrete is developed. Mixture variables in the investigation include aggregate gradation, asphalt content, penetration and viscosity of asphalt, binder blend using flake asphalt and polyethylene, Viadon binder content, and asbestos fibers in mixture. Mixtures are analyzed for suitability to resist compressive stresses in the pavement surface course. The practical application of this procedure to design is shown.

•THE ANALYSIS or design of a mixture for the surface course of a flexible pavement should consider the shear strength properties of the mixture under critical service conditions. Present standard test procedures for the strength of mixtures are empirical and, as such, preclude theoretical analysis. The surface of a flexible pavement structure in service is subjected to flexural, tensile, and compressive stresses. The determination of the resistance of paving mixtures to these stresses for purposes of design necessitates the development of suitable instrumentation for the preparation and testing of test specimens. During the past 2 years, the author designed equipment for the testing of mixtures in flexure, tension, and compression, including the triaxial cell. It is the purpose of this paper to present the instrumentation and test results obtained for various mixtures under varying conditions of test. An analysis of these mixtures by an equation (1, 2) based on shear strength is included. The application to design practice is introduced.

FACTORS IN DESIGN OF FLEXIBLE PAVING MIXTURES

Shear Strength

The resistance which a flexible pavement component offers to plastic displacement from the application of wheel loads depends on the shear strength of the component. Shear strength is developed through intergranular friction as measured by the angle of internal friction, ϕ, and through the internal resistance of the binder to shear as measured by cohesion, c. These stress constants have been determined graphically from Mohr diagrams for this presentation, following an established procedure.

Internal Friction.—This factor is influenced by the density of the mix and by the properties of the aggregate such as hardness, surface texture and shape. Density of mix is a function of (a) aggregate gradation, (b) amount and viscosity of asphalt and (c) compactive effort. For a given gradation of aggregate there is an optimum asphalt content at which the mix will produce maximum density for a given compactive effort. An increase in compactive effort tends to reduce the optimum asphalt content. For a given aggregate and binder content the internal friction, ϕ, varies with density of mineral aggregate. Of primary importance in the design of asphalt mixes is the gradation of the mineral aggregate.

Paper sponsored by Committee on Mechanical Properties of Bituminous Paving Mixtures.

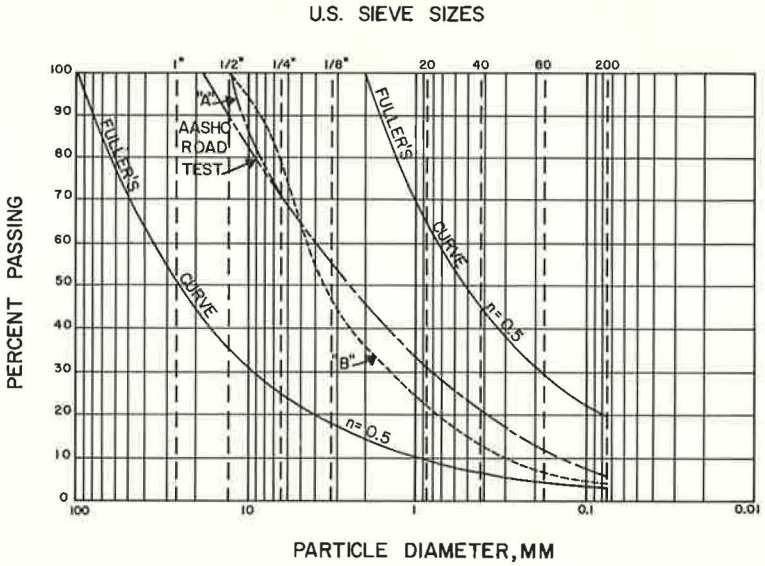

Figure 1. Gradation curves for aggregate used in paving mixtures.

Soon after the beginning of the present century, Fuller showed that aggregate will have a relatively high density when its particle size distribution follows the equation

$$P = 100\left(\frac{S}{M}\right)^n \tag{1}$$

where

P = percent of total aggregate passing any particular sieve,
S = size along side of sieve opening,
M = size of largest piece of aggregate, and
n = a constant.

Since that time Fuller's findings have been widely accepted, with most authorities agreeing that the value of n is approximately 0.5 for both soils and aggregates. The value of 0.5 has become popular, mainly because of the ease with which it may be used. When plotted on a semilogarithmic graph having a vertical arithmetic scale representing P and a horizontal logarithmic scale representing S, Fuller's equation becomes a sagging curve. Figure 1 gives two such curves, along with gradations A and B as used in this investigation.

Fuller's equation becomes a straight line when drawn on a graph having logarithmic scales along both axes. To show how this is possible, we take the logarithms of both sides of Eq. 1, which gives

$$\log P = \log 100 + n \log S - n \log M = K + n \log S \tag{2}$$

where K is some constant which depends only on the size of the largest piece of aggregate. Eq. 2 is in the form of the equation for a straight line having customary x and y axes ($y = ax + b$) if $y = \log P$, $a = n$, $x = \log S$, and $b = K$.

Mixes which plot with a straight-line slope of 0.5 on the log-log graph are very tight and optimum asphalt content is on the low side (4.0 to 5.0 percent for ½-in. maximum size aggregate). Such mixes are difficult to work and would probably present problems in construction. This agrees with work by McLeod (3) in his analysis of void requirements for dense-graded paving mixtures. The plot for gradation B approaches a straight line but has a slope of about 0.65.

Cohesion.—This mix property is dependent on the asphalt binder and is developed through the adhesion of the binder to the aggregate and through the internal resistance of the asphalt to deformation. The amount of cohesion developed in an asphalt mix is influenced by: (a) amount of asphalt cement in the mix, (b) thickness of asphalt film, (c) rate of load application, and (d) temperature of the mix. Viscous resistance is influenced by the rate of deformation; i. e., the higher the rate of application the greater the resistance. The AASHO Road Test showed that static load deflections were about twice those at 50 mph (4). Asphalt is also more viscous at low than at high temperatures. On the basis of shear strength, high summer temperatures are critical and it would be at this time that surface-originated deformations develop.

Voids in Mix

The voids in an asphalt paving mixture are controlled by specifying the range of air voids in the mixture (referred to as voids in total mix), prescribing the range for voids in mineral aggregate which is to be filled with asphalt, and controlling the voids in the mineral aggregate. McLeod (3) has stated that a minimum of 15 percent voids should be provided in the mineral aggregate to assure adequate space for the asphalt binder. This is controlled by aggregate gradation and normally requires some deviation from the Fuller curve ($n = 0.5$). The requirement for air voids in total mix is about 3 to 5 percent with 75 to 85 percent of the aggregate voids filled with asphalt. It is generally a stipulation that voids be determined on the basis of apparent specific gravity of aggregate; however, some procedures require the bulk specific gravity and McLeod (3) suggests that an effective specific gravity should be employed which gives values between apparent and bulk. The problem of selection of the appropriate specific gravity relates to permeable voids in the surface of the aggregate and would be a serious problem only for rather porous aggregates. The purpose of establishing a minimum of air voids in the mix is to provide some space for in-service compaction and to prevent loss of internal friction, ϕ, through lubrication, thus causing excessive surface deformation and possible bleeding of the surface. A maximum permissible air voids content is stipulated to insure a mix of low permeability and to reduce hardening of the asphalt binder by oxidation and loss of volatiles.

Flexibility

Flexibility is a measure of the magnitude of flexural deflection which a component of a flexible pavement structure can withstand without fracture. For more permanent flexible pavements, the deflections should be small. The best flexible pavement is one which produces the least flexural strains. A flexible pavement is designed to resist shear stresses; a rigid pavement is designed to resist flexural stresses. The term flexible should not be taken too literally in the design of asphalt mixtures. The difference in the magnitude of deflection for properly designed rigid and flexible pavements is small.

The requirement for flexibility in an asphalt surface mixture is influenced by the total pavement structure. Flexure failures are normally related to low temperatures of the surface and high moisture content in the subgrade or road base structure. Some flexure cracking may develop through fatigue failure, which is influenced by the magnitude of deflection and the viscosity and amount of binder. It has been shown (6) that for high deflection a thin pavement section can withstand flexural fatigue better than thick sections. Consequently, if a pavement structure is to permit high surface deflections, it might be advisable to provide a thin surface course in design.

Surface Texture

The design of a surface mixture would not be complete without consideration of the non-skid properties and abrasion resistance of the surface. It may be possible to design a mixture satisfying the requirements for shear strength, voids, and flexibility with aggregate of $\frac{1}{8}$-in. maximum size; however, this mixture probably would not provide the skid resistance required on heavy-duty rural roads. The maximum size of aggregate specified for a mixture, and to some extent the gradation, serve to provide desired surface texture.

MIXTURE DESIGN BASED ON SHEAR STRENGTH

Design Equation

The design of flexible pavements should give primary consideration to the shear strength of the various components of the pavement structure. The author has developed a design procedure based on strength theories of soil mechanics (1), which is briefly described here. The design equation is as follows:

$$\gamma z + p\left[1 - \left(\frac{1}{1 + \left(\frac{a}{z}\right)^2}\right)^{3/2}\right] = \gamma z\left[\frac{1 + \sin\phi}{1 - \sin\phi}\right]^2 + \frac{4c}{1 - \sin\phi}\left[\frac{1 + \sin\phi}{1 - \sin\phi}\right]^{1/2} \quad (3)$$

in which

p = surface contact pressure,
a = radius of equivalent circular contact area,
z = thickness of flexible pavement structure,
γ = bulk density (unit weight) of surcharge material,
ϕ = angle of internal friction of bearing material, and
c = cohesion of bearing material.

Eq. 3 is applicable to any layer of the flexible pavement structure. For instance, if z = 0, the equation could be applied to surface mixtures, and would be reduced to

$$p = \frac{4c}{1 - \sin\phi}\left[\frac{1 + \sin\phi}{1 - \sin\phi}\right]^{1/2} \quad (4)$$

The left side of Eq. 3 contains the familiar Boussinesq expression for the vertical intensity of stress along the axis below a circular loaded area, plus the intensity of stress due to the weight of the pavement. The right side of the equation gives the resistance which must be developed in the pavement at depth z if failure of an element from vertical stress is prevented. Lateral confinement is provided by the passive lateral pressure of a wedge of the pavement component subjected to a vertical load equal to the weight of the overlying pavement. Eq. 4 is identical to the McLeod (2) stability equation developed from the Mohr diagram for bituminous paving mixtures.

Because of the various assumptions made in the development of a design procedure based on the strength of materials, such a procedure must be substantiated by engineering practice. This should not detract from the soundness of the procedure but will help explain the reaction of materials to service conditions. Pavement loading and environmental conditions are difficult to simulate in the laboratory, and for this reason a correlation with either service performance or an established design procedure is essential.

Traffic Factor

The design equation for surface mixtures should include a traffic factor, T, to provide for variations in traffic volume and loading. The effect of this factor is to require a thicker and stronger pavement component for a heavy-duty pavement as compared with the requirement for a roadway having light to moderate traffic. The design equation for surface mixtures may then be written:

$$pT = \frac{4c}{1 - \sin\phi}\left[\frac{1 + \sin\phi}{1 - \sin\phi}\right]^{1/2} \quad (5)$$

Suggested traffic factors for design are as follows:

Highway, light traffic, short life—1.0;
Highway, moderate traffic, medium life—1.5;

Highway, heavy-duty—2.0; and
Airport taxiways, aprons, hardstands, runway ends—2.0.

INSTRUMENTATION

Two current standard testing procedures for the determination of the strength of bituminous mixtures (7) are the Marshall method (ASTM Designation: D 1559) and the Hveem method (ASTM Designation: D 1560). These are both empirical tests and because of specimen dimensions and test procedure, the data obtained cannot be subjected realistically to a theoretical analysis of stresses for purposes of pavement design. There exists at present no standard procedure for the testing of paving mixtures in flexure, tension, or triaxial compression. The standard procedure for the testing of paving mixtures in compression (ASTM Designation: D 1074-60) uses a specimen of low height-to-diameter ratio which would be unacceptable in a rational approach to the design of paving mixtures.

For a number of years there appeared in the mix design manual of the Asphalt Institute (8) the Smith triaxial method for the design of asphalt paving mixtures. The procedure is not included in the current issue of this manual. The basis for design by the Smith triaxial method (9) was the shearing resistance of the paving mixture. Correlating studies with pavements in service indicated that the procedure could be used to determine the suitability of mixtures.

For some reason the Smith triaxial method has not been widely accepted, even though desirable test specimen dimensions are used and values of the angle of internal friction and cohesion are obtained. The fact that the closed-system rather than the open-system triaxial test is used should not be a practical deterrent because fewer specimens are required in a testing program even though the data may not be theoretically correct. The primary reasons for the failure of the Smith triaxial method to receive wide acceptance seem to be specimen preparation procedure and specimen size.

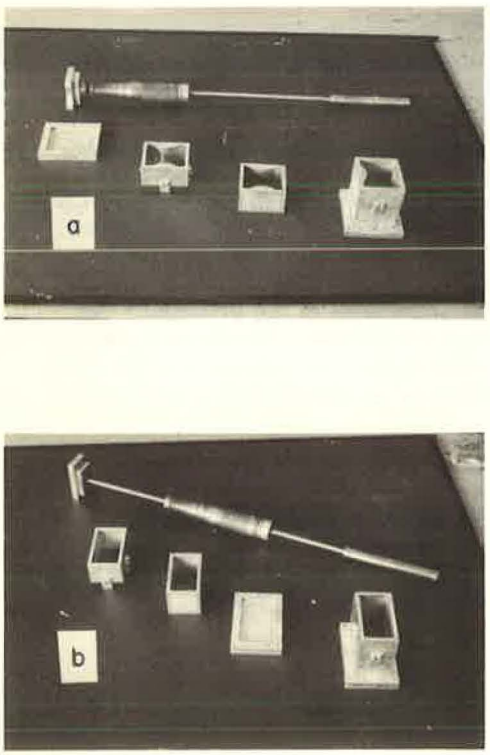

Figure 2. Compaction mold and hammer for (a) tension specimen and (b) compression and flexure specimen.

Specimen Preparation

A practical procedure, which may be applicable to both field and laboratory use, is desirable for the preparation of test specimens for flexure, tension, and triaxial compression. Triaxial specimens should have a ratio of height to minimum cross-section of 2.0. The same compaction procedure should be used for specimens for the flexure, tension and triaxial compression tests. Provision for dynamic compaction of the type used in the preparation of Marshall specimens would be desirable when considering possible field use because of portability.

The author has designed equipment providing specimens of desired dimensions which will require the same compactive effort as the standard Marshall test. All molds were designed to have the same surface area as a Marshall specimen. In this way, the same compactive effort should produce about the same density as the Marshall specimens. The tension specimen

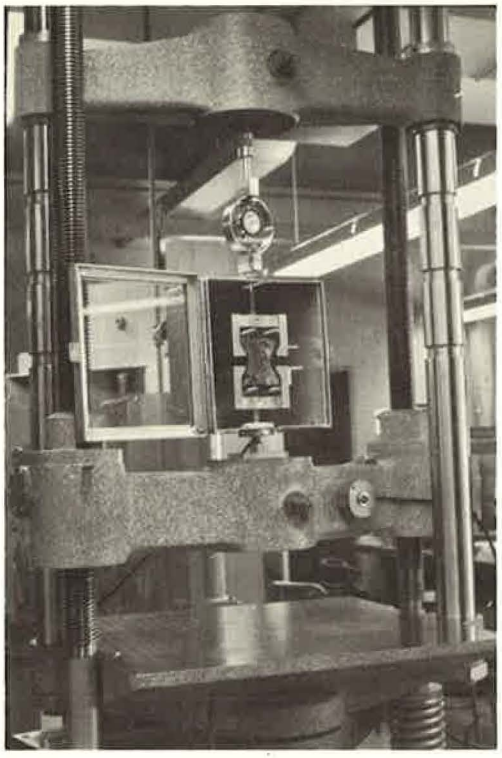

Figure 3. Tension apparatus with specimen in position for test.

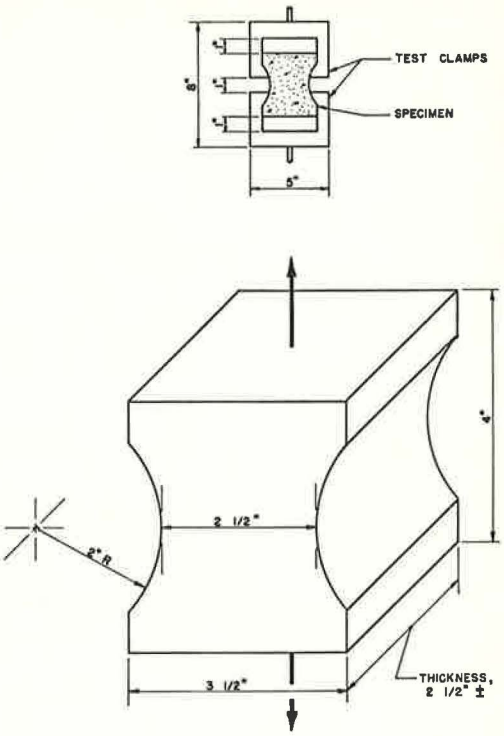

Figure 4. Principal dimensions for tension specimen and tension test clamps.

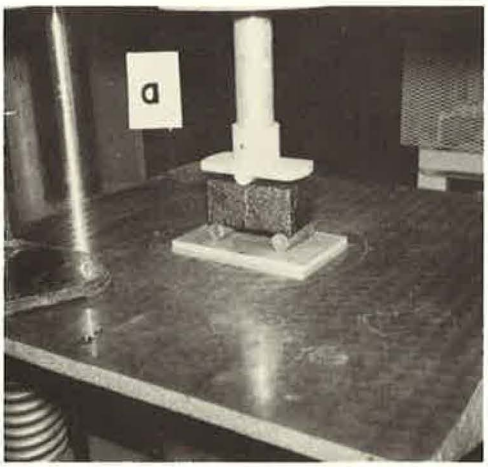

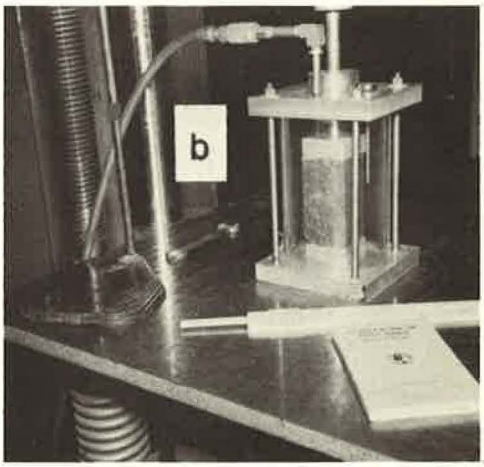

Figure 5. Specimens in position for test: (a) flexure, and (b) triaxial compression.

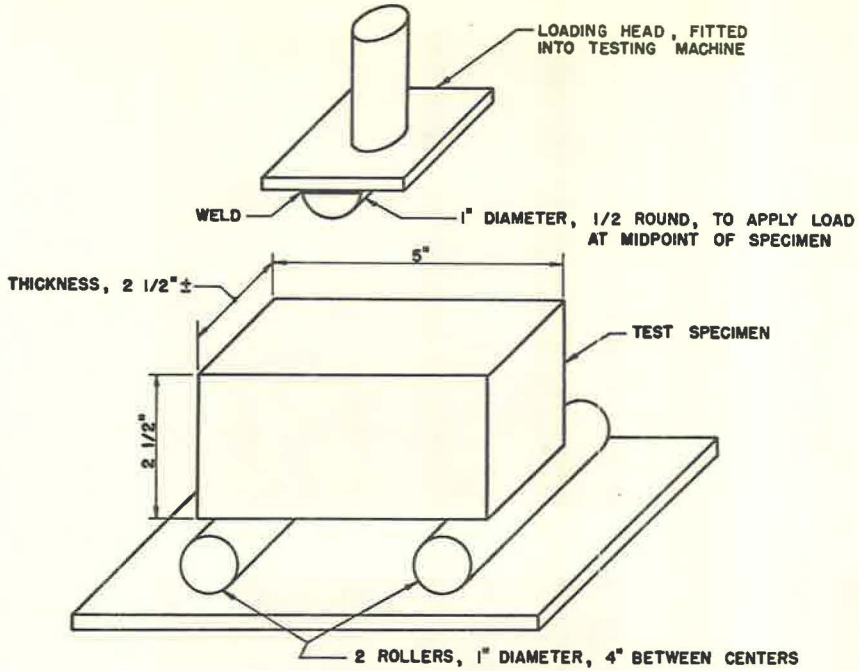

Figure 6. Flexure apparatus.

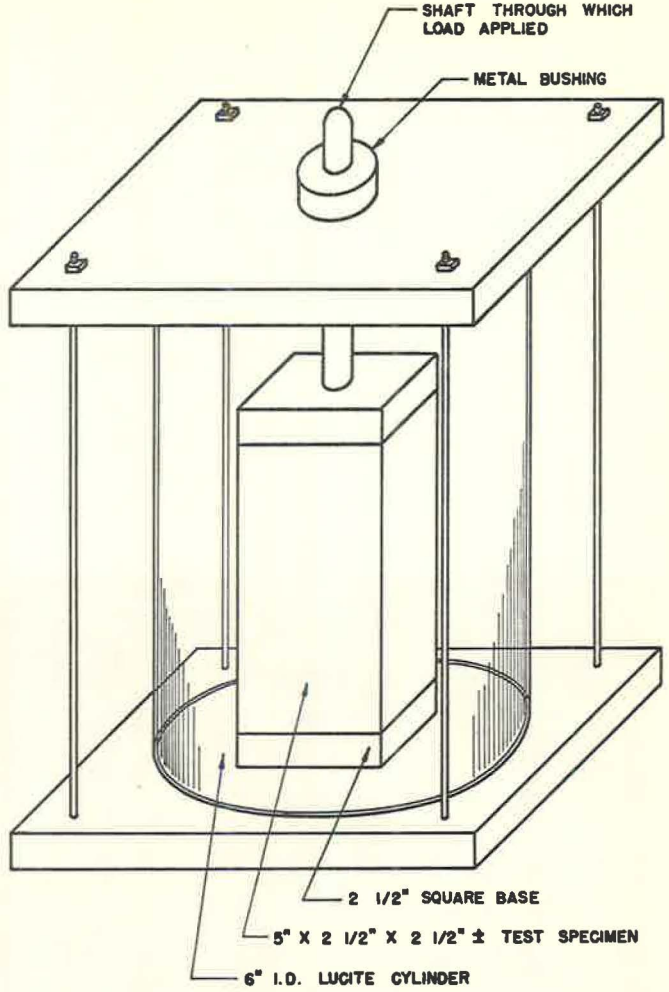

Figure 7. Triaxial cell for specimen having square cross-section.

has a minimum cross-sectional area of 2 ½ in. by the height of the specimen, which may vary slightly from 2 ½ in. Tension specimens are molded with flat top and bottom surfaces and with a shoulder at the ends for tension clamps. The unconfined compression, flexure, and triaxial specimens are made in the same molds and differ fron one another only in the manner in which they are tested. These specimens are 5 in. long, 2 ½ in. wide, and approximately 2 ½ in. high. All specimens are compacted in the same manner as the Marshall specimens—50 blows on each side of the specimen by a 10-lb weight dropping 18 in. The only differences among the compaction hammers are the shapes of the hammer ends necessitated by the different shapes of the molds. The equipment for specimen preparation is shown in Figure 2.

Both the Marshall and Hveem specimens have a minimum dimension of 2 ½ in., which is the same as the minimum dimension for flexure, tension, and triaxial compression specimens prepared in this investigation. The molds used gave satisfactory performance for mixtures having a maximum size aggregate of ½ in. They are considered adequate for mixtures having aggregate as large as ¾ in.

Strength Test Instruments

The tension apparatus used in this investigation is shown in Figures 3 and 4. The tensiometer was adapted to a Universal testing machine. This apparatus was designed with a grooved baseplate and grooved cover plates with the idea that these would be required to hold the specimen in position during the test. It was discovered, however, that the shoulder clamps were adequate. A thermostatically controlled box is provided for temperature control.

Figure 5 shows flexure and triaxial specimens in position for testing. The beam-shaped flexure specimen is tested under simple midspan bending conditions. The specimen is supported on unrestrained 1-in. diameter steel rollers spaced 4 in. apart, and the load is applied vertically through a restrained 1-in. diameter steel bar placed midway between the roller supports. The vertical dimension of the flexure specimen in test position was always 2 ½ in. for the data reported in this paper. A sketch of the flexure test apparatus is shown in Figure 6.

The triaxial cell was designed for testing of a specimen having a square cross-section, as shown in Figure 7, using compressed air for lateral confinement. A rubber membrane surrounds the test specimen and is held in place by rubber bands. An air bleeder valve is provided for drainage from the specimen during the test. The triaxial cell is set in the thermostatically controlled box during test at temperatures other than 80 F. A water bath is used for temperature control before testing.

MATERIALS

Aggregate

The limestone aggregate used in mixtures in this investigation was obtained from the Cayuga Crushed Stone Co., a source approved by the State of New York Department of Public Works for bituminous mixtures.

Aggregate was obtained from stockpiles and was oven-dried before separation into desired fractions with the Gilson machine. The fractions retained on the No. 20 sieve and larger were then washed and oven-dried before batching. This washing operation was considered essential to provide desired control on aggregate composition.

The mixtures were prepared using either gradation A or B, as shown in Figure 1. Actual values for gradation and the apparent specific gravity for each aggregate combination are given in Table 1.

Binder

A number of materials were used in various combinations and at different binder contents. The investigation was designed to show the effect of type of binder on the strength characteristics of paving mixtures. In this connection polyethylene from two sources was used as a part of the binder in some mixtures. The material most widely used, however, was 85-100 penetration grade asphalt cement.

TABLE 1

AGGREGATE PROPERTIES

Property	Value	
	Gradation A	Gradation B
Passing sieve, %:		
½ in.	100	100.0
½ in.	70	78.6
⅛ in.	55	47.1
No. 20	31	21.4
No. 80	12	7.5
No. 200	6	4.3
Apparent sp. gr.	2.723	2.708

TABLE 2

PHYSICAL PROPERTIES OF ATLANTITE 2 FLAKE ASPHALT

Property	Value
Sp. gr. at 60 F	1.06
Wt/gal	8.89
Flash pt. (C. O. C.), °F	560
Softening pt. (R & B), °F	300
Penetration:	
At 77 F, 100 g, 5 sec, 0.01 mm	2
At 150 F, 200 g, 60 sec, 0.01 mm	38
Saybolt Furol viscosity at 450 F, sec	810

TABLE 3

TENITE POLYETHYLENE 840A PHYSICAL PROPERTY DATA

Property	Value
Melt Index	20 ± 3
Density	0.923
Brittleness temp., C	-12
Tensile strength, psi:	
At fracture	1,760
At upper yield	1,840
Elongation, %	50
Thermal coef. of expansion, in./in./° F	11×10^{-5}
Melt temp., F	230
Water absorption, %	0.01

Asphalt cement was obtained at the Three Rivers plant of the Atlantic Refining Co. Flake asphalt (Atlantite 2), having physical properties as presented in Table 2, was provided by the Atlantic Refining Co. from their Philadelphia plant. Asphalt cement of 85-100 penetration was blended at 450 F with 20 percent flake asphalt (Atlantite 5) to obtain a binder having a penetration of 12.

The Allied Chemical Corp. provided A-C polyethylene 629 and A-C polyethylene 680. The 680 grade is slightly harder than the 629 grade. Some of its typical physical properties are as follows:

Softening point, 229 F;
Density, 0.94;
Acid number, 16;
Hardness, 2.

Eastman Chemical Products, Inc., supplied Tenite polyethylene which is a rather tough material of high tensile strength. A melt temperature of 230 F required elevated temperatures for mixture preparation. Typical physical property data for Tenite polyethylene 840 A are given in Table 3.

Both types of polyethylene were of low to medium molecular weight having density slightly below that for asphalt cement. A precaution was taken to prevent prolonged heating of this material at elevated temperatures.

Indopol polybutene (H-300) was provided by the Amoco Chemical Corp. and was used as a blending agent with A-C polyethylene 629. Parallel tests by the Marshall method were conducted to determine the effect of replacing 10 percent A-C polyethylene 629 with polybutene, and there was no significant difference between the Marshall stability and flow values for mixtures having binder contents of 3, 4, 5, 6, and 7, percent.

Viadon, a petrochemical binder, was provided by the Humble Oil and Refining Co. Physical properties are not included in this paper.

Asbestos fibers (7M) were used in one series of tests to show their effect on the strength characteristics of asphalt concrete. These fibers were used at a rate of application of 2 percent of the total mix with gradation B mixture which has 4.3 percent passing the No. 200 sieve.

TEST SPECIMEN PREPARATION

Binder Content

The binder content used for most of the mixtures was determined by the Marshall method of mix design. Duplicate specimens were prepared at various binder contents with the ultimate selection of binder content for various strength specimens based on air voids in total mix and stability. In most instances voids fell within the range of 3 to 5 percent.

Asphalt Concrete

In the preparation of paving mixtures using 85-100 penetration grade asphalt, both the aggregate and asphalt were heated to 300 F. Aggregate had been batched for single specimens and was allowed to remain in an electric oven for a minimum of 12 hr before mixing. The asphalt was brought to temperature in an electric pot from which it was weighed directly into a mixing bowl containing the aggregate for a single specimen. The material was mixed with an electric mixer for 1 min. The mix was then placed in a heated mold, rodded 25 times, and compacted with a dynamic hand-operated compactor. The molds were placed under running water to cool before extrusion. Water was permitted to fall directly on the mold rather than on the specimen to reduce water absorption into the specimen before dry weight for density determination could be made. In most instances, specimens were tested the day after they had been prepared.

The temperature of both aggregate and asphalt was raised to 350 F for mixtures using asphalt cement having a penetration of 12.

Asphalt Cement—Flake Asphalt Binder

Mixtures in which flake asphalt was included in the binder with 85-100 penetration grade were prepared by heating the aggregate to 450 F, adding the flake asphalt in dry form, and mixing until the asphalt was melted and distributed. The desired amount of penetration grade asphalt was then weighed in at 300 F followed by 1 min of mechanical mixing.

A-C Polyethylene

In the preparation of mixtures containing A-C polyethylene 629 or 680 blended with 85-100 penetration grade asphalt, both the stone and asphalt were heated to 300 F, the desired amount of asphalt was added to the aggregate followed by mechanical mixing to obtain uniform distribution, and the polyethylene was added in dry form with additional mechanical mixing.

For the mixture having a binder blend of A-C polyethylene 629, Indopol polybutene H-300, flake asphalt, and 85-100 penetration grade asphalt, the asphalt cement was heated to 450 F and the aggregate to 550 F. Flake asphalt was added first to the heated aggregate, followed by penetration grade asphalt and mechanical mixing. After blending and distribution of the asphalt binder with the aggregate, the A-C polyethylene 629 was added in dry form with continued mixing.

Tenite Polyethylene

Two series of test specimens were made using a blend of Tenite polyethylene and 85-100 penetration grade asphalt. The binder was prepared by heating the asphalt to 500 F and blending Tenite with the asphalt in an asphalt pot. The blend was held at this temperature for application to the stone, also heated to 500 F. The material was then mixed mechanically until thorough distribution was obtained. Compaction temperatures were normally about 350 F.

Mixtures having a blend of flake asphalt (Atlantite 2) and Tenite as binder were prepared by first applying the dry asphalt to stone at 550 F, followed by mechanical mixing, the addition of dry polyethylene, and continued mixing.

Viadon

The procedure recommended by the Humble Oil and Refining Co. for the preparation of laboratory specimens using Viadon binder was followed. This consisted of heating the total aggregate to 425 ± 10 F and placing it in a heated mixing bowl. The dry resin was added while mixing, followed by the addition of the plasticizer and colored paste. The colored paste was weighed on a small piece of polyethylene film, and the film and paste were added to the mix.

TABLE 4

INFLUENCE OF TEST TEMPERATURE ON STRENGTH OF ASPHALT CONCRETE[a]

Temperature (° F)	Flexure (MR) (psi)	Tension (psi)	Triaxial Compression (psi)		
			0-Psi Lat.	15-Psi Lat.	30-Psi Lat.
40	526	120	426	511	641
80	71	14	107	169	221
110	25	6	63	118	179
140	14	1.5	33	83	174

[a]Average of duplicate specimens using gradation A, 6 percent asphalt (85-100 penetration), 0.05-in./min loading.

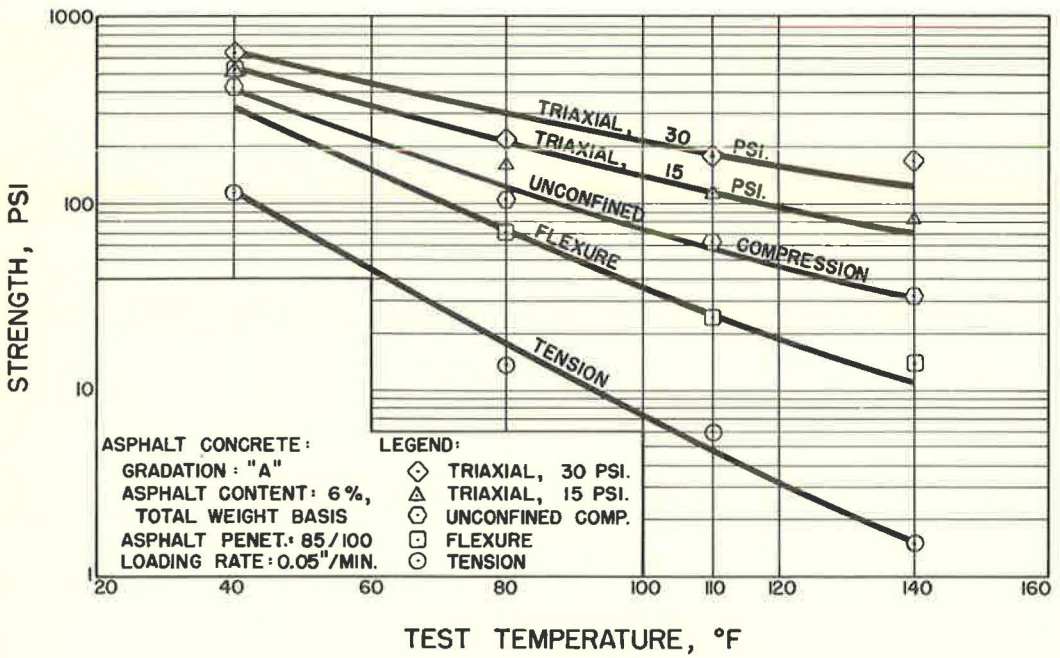

Figure 8. Influence of test temperature on strength of asphalt concrete.

Asbestos Fibers in Mixture

Both the stone and 85-100 penetration grade asphalt were heated to 300 F. The asbestos fibers were added to the dry stone and dry mixed as would be the case in the addition of a mineral filler at the plant. The asphalt was then added with mechanical mixing.

TEST RESULTS AND DISCUSSION

Test Temperature

The influence of test temperature on the strength of asphalt concrete with aggregate gradation A and 6 percent 85-100 penetration grade asphalt, tested at a rate of loading of 0.05 in./min, is indicated in Table 4 and Figure 8. Flexure, tension, unconfined compression and triaxial tests were run. The significant observation from this series of tests is the tremendous influence of temperature on the tensile strength of asphalt concrete. As the temperature is lowered from 140 to 40 F, the tensile strength increases more than 50 times. Lateral confinement of a test specimen tends to reduce the effect of temperature on shear strength.

The Mohr diagram using the unconfined compression and triaxial data was drawn on sheets of 11- by 17-in. graph paper from which the angle of internal friction and cohesion were obtained. A part of this investigation was a determination of whether or not the tension test along with the unconfined compression test could be used to determine the shear strength parameters of friction and cohesion. In Figure 9 the dashed line is made tangent to the tension and unconfined compression curves, giving a visual indication of the difference which may be expected by the two methods. The influence of test temperature on the angle of internal friction and cohesion is indicated in Figure 10 and Table 5. Cohesion increases with a decrease in temperature; however, the angle of internal friction as determined in this test decreases with a decrease in temperature from 140 F to about 95 F, at which point the friction angle as

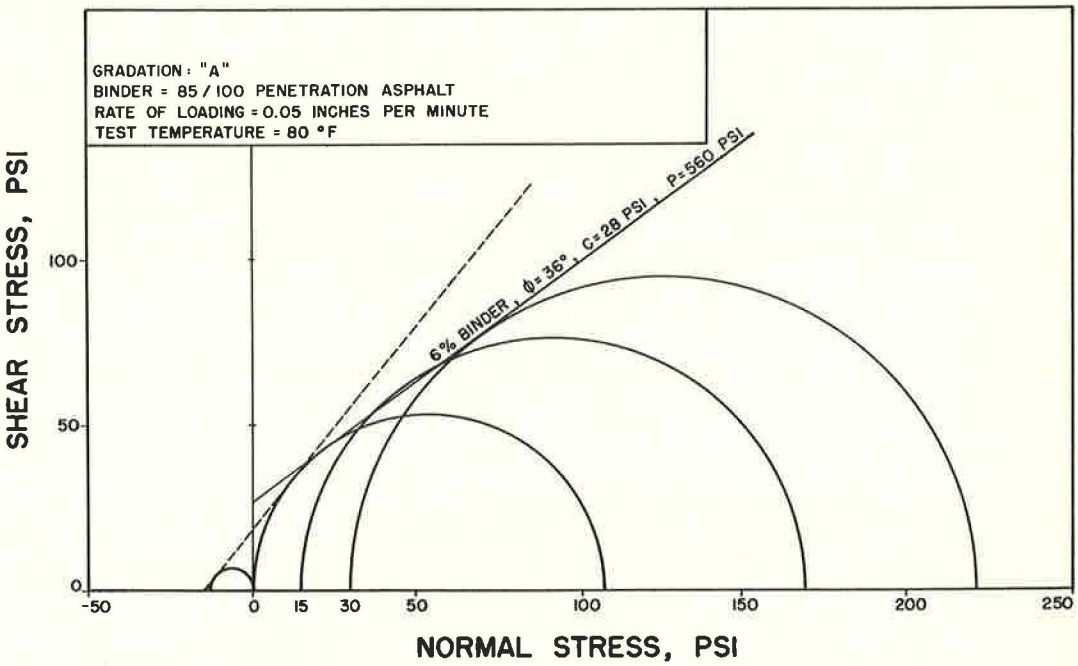

Figure 9. Mohr diagram for asphalt concrete; angle of internal friction and cohesion determined from triaxial compression circles.

TABLE 5

SHEAR STRENGTH PROPERTIES OF ASPHALT CONCRETE[a]

Temperature (° F)	Rate of Load (in./min)	Triaxial Data			Tension-Comp. Data		
		ϕ (deg)	c (psi)	p^b (psi)	ϕ (deg)	c (psi)	p^b (psi)
140	0.002	43	1	29	-	-	-
140	0.05	40	6	145	61	3	372
140	0.5	39	14	310	53	10	600
140	2.0	38	18	390	50	14	653
40	0.05	50	75	3,500	34	115	2,070
80	0.05	36	28	560	51	20	512
110	0.05	36	16	300	55	10	706

[a]Based on duplicate specimens of gradation A, 6 percent asphalt (85-100 penetration).
[b]From Eq. 4.

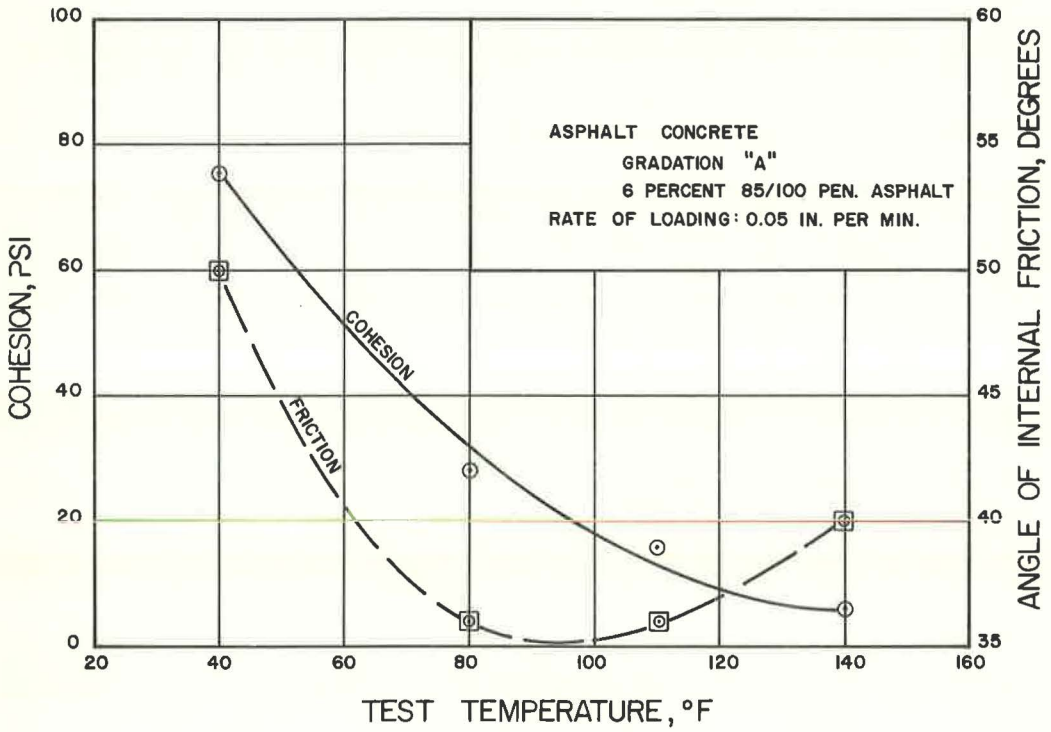

Figure 10. Influence of test temperature on angle of internal friction and cohesion for asphalt concrete.

determined from the Mohr diagram increases rapidly with a further decrease in temperature. Doyle (10) states that, at low temperatures, asphalt reacts somewhat as a solid, so this may be the explanation for the friction curve as shown in Figure 10.

The values of the angle of internal friction and cohesion as shown in Figure 10 were used to compute pavement resistance to vertical contact pressure using Eq. 4. When plotted on a log-log graph (Fig. 11), the relationship between pavement resistance and temperature gives a straight line. In making a determination of the influence of temperature on pavement resistance for purposes of design, it is found that pavement resistance as computed by Eq. 4 is four times greater at 80 F than at 140 F.

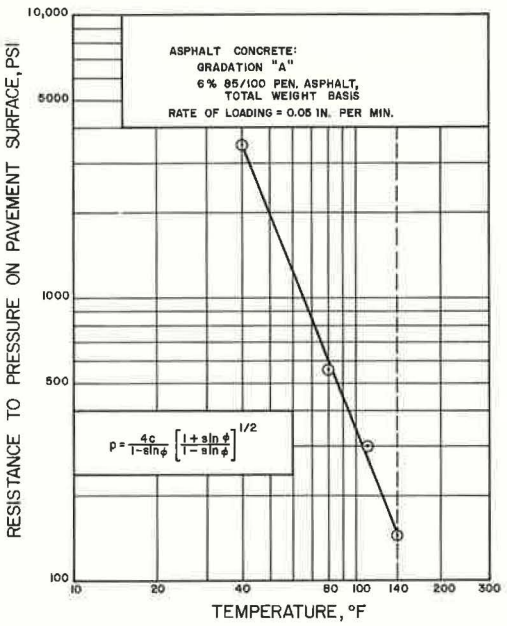

Figure 11. Influence of temperature on pavement resistance to vertical contact pressure.

Rate of Loading

The influence of rate of loading on strength of asphalt concrete is indicated in Table 6 and in Figure 12. It is again apparent that the tensile strength of asphalt concrete is very sensitive to test conditions. The tensile strength at 2.0 in./min is more than 50 times the tensile strength at 0.002 in./min. Lateral confinement of test specimen tends to reduce the effect of rate of loading on strength.

The influence of rate of loading on the angle of internal friction and cohesion for asphalt concrete tested at 140 F is indicated in Table 5 and Figure 13. Also given in Table 5 are values of the angle of internal friction and of cohesion as determined from the tension-unconfined compression data at various test temperatures and rates of loading. It is significant that there is not a consistent relationship between these data and those determined from triaxial compression tests. It was concluded that triaxial tests should be used for the determination of shear strength data.

The influence of rate of loading on pavement resistance to vertical contact pressure as computed using Eq. 4 is indicated in Table 5 and Figure 14.

Table 7 presents data on the influence of test temperature and rate of loading on the flexural strength and magnitude of deflection at failure for asphalt concrete. These data show that the magnitude of deflection at failure increases with an increase in rate of loading and with a decrease in test temperature. The influence of rate of loading on deflection for the flexure test is shown in Figure 15.

Asphalt Content

The influence of asphalt content on unconfined and triaxial compression for asphalt concrete having aggregate gradation B and tested at 80 F and 0.05-in./min rate of loading is shown in Table 8 and in Figure 16. The Mohr diagram for a binder content of 6 percent is shown in Figure 17. This may be compared with the Mohr diagram

TABLE 6

INFLUENCE OF RATE OF LOADING ON STRENGTH OF ASPHALT CONCRETE[a]

Loading Rate (in./min)	Flexure (MR) (psi)	Tension (psi)	Triaxial Compression (psi)		
			0-Psi Lat.	15-Psi Lat.	30-Psi Lat.
0.002	1.6	0.16	4.2	-	-
0.05	14	1.5	33	83	174
0.5	13	6.8	55	94	181
2.0	30	9.8	74	131	199

[a]Average of duplicate specimens of gradation A, 6 percent asphalt (85-100 penetration), 140 F.

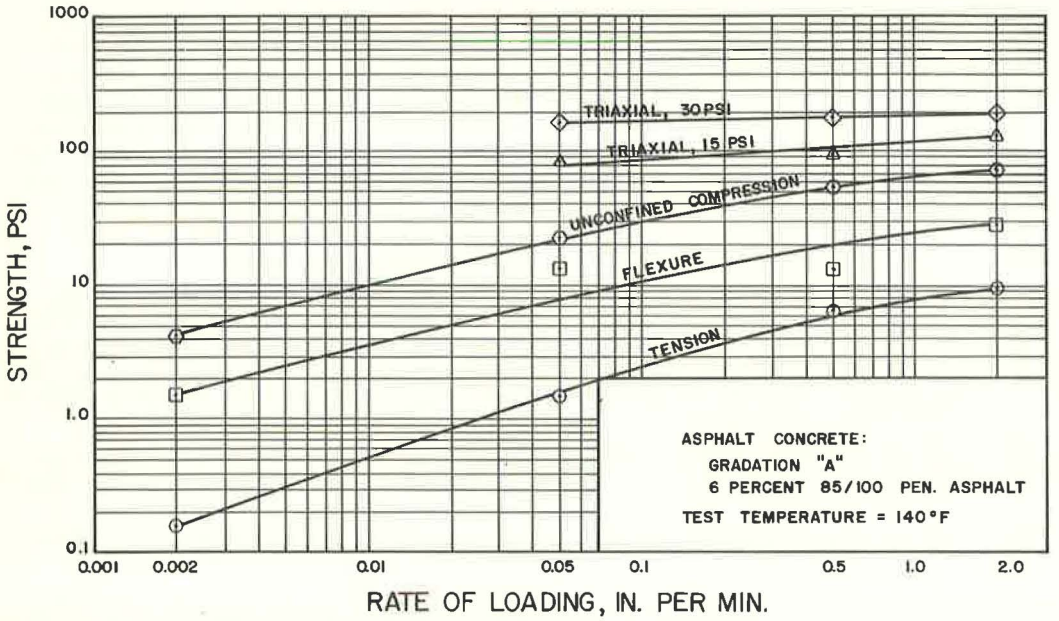

Figure 12. Influence of rate of loading on strength of asphalt concrete.

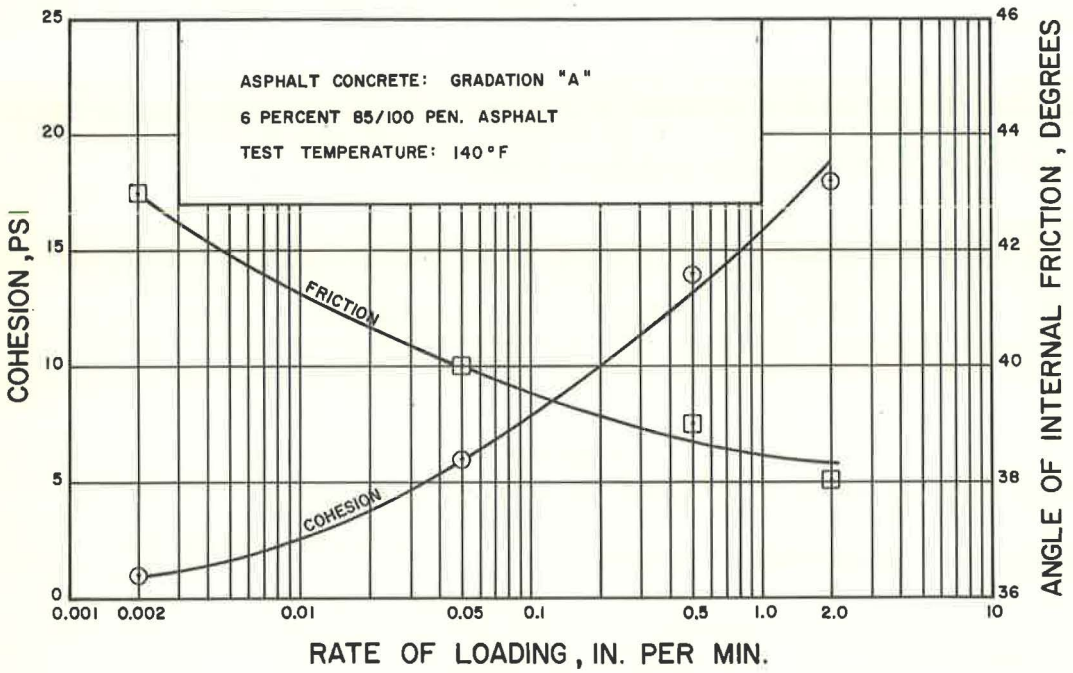

Figure 13. Influence of rate of loading on angle of internal friction and cohesion for asphalt concrete.

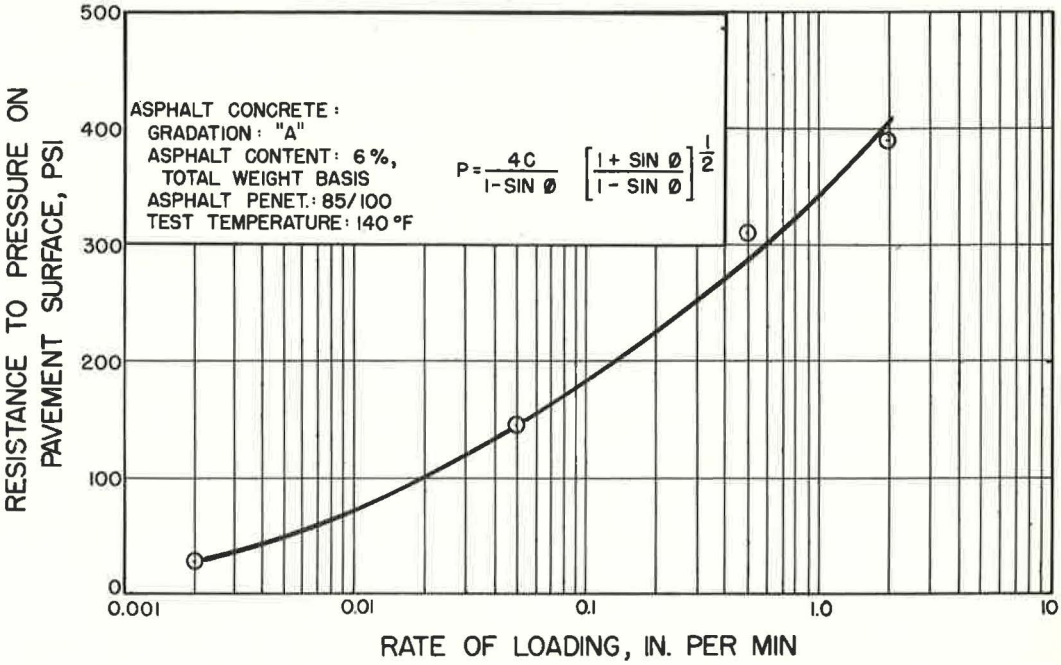

Figure 14. Influence of rate of loading on pavement resistance to vertical contact pressure.

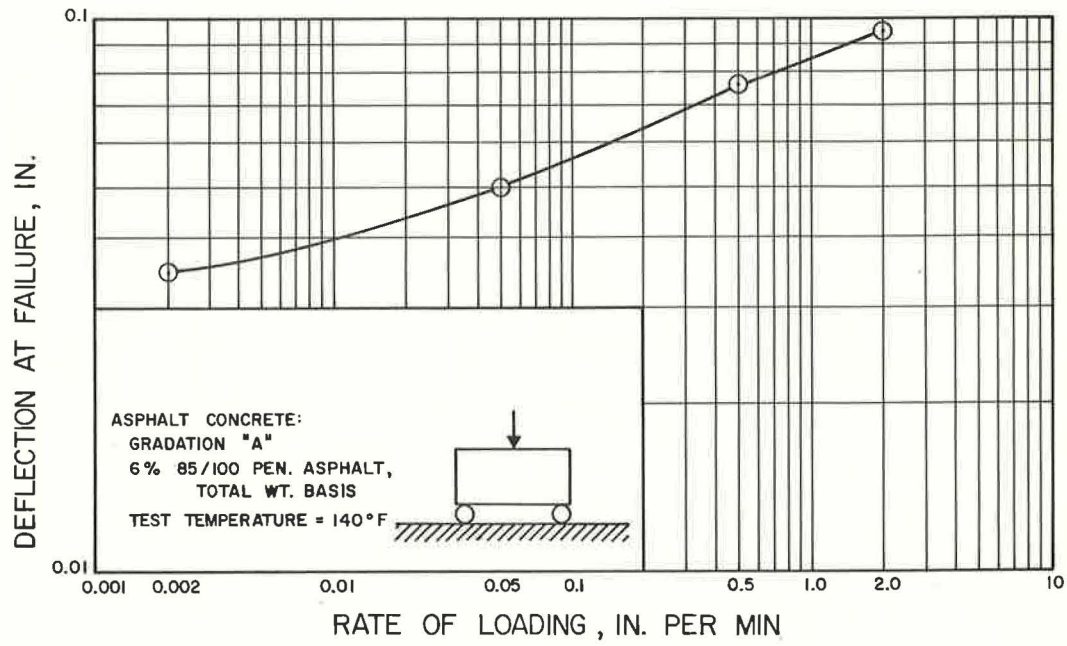

Figure 15. Influence of rate of loading on flexural deflection at failure for asphalt concrete.

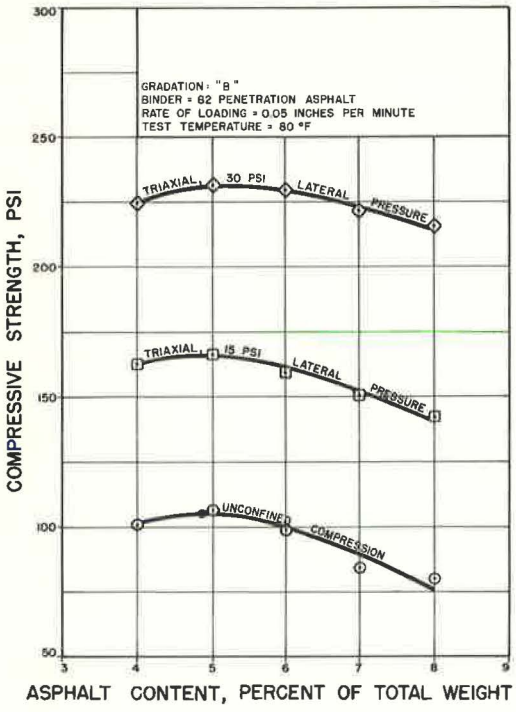

Figure 16. Influence of asphalt content on strength of asphalt concrete in triaxial compression.

presented in Figure 9 for the same conditions of test in which aggregate gradation A was used. Gradation A, which has more fines and is a slightly tighter mix, produces slightly higher cohesion but a lower angle of internal friction than gradation B. The influence of asphalt content on angle of internal friction, cohesion, and pavement resistance to vertical content pressure is shown in Figure 18. Maximum cohesion occurs at 4.5 percent asphalt, whereas the maximum angle of internal friction occurs at 6.5 percent asphalt, and as the

TABLE 7

INFLUENCE OF TEMPERATURE AND RATE OF LOADING ON FLEXURAL STRENGTH AND DEFLECTION[a]

Temperature (°F)	Rate of Load (in./min)	Mod. of Rupture (psi)	Deflection (in.)
140	0.002	1.6	0.035
140	0.05	14	0.050
140	0.5	13	0.076
140	2.0	30	0.095
110	0.05	25	0.080
80	0.05	71	0.089
40	0.05	526	0.105

[a]Average of duplicate specimens for gradation A, 6 percent asphalt (85-100 penetration).

TABLE 8

INFLUENCE OF ASPHALT CONTENT ON STRENGTH OF ASPHALT CONCRETE[a]

Asphalt[b] (%)	Unconf. Comp. (psi)	Triaxial Comp. (psi)		φ (deg)	c (psi)	Pave. Resist. (psi)
		15-Psi Lat.	30-Psi Lat.			
4	102	163	224	37.5	25	508
5	107	167	232	39	25	565
6	98	161	230	40	23	553
7	84	151	221	40	20	482
8	80	142	216	38.5	19	418

[a]Average of triplicate specimens for gradation B, 0.05-in./min rate of loading, 80 F.
[b]82 penetration.

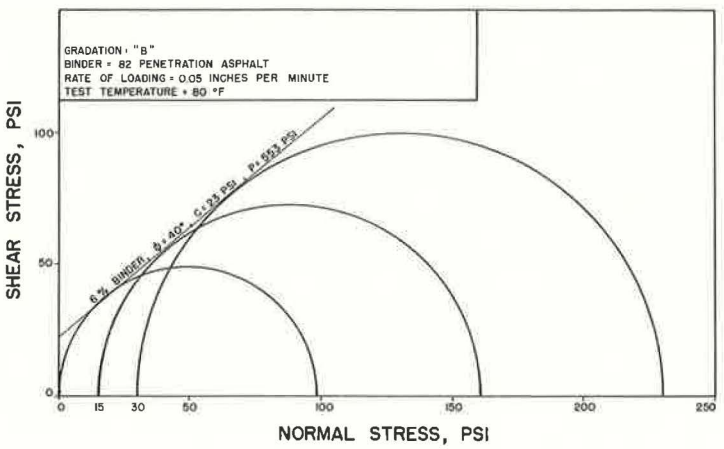

Figure 17. Mohr diagram for asphalt concrete.

asphalt content increases beyond this point the effect of lubrication is pronounced as friction drops rapidly. The effect of film thickness on cohesion at this test temperature is apparent, showing that thick films of asphalt have less resistance to internal shear than thin films. The curve for pavement resistance is similar to curves developed by the standard Marshall method of test and has maximum resistance at an asphalt content of about 5.5 percent.

Figure 19 shows the Mohr diagram for a mixture having 5.75 percent asphalt, with the same mix composition as those mixtures with properties given in Figure 18. The difference in test temperature of 140 F shows the much lower value for cohesion and a higher value for the angle

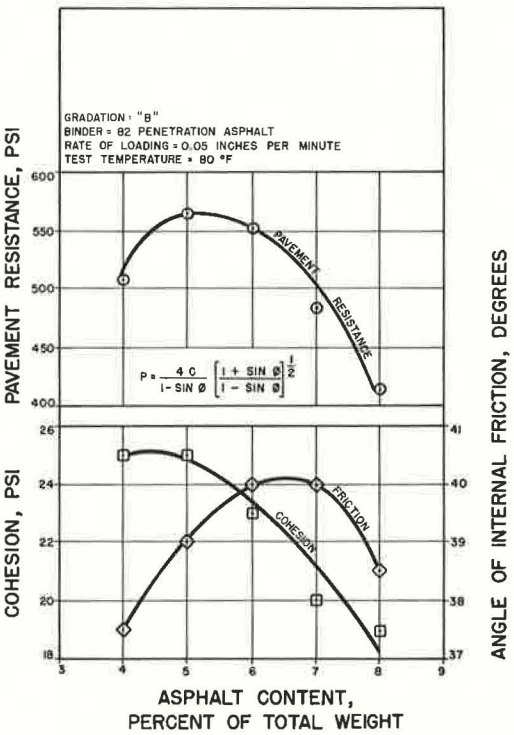

Figure 18. Influence of asphalt content on angle of internal friction, cohesion, and pavement resistance to vertical contact pressure for asphalt concrete.

TABLE 9

STRENGTH OF ASPHALT CONCRETE AT OPTIMUM BINDER CONTENT FOR GRADATION B AGGREGATE[a]

Property	Strength
Marshall stability, lb[b]	1,740
Marshall flow value	12.5
Tension, psi	0.15
Unconfined compression, psi	19
Triaxial, 15-psi lateral, psi	119
ϕ, deg	47.5
c, psi	4.0
Pavement resistance, psi	157

[a]Average of duplicate specimens, 5.75 percent asphalt (85-100 penetration), 0.05-in./min rate of loading, 140 F.
[b]Marshall test at 2.0 in./min.

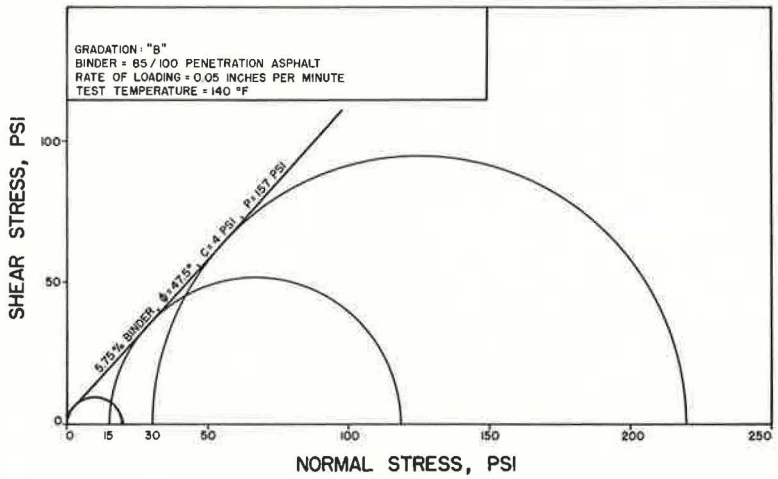

Figure 19. Mohr diagram for asphalt concrete.

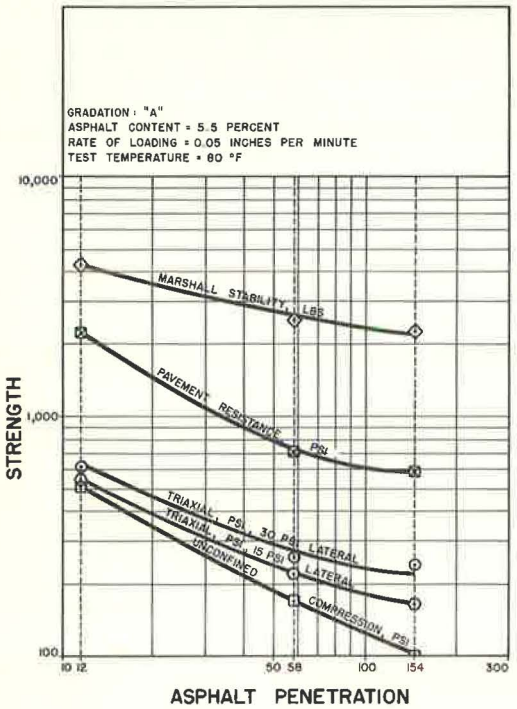

Figure 20. Influence of asphalt penetration on strength of asphalt concrete; Marshall test at 140 F and 2.0 in./min.

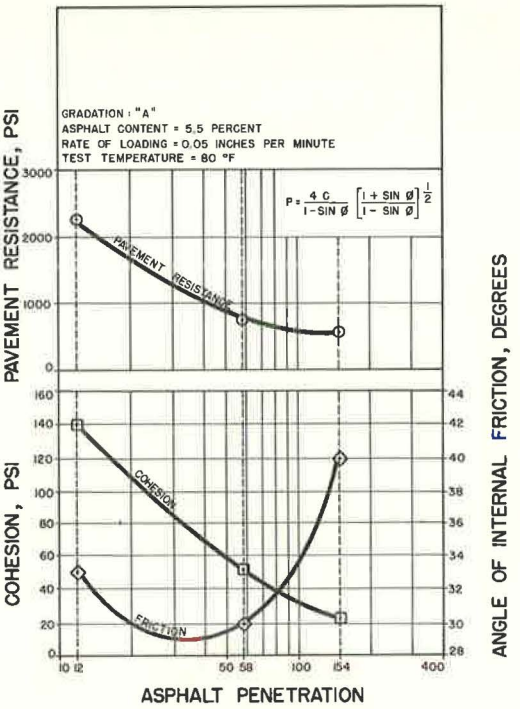

Figure 21. Influence of asphalt penetration on angle of internal friction, cohesion, and pavement resistance to vertical contact pressure.

TABLE 10

INFLUENCE OF ASPHALT PENETRATION AND VISCOSITY ON STRENGTH OF ASPHALT CONCRETE[a]

Property	Strength		
	12 Pen.	58 Pen.	154 Pen.
Viscosity, 10^5 poises	2,000[b]	45.5	7.6
Marshall stability, lb[c]	4,360	2,595	2,375
Marshall flow, 0.01 in.	23	13	24
Flexure (MR), psi	487	161	50
Unconfined compression, psi	514	177	100
Triaxial compression, psi:			
15-psi lateral	547	228	172
30-psi lateral	617	264	240
ϕ, deg	33	30	40
c, psi	140	52	24
Pavement resistance, psi	2,270	720	580

[a]Average of duplicate specimens for gradation A, 5.5 percent asphalt, 0.05-in./min rate of loading, 80 F.
[b]Estimated.
[c]Marshall test at 140 F and 2.0 in./min.

of internal friction. Test values are given in Table 9.

Asphalt Penetration and Viscosity

The influence of asphalt penetration on the strength of asphalt concrete is shown in Figure 20. The standard Marshall test was performed at 140 F and 2.0-in./min rate of loading with unconfined and triaxial compression tests run at 80 F and 0.05 in./min. Figure 21 shows the influence of asphalt penetration on angle of internal friction, cohesion, and pavement resistance to vertical contact pressure. The curve for friction follows the trend developed in the series of tests which showed the influence of test temperature on strength properties (Fig. 10). This shows that at 80 F, asphalt having a penetration below 30 begins to show properties of a solid. The apparent close correlation between Marshall stability and pavement resistance determined from triaxial test data is evident in Figure 20.

It was intended in the design of this experiment that the relationship between absolute viscosity as determined by the sliding plate microviscometer and strength properties be developed. At 77 F, however, it was discovered that the microviscometer did not have the load capacity for the 12 penetration asphalt. Table 10 gives data to show the influence of asphalt penetration and absolute viscosity on the strength of asphalt concrete.

TABLE 11

STRENGTH PROPERTIES OF ASPHALT CEMENT-FLAKE ASPHALT MIXTURES[a]

Flake (%)	Triaxial		p^b (psi)	Marshall	
	ϕ (deg)	c (psi)		Stability (lb)	Flow (0.01 in.)
0	43.5	6.5	195	—	—
5	42.0	7.0	191	2,680	17
10	44.5	7.0	222	2,852	17
15	42.0	7.5	202	2,670	16
20	43.5	7.5	224	3,325	13
25	44.5	8.0	254	3,222	14
30	—	—	—	3,627	12

[a]Based on duplicated specimens for gradation A, 5.5 percent asphalt (85-100 penetration), 0.05-in./min rate of loading, 140 F.
[b]From Eq. 4.

Flake Asphalt—Asphalt Cement Binder

The viscosity of an asphalt binder can be increased at the asphalt mix plant by adding dry asphalt to the pug mill through the mineral filler attachment. This has been done to a limited extent. In this investigation the total binder content remained constant at 5.5 percent and the amount of flake asphalt was increased from 0 to 30 percent of the binder. The influence of flake asphalt in the binder on the strength of mixture is shown in Figure 22 with the influence on the angle of internal friction, cohesion, and pavement resistance given in Table 11. These data show a slight increase in strength with an increase in flake asphalt. It is possible that there was not complete blending of the flake asphalt with the asphalt cement during the

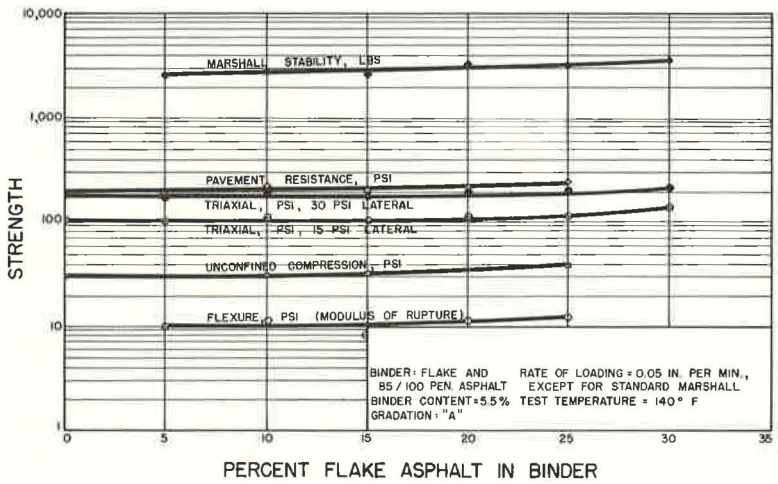

Figure 22. Influence of flake asphalt in binder on strength of asphalt concrete.

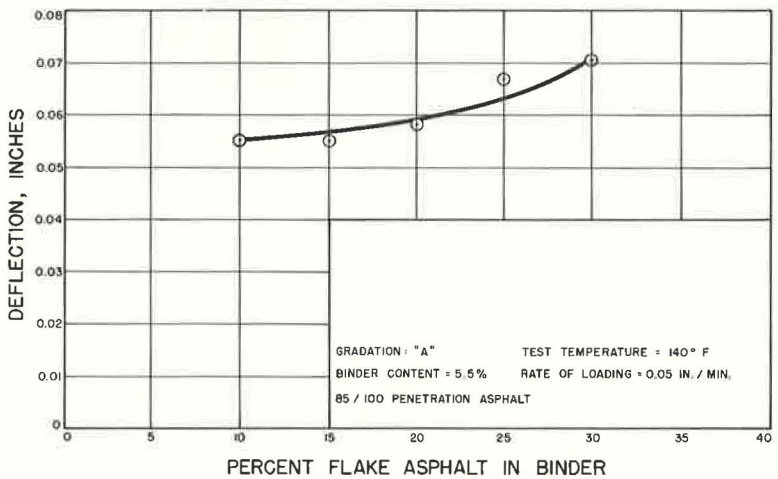

Figure 23. Influence of flake asphalt in binder on flexural deflection at failure for asphalt concrete.

laboratory mixing operation. On the basis of the data relating asphalt penetration and viscosity to the strength of asphalt concrete, it would appear that the effect of flake asphalt would be more pronounced.

Figure 23 shows that the addition of flake asphalt to the binder increases deflection at failure in the flexure test.

TABLE 12

STRENGTH OF MIXTURE HAVING BLEND OF ASPHALT CEMENT, FLAKE ASPHALT AND A-C POLYETHYLENE 629 AS BINDER[a]

Property	Strength
Flexure (MR), psi	60
Tension, psi	8.3
Unconfined compression, psi	119
Triaxial compression, psi:	
15-psi lateral	175
30-psi lateral	245
ϕ, deg	39
c, psi	29
Pavement resistance, psi	660
Marshall stability, lb[b]	3,600
Marshall flow value	11

[a]Average of duplicate specimens for gradation A, 5.5 percent binder (18 percent A-C polyethylene 629, 2 percent Indopol polybutene (H-300), 15 percent flake asphalt, and 65 percent 85-100 pen. asphalt), 0.05-in./min rate of loading, 140 F.
[b]Marshall test at 2.0 in./min.

Polyethylene in Binder

An investigation was made to determine the feasibility of using polyethylene in the binder of paving mixtures. A-C polyethylene 629 blended with polybutene, flake asphalt, and 85-100 penetration grade asphalt provided a binder which gave desirable strength characteristics to the mixture. Pavement resistance at 140 F was high as a result of high cohesion in the mixture. Strength data are given in Table 12. The influence of test temperature on the flexural strength of this mixture is shown in Figure 24.

The Marshall test was used to determine the influence of the amount of A-C polyethylene 629 blended with 85-100 penetration asphalt on the strength of mixtures. The results of this series are given in Table 13. The addition of A-C polyethylene 629 did permit a lower binder content for the mixtures.

The influence of A-C polyethylene 680 blended with 85-100 penetration asphalt on the strength of a mixture is indicated in Table 14. Marshall, unconfined compression and triaxial compression tests

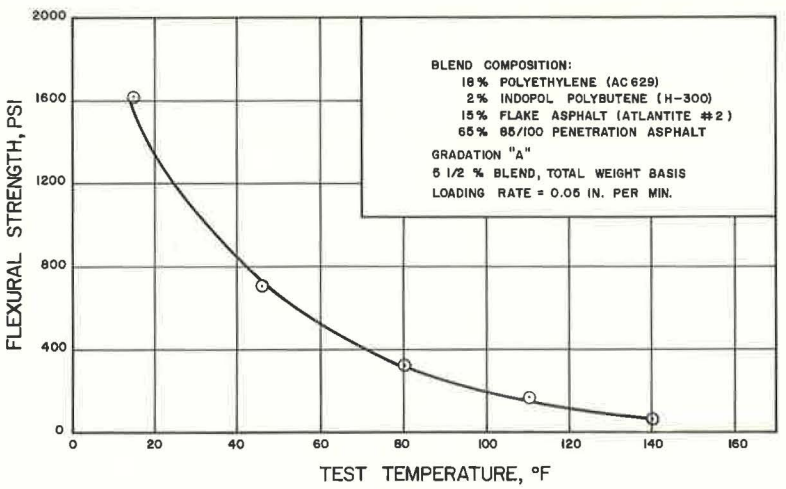

Figure 24. Influence of test temperature on modulus of rupture for mixture having binder composition of A-C polyethylene 629, Indopol, flake asphalt and penetration grade asphalt.

TABLE 13

STANDARD MARSHALL STABILITY FOR MIXTURES HAVING A-C POLYETHYLENE 629 IN BINDER WITH 85-100 PENETRATION ASPHALT[a]

Polyethylene in Binder (%)	Binder (%)	Marshall Stability (lb)
0	6.0	2,075
20	4.0	2,455
50	4.0	3,250
100	4.0	5,400

[a]Average of triplicate specimens.

TABLE 14

STRENGTH OF MIXTURE HAVING BLEND OF ASPHALT CEMENT AND A-C POLYETHYLENE 680 AS BINDER[a]

Property	Strength
Marshall stability, lb[b]	2,510
Marshall flow, 0.01 in.	9
Flexure (MR), psi	135
Unconfined compression	168
Triaxial compression, psi:	
15-psi lateral	212
30-psi lateral	250
ϕ, deg	28
c, psi	51
Pavement resistance, psi	640

[a]Average of triplicate specimens for gradation B, 5 percent binder (80 percent 85-100 penetration asphalt, 20 percent A-C polyethylene 680), 0.05-in./min rate of loading, 80 F.
[b]Marshall test at 140 F and 2.0 in./min.

TABLE 15

STRENGTH AT OPTIMUM BINDER CONTENT OF MIXTURES HAVING ASPHALT CEMENT-TENITE POLYETHYLENE BINDER[a]

Property	Strength	
	20% Tenite	35% Tenite
Binder content, %	6.0	7.0
Flexure (MR), psi	72	86
Tension, psi	21	--
Unconfined compression, psi	94	162
Marshall stability, lb[b]	3,590	3,975
Marshall flow, 0.01 in.	9	8.5

[a]Average of duplicate specimens for gradation A, 85-100 penetration asphalt, 0.05-in./min loading, 140 F.
[b]Marshall test at 2.0 in./min.

were run. A comparison with Tables 8 and 9 shows that 20 percent A-C polyethylene 680 in the binder tested at 80 F and 0.05 in./min produces an increase in the strength of the mixture of only about 15 percent. However, in testing by the Marshall method at 140 F and 2.0 in./min, there is an increase in strength of about 50 percent with the addition of 20 percent A-C polyethylene 680. The significance of this is that A-C polyethylene 629 or 680 could be used to advantage where it was desirable to increase strength characteristics at high temperatures.

Tenite polyethylene was used in mixtures in two ways. In one case a previously blended binder of Tenite and asphalt cement was used in the preparation of mixtures for the Marshall, flexure, tension, unconfined compression, and triaxial tests. The results of these tests are given in Table 15. In the second series of tests, Tenite polyethylene and flake asphalt were both added in dry form to the hot stone to provide the binder. The asphalt was added first. Various combinations of the binder were used, with the results presented in Table 16 and Figure 25. This binder was very strong as is shown by a modulus of rupture of 592 psi at 140 F where the binder consists of 80 percent Tenite. It produces a relatively rigid mixture which has low flexural deflections at failure. This was also observed when there was not a great difference in strength between the unconfined and triaxial compression tests.

Viadon

Mixtures were prepared using 5.5 and 7.4 percent Viadon as binder. The effect of binder content appears to be influenced by rate of loading as is indicated in Table 17. All tests were at 140 F. For the Marshall test which has a rate of loading of 2.0 in./min, the stability was greater at a binder content of 7.4 percent. However, on the basis of triaxial compression data as shown in Figure 26 in which the rate of loading was 0.05 in./min, the strength at 5.5 percent binder was more than twice that at 7.4 percent binder.

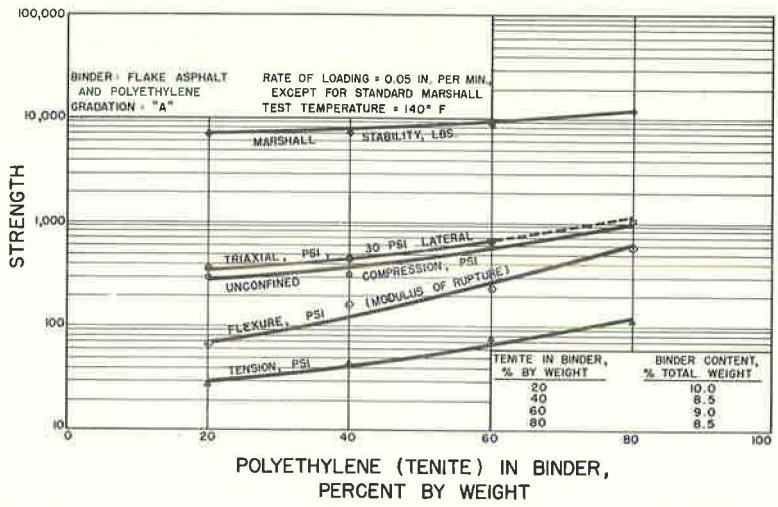

Figure 25. Influence of binder composition on strength of flake asphalt-tenite polyethylene mixtures.

TABLE 16

STRENGTH AT OPTIMUM BINDER CONTENT OF MIXTURES HAVING FLAKE ASPHALT-TENITE POLYETHYLENE BINDER[a]

Property	Strength			
	20% Tenite	40% Tenite	60% Tenite	80% Tenite
Binder content, %	10.0	8.5	9.0	8.5
Flexure (MR), psi	66	165	240	592
Tension, psi	29	45	76	121
Unconfined compression, psi	299	325	-	1,096
Triaxial, 30-psi lateral, psi	366	453	665	-
Marshall stability, lb[b]	6,865	7,035	8,860	13,200
Marshall flow, 0.01 in.	13	10.5	10	9.5

[a]Average of duplicate specimens for gradation A, 0.05-in./min rate of loading, 140 F.
[b]Marshall test at 2.0 in./min.

TABLE 17

STRENGTH OF VIADON[a]

Property	Strength	
	5.5% Binder	7.4% Binder
Marshall stability, lb[b]	3,185	3,690
Marshall flow, 0.01 in.	18	35
Tension, psi	--	8
Unconfined compression, psi	99	50
Triaxial compression, psi:		
15-psi lateral	159	101
30-psi lateral	218	148
ϕ, deg	37	32.5
c, psi	25	14
Pavement resistance, psi	505	220

[a]Average of triplicate specimens for gradation A, 0.05-in./min rate of loading, 140 F.
[b]Marshall test at 2.0 in./min.

Asbestos Fibers in Binder

Asbestos fibers were added to a mixture using aggregate gradation B at a rate of 2 percent of the weight of the mixture. Test results are presented in Table 18. A comparison with Tables 8, 9, and 10 indicates that the addition of 2 percent asbestos fibers has about the same effect on strength as a 2 percent increase in the fines content in the aggregate. Cohesion is increased but there is some reduction in the angle of internal friction. The triaxial data show a greater effect of asbestos fibers on the strength of the mixture than do the Marshall stability data. It is possible that this strength variation with test procedure is also related to the rate of load application.

DESIGN APPLICATION

The design of flexible paving surfaces must provide shearing resistance in the pavement to excessive compression deformation under critical service conditions. The most critical condition of the pavement, with respect to shearing resistance, occurs when the pavement is at the maximum temperature and loads on the pavement are moving at a slow rate. A realistic design temperature is considered to be 140 F. The selection of a rate of load application to simulate actual loading of the pavement in service is not as easy. Although static loading would be most critical, as in the case of parked vehicles, this would not be practical for use in the design of pavements

for highways, airport runways or streets. Also, it would not be practical to design a pavement for the shear stresses which would develop for vehicles moving at the design speed of the roadway. Another factor to be considered is the magnitude of compressive deformation in the surface and the relationship of this deformation to the total deformation of a pavement surface with loading, a part of which would be due to flexure resulting from the total deformation of the flexible pavement structure. A rate of loading of 0.05 in./min would be realistic for laboratory testing of specimens in unconfined and triaxial compression. Data obtained under these conditions of temperature and loading should be evaluated on the basis of pavement performance to determine a correlation.

On the basis of data obtained in this investigation of asphalt concrete and as provided in Tables 4 through 6 and Figures 8 and 10 through 14, mixtures tested at a rate of loading of 0.05 in./min are 4 times as strong at 80 F as at 140 F. Also, specimens tested at 140 F are twice as strong when tested at a rate of loading of 0.5 in./min as when tested at 0.05 in./min. These and other established relationships developed for asphalt concrete were used to convert computed values for pavement resistance to vertical contact pressure for various materials tested in this investigation to a design bearing capacity at 140 F and 0.05-in./min rate of loading for purposes of comparison. This also shows the feasibility and practicability of testing at 0.05-in./min rate of loading and at a temperature of 80 F and reducing the computed pavement resistance by a factor of 4 to determine bearing values for design. Table 19 gives the bearing capacity of various mixtures as tested in this investigation, and as adjusted if necessary to 140 F and 0.05 in./min.

The values of bearing capacity as shown in Table 19 may be considered ultimate bearing capacity and have not

TABLE 18

STRENGTH OF ASPHALT CONCRETE CONTAINING TWO PERCENT ASBESTOS FIBERS[a]

Property	Strength
Marshall stability, lb[b]	1,895
Marshall flow, 0.01 in.	17
Flexure (MR), psi	122
Unconfined compression, psi	158
Triaxial compression, psi:	
15-psi lateral	208
30-psi lateral	257
ϕ, deg	32.5
c, psi	44
Pavement resistance, psi	690

[a]Average of triplicate specimens for gradation B, 6.0 percent asphalt (85-100 penetration), 0.05-in./min rate of loading, 80 F.
[b]Marshall test at 140 F and 2.0 in./min.

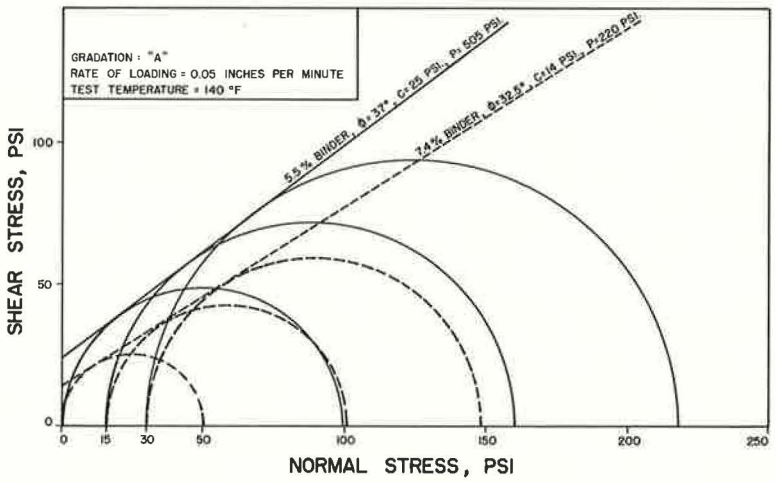

Figure 26. Mohr diagram for Viadon at two binder contents.

TABLE 19

DESIGN BEARING CAPACITY FOR VARIOUS MIXTURES

Aggregate Gradation	Binder		Test		Bearing Capacity		
	Type	%	Temp (° F)	Load Rate (in./min)	Test (psi)	Test Factor	Design[a] (psi)
A	A-C 629, A.C., flake	5.5	140	0.05	660	1	660
A	Viadon	5.5	140	0.05	505	1	505
A	Viadon	7.4	140	0.05	220	1	220
A	15% flake	5.5	140	0.05	200	1	200
A	25% flake	5.5	140	0.05	255	1	255
A	85-100 pen.	6.0	140	0.05	145	1	145
A	85-100 pen.	6.0	140	0.5	310	2	155
A	85-100 pen.	6.0	80	0.5	560	4	140
A	85-100 pen.	6.0	110	0.5	300	2	150
A	154 pen.	5.5	80	0.05	580	4	145
A	58 pen.	5.5	80	0.05	720	4	180
A	12 pen.	5.5	80	0.05	2,270	4	568
B	85-100 pen.	5.75	140	0.05	157	1	157
B	82 pen.	4.0	80	0.05	508	4	125
B	82 pen.	5.0	80	0.05	565	4	140
B	82 pen.	6.0	80	0.05	553	4	138
B	82 pen.	7.0	80	0.05	482	4	120
B	82 pen.	8.0	80	0.05	418	4	105
B	2% asbestos 85-100 pen.	6.0	80	0.05	690	4	173

[a]For 140 F and 0.05-in./min unadjusted for traffic factor.

TABLE 20

PERFORMANCE RATING OF PAVING MIXTURES FOR HEAVY-DUTY HIGHWAYS

Traffic Factor, T	Bearing Capacity (psi)	Performance Rating
1.0	75	Poor
1.5	115	Fair
2.0	150	Good
2.5	190	Excellent

TABLE 21

FLEXURAL STRENGTH OF VARIOUS MIXTURES[a]

Binder Type	Binder (%)	Flexure (MR) (psi)	Deflection (in.)
85-100 penetration asphalt	6.0	14	0.050
15% flake, 85% asphalt cement	5.5	8	0.055
25% flake, 75% asphalt cement	5.5	14	0.067
18% A-C polyethylene 629, 2% polybutene, 15% flake asphalt, 65% asphalt cement	5.5	60	0.055
100% A-C polyethylene 629	4.5	122	0.049
20% Tenite, 80% asphalt cement	6.0	72	0.028
20% Tenite, 80% flake asphalt	10.0	66	0.019
40% Tenite, 60% flake asphalt	8.5	165	0.025
Portland cement	-	955	0.024

[a]Gradation A, 0.05-in./min rate of loading, 140 F.

been subjected to a safety factor or traffic factor. To determine the suitability of these various mixtures to roadway requirements, it would be necessary to consider design loads and pavement category. For instance, if a pavement is for a heavy-duty highway where contact pressures are 75 psi, it would be essential that the design bearing capacity be 150 psi, as computed in Table 19, if the pavement is to have a traffic factor of 2.0. Similarly, it might be expected that a paving mixture having a bearing capacity of 75 psi would show early surface deformations if placed on a heavy-duty highway. A means of rating the expected performance of paving mixtures for heavy-duty highways on the basis of bearing capacity is given in Table 20.

There are problems in the design of flexible paving mixtures other than those relating to shear strength. Of considerable importance are the flexibility of the pavement layer (its ability to deform in flexure without cracking) and the ability of the pavement to resist tensile stresses with changes in environmental conditions without cracking. A flexible paving mixture cannot be designed to resist flexural stresses without reinforcement if excessive flexural deflections are permitted. The problems related to the flexural and tensile stresses and deformations of flexible paving mixtures

should be the subject of an intensive investigation. Most of the research relating to pavement strength as applied to design practice has been in the area of shear strength. Research on the flexural or tensile strength of paving mixtures has not been extended to a consideration of design and it is in this area that work needs to be done (11, 12, 13, 14).

Table 21 gives a comparison of the flexural strength and deflection at failure for various mixtures. This is probably of more interest for a comparison of the flexibility of these mixtures as measured by deflection than by modulus of rupture.

CONCLUSION

Instrumentation has been developed for specimen preparation and the testing of flexible paving mixtures in flexure, tension, and triaxial shear. The influence of test temperature and rate of loading on asphalt concrete tested by these procedures was shown. Various mixtures were tested and analyzed for suitability to resist compressive stresses in the pavement. The practical application of this procedure to design is shown.

ACKNOWLEDGMENTS

The author is grateful to the Graduate Faculty of Cornell University and to the College of Engineering for faculty research grants which made this investigation possible. The author is also indebted to David Powers for his suggestions concerning equipment design and for supervision during its manufacture.

Appreciation is extended to the Cayuga Crushed Stone Co., Atlantic Refining Co., Allied Chemical Corp., Amoco Chemical Corp., Eastman Chemical Products, Inc., and the Humble Oil and Refining Co.

Mixtures were prepared and tested in the Transportation Laboratory by Ray Balfour, John Curtis, John Lukens, Mike Preg and Joost Van Hamel, under the direction and supervision of the author. Illustrations were prepared by Ray Balfour and Mrs. John Lukens.

REFERENCES

1. Hewitt, W. L. Analysis of Stresses in Flexible Pavements and Development of a a Structural Design Procedure. Highway Research Board Bull. 269, pp. 66-74 1960.
2. McLeod, N. W. A Rational Approach to the Design of Bituminous Paving Mixtures. Proc. AAPT, Vol. 19, p. 99, 1950.
3. McLeod, N.W. Void Requirements for Dense-Graded Bituminous Paving Mixtures. ASTM Spec. Tech. Pub. No. 252, 1959.
4. The AASHO Road Test. Highway Research Board Spec. Rept. 61, 1962.
5. Hveem, F.N. Pavement Deflections and Fatigue Failures. Highway Research Board Bull. 114, pp. 43-87, 1955.
6. Jimenez, R. A., and Galloway, B. M. Behavior of Asphaltic Concrete Diaphragms to Repetitive Loadings. Proc. Int. Con. on Structural Design of Asphalt Pavements, Univ. of Michigan, pp. 339-344, 1962.
7. ASTM Standards on Bituminous Constructional Materials. 9th ed., 1962.
8. Mix Design Methods for Hot-Mix Asphalt Paving. Asphalt Inst., 1956.
9. Smith, V. R. Application of Triaxial Test of Bituminous Mixtures—California Research Corporation Method. ASTM Spec. Tech. Pub. 106, 1951.
10. Doyle, P. C. Cracking Characteristics of Asphalt Cement. Proc. AAPT, Vol. 27, p. 123, 1958.
11. Monismith, C. L., Secor, K. E., and Blackmer, E. W. Asphalt Mixture Behavior in Repeated Flexure. Proc. AAPT, Vol. 30, p. 188, 1961.
12. Papazin, H. S., and Baker, R. F. Analysis of Fatigue Type Properties of Bituminous Concrete. Proc. AAPT, Vol. 28, p. 179, 1959.

13. Wood, L. E., and Goetz, W. H. The Strength of Bituminous Mixtures and Their Behavior Under Repeated Loads. Highway Research Board Proc., Vol. 35, pp. 405-417, 1956.
14. Davis, E. F., Krokosky, E. M. and Tons, E. Stress Relaxation of Bituminous Concrete in Tension. MIT Dept. of Civil Eng., Res. Rept. R63-40, Aug. 1943.

Discussion

W. H. CAMPEN, Manager, Omaha Testing Laboratories —Asphalt paving mixtures must resist displacement to prevent shoving and rutting when subjected to the application of loaded tires. It may be possible to measure this resistance by shear but it should be pointed out emphatically that stability tests such as the Marshall and the Hveem do measure this resistance fairly accurately. For instance, it is well known that a Marshall stability of about 2,000 lb does prevent shoving and rutting under heavy truck traffic.

I might add that in my part of the country, shoving and rutting are a thing of the past. The change has been brought about by using stability tests as the principal criteria for design. Furthermore, stability has been correlated with type of traffic for economic reasons. Marshall stabilities of about 1,000 lb for light traffic, 1,500 lb for medium traffic, and 2,000 lb for heavy traffic are sufficient.

WILLIAM L. HEWITT, Closure—Flexible paving mixtures provide resistance to plastic deformation through intergranular friction and through the internal resistance of the binder to shear stresses. Shearing and rutting are forms of plastic failure in the pavement. The pavement component fails in compression while laterally supported. The triaxial test provides a good measure of the resistance offered by paving mixtures under these conditions. Marshall and Hveem stability values give some measure of the combined effect of intergranular friction and internal resistance of the binder, though Marshall stability may be influenced primarily by the internal resistance of the binder and Hveem stability may be influenced primarily by intergranular friction. Therefore, they too provide an indication of the resistance offered by paving mixtures to displacement when subjected to the application of loaded tires. The author is of the opinion that the triaxial test as described in this paper provides a better measure of resistance to the plastic deformation of paving mixtures than either Marshall stability or Hveem stability.

Pavement resistance values computed from triaxial data may be adjusted by a traffic factor to provide design values for various traffic conditions (Tables 19 and 20). This would serve the same purpose as varying Marshall stability for traffic category as suggested by M. Campen.

Effect of Degree of Aging on Creep and Relaxation Behavior of Sand-Asphalt Mixtures

F. MOAVENZADEH and O. B. B. SENDZE
Respectively, Assistant Professor, Department of Civil Engineering; and International Road Federation Fellow, Ohio State University

Previous work on the study of aging is reviewed. The creep parameters of mixture viscosity and modulus of recovery developed by Wood and Goetz were selected for use in comparing the creep characteristics of the aged and unaged mixes.

A 60-70 penetration asphalt was used. Ottawa sand of maximum size No. 16 was used as aggregate. The gradation was within the limits of ASTM Designation: D 1663-59T. Three different mixes were made with 9, 12, and 15 percent asphalt content by weight of aggregate. Three degrees of aging were used: 77 F (unaged), 140 F, and 225 F for 1 wk. Specimens, 3.5 cm in diameter and 7 cm high, were made and tested in creep and relaxation. Maximum creep strain was limited to 1.2 percent and the relaxation strain was 1.4 percent.

The rate of creep generally decreased with increase in the degree of aging. With the higher asphalt content mixes, the difference in the creep rates was less marked. The maximum relaxation load increased with aging.

For the particular results obtained, a semilog relation was developed showing the variation of mixture viscosity with the degree of aging. A similar expression was developed relating the maximum relaxation load to the degree of aging.

•WORK ON the aging of bituminous materials with time has continued since the first paper on the subject was presented by Hubbard (7) in 1913. Hubbard showed that the hardening of asphaltic materials on exposure was due to both volatilization and oxidation. Reeve (20) next showed that polymerization and intermolecular reactions induced by heat, in addition to volatilization, were responsible for hardening. Sabbrow (22), after undertaking research on the aging of road tar in France, concluded that the effect of evaporation was far greater than that of oxidation.

Most recent researchers have agreed that the main causes of age hardening of bituminous materials are oxidation, photooxidation, volatilization, polymerization, thixotropy, syneresis and separation (27). The main effect of these processes, in varying degrees, is to cause asphalt to become less ductile, lose its penetration, and gradually develop a structure, thereby causing brittleness and failure of pavements. The most important causes of hardening are oxidation, volatilization and polymerization.

To study these effects, asphalts are usually artificially aged in the laboratory by the technique of accelerated weathering. Ovens are to reproduce various conditions representing long periods of aging in actual practice. High-temperature weathering is used in the study of volatilization and oxidation. Artificial light is used to study the effects of photooxidation, and infrared and ultraviolet weathering are used to study the effects of the sun's radiant energy. Selection of an aging method depends on the effect being studied.

Paper sponsored by Committee on Mechanical Properties of Bituminous Paving Mixtures.

Because the problem of aging is an important factor in the life of a bituminou pavement, investigators have directed their research to its effects on particular properties of bituminous materials and mixtures. Aging is not a physical property which can be measured in numerical terms. There is, therefore, as yet no scale for it. The main problem has been to find some way of measuring the rate of change due to aging of any particular property of bituminous materials with time and thereby to deduce a method of measuring the durability of an asphaltic pavement.

Of historical interest is the work of Sabbrow and Renausie (23) who put forward a method of measuring the aging effects of road binders by means of an aging coefficient. He used the following equation to measure the likelihood of a binder softening during the summer months:

$$C_{v/t} = \frac{V_v - V_p}{A_p} \qquad (1)$$

where

$C_{v/t}$ = aging coefficient at temperature t;

V_v = viscosity after artificial aging at temperature t;

V_p = viscosity of original binder; and

A_p = loss in weight during aging.

This, therefore, used change in viscosity as a measure of aging. They in fact carried out field studies to correlate the aging coefficient with the development of cracks in pavements.

Some investigators measured changes in the penetration of the asphalt, for they felt that this was a very important property. Hubbard (8) indicated that a penetration of 30 or less for asphalts subjected to freezing may result in cracking. Powers (19), as a result of his own studies, concluded that pavements containing asphalts with a penetration of less than 10 would be subject to cracking.

McKesson (15), on the other hand, felt ductility was a better measure of hardening than penetration. Vokar (31) used the softening point of asphalt together with changes in ductility and penetration to measure the hardening of asphalts.

The U. S. Bureau of Public Roads (11) developed the thin-film oven test which is used in its work. The Bureau has published data showing the relation between loss of penetration and changes in softening point of various film thicknesses of asphalt after aging under high-temperature weathering for as long as 10 hr.

California (25) developed a test in which Ottawa sand is coated with various films of asphalt, weathered for specified periods in a weathering machine, and then subjected to the abrasive action of 100 gm of steel shot falling 1 m. Loss of weight is used as a measure of the durability of the asphalt.

With the development of the microviscometer by Shell (5), much work on aging has been based on measuring the change in viscosity after aging using the aging index, defined as the ratio of the viscosity of the weathered to the unweathered material as measured by the microviscometer. The results presented by Shell Development Co. show that as the duration of high-temperature weathering is increased, the aging index rises sharply. The microviscometer method of determining the change in the viscosity of the asphalt due to aging is being widely used in research. The value of the aging index can be used as a measure of the durability of the pavement by correlating it with the behavior of the pavement.

Traxler (29) investigated the effect of prolonged heating of asphalt films of 15 μ at 325 F in air. His results also reveal a rapid increase in the viscosity of an asphalt with the duration of aging by direct heat. This information is very helpful in determining the choice of aging temperatures and the duration of aging.

In undertaking any aging experiments, therefore, the choice of the method, duration and temperature of aging is very important. Most often the method of aging is deter-

mined by the property being studied and its correlation with the actual conditions in a pavement. Vallerga et al. (30) studied the relative effects of different types of laboratory aging techniques and found that the effect on either penetration or softening point varied depending on whether the method used was direct heating in no light, aging in ultraviolet light, or aging in infrared light. The most important thing, therefore, is the correlation of results with field conditions. Hveem, Zube, and Skog (9), using the California infrared machine, showed that exposing asphalt for 1,000 hr in such a device was equivalent to 5 yr of pavement life. It has been estimated that most of the aging takes place within this period of time. Clark (2), on the other hand, carried out a set of correlation studies which compared the weathering of asphalt in an oven for weeks at 150 F with the aging of pavement. He concluded that 1 wk of aging at 150 F was equivalent to 1 yr of natural weathering of a pavement. Comparison of laboratory aging with life of bituminous materials in the field is of great importance in using the laboratory data for design.

Most investigators have felt that, because asphalt is the main cause of loss of durability, it should be isolated and studied independently; therefore, most work on the aging of bituminous concrete has been confined to analyzing the change in the properties of pure asphalt.

Recently, investigators have begun to study the aging of the bituminous concrete mass. Although the study of asphalt film is easier, it cannot be a proper substitute for the study of the mix. Analyzing this approach, Mack (14) states that the mechanical strength of mineral aggregate is greater than that of the asphalt. The adhesion energy between asphalt and aggregate is greater than the cohesive energy of the asphalt. Failure in a pavement, therefore, occurs when the external forces exceed the cohesive forces in the asphalt film. Mack further states that there is sufficient evidence to indicate that even simple liquids in thin films have properties different from those in the mass. Principal effects are considerably increased viscosity and greater elastic strength of the liquid near the surface of the solid. In bituminous pavements, asphalt films behave like solids. He concludes that, in view of these factors, the consistency of asphalts in mass cannot be extrapolated to thin films and any evaluation of the hardening effect in relation to their suitability as binders is best carried out on bituminous mixtures.

Mack measured the bearing strength of asphalt-sand mixtures for aged and unaged specimens and arrived at the following significant conclusions:

1. The bearing strength of unaged asphalt-sand mixtures decreases generally with deviation from Newtonian flow of the asphalt used; and
2. Aging increases the bearing strength markedly at 77 F in all cases, but only in two cases at 60 F.

In view of the increased consistency of the asphalts, the latter result is interesting in that bearing strength bears no relationship to the consistency of the asphalt. Mack indicated that strains in the asphalt-sand mixtures are not independent of the degree of compaction. To eliminate compactive effort, measurements must be carried out on mixtures of the same dimensions for a given weight. Aging does not affect the total strain.

There are also other factors which make the investigation of the asphalt aggregate mixture a closer approximation to what actually happens in the field. There is a substantial amount of hardening through loss of penetration during mixing (1). Because the duration of mixing also greatly affects hardening, a maximum length of time is required in most specifications for mixing. Other variables are the degree of compaction, void content, and permeability of the mix (14). In investigating aggregate asphalt mixtures, therefore, most of these effects will be present.

To evaluate the hardening effects on the mass by mechanical tests as recommended by Mack, the properties to be studied and the parameters involved must be carefully selected if any useful results are to be obtained. Fink (3), in his recommendations, indicated that measurement of an appropriate physical property of an asphalt before and after aging was the key factor in hardening studies. He thought it would be ideal to obtain a complete picture of rheological behavior as a function of loading time and temperature.

The results of recent research have confirmed that the stress characteristics of flexible pavements are time dependent. Mack (13) showed that deformation of a bituminous mixture consists of an elastic (recoverable) part and a nonrecoverable part. The type of behavior in deformation shown by asphaltic mixtures is termed viscoelastic behavior, the analysis of which belongs to the study of rheology of materials. To evolve theoretical equations representing the stress and strain characteristics of linear viscoelastic materials, model representation is used. The models consist essentially of various arrangements of springs and dashpots which represent the elastic and viscous behavior of the materials.

The stress-strain characteristics of asphaltic mixtures as obtained from creep tests consist of three essential parts (13): (a) an instantaneous elastic strain independent of time; (b) a retarded elastic strain which is a function of time; and (c) viscous strain whose rate decreases with time. Various attempts have been made to develop the simplest model that will duplicate all these features in its stress-strain curve. Burger's model (12, 15, 16, 29) seems adequate as it exhibits all the foregoing features in its stress-strain curves. This model consists of four elements which combine the Maxwell and Kelvin models.

The equation of deformation of the model is represented by:

$$\frac{d\gamma}{dt} = \frac{\tau}{\eta_1} + \frac{d\tau}{dt}\frac{1}{G_1} + \frac{d}{dt}\left[\frac{1}{\eta_2} e^{-\frac{G_2 t}{\gamma_2}} \int \tau\, e^{-\frac{G_2 t}{\gamma_2}}\, dt\right] \qquad (2)$$

where

G_1, G_2 = spring constants (spring modulus),
η_1, η_2 = dashpot constants (viscosity),
τ = applied stress, and
γ = deformation.

In creep tests where the creep load is static and constant $d\tau/dt = 0$. Solving Eq. 2 for a static creep load gives:

$$\gamma = \frac{\tau}{G_1} + \frac{\tau}{G_2}\left(1 - e^{-\frac{G_2 t}{\eta_2}}\right) + \frac{\tau}{\eta_1} t \qquad (3)$$

where

τ/G_1 = instantaneous elastic deformation,
$\tau/\eta_1 t$ = permanent deformation after time t, and
$\frac{\tau}{G_2}[1 - \exp(-G_2/\eta_2 t)]$ = retarded elastic strain.

It has been argued that this model configuration does not truly represent the behavior of the asphalt mixture in practice. Pister and Monismith (18) show that in Burger's model the instantaneous elastic strain is equal to the elastic rebound regardless of the duration of loading, whereas in practice this is not the case. The amounts of elastic recovery vary with the duration of loading. Hence, they felt that a model similar to Burger's but incorporating this variability of elastic recovery with time would be more appropriate. For the scope of the present work, however, Burger's model is assumed because of its relative simplicity.

Mathematical analysis of Burger's model and its various modifications become complex except in very simple cases. Using the model as a basis for evaluation, an empirical study of the actual curves obtained from creep tests are used in the present work. The study of the effects of hardening on the viscoelastic characteristics of the mixtures is essentially concerned with comparison and not with actual solutions of the equations which represent the behavior of the material as obtained from model analysis. Therefore, the derivation of parameters which can be affected by various hardening effects is bound to be the best approach.

In this connection, the work of Wood and Goetz (32) seems the most significant. They studied the rheological characteristics of sand-asphalt mixtures by undertaking unconfined compression creep tests on various specimens and thereby obtaining the deformation time curves for the mixtures.

Using Burger's model, they analyzed the curves from two main properties, elastic instantaneous strain and viscous deformation. The second term in Eq. 3 shows retarded elasticity of the Kelvin element. The effect of this element is usually pronounced in the first section of the creep curve, giving it the parabolic shape. As the test continues, this effect quickly dies out and, as Wood and Goetz pointed out, the remainder of the curve is for all practical purposes straight with a fairly constant slope.

If, therefore, the parabolic section of the curve is ignored, the slope of the straight portion could be measured and used as a parameter. This section of the curve can be said to be represented by the last term in Eq. 3. The reciprocal of the slope of the curve at this section represents the viscosity of the mixture. Wood and Goetz defined the product of the applied stress and the reciprocal of this slope as the mixture viscosity (V) in pound-seconds per square inch.

To measure the elastic component, they divided the applied stress by the rebound strain to obtain a second parameter which they termed the modulus of recovery (R). They showed that within the limits of experimental error the modulus of recovery and the mixture viscosity are independent of the applied stress. This property, if exact, makes these two parameters useful tools in the study of aging. The effects of aging on the values of these two parameters provide a useful basis for comparing the degrees of age hardening. The two parameters depend on properties affected by aging, namely, the viscous behavior of the mixture and its elastic or rigid behavior. Their use should, therefore, prove fruitful.

In discussing the foregoing results, Mack (32) pointed out that if the strain is plotted against the log of time, the parabolic section of the creep curve comes out as a straight line. This becomes obvious on examining the exponential nature of this part of the curve. If a straight line is obtained, its slope could also serve as a parameter, since it depends on the viscosity, which could then also be investigated as a possible third parameter for use in aging.

For a complete study of the rheological properties, an examination of the stress relaxation behavior of the mixture would provide a useful comparison. The best model representation of relaxation behavior has been shown to be the generalized Maxwell model with a series of elements (18).

Stress at any time is represented by the following equation:

$$\sigma = \epsilon \int_0^{\infty} G\,(T_{rel})\; e^{-\frac{t}{T_{rel}}}\; d\,(T_{rel}) \qquad (4)$$

where T_{rel} is relaxation time and ϵ is strain. The ratio of stress to strain is known as the relaxation modulus, $E_r\,(t)$. This gives another parameter which can be used to compare the properties of the mixture. The modulus of relaxation is widely used in work on polymers (30). Since the relaxation behavior depends on the viscous properties of the mix, hardening should have a marked effect on the modulus of relaxation and could also be used as a basis of comparing the degree of aging.

MATERIALS AND TEST PROCEDURE

Aggregate

To study properly the effects of aging, it was considered necessary to eliminate any unknown factors caused by the properties of the aggregate. To eliminate disintegration and aggregate reactivity with asphalt in the mix, the aggregate had to be inert, sound, and durable. Aging effects, thereby, would be confined to changes in the asphalt properties. Ottawa sand was chosen as meeting these requirements, and silica sand powder was used as mineral filler.

It was desirable that the gradation of the sand be within the specification limits of ASTM Designation: D 1663-59T for sheet asphalt. By plotting the specification limits on a log plot, a straight line lying within the specified range was obtained. This straight line represented a gradation shown mathematically as:

$$P_i = P_o\left(\frac{d_i}{D_o}\right)^n \tag{5a}$$

or

$$\log P_i = \log P_o + n \log \left(\frac{d_i}{D_o}\right) \tag{5b}$$

where

P_i = percent passing sieve size being considered,
P_o = percent passing maximum sieve size,
d_i = diameter of required size,
D_o = diameter of maximum size aggregate.

The exponent, n, is the slope of such a line and when its value is approximately 0.5, the equation will be the same as Fuller's for maximum density. Table 1 gives the gradation analysis of dry sand used in this study.

The specific gravity of the aggregate was determined using the hydrometer method of ASTM Designation: C 188-44. This method was considered suitable because of the high percentage of fines in the aggregate.

Asphalt

A 60-70 penetration asphalt available in the laboratory was used. The properties of this asphalt have been determined in other tests (33). Three different asphalt contents were chosen, of which two, and 12 percent, were within ASTM specification limits and one, 15 percent, was higher than specified.

Preparation of Mix

The method adopted was similar to the California test method (No. Calif. 350-A) (9). The sand was divided into three equal batches and preheated to a temperature of 325 F in an oven. The asphalt was also heated to a uniform temperature of 325 F and the required amount was poured on the preheated sand and mixed thoroughly in a large bowl for 2 min, insuring that all the sand was evenly coated. To reduce the amount of aging, no further heating was done during this process. After mixing, the sample was portioned into three equal parts and spread out in open containers in preparation for aging.

TABLE 1

SIEVE ANALYSIS OF OTTAWA SAND[a]

Sieve Size	% Passing	% Retained	Wt of Materials (gm)
No. 16	100	0	—
No. 30	75	25	1,750
No. 50	45	55	2,100
No. 100	26	74	1,330
No. 200[b]	15	85	770
			1,050
Total			7,000

[a]Hydrometer analysis: avg. sp. gr., 2.645; value used, 2.65.
[b]Silica sand used for sizes ≤ 200.

Method of Aging

It was decided to age the mixtures at three different temperatures which had been previously employed in other work on aging: 77, 140, 225 F. The standard temperature of 77 F was selected as a basis for comparison; 140 F is used for the Shell aging index (5), and 225 F is widely used in aging work (9, 29).

The aging was undertaken in electric ovens in the presence of air. It was decided to use an aging period of 1 wk, based on the work of Clark (2) and Traxler (29). Clark indicated that 1 wk of aging in a

TABLE 2

DENSITIES OF SPECIMENS

Specimen	A/C Content (%)	Avg. Weight (gm)	Height (cm)	Density (gm/cu cm)	Theoretical Max. Density	Voids (%)
A-9	9	140	7.0	2.09	2.35	11
B-9		140	7.0	2.09	2.35	11
C-9		140	7.0	2.09	2.35	11
A-12	12	135	7.0	2.00	2.25	11.1
B-12		135	7.0	2.00	2.25	11.1
C-12		135	7.0	2.00	2.25	11.1
A-15	15	130	7.0	1.91	2.15	11.1
B-15		130	7.0	1.91	2.15	11.1
C-15		130	7.0	1.91	2.15	11.1

laboratory oven at 150 F was equivalent to 1 yr of aging in the field. By using the same duration, it was hoped to eliminate the time element from the number of variables. The three samples were spread out so that most of the material was exposed to the effects of heating. The principal agents in this type of aging would be volatilization and oxidation. After aging, the mixtures were stored in an inert atmosphere of carbon dioxide until ready for use.

Preparation of Specimens

The specimens were prepared in molds of 1 3/8-in. diameter with 2 7/8-in. internal dimensions. The molds were preheated in an oven to a temperature of 270 F. The aged sand-asphalt mixture was divided into four portions weighing 140 gm each. It was estimated that about 0.3 lb, or 134 gm, would be necessary for each specimen.

Each portion was then reheated in an oven to a temperature of 270 F for a period of 15 min. It was removed and the mold filled in four equal lifts. Compaction was done with the help of a Harvard miniature compactor, using 20 blows of 45 lb for each lift. The sample was extruded from the mold with a special extractor and allowed to cool before weighing.

In the case of samples with asphalt contents of 12 and 15 percent, the extraction from the mold could not be done immediately after compaction because the specimens tended to lose shape and collapse when hot. After compaction, the molds and the specimens were placed in a refrigerator and allowed to cool down completely. They were then removed and the outside of the molds were heated until heating effects just showed on the inside edges of the samples, but the middle cores were not affected. The molds were then placed in the extractor and the samples were forced out, numbered, and stored in a refrigerator in the presence of CO_2 until ready for testing.

Creep Tests

The creep test apparatus consisted of a triaxial cell, and loading was done by consolidation weights applied to the loading frame. Water at a constant 25 C was circulated around the test cell to insure testing at a constant temperature.

Deformation was recorded by means of an LVDT transducer connected to a Varian recorder (Model G-14). The recorder had two chart speeds of 1ft/min and 1 in./min, either of which was used depending on the speed of deformation of specimen and sensitivity required.

The amount of deformation allowed on the sample was limited to 1 or 2 percent, avoiding stressing the material to failure. In practice, deformation was limited to 0.03 in. The average height of a specimen was 2 3/4 in. This, therefore, represented a strain of 1.1 percent. After the set deformation was attained, the load was removed.

The recorder was allowed to run until the deformation became constant. At least two tests were run for each specimen for the same load. Three sets of loadings were used for each set of specimens.

Relaxation Tests

Six specimens were selected from the 9 and 12 percent asphalt content specimens and for the three degrees of aging. The relaxation tests were carried out on an Instron testing machine which measures and records both stresses and strains automatically and can record either variable load at constant strain or variable deformation at constant stress. To test the specimens, a deformation of 1 mm was applied to the specimen within a period of 0.1 min and maintained. The maximum load induced and subsequent stress relaxation were automatically recorded on a chart.

As mentioned previously, the strains obtained in the creep test are not independent of the degree of compaction. To limit any variation in the results due to variation in the density of the specimen, great control was exercised in the compaction. The densities obtained for each asphalt content were in agreement to within 1 percent. Table 2 gives the average bulk densities and percent voids of various mixtures used in this study.

The main difficulty in conducting creep tests was in the application of the creep load. The range of strain measured was only 1.2 percent maximum (i.e., about 0.035 in.). This measurement could easily be upset by the slightest vibration produced in placing the weights. Any erratic initial developments were usually noted and used as the zero error.

The specimens tested in creep generally showed an instantaneous and a delayed strain. When unloaded, the specimens showed an instantaneous rebound, a delayed rebound, and a permanent strain. When the same specimens were reloaded, the magnitude of instantaneous rebound was closer to instantaneous strain than during the first loading. It was decided, therefore, to load and unload each specimen at least twice. For consistency, only the curves obtained from the first reloading were used in computations.

The creep tests on the 15 percent A/C mix were carried out with as little delay as possible because the specimens tended to slump if left in the cell at the test temperature of 77 F. They were usually not removed from storage until a short time before testing.

To obtain the rebound modulus, the instantaneous rebound strain was measured from the recorder charts. It was difficult to measure this quantity because it was difficult to know precisely how much of the rebound was instantaneous and how much was retarded. The rebound modulus (12) was calculated as follows:

$$R = \frac{T}{E_R} \tag{6}$$

where T is applied stress (kg/sq cm), and E_R is rebound strain.

The slopes S of the stress-strain creep curves at the point where the slope is almost constant were measured as follows:

$$S = \frac{\Delta e}{\Delta t} \tag{7}$$

From this the mixture viscosity (V) can be obtained as follows:

$$V = T/S = \frac{T}{\frac{\Delta e}{\Delta t}} \text{ kg/sq cm-sec} \tag{8}$$

RESULTS AND DISCUSSION

Typical creep curves obtained for various mixes are shown in Figures 1 through 3, and values of mixture viscosity, creep modulus, and modulus of recovery (R) are given in Tables 3 through 6.

No relaxation tests could be undertaken on the 15 percent asphalt content mixtures because by the end of the creep tests (in waiting for the cell to drain out before removal of the specimen) the samples had slumped badly and could not have given useful results. The relaxation curves shown in Figures 4 and 5 are for 9 and 12 percent A/C mixtures. Tables 7 and 8 give the values obtained and the calculated values of the relaxation modulus.

An examination of the deformation time curves in Figures 1 through 3 shows that the general outlines of these curves exhibit the predicted characteristics, i.e., an instantaneous elastic deformation and rebound, a time-dependent deformation, and a permanent deformation.

The results showed that the creep curves obtained for the specimens under the first application of load had a very high initial value of instantaneous deformation, far larger than the elastic rebound. It was felt that this was most likely due to initial compression of the specimens. Despite the dense gradation of the mixtures, Table 2 indicates that the mixes contained relatively high percentages of voids. After the initial loading, the material settled and gave more consistent results.

An examination of the creep curves for the various degrees of aging shows a definite difference in the rate of creep (Figs. 1, 2, and 3). For the 9 and 12 percent asphalt content, mix A shows the highest rate of creep, followed by mix B and mix C. The high degree of aging to which mix C was subjected seems to reduce the viscous component of the mix, producing a low viscous deformation. The closeness of curves A and B in Figures 2 and 3 indicates that the degree of aging to which B was subjected was not high enough to make a marked difference as in C. For the 15 percent asphalt content mix (Fig. 3), the slope of curve C is again much lower, but a close examination of the curves shows that the difference between the curves is less marked. This is probably due to a lower degree of aging taking place in the mix with higher asphalt content. It is clear, therefore, that aging does affect the rate of creep and the elastic deformation. The next problem is how to measure these changes.

Earlier, some parameters were developed for measuring the characteristics of the mix based on Burger's model. This model assumes that the viscoelastic behavior of the material is linear. For this linearity to be satisfied, the instantaneous elastic deformation and the retarded elastic deformation (represented by the parabolic section of curve) should be a mirror image of the rebound strain section. The only curves that seem to satisfy this property are those for the group C specimens. The groups A and B specimens indicate that their viscoelastic behavior is not exactly linear. Linearity, however, can be used as an approximation for these mixtures. Table 9 gives the values of its constants for various mixes used in this study.

Wood and Goetz (32), using Burger's model, evolved the parameters of modulus of recovery (R) and mixture viscosity (V). They further suggested the use of these parameters as measures of the degree of aging of mixtures. As indicated before, the creep curves were affected by the aging process; therefore, R and V were calculated to see if any possible interpretation could be made of possible trends in their values. The values obtained appear in Tables 6 and 10. The modulus of recovery values obtained, apart from a few scattered values which do not obey the trend and are obviously erratic, showed a decrease with the degree of aging. To use such a parameter for design, it is necessary to evolve some relationship linking the value of the modulus of recovery to the degree of aging measured, perhaps in terms of temperature or degree-days.

The main problem in measuring the modulus of recovery is the difficulty of measuring the instantaneous rebound. It is difficult to determine exactly where this rebound ends and the retarded rebound begins. It might be possible to measure this value more accurately if, for example, a higher recorder chart speed is used. Even then, removing the load instantaneously to record the rebound is difficult unless an automatic loading

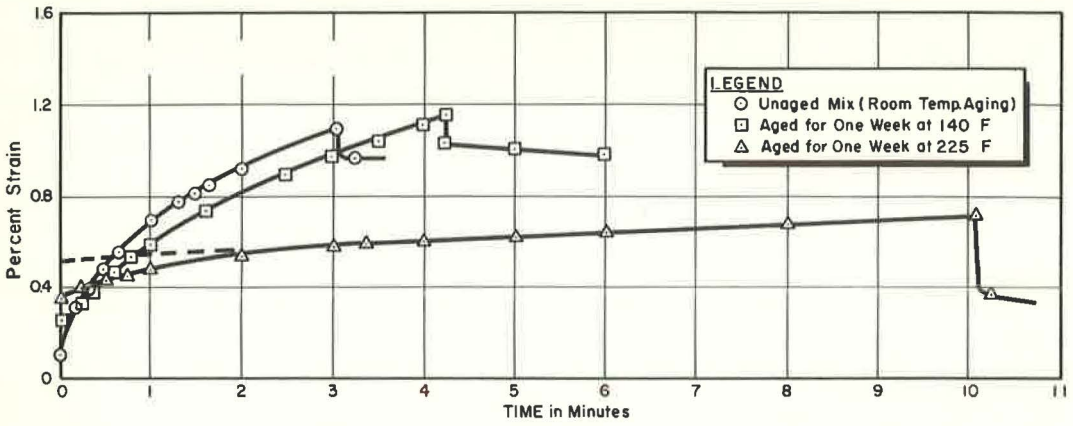

Figure 1. Creep curves, 9 percent A/C, 50 kg (5.2 kg/sq cm) load.

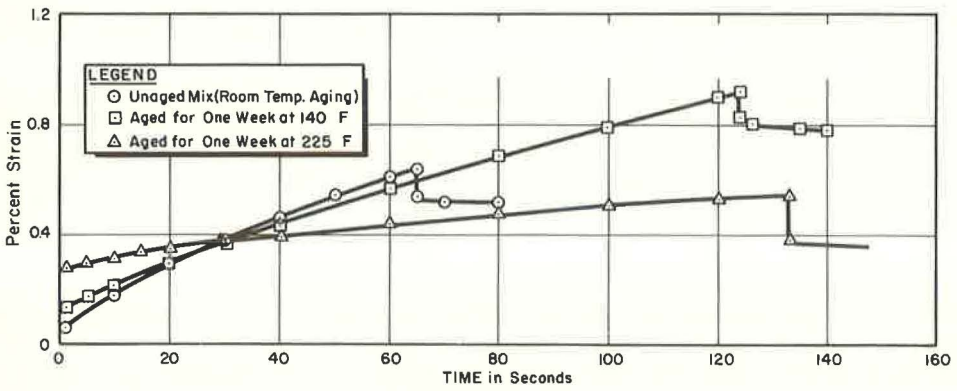

Figure 2. Creep curves, 12 percent A/C, 5 kg (0.52 kg/sq cm) load.

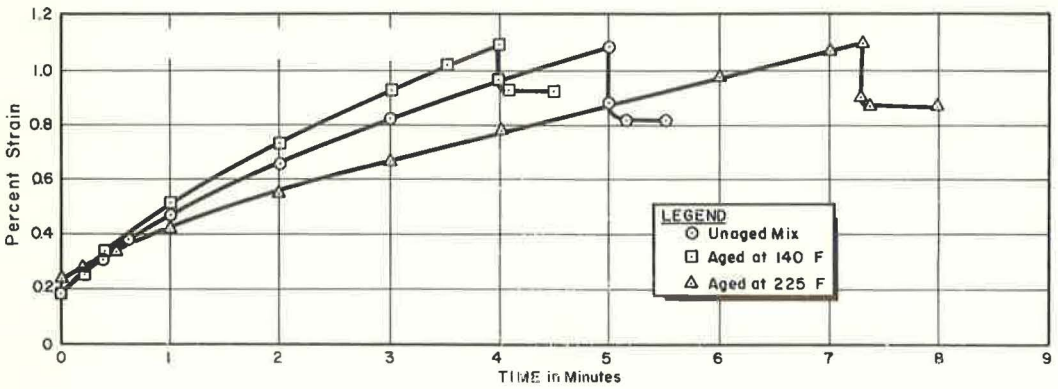

Figure 3. Creep curves, 15 percent A/C, 2 ½ kg (0.263 kg/sq cm) load.

TABLE 3

CREEP TEST, 9 PERCENT A/C MIXTURES

Specimen A-9[a]				Specimen B-9[a]				Specimen C-9[a]			
t (min)	γ ($\times 10^{-3}$ in.)	ϵ ($\times 10^{-3}$)	$E_c(t)$ (kg/sq cm)	t (min)	γ ($\times 10^{-3}$ in.)	ϵ ($\times 10^{-3}$)	$E_c(t)$ (kg/sq cm)	t (min)	γ ($\times 10^{-3}$ in.)	ϵ ($\times 10^{-3}$)	$E_c(t)$ (kg/sq cm)
0	2.5	0.91	5710	0	3.0	1.1	4700	0	9.5	3.4	1530
0.25	18.8	3.20	1800	0.2	7.0	2.54	2050	0.25	10.8	3.86	1350
0.5	13.0	4.73	1100	0.6	12.5	4.55	1170	0.5	11.8	4.24	1230
0.66	15.0	5.45	953	1.0	14.5	5.82	890	0.75	12.5	4.48	1160
1.0	18.8	6.84	750	1.4	19.0	6.91	752	1.0	13	4.67	1110
1.33	21.0	7.64	680	1.8	21.3	7.72	673	2	14.5	5.22	990
1.66	23.0	8.39	620	2.0	22.3	8.48	613	3	15.8	5.69	915
2.0	25.0	9.10	570	3.0	26.5	9.64	541	4	16.5	5.94	877
2.3	26.5	9.65	540	3.4	28	10.2	510	5	17.0	6.1	854
2.6	28	10.70	486	3.8	29.3	10.65	487	6	17.5	6.3	826
3.0	29.5	10.70	-	4.0	30	10.9	476	8	18.5	6.7	776
3.05	26.5	9.65	-	4.2	31.25	11.45	454	10	19.5	7.00	743
3.5	23.5	8.54	-	4.2	28	10.2	-	10.1	19.5	7.00	743
4.0	23.0	8.36	-	4.4	28	10.2	-	10.1	10.0	3.65	-
10.0	22	8.00	-	6.0	27.5	9.8	-	10.2	9.8	3.56	-
								12	7.5	2.73	-

[a]Load: 50 kg (5.2 kg/sq cm).

TABLE 4

CREEP TEST, 12 PERCENT A/C MIXTURES

Specimen A-12[a]				Specimen B-12[a]				Specimen C-12[a]			
t (sec)	γ ($\times 10^{-3}$ in.)	ϵ ($\times 10^{-3}$)	$E_c(t)$ (kg/sq cm)	t (sec)	γ ($\times 10^{-3}$ in.)	ϵ ($\times 10^{-3}$)	$E_c(t)$ (kg/sq cm)	t (sec)	γ ($\times 10^{-3}$ in.)	ϵ ($\times 10^{-3}$)	$E_c(t)$ (kg/sq cm)
0	1.0	0.36	1440	0	3.2	1.11	470	0	4	1.46	356
2	1.5	0.54	963	2	3.5	1.28	408	1	7.5	2.72	191
5	2.5	0.91	572	5	4.5	1.65	315	5	8.0	2.90	179
10	4.5	1.63	319	10	6.0	2.19	238	10	8.5	3.08	169
20	8.0	2.90	179	20	8.0	2.92	178	15	9.0	3.26	159
30	10.5	3.80	137	30	9.90	3.62	144	20	9.5	3.45	151
40	12.5	4.65	112	40	12.0	4.38	119	30	10.3	3.74	139
50	15.0	5.42	96	60	15.6	5.68	92	40	11.0	3.99	130
60	16.8	6.12	85	80	18.9	6.89	73.6	60	12.0	4.35	119
65	17.5	6.36	82	100	21.8	7.91	65.8	80	13.0	4.72	110
66	14	5.09	-	120	24.7	9.00	57.9	100	14.0	5.09	102
67	14	5.09	-	124	25.6	9.31	56	120	14.5	5.28	98.4
70	14	5.09	-	125	22.6	8.2	-	133	15.0	5.42	96.0
				135	21.6	7.86	-	134	10.5	3.80	-
				140	21.4	7.80	-	135	10.3	3.70	-
								150	10.0	3.64	-

[a]Load: 5 kg (0.52 kg/sq cm).

TABLE 5

CREEP TEST, 15 PERCENT A/C MIXTURES

Specimen A-15[a]				Specimen B-15[a]				Specimen C-15[a]			
t (min)	γ ($\times 10^{-3}$ in.)	ϵ ($\times 10^{-3}$)	$E_c(t)$ (kg/sq cm)	t (min)	γ ($\times 10^{-3}$ in.)	ϵ ($\times 10^{-3}$)	$E_c(t)$ (kg/sq cm)	t (min)	γ ($\times 10^{-3}$ in.)	ϵ ($\times 10^{-3}$)	$E_c(t)$ (kg/sq cm)
0	5	1.8	1.46	0	5	1.8	1.41	0	6.5	2.36	110
0.2	6.9	2.5	105	0.2	68	2.46	1.07	0.1	7.0	2.54	102
0.4	8.8	3.1	84.7	0.4	8.8	3.20	0.823	0.2	7.75	2.71	95.5
0.6	10.3	3.75	70.1	0.6	9.5			0.3	8.25	3.00	86.3
1.0	13.0	4.73	55.7	1	14.0	5.09	0.517	0.5	9.25	3.36	77
2.0	18.3	6.65	39.6	2	20.0	7.25	0.363	1.0	11.25	4.08	63.5
3.0	22.8	8.28	31.8	3	25.8	9.35	0.282	2.0	15.0	5.45	47.5
4.0	26.5	9.63	27.6	3.5	28.3	10.20	0.258	3.0	18.5	6.72	38.5
5.0	30.0	10.9	24.0	4	26	10.90	0.241	4.0	21.5	7.8	33.2
5.1	22.5	8.2	3.20	4.5	26	9.44	-	5.0	24.5	8.9	29.1
5.2	22.5	8.2	3.20	-	-	9.44	-	6.0	27.0	9.8	26.4
5.6	22.5	8.2	3.20	6	26	9.44	-	7.0	29.5	10.7	24.2
6.0	22.5	8.2	3.20	6.5	26			7.3	30	10.9	23.7
								8.0	24	8.7	

[a]Load: 2 ½ kg (0.263 kg/sq cm).

TABLE 6

MODULUS OF RECOVERY

Specimen	Load (kg)	Rebound Strain ($\times 10^{-3}$)	Modulus of Recovery
A-9	50	1.0	5,200
B-9	50	1.25	4,160
C-9	50	3.35	1,550
A-12	5	1.27	410
B-12	5	1.11	470
C-12	5	1.63	320
A-15	2 ½	1.5	173
B-15	2 ½	1.5	173
C-15	2 ½	1.6	162

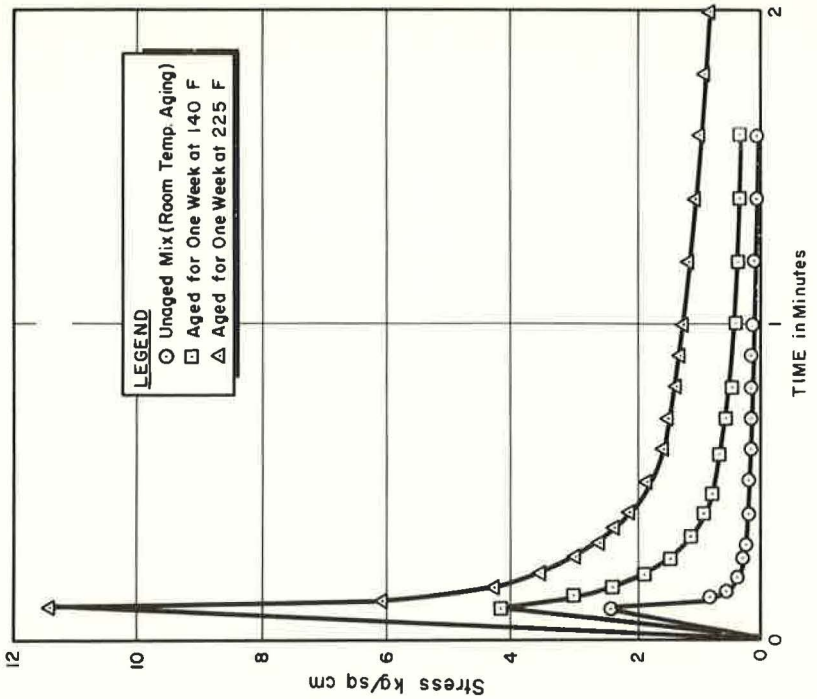

Figure 5. Stress relaxation curves, 12 percent asphalt content.

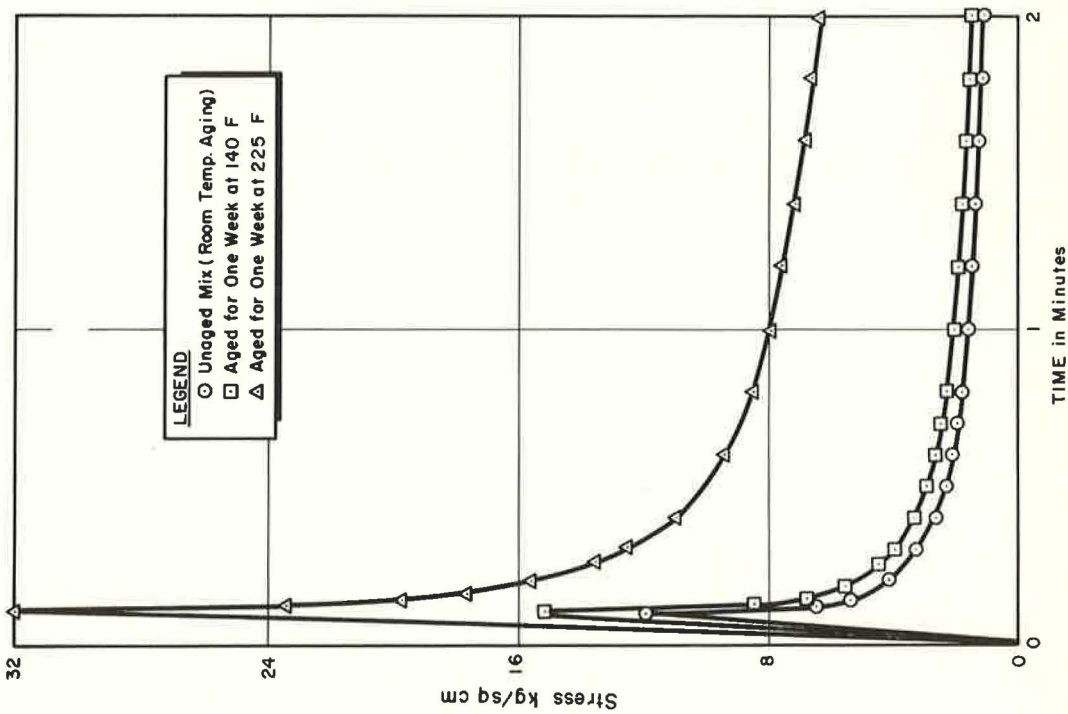

Figure 4. Stress relaxation curves, 9 percent asphalt content.

TABLE 7

RELAXATION TESTS, 9 PERCENT A/C MIXTURES

Specimen A-9-1				Specimen B-9-1				Specimen C-9-1							
Time (min)	Load (kg)	Stress (kg/sq cm)	$E_{R(t)}$ (kg/sq cm)	Time (min)	Load (kg)	Stress (kg/sq cm)	$E_{R(t)}$ (kg/sq cm)	Time (min)	Load (kg)	Stress (kg/sq cm)	$E_{R(t)}$ (kg/sq cm)	Time (min)	Load (kg)	Stress (kg/sq cm)	$E_{R(t)}$ (kg/sq cm)
0.1	115	11.95	870	0.1	145	15.1	1100	0	0	0	-	-	-	-	-
0.12	62	6.44	470	0.12	80	8.3	606	0.1	310	32.2	2340	1.2	72	7.5	545
0.13	52	5.4	3.94	0.14	65	6.75	492	0.12	225	23.4	1700	1.4	68	7.09	515
0.16	49	5.1	3.21	0.20	50	5.2	380	0.14	190	19.7	1440	1.6	65	6.75	492
0.18	46	4.8	348	0.25	43	4.46	326	0.16	170	17.7	1290	1.8	63	6.55	476
0.20	40	4.15	303	0.30	38	3.94	288	0.18	155	16.1	1170	2.0	60.2	6.27	456
0.25	35	3.64	265	0.35	35	3.63	266	0.20	150	15.6	1135	2.5	57.8	6.0	438
0.30	31	3.22	235	0.40	32	3.32	242	0.25	130	13.5	985	3.0	53	5.5	400
0.35	28.5	2.95	216	0.45	30.2	3.14	229	0.30	120	12.5	910	3.5	50	5.2	380
0.40	26	2.7	197	0.50	28.5	2.96	218	0.35	112	11.5	850	4.0	48	5.0	364
0.50	23	2.4	174	0.60	26	2.7	197	0.40	106	11.0	803	4.5	46	4.8	350
0.60	21	2.18	159	0.7	24	2.5	182	0.45	102	10.1	774	5.0	44.2	4.57	335
0.70	19	1.97	144	0.8	22.5	2.34	170	0.50	98	10.0	743	5.5	43	4.47	326
0.80	18	1.87	136	1.0	20.4	2.12	154.5	0.60	91	9.45	690	6.0	42	-	318
0.90	16.8	1.74	127	1.2	18.6	1.94	141	0.70	86	8.94	650	6.5	41	-	310
1.0	15.8	1.64	120	1.4	17.4	1.80	132	0.80	82	8.52	620				
1.2	14.4	1.5	109	1.6	16.4	1.7	124	0.90	80	8.31	606				
1.4	13.3	1.38	101	1.8	15.4	1.6	116.5	1.0	76.5	7.95	580				
1.6	12.3	1.28	93	2.0	14.5	1.5	105								
1.8	11.6	1.20	88	2.5	13.2	1.37	95.5								
2.0	11.0	1.14	83.4	3.0	12.1	1.26	89								
2.5	9.8	1.00	74.2	3.5	11.4	1.18	82								
3.0	9.0	0.935	68	4.0	10.7	1.11	78								
4.0	7.8	0.81	59	4.5	10.1	1.05	73								

TABLE 8

RELAXATION TESTS, 12 PERCENT A/C MIXTURES

Specimen A-12-4				Specimen B-12-3				Specimen C-12-3							
Time (min)	Load (kg)	Stress (kg/sq cm)	$E_{R(t)}$ (kg/sq cm)	Time (min)	Load (kg)	Stress (kg/sq cm)	$E_{R(t)}$ (kg/sq cm)	Time (min)	Load (kg)	Stress (kg/sq cm)	$E_{R(t)}$ (kg/sq cm)	Time (min)	Load (kg)	Stress (kg/sq cm)	$E_{R(t)}$ (kg/sq cm)
0	0	0	-	0	0	0	-	0	0	0	-	1.2	10.8	1.12	82
0.1	23	2.39	166.8	0.1	40	4.16	303	0.1	110	11.4	834	1.4	9.9	1.04	75
0.12	8	0.82	58	0.12	35	3.54	267	0.12	58	6.02	438	1.6	9.2	0.95	69.7
0.14	6	0.624	43.4	0.14	29	3.02	220	0.14	47	4.89	356	1.8	8.6	0.89	65
0.16	5	0.52	36.2	0.16	23	2.39	174.2	0.16	41	4.26	310	2.0	8.2	0.85	62
0.18	4.4	0.457	31.9	0.18	20	2.08	151.3	0.18	37	3.85	280	2.5	7.2	0.75	54.5
0.20	3.6	0.374	26.4	0.20	18	1.87	136.2	0.20	33.5	3.5	255	3.0	6.5	0.68	49.2
0.25	2.8	0.29	20.2	0.25	14	1.45	106	0.25	28.3	2.95	214	3.5	6.0	0.624	45.4
0.30	2.3	0.24	17.4	0.30	11.5	1.2	87.1	0.30	25	2.6	189	4.0	5.6	0.58	42.4
0.35	2.0	0.208	15.1	0.35	10	1.04	75.6	0.35	22.5	2.35	170	4.5	5.2	0.54	39.4
0.40	1.8	0.187	13.6	0.40	9	0.93	68.2	0.40	20.5	2.14	155	5.0	4.9	0.50	22
0.45	1.6	0.166	12.6	0.50	7.5	0.78	56.8	0.45	19.2	1.98	145	5.5	4.6	0.47	19.7
0.5	1.4	0.145	10.6	0.60	6.4	0.66	48.4	0.5	18.0	1.87	136	6.0	4.4	0.45	18.1
0.6	1.22	0.127	9.24	0.70	5.5	0.57	41.6	0.6	16.2	1.6	122				
0.7	1.1	0.114	8.34	0.80	5.0	0.52	37.9	0.7	14.8	1.54	112				
0.8	1.0	0.104	7.57	0.90	4.5	0.47	34.1	0.8	13.6	1.40	103				
0.9	0.9	0.094	6.8	1.0	4.3	0.45	32.6	0.9	12.8	1.34	96.8				
1.0	0.82	0.085	6.2	1.2	3.7	0.39	28	1.0	12.0	1.25	91				
1.2	0.7	0.073	5.3	1.4	3.3	0.34	25								
1.4	0.65	0.068	4.92	1.6	3.0	0.31	22.7								
1.6	0.53	0.055	4.01	1.8	2.8	0.29	21.2								
1.8	0.51	0.053	3.96	2.0	2.5	0.26	18.9								
2.0	0.49	0.051	3.7	2.2	2.4	0.25	18.2								

TABLE 9

MODEL CONSTANTS[a]

Specimen	Asphalt	Condition	G_1 (kg/sq cm)	G_2 (kg/sq cm)	η_1 (kg-sec/sq cm)	η_2 (kg-sec/sq cm)
A-9	9	A	4,330	1,040	1.01×10^5	3.4×10^4
B-9	9	B	2,370	1,530	1.43×10^5	8.2×10^4
C-9	9	C	1,530	3,080	1.82×10^6	19.4×10^4
A-12	12	A	1,300	346	6.63×10^3	5.32×10^3
B-12	12	B	472	371	6.73×10^3	7.41×10^3
C-12	12	C	193	520	1.92×10^4	1.80×10^4
A-15	15	A	140	158	9.63×10^3	1.30×10^3
B-15	15	B	140	141	6.86×10^3	0.554×10^3
C-15	15	C	114	169	1.39×10^4	1.06×10^3

[a]For curves shown only.

TABLE 10

MIXTURE VISCOSITY

Specimen	Load (kg)	Slope of Curve ($\times 10^{-6}$)	Mixture Viscosity ($\times 10^{6}$ kg-sec/sq cm)	Average ($\times 10^{6}$ kg-sec/sq cm)
A-9-1	20	30	0.67	
A-9-3	50	29	1.7	1.14
B-9-1	20	5.16	3.87	
B-9-2	50	23.2	2.16	3.01
C-9-1	20	1.13	17.8	
C-9-4	50	2.86	16.9	17.4
A-12-1	5	73.6	0.068	
A-12-2	10	930	0.1075	
A-12-3	20	242	0.082	0.085
B-12-1	5	41.6	0.12	
B-12-2	20	18.8	0.106	0.113
C-12-1	5	14	0.357	
C-12-2	10	3.4	2.94	
C-12-3	20	1.47	1.36	2.15
A-15-1	5	1.36	0.037	
A-15-2	10	310	0.032	0.035
B-15-1	2.5	25.4	0.099	
B-15-2	5	46.2	0.082	
B-15-3	10	120	0.108	0.093
C-15-1	2.5	24	0.111	
C-15-2	5	37.5	0.133	
C-15-3	10	95.0	0.103	0.116

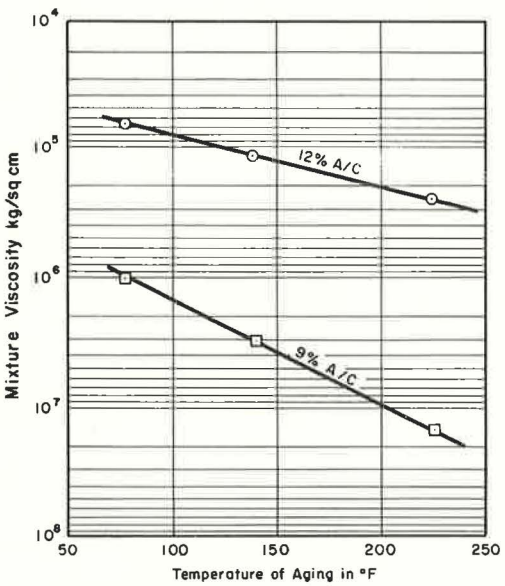

Figure 6. Log mixture viscosity vs temperature of aging.

system is used. On the whole, because of the practical difficulty of finding the correct value of rebound, it does not seem that the modulus of recovery could be used as a practical parameter for aging measurements.

The mixture viscosity values obtained showed a more promising trend. It is clear from the results given in Table 10 that mixture viscosity increases with the degree of aging. This seems a more reliable parameter, easier to measure and to control. With the limited range of values obtained in this experiment, it is not possible to say categorically what sort of relation can be evolved relating the mixture viscosity to the degree of aging. However, the observed data appear to indicate that a semilog relationship exists. The log V vs temperature generated a straight line (Fig. 6) which results in the following relation:

$$V = e^{kT_A} \qquad (9)$$

where T_A is aging temperature, and k = a constant which varies with percent asphalt in mix. To confirm the existence of such a relationship, which could be of great use in the study of mixes, more experiments would be necessary.

To obtain a reliable value of V, great care must be exercised in selecting loading cycles to insure consistency. As the sample is loaded and unloaded several times,

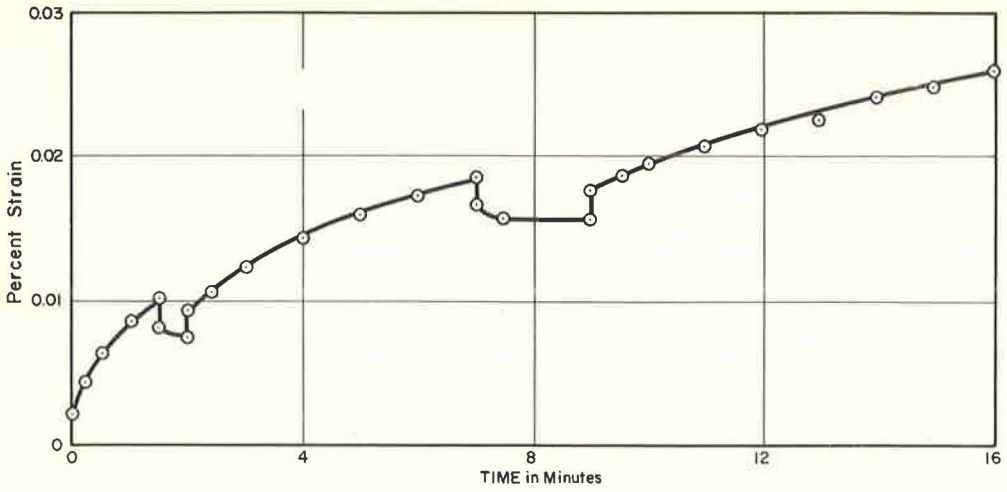

Figure 7. Effect of repeated loading on creep, 15 percent A/C, 2½ kg (0.263 kg/sq cm) load.

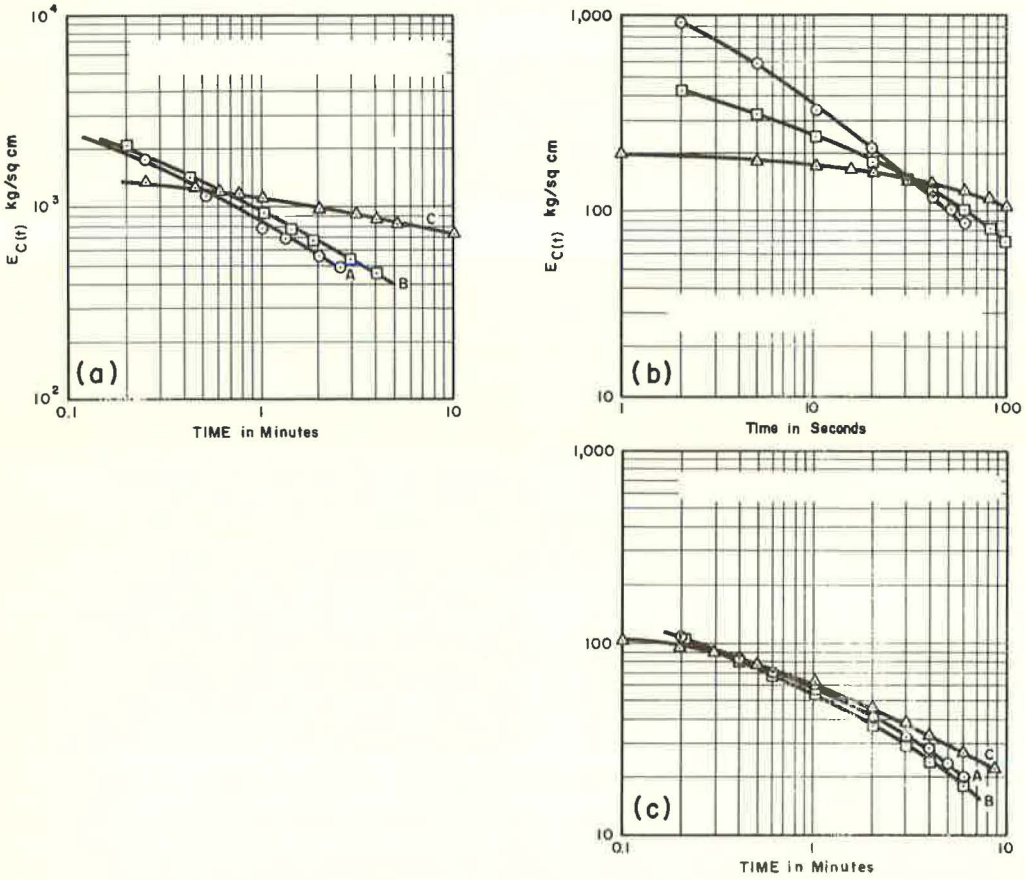

Figure 8. Log-log plots of creep modulus vs time: (a) 9 percent A/C, 50 kg (5.2 kg/sq cm) load; (b) 12 percent A/C, 5 kg (0.52 kg/sq cm) load; and (c) 15 percent A/C, 2½ kg (0.263 kg/sq cm) load.

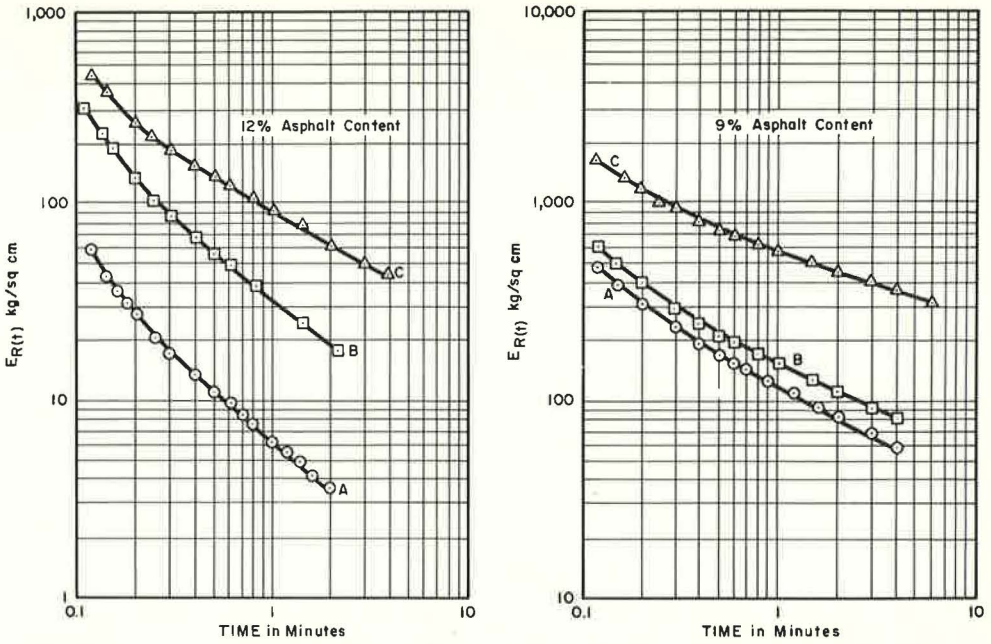

Figure 9. Log-log plot of relaxation modulus vs time.

the slope of the creep curves progressively decreases as shown in Figure 7. It is necessary, therefore, to select the same load cycle for all the specimens before evolving values. The decrease in the slope of the creep curve provides further evidence that the viscoelastic behavior of the asphalt mixture may not be exactly linear. This decrease in the rate of creep with repeated load may be caused by stiffening of the mixes due to densification of specimens.

A plot was made of the log of creep modulus vs the log of time (Fig. 8). Although no obvious trend was noticed in these curves, future results may indicate one.

The relaxation curves in Figures 4 and 5 again show differences due to aging. These curves, like the creep curves, also showed that for the duration of aging employed, the 140 F aging temperature did not alter the viscoelastic characteristic of material significantly, whereas aging at 225 F changed this behavior considerably. A plot of relaxation modulus vs log of time did not produce a straight line, thus indicating that the relaxation behavior of these asphaltic mixtures may be that of a complex model.

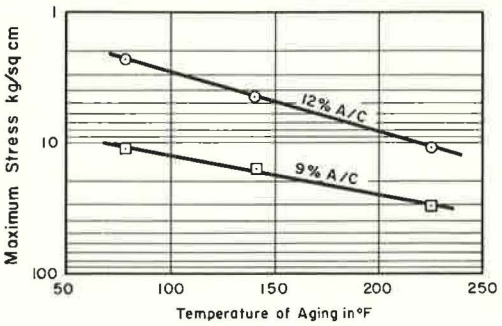

Figure 10. Log maximum relaxation stress vs aging temperature.

A plot of the log of relaxation modulus vs log of time shown in Figure 9 exhibits marked curvature which again indicates that a simple viscoelastic model may not be representative of the mixtures used.

An investigation was made of the possible existence of a relation between the degree of aging and the maximum relaxation stress attained by the material for the 1-mm deformation of 1.42 percent strain. It appears that a semilog relation is possible and that a relationship of the form, $P_R = e^{bT_R}$, might be possible where P_R is maximum relaxation stress, T_R is temperature of aging in degrees Fahrenheit and b is a constant (Fig. 10). This relation, if it

exists, could also be useful in studying the effect of aging on mechanical properties of asphaltic mixtures. It is difficult to confirm definitely the existence of this relation with the limited data obtained. The relationship, however, would be much easier to measure than the other parameters mentioned earlier if the right equipment were used.

CONCLUSION

The results of this study appear to justify the following conclusions. It should be realized that these conclusions are applicable only to the particular kinds of mixtures used in this investigation. Within the limitations of the tests performed and the data obtained, it would seem that:

1. Aging does affect the creep and relaxation characteristics of the mixtures studied;
2. Aging reduces the rate of creep of the mix, resulting in a harder mix with a higher elastic response and a lower viscous component;
3. Within the range of the materials studied and the procedures used in this study, there appears to be a certain relationship between mixture viscosity and aging temperature, and a maximum relaxation stress and aging temperature; and
4. The creep modulus did not seem to indicate any significant relation with aging, but the relaxation modulus showed a more significant variation with the degree of aging.

REFERENCES

1. Bright, R., and Reynolds, E. T. Effect of Mixing Temperature on Hardening of Asphaltic Binders in Hot Bituminous Concrete. Highway Research Board Bull. 333, pp. 20-38, 1962.
2. Clark, R. C. Practical Results of Asphalt Hardening on Pavement Life. Proc. AAPT, Vol. 27, p. 196, 1958.
3. Fink, D. F. Research Studies and Procedures. Proc. AAPT, Vol. 27, p. 176, 1958.
4. Goetz, W. H., McLaughlin, J. F., and Wood, L. E. Load Deformation Characteristics of Bituminous Mixtures Under Various Conditions of Loading. Pro. AAPT, Vol. 26, p. 241, 1957.
5. Griffin, R. L., Miles, T. K., and Penther, C. J. Microfilm Durability Test for Asphalt. Proc. AAPT, Vol. 24, 1955.
6. Resistance of Bituminous Materials to Deterioration Caused by Physical and Chemical Changes. Highway Research Board Bibliography No. 9, 1951. 89 pp.
7. Hubbard, Prevost, and Reeve, C. S. The Effect of Exposure on Bitumens. J. Ind. Eng. Chem., Vol. 5, No. 15, 1913.
8. Hubbard, P., and Gollomb, R. The Hardening of Asphalt in Relation to Development of Cracks in Asphaltic Concrete Pavements. Proc. AAPT, Vol. 9, Dec. 1937.
9. Hveem, F. N., Zube, E., and Skog. J. Proposed New Tests and Specifications for Paving Grade Asphalts. Proc. AAPT, Vol. 32, p. 282, 1963.
10. Krchma, L. C. Relationship of Mix Design to Hardening. Proc. AAPT, Vol. 27, p. 186, 1958.
11. Lewis, R. H., and Halstead, W. J. Behavior of Asphalts in Thin Films. Public Roads, Vol. 22, No. 2, Apr. 1941.
12. Mack, C. Rheology of Bituminous Mixtures in Relation to Properties of Asphalts. Proc. AAPT, Vol. 13, 1942.
13. Theory of Deformation Mechanism and Bearing Strength of Bituminous Pavements. Proc. AAPT, Vol. 23, 1954.
14. Mack, C. Physical Aspects of Hardening of Paving Asphalts. Proc. AAPT, Vol. 27, p. 183, 1958.
15. McKesson, C. L. Durability of Asphaltic Binders. Proc. Montana Bituminous Conf., 1958.
16. Secor, K. E., and Monismith, C. L. Viscoelastic Properties of Asphalt Concrete. Highway Research Board Proc., Vol. 41, pp. 299-320, 1962.

17. Secor, K. E., and Monismith, C. L. Analysis of Triaxial Test Data on Asphalt Concrete Using Viscoelastic Principles. Highway Research Board Proc., Vol. 40, pp. 295-314, 1961.
18. Pister, K. S., and Monismith, C. L. Analysis of Viscoelastic Flexible Pavements. Highway Research Board Bull. No. 269, pp. 1-15, 1960.
19. Powers, J. W. Hardening of Asphalt Cement in Asphaltic Concrete Pavements. Proc. Montana Nat. Bituminous Conf., 1937.
20. Reeve, C. S., and Lewis, R. H. The Effects of Exposure on Some Fluid Bitumens. J. Ind. Eng. Chem., Vol. 9, No. 743, 1917.
21. Reiner, M. Building Materials, Their Properties, Plasticity and Inelasticity. New York, Interscience Pub., 1954.
22. Sabbrow, S. Aging of Road Tars. Cong. de l'Industrie de Gaz, Paris, June 1934.
23. Sabbrow, S., and Renausie, E. M. A Study of the Aging of Coal Tar Road Binders. 14th Congr. Chim. End., Paris, Oct. 1934; Chemical Abstracts, Vol. 29, p. 6389, 1935.
24. Skog, J. B. The Operation, Control and Application of Infra-red Weathering Machine California Design. 2nd Pacific Area Nat. Meet., ASTM, Calif., 1956.
25. Stanton, T. E., and Hveem, F. N. Test Methods for Performing Accelerated Durability Tests on Asphalt. ASTM STP No. 94, 1950.
26. Tobolsky, S. V. Stress Relaxation Studies of the Viscoelastic Properties of Polymers. Jour. Appl. Physics, Vol. 27, No. 7, July 1956.
27. Traxler, R. M. Durability of Asphalt Cements. Proc. AAPT, Vol. 32, No. 44, 1963.
28. Traxler, R. N. Pavement Performance and Durability as Affected by Asphalt Properties. Proc. AAPT, Vol. 32, p. 229, 1963.
29. Traxler, R. N. Asphaltic Composition and Hardening by Volatilization. Proc. AAPT, Vol. 30, p. 359, 1961.
30. Vallerga, B. A., Monismith, C. L., and Grantham, K. C. A Study of Some Factors Influencing Weathering of Paving Asphalts. Proc. AAPT, Vol. 26, p. 127, 1957.
31. Vokar, R. Correlation of Laboratory Tests of Bituminous Mixtures with Service Behavior. Proc. Montana National Bituminous Conf., Sept. 1937.
32. Wood, L. E., and Goetz, W. H. The Rheological Characteristics of a Sand-Asphalt Mixture. Proc. AAPT, Vol. 28, p. 211, 1959.
33. Sendze, O. B. B. The Effect of the Degree of Aging on the Creep and Relaxation Behavior of Sand Asphalt Mixtures. Unpubl. M. S. Thesis, Ohio State Univ., 1964.

Effect of Asphalt Viscosity on Rheological Properties of Bituminous Concrete

CHARLES A. PAGEN and BEE KU
Respectively, Assistant Professor of Civil Engineering, and Research Associate, Transportation Engineering Center, Ohio State University

The mechanical properties of bituminous concrete and the rheological response of asphalt greatly influence the design and construction of multilayer flexible pavement structures and are directly related to the reponse of bituminous concrete structures to traffic under various environmental conditions. The experimental phase of this research involved the testing of five different types of asphaltic concrete mixtures in which two aggregate types, two aggregate gradations, and two asphalt types are used. Correlations between asphalt viscosity, rheological strength moduli, and deformations of the bituminous mixes were developed over an extensive range of loading times and temperatures. The application of the linear viscoelastic theory and the time-temperature superposition concept to define the mechanical properties of asphaltic concrete mixtures was rigorously investigated. An equation of state to describe the load, deformation, time, and temperature-dependent behavior of asphalt concrete is presented. The agreement of the data in this experimentation provides a verification of the ability of the linear viscoelastic theory to describe the response of asphaltic concrete, as well as of the application of the derived equations of state and the time-temperature superposition concept to these materials.

•THE MECHANICAL PROPERTIES of the asphaltic concrete layers of flexible pavements and the rheological properties of the asphalt component of these layers greatly influence the design and construction of multilayer flexible pavements. The response of asphaltic concrete structures to traffic and environmental conditions is directly related to these factors. However, considerable data remain to be accumulated to establish the usefulness of viscoelastic analysis in design and to explain the mechanical behavior of asphalts and mixtures of asphalt and aggregates.

Research at The Ohio State University to date has demonstrated that, as an engineering approximation, asphalt-aggregate mixtures may be considered linear viscoelastic materials and thermorheologically linear materials (1, 2). The time- and temperature-dependent mechanical properties of bituminous concrete have also been investigated by Secor and Monismith (3) and by Krokosky and Chen (4), and this research may be used as a tool by asphalt technologists in evaluating the complex nature of such materials. Data have been obtained demonstrating the loading time and temperature dependence of such physical properties as the complex moduli, Marshall test stability, stress relaxation moduli, and creep moduli. It is possible that this rheological approach may only serve as an engineering approximation to the behavior of asphaltic concrete under definite conditions of traffic and certain ranges of temperature. However, rheological concepts provide a much higher level of approximation than the presently available elastic design theories. The objective of this research is to relate

Paper sponsored by Committee on Mechanical Properties of Bituminous Paving Mixtures.

changes of asphalt viscosity or temperature to the mechanical properties of asphaltic concrete mixtures. The data obtained may be used to evaluate: (a) limits of asphalt viscosity which will produce specified changes of material rheological strength properties and material deformation, and (b) procedures to predict strength moduli and mixture strain based on binder viscosity over a range of loading times and temperatures.

PROCEDURE

The experimental phase of the research project involved the testing of five different types of asphaltic concrete mixtures comparable to several major categories used for road surfacing in which two aggregate types, two aggregate gradations, and two asphalt types are used. The two 85-100 penetration asphalts used in the study were obtained from different sources; one has a high temperature susceptibility as measured by microviscometer tests, and the other has a relatively low temperature susceptibility. One aggregate type is a crushed river gravel and the other is a limestone. Two aggregate gradations falling within the Ohio T-35C specifications were used, one with a maximum size of $\frac{1}{2}$ in. and the other with a maximum size of $\frac{3}{8}$ in. Test specimens, 4 in. in diameter and approximately 8 in. high, were prepared using a kneading compactor.

Constant-load compressive tests were performed on unconfined test cylinders. The experimental loads and temperatures were varied over a wide range. A standard creep testing program was used to record and analyze the instantaneous elastic, retarded elastic, and viscous deformations. Cyclic repetition of loading and unloading was also studied. Kinematic viscosity of the original asphalts used in the mixtures was measured with a sliding plate microviscometer.

Correlations between the original asphalt viscosity, mixture rheological strength moduli, and mixture deformations under load were developed for a wide range of loading times and temperatures. The application of the linear viscoelastic theory and the time-temperature superposition concept to define the mechanical properties of asphaltic concrete mixtures were rigorously investigated and validated. An equation of state to describe the stress, strain, time, and temperature-dependent mechanical behavior of the asphaltic concrete mixtures studied is presented. Two methods were employed to determine the equation of state: (a) curve-fitting procedures utilizing equations of the form of a generalized Voigt model, and (b) a Scatran computer program where the equation of state developed was in the form of sixth-degree polynomials. The equation of state developed by both methods was applied to predict the response of the material over an extensive range of loading times and temperatures.

NOTATIONS

σ = stress,

ϵ = strain,

J = creep compliance,

E = creep modulus and elastic constants,

α_T = temperature shift factor,

t = time,

T = temperature,

ζ = characteristic retardation or relaxation time,

δ = deformation,

T_o = standard reference temperature,

k = slope of asphalt viscosity-temperature curve on semilog plot or slope of log α_T vs temperature plot,

η = dashpot constants and asphalt viscosity,

C = constant, and

e = base of natural logarithms.

EXPERIMENTATION

The different test programs available for the investigation of the rheological properties of bituminous concrete may include constant-load creep tests, stress-relaxation tests, and direct sinusoidal-stress dynamic tests. Stress-relaxation tests are usually difficult to perform, and direct dynamic tests yield information applicable only at the frequency used in the test. The creep test, which was primarily used in this study, is relatively easy to conduct and yields information over a wide range of loading time or over a range of frequencies when transformed to the frequency domain. In the viscoelastic theory (5), creep deformation consists of instantaneous elastic, time-dependent elastic, and viscous deformation. To investigate these three components, and particularly to separate the elastic and viscous deformation from the total deformation, one must observe the rebound behavior of the material after unloading. The loading and unloading duration should be determined by comparing it with the longest retardation time. For utility and standardization of the testing procedure, a 1-hr loading and equal unloading duration were adopted in this research.

Many engineering materials exhibit the phenomenon of mechanical conditioning which can be conveniently analyzed by repetition-of-load application. Hence, the present testing program includes the following three phases: (a) constant-load creep tests, (b) creep recovery tests, and (c) repetition-of-load tests.

An independent test program to investigate the viscosity of asphalt was also performed. These experiments included the measurement of original asphalt viscosity (before mixing) by means of a Hallikainen sliding plate microviscometer.

Materials

The bituminous concrete mixtures investigated included two different asphalt types, two aggregate types, and two aggregate gradations. The two asphalts were from a Venezuela crude and California crude and have, respectively, a low and a high temperature susceptibility. The viscosities of the original asphalts are shown in Figure 1 for a range of temperatures from approximately 55 to 100 F. The two aggregate types used were a limestone and a crushed river gravel. The two gradations of the aggregates (Table 1) are within type T-35C of the Ohio Department of Highways specification. There are approximately 30 specimens in each series. An asphalt content of 5.7 percent was selected for all mixes because this value was found to be close to the optimum asphalt content for stability of the materials tested. The following series numbering system for the asphaltic concrete mixes was used:

A = Asphalt type
   1. Low temperature susceptible asphalt
   2. High temperature susceptible asphalt

B = Gradation, type T-35C
   1. Ohio minimum specification
   2. Ohio intermediate specification

C = Aggregate type
   1. Limestone
   2. River gravel

The asphalt and aggregate were proportioned on the basis of weight. Before mixing, aggregates were first heated to 300 F and kept in the oven at this temperature for at least 8 hr; then the asphalt was heated to 290 F and mixed with the aggregate by a mechanical mixer. A kneading compactor was used to compact the samples. Each mix was fed to the mold in five layers, and each layer was compacted with 25 blows. On each blow the booster exerted a compactive force of 10,900 lb. The dwell duration time for the applied load was, respectively, 4, 5, 6, 5, and 4 sec at the five layers to

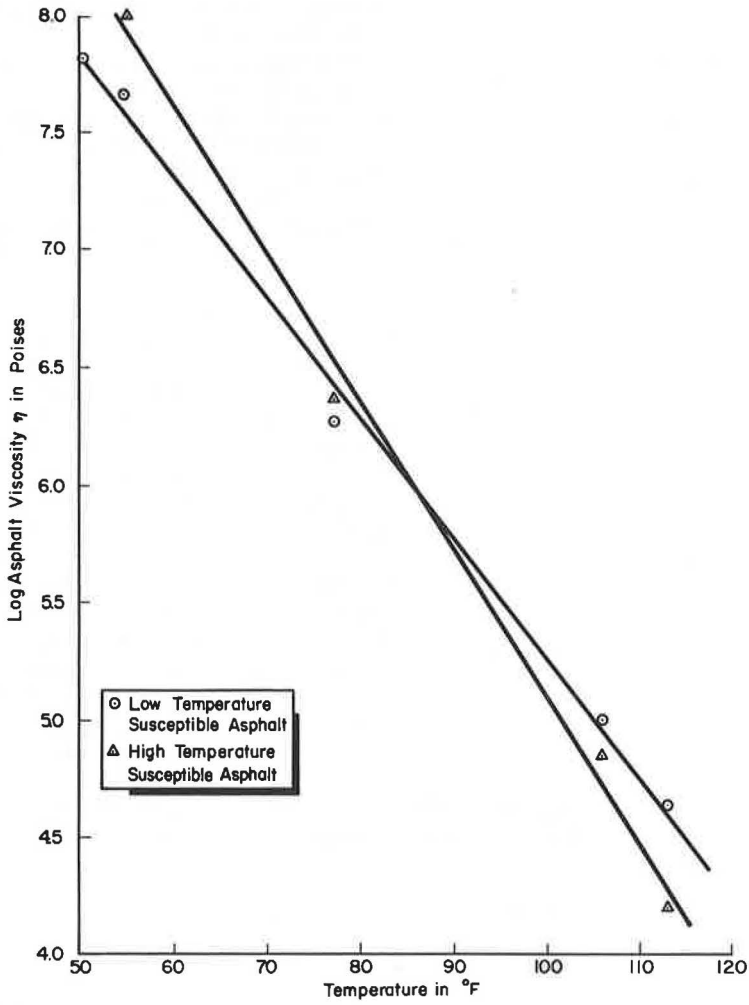

Figure 1. Asphalt viscosity vs temperature.

produce relatively homogeneous and isotropic specimens. After the compaction procedure was completed, a static load of 10,900 lb was immediately applied to the specimen and maintained constant for 5 min. The specimens prepared were 4 in. in diameter and approximately 8 in. high.

Description of Tests

Each series of specimens was investigated at three different temperatures: 41, 77, and 104 F. At each temperature, three stress levels were studied. The level of stress was different at each temperature, as indicated in Table 2.

All specimens were stored at room temperature until tested. The samples were submerged in a temperature-controlled water bath approximately 8 hr before testing. Creep experiments were also conducted at 60 and 90 F to supplement the research program. The reproducibility of the test results was also checked. As pointed out by Bland (6), the stress and strain are proportional in the linear viscoelastic range. If the strain-time curves are reduced to a curve corresponding to a standard stress by multiplying the strain-time curves by the ratio of the standard stress to the actual

TABLE 1

BITUMINOUS CONCRETE MIX PROPORTIONS

Passing U.S. Sieve	Retained on U.S. Sieve	Percent by Wt of Agg.	Percent by Wt of Total Mix	Wt/Mix (gm)
		(a) Mix 1		
½ in.	⅜ in.	0	0	0
⅜ in.	No. 4	25.44	24.0	960
No. 4	No. 6	17.00	16.0	640
No. 6	No. 16	25.40	24.0	960
No. 16	No. 30	6.36	6.0	240
No. 30	No. 50	5.30	5.0	200
No. 50	No. 100	7.42	7.0	280
No. 100	No. 200	8.52	8.0	320
No. 200		4.56	4.3	172
		100.00	94.3	3,772
85-100 Bitumen			5.7	228
			100.0	4,000
		(b) Mix 2		
½ in.	⅜ in.	4.24	4	160
⅜ in.	No. 4	28.60	27	1,080
No. 4	No. 6	17.00	16	640
No. 6	No. 16	24.40	23	920
No. 16	No. 30	7.43	7	280
No. 30	No. 50	6.35	6	240
No. 50	No. 100	5.30	5	200
No. 100	No. 200	5.30	5	200
No. 200		1.38	1.3	52
		100.00	94.3	3,772
85-100 Bitumen			5.7	228
			100.0	4,000

stress, a means of comparison is obtained. If the reduced strain functions obtained are within experimental error, the definitions of linearity and reproducibility of test results are satisfied. In this research the strain-time curves will form a band, rather than exactly coincide. Thus, the linearity and reproducibility of experiments are satisfied within a range of testing error. The maximum deviation for this research is approximately 15 percent, which the authors consider satisfactory for this type of experimentation. Due to inherent variation in all materials, some scatter is noted and expected in the experimental results. However, this research indicates that the mechanical response of asphaltic concrete mixtures can be approximately described by the linear viscoelastic theory. It can be rigorously argued that there are no true elastic or viscous materials (7, 8), and there is no reason to assume that a perfectly linear viscoelastic material should exist. It is important to consider whether this engineering idealization will aid highway engineers to evaluate pavement performance and assist in establishing better pavement design procedures. More sophisticated approaches are, of course, available if this engineering approximation does not prove sufficiently accurate. However, more complex methods may prove troublesome when applied to practical problems.

EXPERIMENTAL RESULTS

Creep Tests

The experimental loading data of the constant-load creep tests are shown in Figures 2 through 6. Each graph contains the strain-time data of one complete series of an asphaltic concrete mixture, with each curve representing the average of six experiments, with the exception of the 60 and 90 F tests. The six tests were performed at the same temperature under isothermal conditions, but in each case two samples were tested at three different stress levels. By application of the linear viscoelastic assumption, the six individual creep experimental results were reduced to one curve corresponding to a 10-kg loading at the experimental temperature indicated. The results, reasonably close to the average strain curve of the six creep tests, verify the application of the linear viscoelastic concepts to the asphaltic concretes investigated.

TABLE 2

Temperature (°F)	Axial Stress Level (psi)		
	σ_1	σ_2	σ_3
41	26.3	52.6	78.9
77	10.5	21.0	31.5
104	3.5	7.0	10.5

Values of the creep compliance are also indicated on the right ordinate in the foregoing figures, for convenience. The creep compliance, J, is defined as the time-dependent strain divided by the constant stress. Tabular and graphical representations were used to present the results. However, it is not possible to present all the data here, and only typical results are shown.

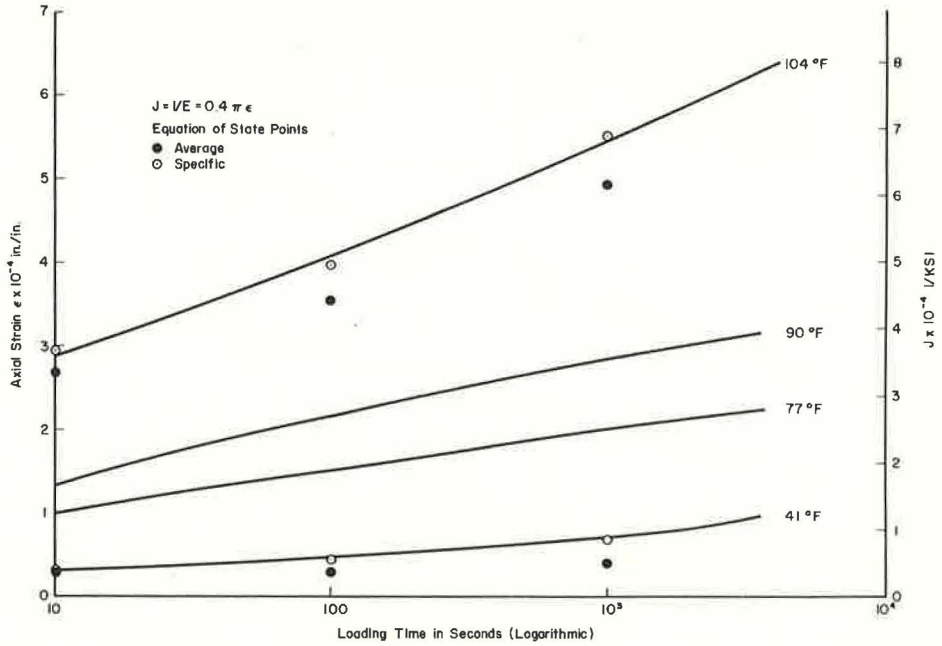

Figure 2. Strain-time data of creep tests reduced to 10-kg load, asphaltic mix 111.

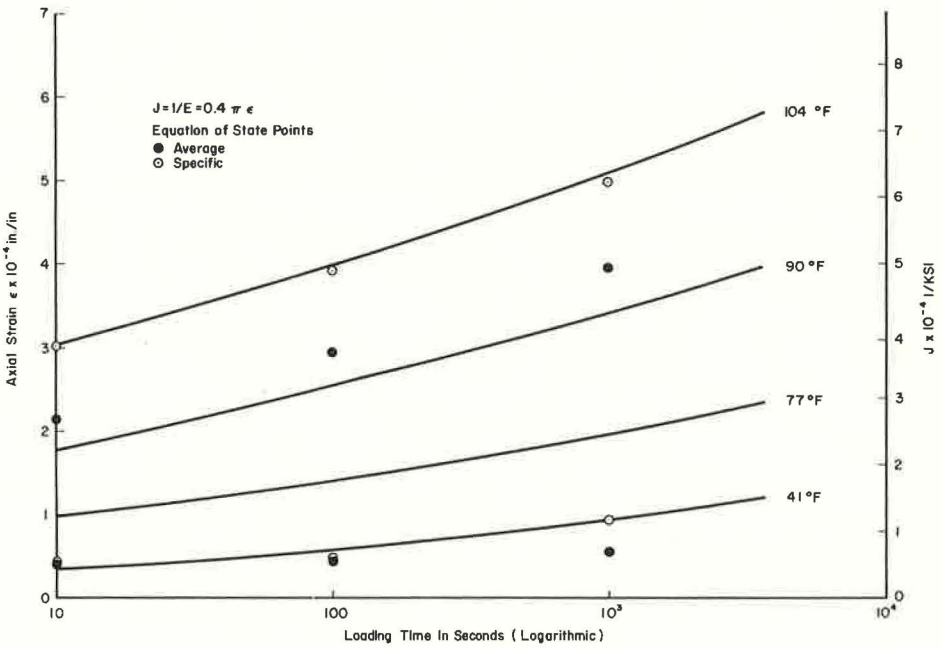

Figure 3. Strain-time data of creep tests reduced to 10-kg load, asphaltic mix 112.

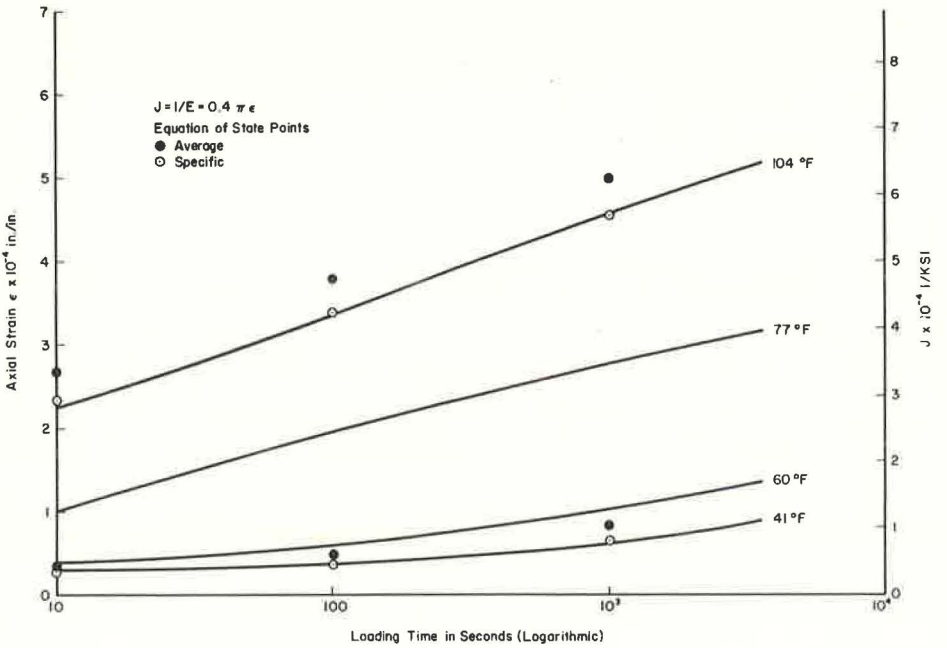

Figure 4. Strain-time data of creep tests reduced to 10-kg load, asphaltic mix 121.

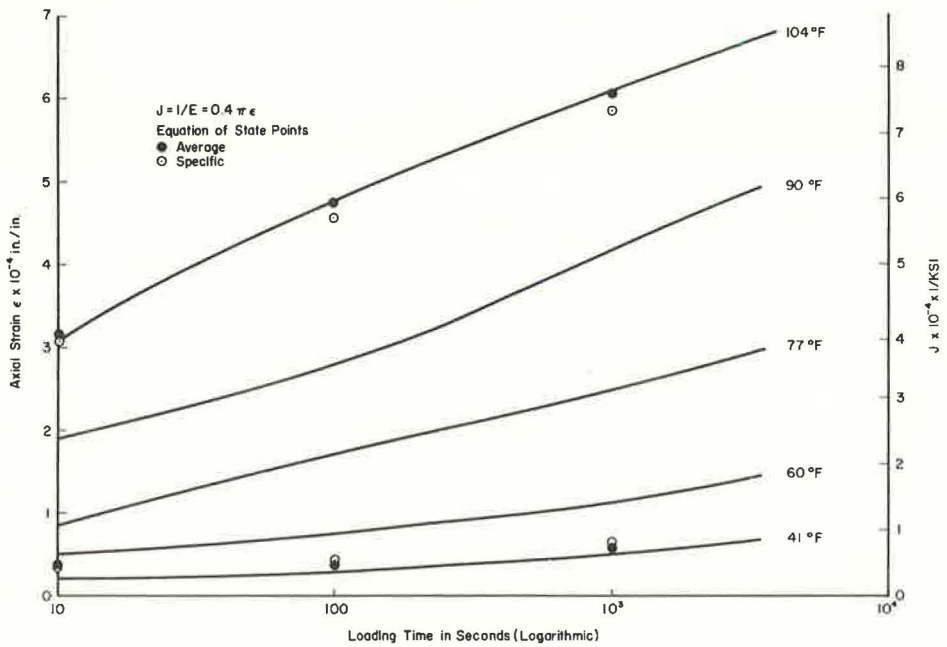

Figure 5. Strain-time data of creep tests reduced to 10-kg load, asphaltic mix 122.

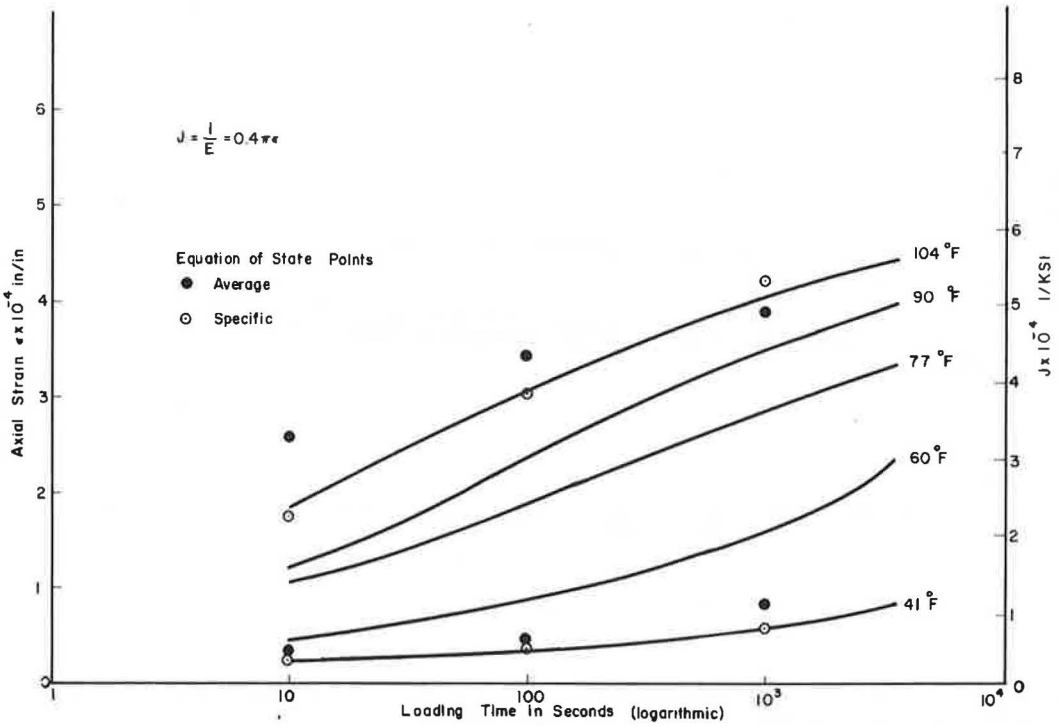

Figure 6. Strain-time data of creep test reduced to 10-kg load, asphaltic mix 222.

Repeated Loading

Figures 7 through 9 show the typical response of asphaltic concrete to repeated loading and unloading cycles and the relative creep strain for such loading patterns. The relative creep strain is defined as the total strain minus the residual viscous

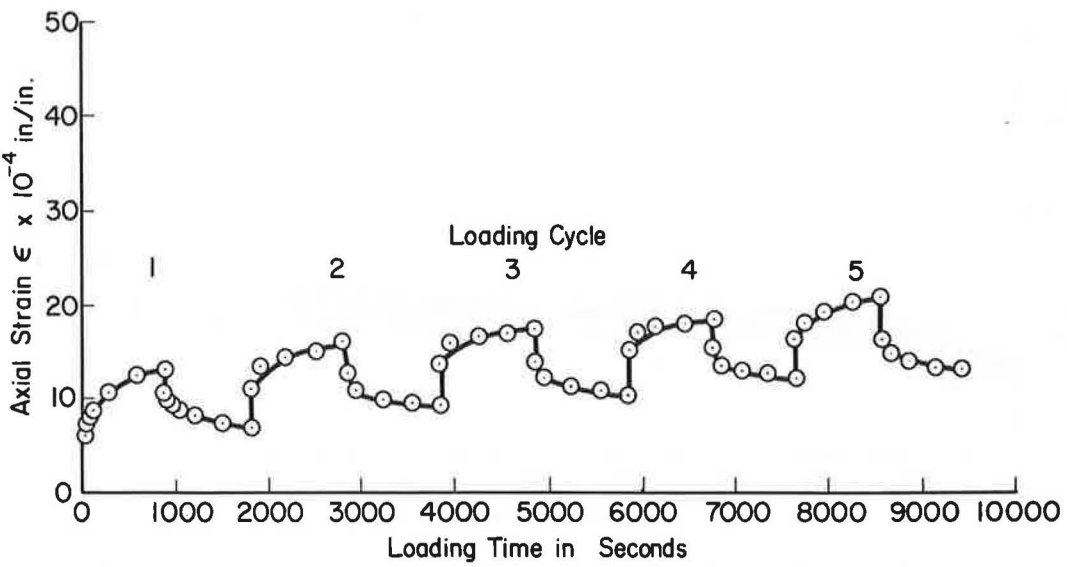

Figure 7. Creep strain under repeated 60-kg loading, 77 F, asphaltic mix 121.

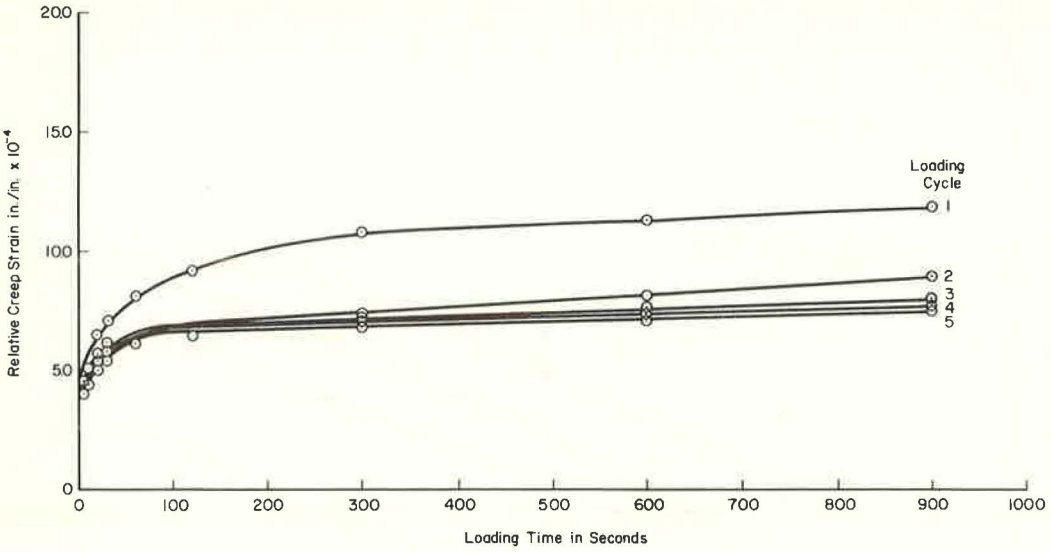

Figure 8. Relative creep strain vs loading time, 60-kg load, 77 F, asphaltic mix 121.

strain in the specimen just before loading. For all tests the relative strain for the first loading cycle had greater magnitude than in later cycles. The subsequent loading and unloading cycles had progressively smaller deviations.

The foregoing observation suggests that mechanical conditioning (9) is also possible for asphaltic concrete. From the experimental data obtained, the elastic and retarded elastic components of the total strain were found to approach a steady-state condition

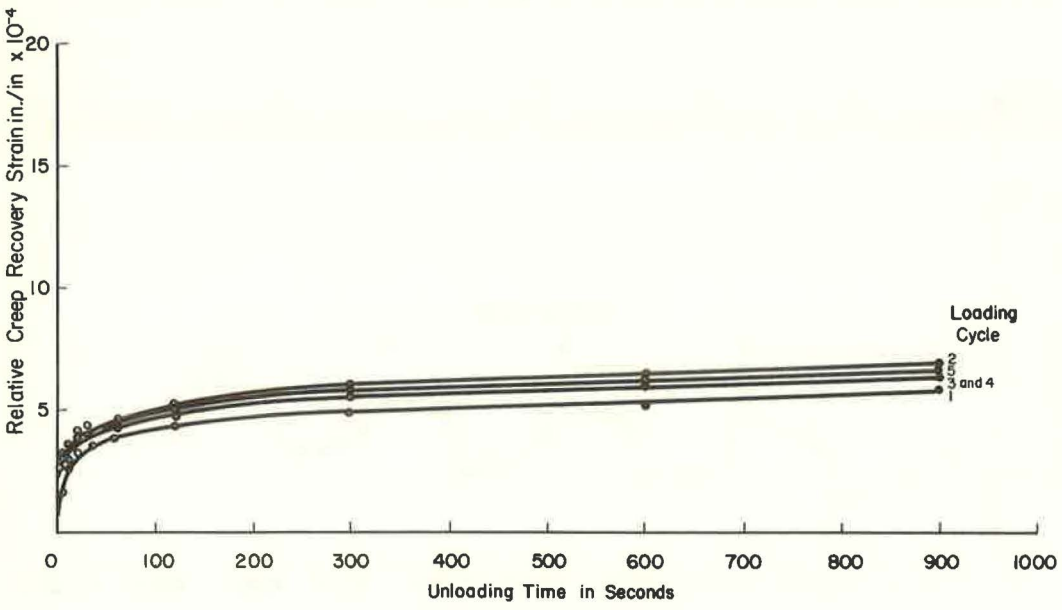

Figure 9. Relative creep recovery strain vs unloading time, 60-kg load, 77 F, asphaltic mix 121.

after approximately three or four loading cycles, but the plastic part of deformation, as expected, continued to increase at a uniform rate. After mechanical conditioning occurs, the material seems to follow the linear viscoelastic assumption to a higher degree of approximation at the conditions investigated.

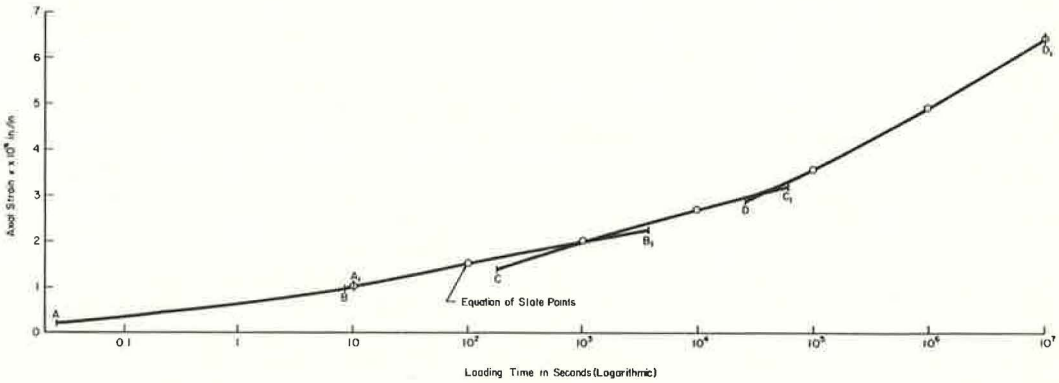

Figure 10. Composite master creep strain curve for asphaltic mix 111, 10-kg load, 77 F.

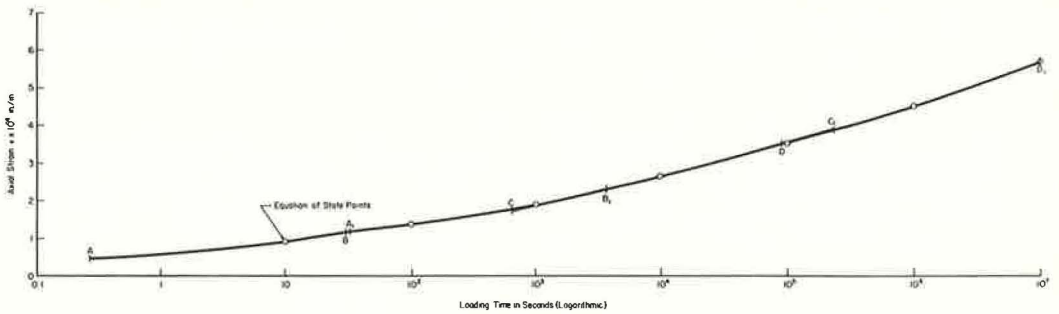

Figure 11. Composite master creep strain curve for asphaltic mix 112, 10-kg load, 77 F.

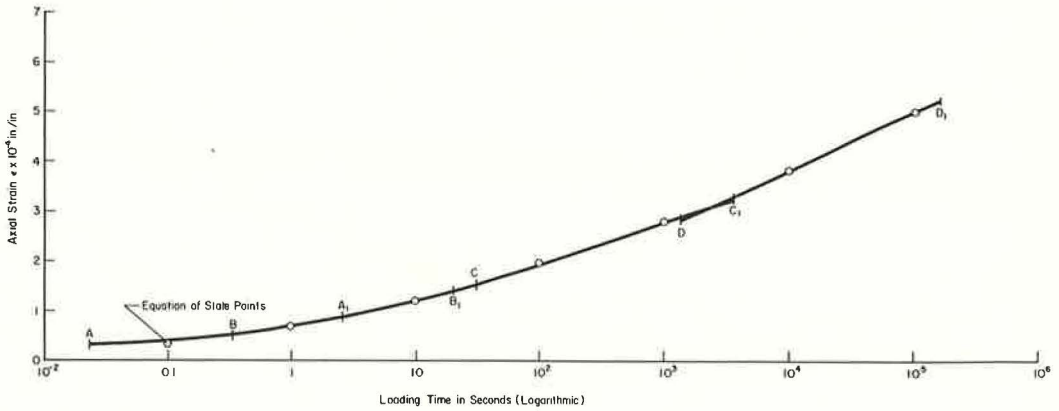

Figure 12. Composite master creep strain curve for asphaltic mix 121, 10-kg load, 77 F.

Time-Temperature Superposition Principle

The time-temperature superposition concept (10, 11, 12), was used to obtain master strain-time curves at 77 F for each series of asphaltic concrete mixes tested, as shown in Figures 10 through 14. The composite master curves were derived from the strain-time curves of Figures 2 through 6, respectively, by means of horizontal translations parallel to the time scale. Similar master strain functions can also be obtained by means of activation energy relations and a form of the Arrhenius equation (10). The curves shown represent master plots of the creep moduli over an extended portion of the time scale. By calculation of time ratios and by inspection, values were determined for the temperature shift factor, α_T, which permit horizontal shifting of the 41, 60, 90, and 104 F data to coincide with the 77 F creep data and thereby form a relatively smooth continuous master curve.

An absolute temperature factor, T_0/T, and a density factor, P_0/P, theoretically enter into the reduction scheme due to the theory of rubberlike elasticity (10) and density changes with temperature, have been omitted from calculations since they are within experimental error and approach unity. These theoretical density and temperature corrections lead to small vertical shifts of the experimental data.

The values of log α_T obtained from the tests are plotted in Figure 15. The values obtained are in close agreement with those found for another asphalt mixture similar to the test materials investigated in this research at Ohio State University (1), as shown in the figure. The solid circles indicate the sample mean, and the intervals indicate the 95 percent confidence limits of the population means (13). The straight line is the empirical regression line. The significance of the concept of reduced variables becomes more apparent when one considers that: (a) the number of experiments needed to evaluate the mechanical response of the material over a wide range

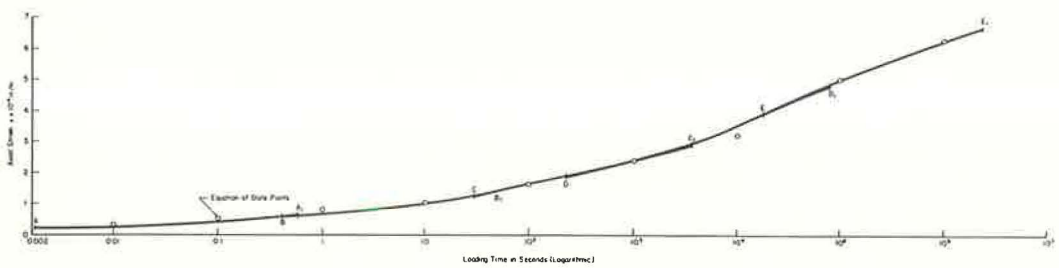

Figure 13. Composite master creep strain curve for asphaltic mix 122, 10-kg load, 77 F.

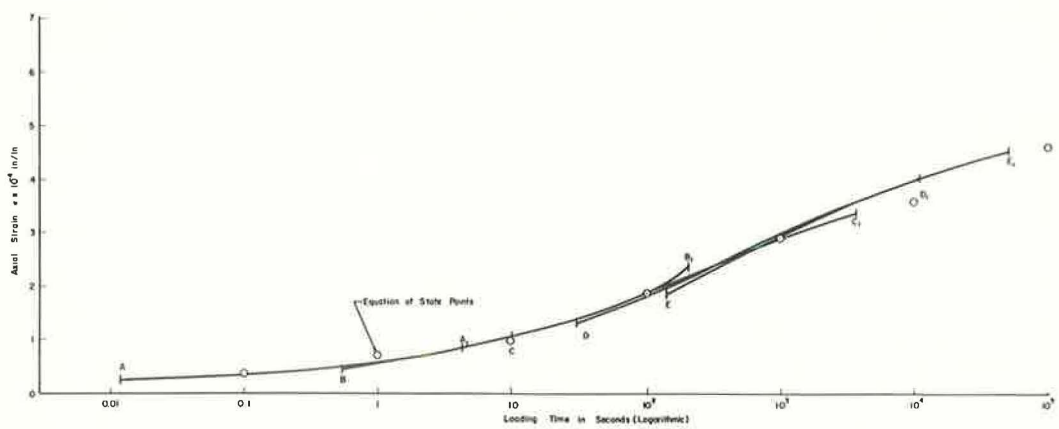

Figure 14. Composite master creep strain curve for asphaltic mix 222, 10-kg load, 77 F.

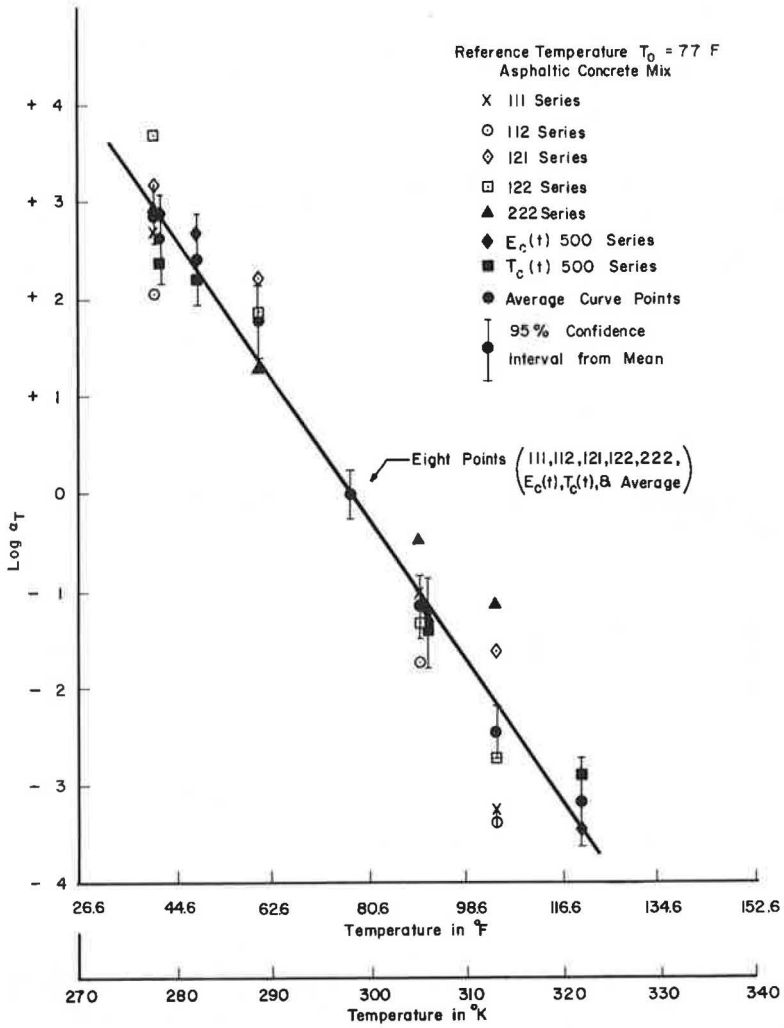

Figure 15. Temperature dependence of shift factor, a_T.

of temperature and time can now be greatly reduced; (b) the experimental data can be projected to loading times both shorter and longer than can normally be obtained experimentally; and (c) the creep compliance, creep moduli, and mixture strain can be predicted at any intermediate temperature in the experimental range for extended loading times.

Equation of State

The most important variables in investigating the mechanical response of a viscoelastic material such as asphaltic concrete are stress, strain, time, and temperature. Bituminous concrete mixes are three-phase systems and may be viscoelastic materials in which the asphalt component is the most susceptible to loading time and to environmental temperature variations. Thus, in this study, it was necessary to investigate the effect of these principal variables on the rheologic properties of the material as influenced by the asphalt phase.

A constant load applied to a linear viscoelastic material produces a deformation which increases with time. This fact can be described mathematically by the following expression (14, 15):

$$\epsilon(t) = \sigma\left[\frac{1}{E_o} + \sum_{i=1}^{n}\frac{1}{E_i}\left(1 - e^{-\frac{E_i}{\eta_i}t}\right) + \frac{t}{\eta_o}\right] \quad (1)$$

Eq. 1 shows that stress and strain are linearly related. If the stress is doubled, the resulting strain is doubled; conversely, if the strain is doubled, the resulting stress is also doubled.

A k value, defined as the slope of a straight line on a semilog asphalt viscosity-temperature plot (2), is related to the temperature shift factor, $\alpha(T)$, at a reference temperature, T_o,

$$\ln \alpha_{T_o}(T) = -k(T - T_o) \quad (2)$$

Thus, the general equation of state for the material can be written in a form similar to that of a generalized Voigt model:

$$\epsilon(t, T) = \sigma\left[\frac{1}{E_o} + \sum_{i=1}^{n}\frac{1}{E_i}\left\{1 - \exp\left(\frac{-E_i t}{\alpha_{T_o}(T)\,\eta_i(T_o)}\right)\right\} + \frac{t}{\alpha_{T_o}(T)\,\eta_o(T_o)}\right] \quad (3)$$

which describes the mechanical response over a range of loading times and temperatures.

Making use of Eq. 2, Eq. 3 can be written as:

$$\epsilon(t, T) = \sigma\left[\frac{1}{E_o} + \sum_{i=1}^{n}\frac{1}{E_i}\left\{1 - \exp\left(\frac{-e^{k(T - T_o)}E_i t}{\eta_i(T_o)}\right)\right\} + \frac{t}{\eta_o(T_o)\,e^{-k(T - T_o)}}\right] \quad (4)$$

which is the relation desired.

Curve-Fitted Equation

By using the graphical procedures described in an earlier report (2), the coefficients of the equations in the form of Eq. 1 were found to represent the master curves shown in Figures 10 through 14. The analytical expression for the 111 series asphaltic mix master curve under a 10-kg load at 77 F is as follows:

$$\epsilon(t) = 1.49 \times 10^{-4}\left(1 - e^{-4.61 \times 10^{-7}t}\right) + 1.21 \times 10^{-4}\left(1 - e^{-4.072 \times 10^{-6}t}\right) + 5.85 \times 10^{-5}\left(1 - e^{-3.4 \times 10^{-5}t}\right) + 7.40 \times 10^{-5}\left(1 - e^{-4.18 \times 10^{-4}t}\right)$$

$$+ 4.00 \times 10^{-5}\left(1 - e^{-4.36 \times 10^{-3}t}\right) + 5.63 \times 10^{-5}\left(1 - e^{-4.4 \times 10^{-2}t}\right)$$
$$+ 2.6 \times 10^{-5}\left(1 - e^{-3.815 \times 10^{-1}t}\right) + 2.57 \times 10^{-5}\left(1 - e^{-4.4t}\right)$$
$$+ 5.9 \times 10^{-12}t + 2.55 \times 10^{-5} \qquad (5)$$

The strain-time values calculated from the equations of state check very closely with the experimental values at 77 F shown in the form of master curves in Figures 10 through 14. Using the shifting factors shown in Figure 15, the k values are computed according to Eq. 2. These values are given in Table 3.

By rewriting Eq. 5 in the form of Eq. 4, the following equation was obtained for the 111 series mix:

$$\epsilon(t, T) = 1.49 \times 10^{-4}\left(1 - e^{-4.61 \times 10^{-7}t \exp[k(T-77)]}\right)$$
$$+ 1.21 \times 10^{-4}\left(1 - e^{-4.072 \times 10^{-6}t \exp[k(T-77)]}\right)$$
$$+ 5.85 \times 10^{-5}\left(1 - e^{-3.4 \times 10^{-5}t \exp[k(T-77)]}\right)$$
$$+ 7.40 \times 10^{-5}\left(1 - e^{-4.18 \times 10^{-4}t \exp[k(T-77)]}\right)$$
$$+ 4.0 \times 10^{-5}\left(1 - e^{-4.36 \times 10^{-3}t \exp[k(T-77)]}\right)$$
$$+ 5.63 \times 10^{-5}\left(1 - e^{-4.4 \times 10^{-2}t \exp[k(T-77)]}\right)$$
$$+ 2.6 \times 10^{-5}\left(1 - e^{-3.815 \times 10^{-1}t \exp[k(T-77)]}\right)$$
$$+ 2.57 \times 10^{-5}\left(1 - e^{-4.4t \exp[k(T-77)]}\right)$$
$$+ 5.9 \times 10^{-12}t \exp[k(T-77)] + 2.55 \times 10^{-5} \qquad (6)$$

Analogous equations were obtained for all the materials studied.

Eq. 6 can be used to calculate the creep strain for any temperature and loading time, provided the k values are defined. Using the k values listed in Table 3, the strains calculated by Eq. 6 and similar equations are shown in Figures 2 through 6 for temperatures of 41 F and 104 F. When the specific k values are used, the calculated strains fall almost exactly on the experimental curve. When the average k values are used, the agreement between the calculated strain and observed strain is still very good, implying that the specific k value is desirable if extreme accuracy is required.

TABLE 3

"k" VALUES[a]

Asphaltic Concrete Series	Specific		Best Line
	41 F	104 F	
111	0.1690	0.2885	0.2545
112	0.1299	0.2898	0.2017
121	0.2030	0.1390	0.1740
122	0.2361	0.2388	0.2455
222	0.1874	0.0975	0.1498

[a]Specific k values computed for particular temperatures concerned; best line k values computed for range of temperatures by drawing best straight lines through experimental points.

Computer Equations

The master curve data for the materials studied shown in Figures 10 through 14 were used to write a Scatran computer program and calculate similar equations of state, but of a sixth-degree polynomial form:

$$\epsilon(t) = C_0 + C_1 \log t + C_2 (\log t)^2 + \ldots + C_n (\log t)^n \quad (7)$$

The coefficients of the polynomial equation were calculated by an IBM 7094 computer and printed out as C_0, C_1, ..., C_6. For this research, the sixth-degree polynomial

TABLE 4

VALUES FOR POLYNOMIAL COEFFICIENTS FOR ASPHALTIC CONCRETE MIXES

Mix	Coefficients						
	C_0	C_1	C_2	C_3	C_4	C_5	C_6
111	0.641261719	0.324797884	0.055929484	-0.000518209	-0.005969534	0.001864175	-0.000137133
112	0.589549825	0.285540815	0.134473095	-0.080792851	0.029345342	-0.004377093	0.000232387
121	0.680619359	0.408324849	0.139726138	-0.014161315	-0.009319783	0.004103141	-0.000416568
122	0.706186898	0.317805842	0.049930007	0.008847243	0.002605793	-0.000233102	-0.000032063
222	0.558999084	0.339170013	0.150620632	0.017126073	-0.007738411	0.000657460	-0.000046117

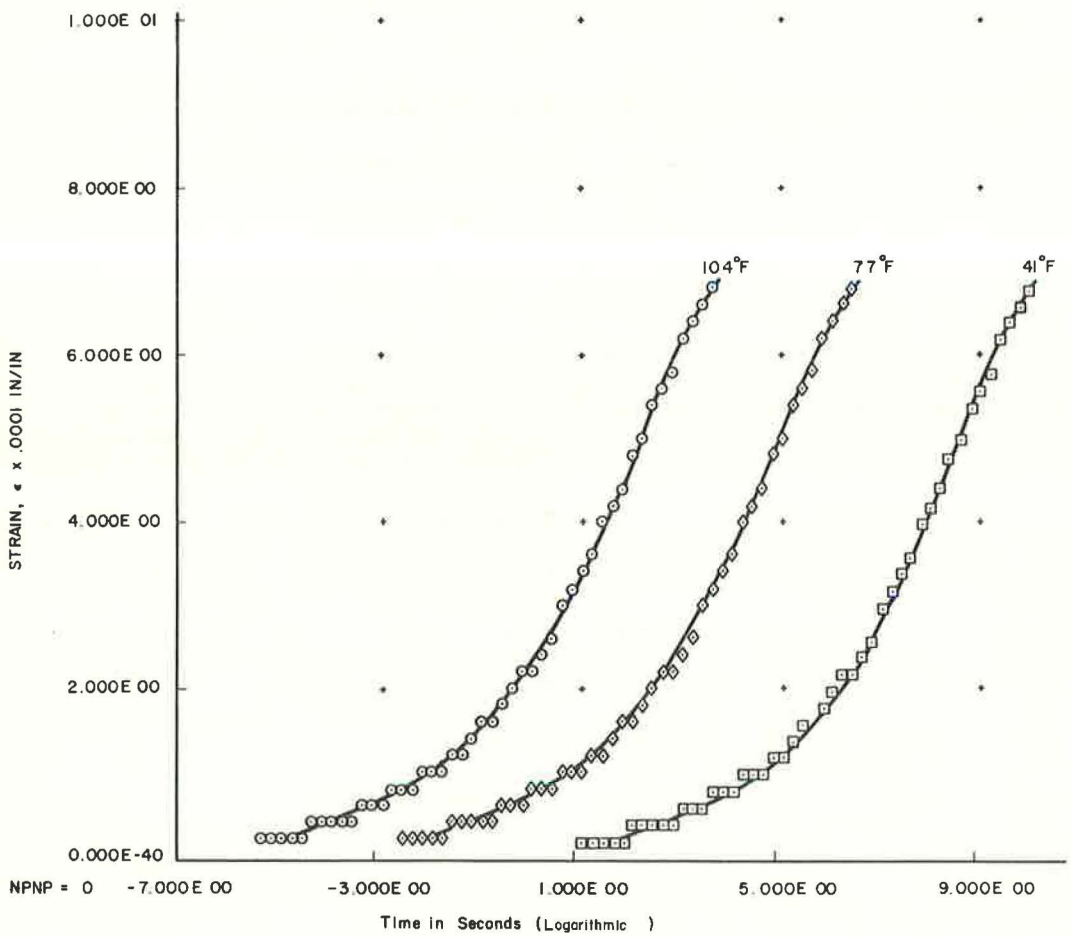

Figure 16. Computer master strain curves at three temperatures, asphaltix mix 122, 10-kg load.

equation was selected and yields a 3 percent root-mean-square error. Greater accuracy is possible by using higher order polynomials. The values of the polynomial coefficients are given in Table 4.

A second Scatran program was written to evaluate the master strain-time curves of the materials studied at any temperature in the experimental range by means of the specific temperature shift factors and the computer equations. The results were tabulated and roughly plotted by the computer as shown for the 122 series mixture in Figure 16 for the 41, 77, and 104 F master curves.

Correlation of Equation of State and Time-Temperature Superposition Concept

By comparing the strain-time values evaluated by the time-temperature superposition concept and by the equation of state, the correlation of results may be observed between both types of analyses. Values of ϵ (t), J, and E may be compared at the common experimental temperatures and loading times. The agreement between the measured and predicted strain values are shown in Figures 2 through 6 for the 41 and 104 F curves. These correlations were considered good for all experimental data analyzed. The agreement in this experiment provides a verification of the ability of the linear viscoelastic theory to describe the response of asphaltic concrete. It also provides verification of the application of the derived equation of state and the time-temperature superposition concept to these materials.

SUMMARY AND CONCLUSIONS

The major objective of this study was to relate changes of asphalt viscosity or temperature to changes in the mechanical properties of asphaltic concrete mixes. Research has shown that a correlation between these properties can be obtained. In the linear viscoelastic range of stress and in the thermolinear range of temperature, an equation of state which correlates stress, strain, time, and temperature has been derived. By a relatively few tests, this equation allows the mechanical properties of bituminous concrete to be described over a range of conditions.

For the materials and conditions studied, the following are the major conclusions of this investigation:

1. The experimental data indicate that the time-temperature superposition concept is applicable to the bituminous-aggregate compositions tested at a satisfactory level of approximation.
2. Experimentation on the phenomenological level has demonstrated that the mechanical properties of the dense bituminous concrete mixtures investigated can be expressed by the linear viscoelastic theory to a useful degree of approximation.
3. An equation of state incorporating load, deformation, time and temperature is valid for predicting deformation and strength properties of the bituminous mixes studied. This equation provides an additional, independent check of the time-temperature superposition concept used in this study.
4. Rheological experimentation is usually conducted on samples previously untested because the loading history influences the mechanical behavior of the materials. Usually, experimentation with untested specimens is all that is required to obtain the desired results in a research program. However, an asphaltic concrete exhibits mechanical conditioning and, when the material is tested, the deformation and the strength properties measured will vary with subsequent repetitions of loading and unloading. After several standard repetitions of load, the instantaneous phase, viscoelastic phase, and plastic phase of the total deformation were observed to be approximately constant for each loading and rebound cycle, suggesting that a conditioning of the samples may yield more realistic results in the case of highway pavement studies. In this research, the three rheological components of the total deformation asymptotically approached limiting values after several loading cycles, making the application of linear theory to these materials an even more valid approximation.
5. The total deformation could be separated into three components: instantaneous elastic, retarded elastic, and plastic or viscous. Evidence was obtained that the

measured instantaneous deformation of asphaltic concrete is highly dependent on testing procedure, sample preparation, and equipment used. Thus, scattering of results for this component is not unusual. The plastic component, evaluated after a specified rebound time, deviated most from the linear assumption. The retarded elastic phase was statistically linear to a high degree of approximation.

6. Application of changes in asphalt viscosities to produce desired changes in the mechanical properties of asphaltic concrete has been verified.

ACKNOWLEDGMENTS

The material presented in this paper was partially secured from Research Project EES 191, conducted by the Transportation Engineering Center and sponsored by the Ohio Department of Highways in cooperation with U.S. Bureau of Public Roads. The continued interest and cooperation of these agencies are gratefully acknowledged.

The authors wish to express their appreciation for the efforts of the staff of the Engineering Experiment Station in the preparation of this paper. Special thanks are due to Ravi Bhatia, Tom Snider, David Wu, and Barbara Fravel for their valuable assistance.

REFERENCES

1. Pagen, C.A. Rheological Response of Bituminous Concrete. Highway Research Record No. 67, pp. 1-26, 1965.
2. Pagen, C.A., and Ku, B. Effect of the Viscosity of Asphalt on the Rheological Properties of Bituminous Mixes. Ohio State Univ., Eng. Exp. Sta., Ann. Rept. No. EES 191-3.
3. Secor, K.E., and Monismith, C.L. Analysis and Interrelation of Stress-Strain-Time Data for Asphalt Concrete. Paper presented to Winter Mtg. Soc. of Rheology, Claremont, Calif., 1964.
4. Krokosky, E.M., and Chen, J.P. Viscoelastic Analysis of the Marshall Test. Paper presented to AAPT Ann. Mtg., Dallas, Tex., 1964.
5. Stuart, H.A. Die Physik Der Hochpolymeren. Berlin, Springer-Verlag, 1956.
6. Bland, D.R. The Theory of Linear Viscoelasticity. London, Pergamon Press, 1960.
7. Baker, R.F. Pavement Design Using Rheologic Concepts. Proc. Int. Conf. on Structural Design of Asphalt Pavements, Ann Arbor, Mich., 1962.
8. Reiner, M. Building Materials, Their Elasticity and Inelasticity. Amsterdam, North-Holland Pub. Co., 1954.
9. Freudenthal, A.M. The Inelastic Behavior of Engineering Materials and Structures. New York, John Wiley and Sons, 1950.
10. Ferry, J.D. Viscoelastic Properties of Polymers. New York, John Wiley and Sons, 1961.
11. Leaderman, H. Elastic and Creep Properties of Filamentous Materials and Other High Polymers. Washington, D.C., Textile Found., 1943.
12. Broadnyan, J.G. Use of Rheological and Other Data in Asphalt Engineering Problems. Highway Research Board Bull. 192, pp. 1-19, 1958.
13. Hald, A. Statistical Theory with Engineering Applications. New York, John Wiley, and Sons, 1961.
14. Eirich, F.R., ed. Rheology, Theory and Application. Vol. 1-3. New York, Academic Press, 1961.
15. Alfrey, T., and Doty, P. Mechanical Behavior of High Polymers. Jour. Appl. Phys., 1948.

Expansion and Contraction of Asphalt Concrete Mixes

ERNEST ZUBE and JAMES CECHETINI
Respectively, Assistant Materials and Research Engineer and Materials and Research Engineering Associate, California Division of Highways

The Materials and Research Department of the California Division of Highways has been conducting a research study on the expansion and contraction of asphalt concrete mixes using aggregates ranging from nonabsorptive to highly absorptive. Data indicate that AC test specimens fabricated from absorptive aggregates and exposed to normal atmospheric conditions absorb moisture from the air which may cause considerable expansion. During the warmest hours of the day, these expanded specimens contract, causing transverse or so-called block cracking. Identical specimens kept in a dry storage cabinet did not exhibit this phenomenon. The type of cracking found in pavements appears the same as observed in laboratory specimens when both are fabricated from the same highly absorptive aggregates. Strains created in pavement by this cycle of expansion and contraction, together with deflections imposed by loads, may cause a serious reduction in service life.

This study presents data showing that expansion can be reduced by certain mineral fillers and increased by others. Expansion can also be greatly reduced by increasing the asphalt content of the mix consistent with other specification requirements.

•AGGREGATES of varying degrees of absorption are the only economical sources of road building material available in certain areas of California. Although these aggregates appear to present no great problem when used in the construction of bases and subbases, some evidence of distress is noted when they are used in the construction of asphalt concrete surfacing. Considerable mileage of pavement has been placed using these aggregates.

It can be generally stated that the California Division of Highways has had more failures and distress with asphalt concrete pavements containing absorptive aggregates than with pavements using nonabsorptive aggregates. Two main types of distress appear to be related to the degree of absorption of the aggregate. The first is drying out and raveling of the mix caused by rapid oxidation of the binder, insufficient asphalt in the mix, or the capacity of the aggregates to continue absorbing the asphaltic binder. The second is the appearance, in a few years, of excessive shrinkage cracks. On one road these shrinkage cracks, about 1 in. wide, were at right angles to the centerline and at intervals of about 15 to 30 ft. Our new test method, described later, indicated that the aggregates were highly absorptive. There was no evidence that this cracking was caused by reflection from the base. Similar cracks often appear in short sections of AC pavement which are closed to traffic pending extension by future construction.

Paper sponsored by Committee on Mechanical Properties of Bituminous Paving Materials.

The most widely accepted theories of asphalt concrete pavement failures are (a) pavement fatigue (1-6), (b) excessive deflections (1, 6), (c) radius of curvature of deflected pavement (7), and (d) rapid hardening of the asphalt binder (8).

In addition to these, at least one more factor should be included, i.e., the expansion-contraction cycle of asphalt concrete mixes using absorptive aggregates.

One prime difficulty in the use of absorptive aggregates is the determination of the optimum asphalt content so that sufficient asphalt can be introduced to prevent drying out of the pavement while sufficient stability is provided to prevent rutting or shoving of the mix at the time of construction. About 20 yr ago we developed the Centrifuge Kerosene Equivalent (CKE) test (9) which provides an optimum asphalt content based on a combination of surface area and absorption. This test has given excellent service and our standard specifications contain certain limiting factors (k factors) obtained from the CKE test to eliminate or reduce the number of highly absorptive aggregates used. The CKE test is now being modified to provide separate quantitative measures of the surface area and absorbency of the aggregate. Therefore, in future specifications this determination will permit us to limit the absorption factor. A tentative limit of 0.5 percent absorption has been adopted for future specifications. A brief description of the modified CKE test is presented in this paper.

The excessive shrinkage cracking in pavements containing absorptive aggregates has been of concern to the Materials and Research Department for a number of years. Laboratory studies indicate that the most likely cause of this form of distress is absorption of moisture from the air through the asphalt film which causes considerable expansion of the pavement. When the pavement dries, contraction and cracking appear. Studies indicate that nonabsorptive aggregates do not exhibit this phenomenon. There is little doubt that strains created in the pavement by this cycle of expansion and contraction, together with deflections imposed by loads, lead to a serious reduction in service life of the pavement.

The purpose of this report is to present the development of laboratory tests for studying the expansion and contraction of asphalt concrete mixtures using absorptive aggregates during cycling under moist and drying conditions and the tentative correlation of the results with pavement performance. A method for measuring the degree of absorption of the aggregate and expansion of the mixture is outlined. Also, methods for reducing the degree of expansion are presented, together with future studies on the probable causes of these findings.

LABORATORY STUDIES

Our laboratory studies are grouped under three parts: (a) early studies on compacted AC briquettes, (b) study on compacted AC slabs, and (c) present studies on compacted AC bars.

Early Studies on Compacted AC Briquettes

In 1958 a series of AC briquettes, 3 in. high and 4 in. in diameter, were made from highly absorptive and nonabsorptive aggregates. These briquettes, made primarily for visual observation, were compacted by our kneeding compactor. Half of the specimens were compacted at 500 psi and the remaining samples at 350 psi. The laboratory test results for these briquettes are given in Table 1.

Previous data indicated that specimens compacted at 350 psi are approximately equal in density and stability to a newly compacted AC pavement, whereas a compaction pressure of 500 psi, as used in our standard laboratory procedure, produces a specimen approximately equal to the density of a pavement after a period of time under traffic.

Some of the AC briquettes made from absorptive and nonabsorptive aggregates were encapsulated in epoxy resin. We felt that by coating the briquettes, oxidation of the asphalt binder would be negligible. Therefore, any change in the hardness of the asphalt would be caused by the aggregates. Briquettes, both encapsulated and nonencapsulated, were divided into identical groups and weathered under the following conditions:

TABLE 1

TEST RESULTS—COMPACTED AC BRIQUETTES

Sample	Agg. Class.[a]	Absorp.[b] (%)	Asph. 85-100 (%)	Stability[c]		Cohesion[d]		Specific Gravity	
				350-Psi	500-Psi	350-Psi	500-Psi	350-Psi	500-Psi
57-854 (non-absorptive)	Quartsitic meta sandstone, diabase (river sand and gravel)	0.0	5.3	32	42	420	683	2.35	2.37
57-1236 (absorptive)	Volcanic dacite and rhyolite, feldspar, quartz, calcite and mica	1.0	6.3	34	38	227	312	2.07	2.09

[a]By X-ray diffraction and DTA.
[b]By modified CKE test.
[c]Stabilometer value.
[d]Cohesiometer value.

Group 1—placed on roof of laboratory exposed to normal climate;
Group 2—inserted into previously cored holes of an existing AC pavement; and
Group 3—placed in darkened cabinet.

Group 1.—During a periodic inspection of the briquettes on the roof shortly after exposure, the specimens made from highly absorptive aggregates and compacted at 500 psi showed signs of expanding. Hairline cracking and stretch marks were visible in the epoxy coating. About 3 mo from the time the specimens were placed on the roof, the first signs of cracking appeared in the epoxy coating. The other briquettes, nonabsorptive and uncoated, showed no signs of stress under the same environment. This also includes the highly absorptive specimens compacted at 350 psi. However, at the end of 6 mo, signs of distress were visible in the coating of the absorptive specimens compacted at 350 psi (Fig. 1). We believe the highly absorptive specimens compacted at 500 psi ruptured their epoxy coating before identical AC samples compacted at 350 psi primarily because of insufficient void space. The additional void space of

Figure 1. Epoxy-coated specimens, made from absorptive aggregates, exposed on roof 6 mo: left, specimen compacted at 500 psi; right, specimen compacted at 350 psi.

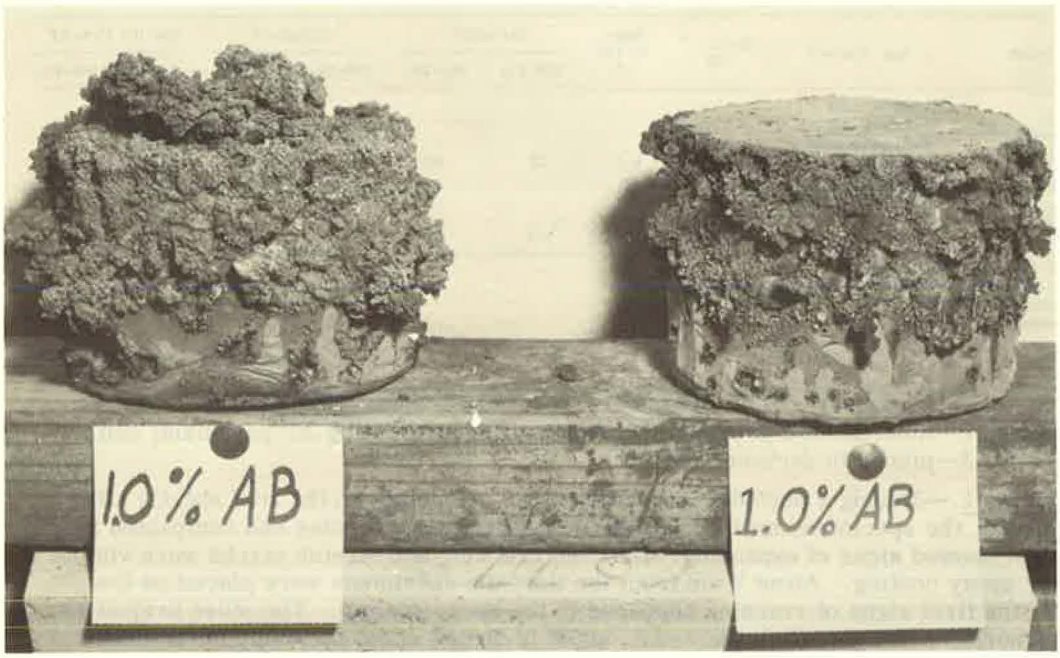

Figure 2. Same specimens as in Figure 1 after 1 yr.

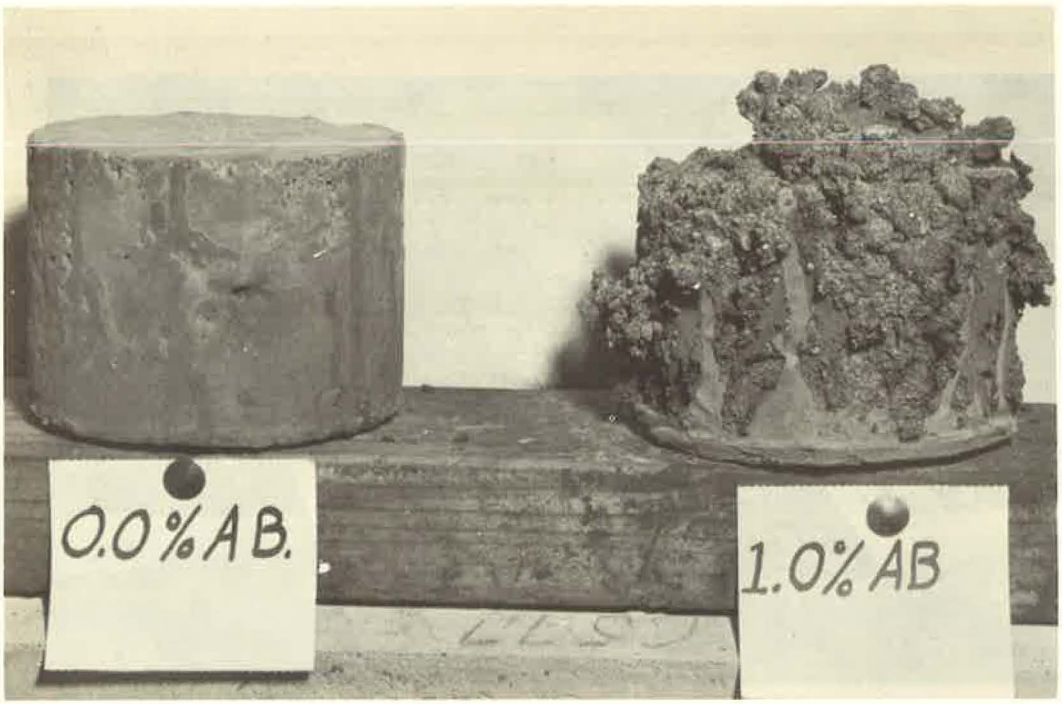

Figure 3. Epoxy-coated specimens after 1 yr: left, nonabsorptive aggregate; right, absorptive aggregate.

Figure 4. Nonencapsulated specimens exposed on roof 6 mo: left, nonabsorptive aggregate; right, absorptive aggregate.

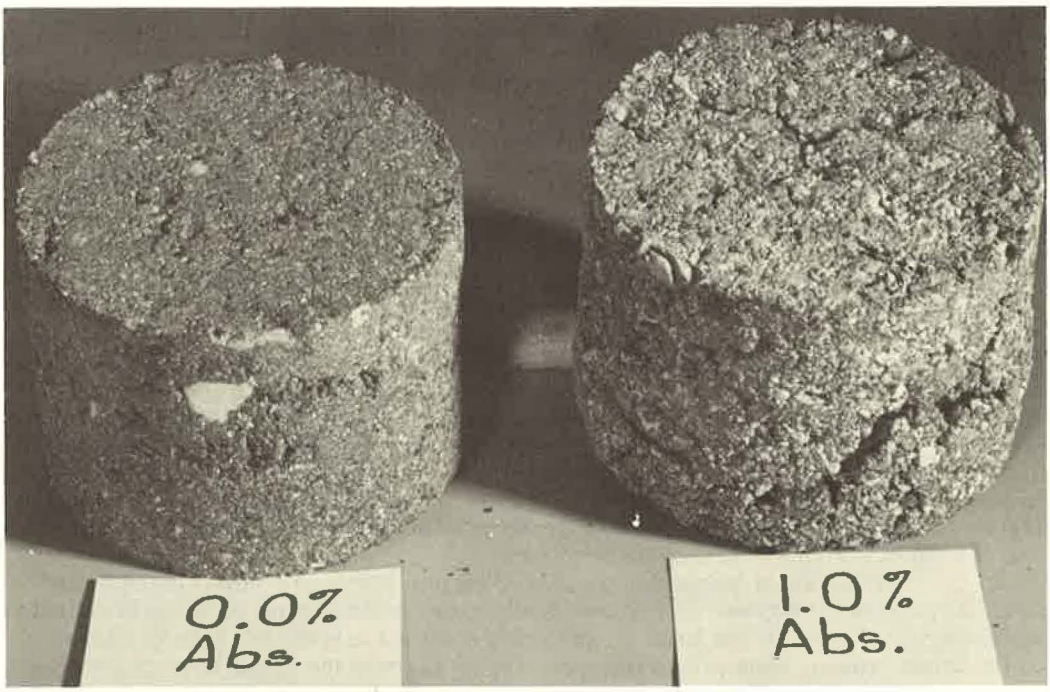

Figure 5. Same briquettes as shown in Figure 4; after 6 yr, briquette made from absorptive aggregates (1.0 percent) increased in volume 18.8 percent; no increase in volume was seen in briquette fabricated from nonabsorptive (0.0 percent) aggregate.

Figure 6. Stainless steel pins cemented to sides of specimen to measure volume changes.

specimens compacted at 350 psi permitted the absorptive aggregates to expand without bursting their epoxy coating. However, when the aggregate's volume increase became greater than the available voids in the compacted briquette, the specimens compacted at a lower pressure also ruptured.

At the end of 1 yr, the highly absorptive specimens compacted at 350 and 500 psi had completely ruptured their epoxy coating (Fig. 2), but the nonabsorptive encapsulated specimens remained in excellent condition (Fig. 3).

The nonencapsulated specimens showed the same trend. The absorptive briquettes had cracks over the entire surface, whereas the nonabsorptive briquettes had no indication of cracking. Figure 4 shows their appearance after 6 mo. After 6 yr, the diameter of the absorptive (1.0 percent) specimen increased from 4.0 in. to an average of 4.25 in. The height increased from 3.0 to 3.15 in. This is an increase of 18.8 percent in volume. No expansion in volume occurred in the nonabsorptive briquette (Fig. 5).

After noticing this volume change in the absorptive AC specimen, we made our first attempt to measure the expansion. Stainless steel reference pins, $\frac{1}{2}$ in. long, were cemented with epoxy resin to the vertical sides of the test specimens made from absorptive and nonabsorptive mixes (Fig. 6). The specimens were then placed on the roof and expansion measurements were made. However, after about 1 wk, the weight of the pins and the ambient temperature caused the mix aroung the pins to soften and disintegrate. As is mentioned later, this problem was overcome by measuring the volume change of a slab and test beam specimen.

Group 2. —This group of briquettes was inserted into previously cored holes in an existing AC pavement, between and in the wheel track, to determine what visible effects the different wheel loads might have. The tightly confined briquettes, both in and between the wheel tracks, showed hairline cracking on the surface of the absorptive types. However, no signs of cracking appeared on the nonabsorptive briquettes. The surface cracking on the absorptive specimens indicates that expansion and subsequent shrinkage had occurred; apparently the force of expansion was sufficient to move the surrounding pavement slightly.

Figure 7. Absorptive and nonabsorptive AC briquettes; dark-colored specimens stored in cabinet for 6 yr, and light-colored specimens exposed on roof for 6 yr.

Group 3.—Both absorptive and nonabsorptive briquettes stored in a cabinet free from sunlight and moisture remained in excellent condition. Figure 7 shows the appearance of these specimens after 6 yr. For comparison, identical specimens stored on the roof for 6 yr are shown in Figure 5.

We had intended to recover the asphalt from the briquettes in Group 1 and determine if the absorptive aggregates harden the asphalt more rapidly. However, due to the ruptured epoxy coating, we were not able to complete this phase.

The excessive expansion of the absorptive samples and the slight or no expansion of the nonabsorptive samples weathered on the roof and in the pavement raised the following questions:

1. Why did the absorptive AC samples expand so rapidly?
2. Why did the nonabsorptive samples not expand?
3. What is the maximum expansion that can be expected from absorptive AC mixes?

In answer to the first question, we might state that there probably were microscopic holes in the epoxy coating and asphalt binder through which moisture could pass. The absorption of moisture by the aggregates caused a sufficient increase in volume to crack the epoxy coating. This destructive cycle of moisture absorption and expansion continued until the AC briquettes were completely ruptured (Fig. 2).

The absorptive briquettes which were not encapsulated (Fig. 4) had noticeable cracks over their entire surface. Their movements were not confined, allowing expansion and contraction to occur without complete rupture, which was not the case with the encapsulated briquettes.

In answer to the second question, we feel that the absence of visible signs of stress in both the encapsulated and nonencapsulated absorptive briquettes indicated that no increase in volume had occurred. We believe the moisture that did enter the briquettes was adsorbed and retained in the void spaces. The hard nonabsorptive aggregates did not absorb moisture; therefore, no overall expansion was noticed.

In answer to the third question, we may state that the maximum longitudinal expansion recorded to date on one of the test specimens (as described later) was about 0.2 in.

Study on Compacted AC Slab

To obtain better measurements, we constructed a test slab 1 ft by 2 ft by 3 in. thick. A sample of absorptive aggregate (Table 1) was mixed with 6.3 percent of 85-100 penetration paving asphalt. The aggregates and asphalt were mixed under controlled conditions in a Hobart mixer. This procedure for mixing had been calibrated previously for studies on asphalt hardening against field pug mill mixing. The slab was made in two layers and a syntron hammer was used for compaction. The specimen required about 65 lb of aggregate and was compacted to a density of 126 pcf.

After the test slab was compacted in a heavy wooden split frame, the top portion of the frame was removed and replaced with aluminum sides which permitted free expansion and contraction. The unrestrained movement was recorded by six dial indicators reading to the nearest 0.001 in. and located around the surface course (Fig. 8).

In June 1961, this fabricated slab was exposed to the outside atmosphere. Dial measurements were made every 2 hr during the working day, and the air and surface temperatures were also recorded 5 times daily.

Figure 9 shows the expansion and contraction that occurred in a 1-wk period during the study, which lasted about 3 mo. Figure 10 shows the expansion that occurred during the entire length of test. The cyclic pattern illustrates that maximum expansion for this AC mix occurs during the early morning hours when a considerable amount of moisture is in the atmosphere, and maximum contraction occurs during the warmest hours of the day. The test specimen failed to return to its original dimensions during the contraction period, probably because of structural breakdown of individual aggregates exposed to moisture during the wet cycle. The maximum expansion in width, 0.142 in., occurred on a day following a rainstorm in September, about 3 mo after the starting date of the test. This expansion would have been considerably higher if the lower wooden form had not broken under the tremendous force of the expanding asphalt concrete.

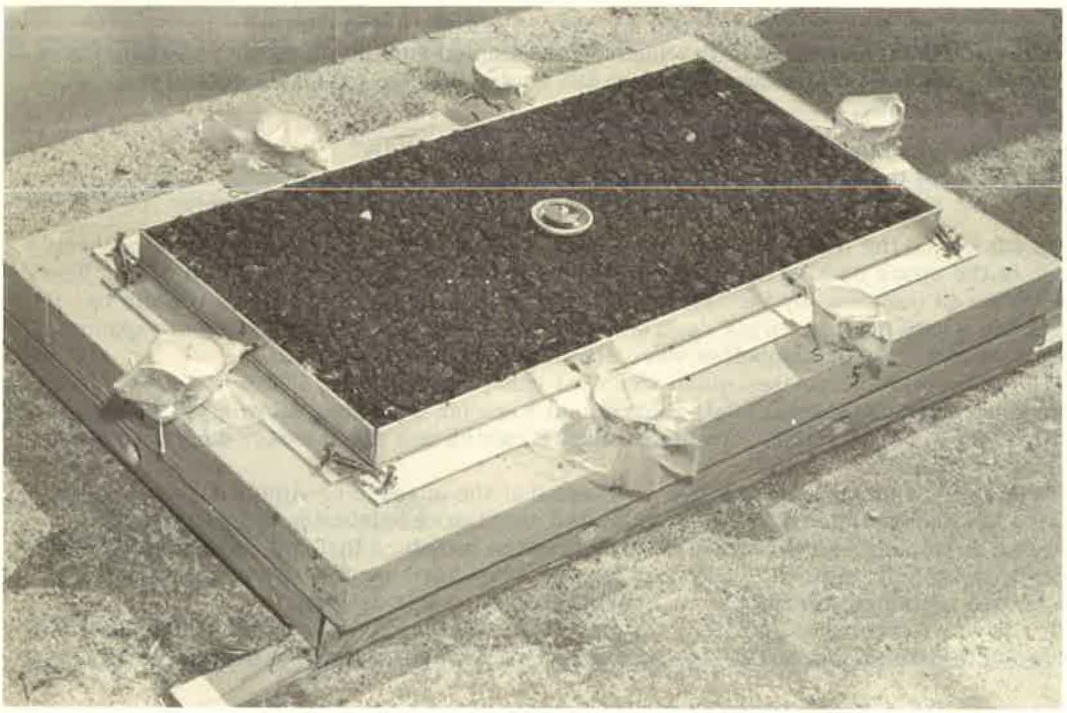

Figure 8. Slab specimen 1 ft by 2 ft by 3 in.; note springs holding aluminum sides surrounding surface course.

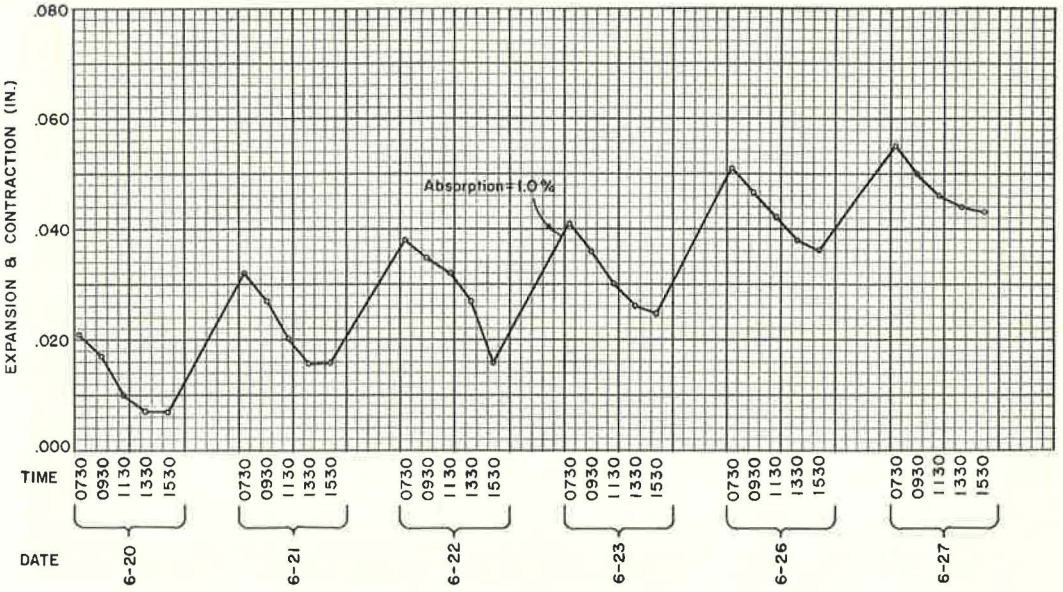

Figure 9. Test 57-1236.

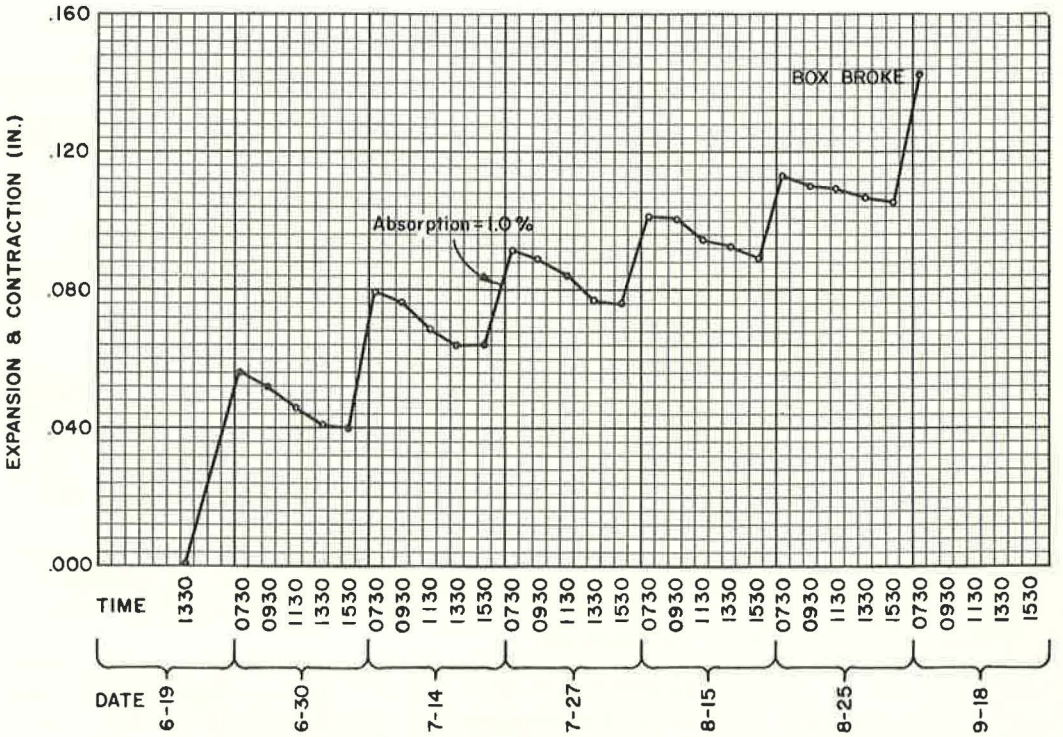

Figure 10. Test 57-1236.

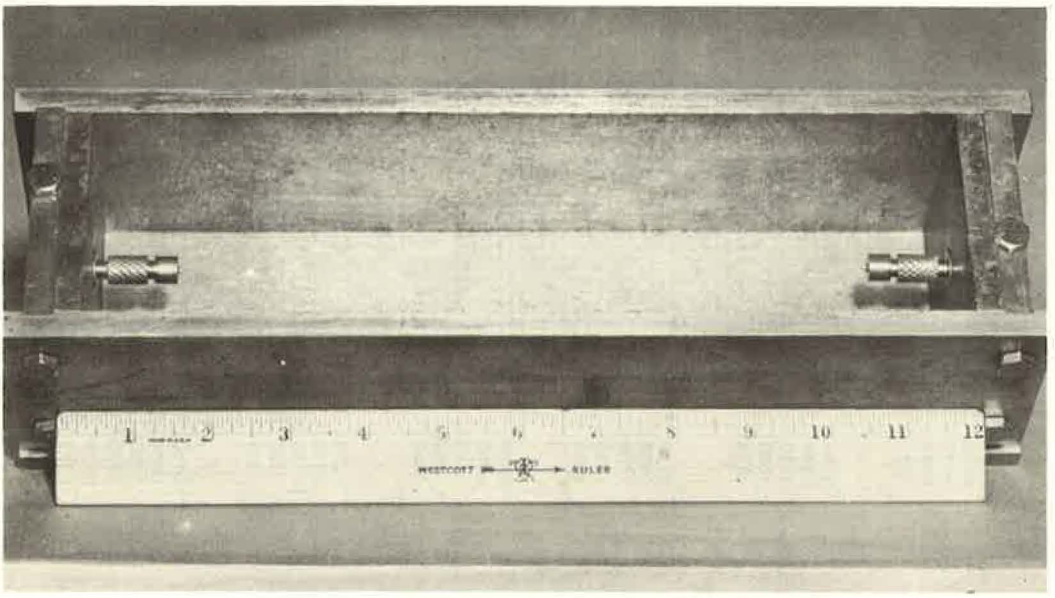

Figure 11. Steel mold, 3 by 3 by 11.25 in., for fabricating bars; note steel pins in end of plates for measuring AC bars.

The total expansion in length and width, as recorded, shows an increase in volume of 1.4 percent. However, the actual volume increase undoubtedly would have been much greater if the box had not broken and if we had arranged to determine the increase in thickness of the test specimen.

The foregoing method for fabricating AC mixes to determine the amount of expansion and contraction was discontinued for the following reasons:

1. The amount of material needed for one sample was approximately 65 lb;
2. The cost of the box and the six dial indicators for each specimen tested was considered too high; and
3. The time required for preparing one sample was excessive.

Measurement of AC Bars

To reduce the expense of constructing large test samples, a new method was adopted. Asphalt mixes were compacted into 3- by 3- by 11.25-in. steel molds (Fig. 11). Briefly, the method consists of heating the AC mixture to 230 F, rodding it into two layers in the preheated mold, and compacting it with the kneading compactor. On cooling, the mold is stripped and the steel pins at the end of the specimen are fastened into place with epoxy. The bar is cured in a 100 F oven for 3 days and then subjected to the weathering cycles, one cycle consisting of 7 days in a moist room and 7 days in a 100 F oven. Daily measurements of the specimen are made and any cracks or unusual behavior recorded. The specimen is subjected to a total of 3 to 6 weathering cycles. Detailed procedure is given in the Appendix.

Following this new procedure, test bars were made from AC samples obtained from current construction projects throughout the state, as well as from proposed aggregate sources showing varying absorptive characteristics (0.0 to 2.8 percent). Figure 12 and Table 2 present results from the first AC bars tested. These bars were fabricated from highly absorptive aggregates from two different sources.

Cracks appeared in sample 62-1863 during the drying period of the first cycle. During the third cycle, the sample expanded over 0.2 in. with block cracking throughout. This expansion of more than 0.2 in. in a 11.25-in. bar (1.8 percent expansion)

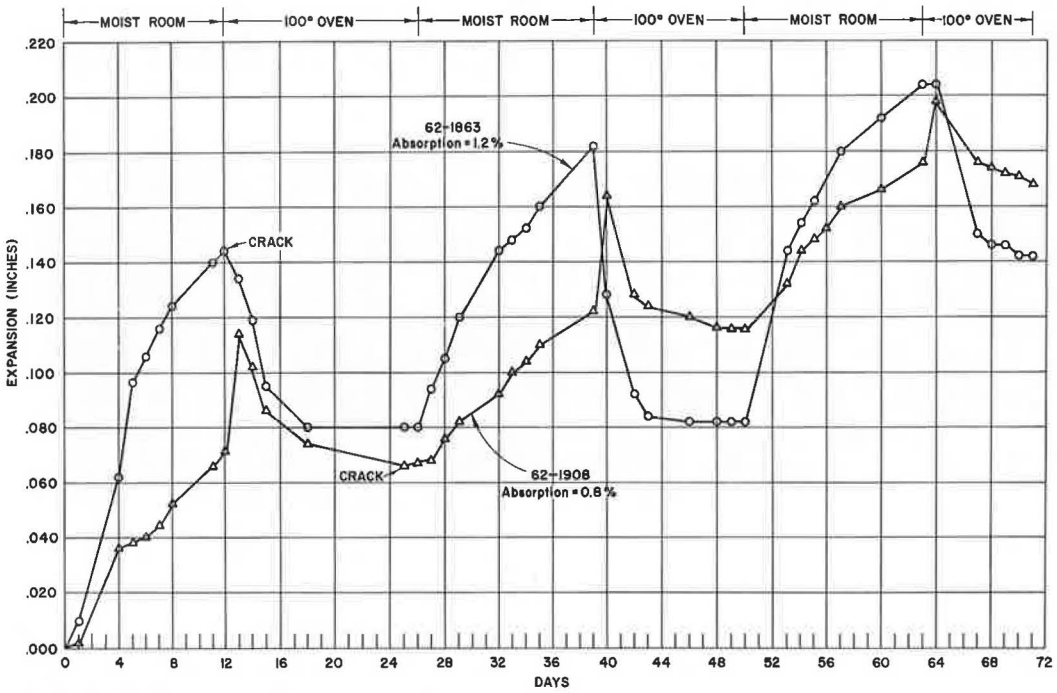

Figure 12. Tests 62-1863 and 62-1908.

is the maximum longitudinal increase recorded to date for AC bars and was reached after 64 days (Fig. 12) of exposure to wet and dry periods.

Transverse cracks were visible on sample 62-1908 at the end of first cycle (Fig. 13). Rapid expansion (0.045 in.) at the beginning of the drying cycle suggests that this specimen is susceptible to moisture in the vapor state. This sample also exhibited several transverse cracks at the end of the third cycle.

Results show sample 62-1908 required 13 days in a 100 F oven before contraction remained constant. This unusually long period was probably due to the sample's susceptibility to moisture vapor. Sample 62-1863 stopped contracting at the end of 6 days.

Data show that the average time required for maximum expansion and contraction is approximately 7 days for each wet and dry cycle.

TABLE 2

TEST RESULTS—AC BARS

Sample	Agg. Class.[a]	Absorb.[b] (%)	Asph. 85-100 (%)	Stab. Value	Coh.	Sp. Gr.
62-1863	Weathered andesite	1.2	6.9	37	255	2.11
62-1908	Weathered andesite, some tuff, minor quartz	0.8	6.5	39	279	2.13

[a]By X-ray diffraction and DTA.
[b]By modified CKE test.

Figure 13. Test bar 62-1908; transverse cracks appeared after first cycle.

AC pavements constructed with aggregates from the same source as sample 62-1863 have shown considerable distress in the form of cracking. This aggregate source has now been eliminated for constructing AC pavements, even though the material generally passes all routine physical tests.

Figure 14 is a close-up of test bar 62-1863. Transverse cracks appeared first on the surface of the specimen, then progressed downward. At the end of the third cycle, the bar was completely block cracked.

INVESTIGATION OF PAVEMENT FAILURE

In 1962 we were asked to investigate an AC pavement failure in one of our districts. This failure (Fig. 15) consists of transverse cracks from $\frac{3}{4}$ to $1\frac{1}{2}$ in. wide in the surfacing at irregular intervals ranging from 10 to 20 ft apart throughout the entire

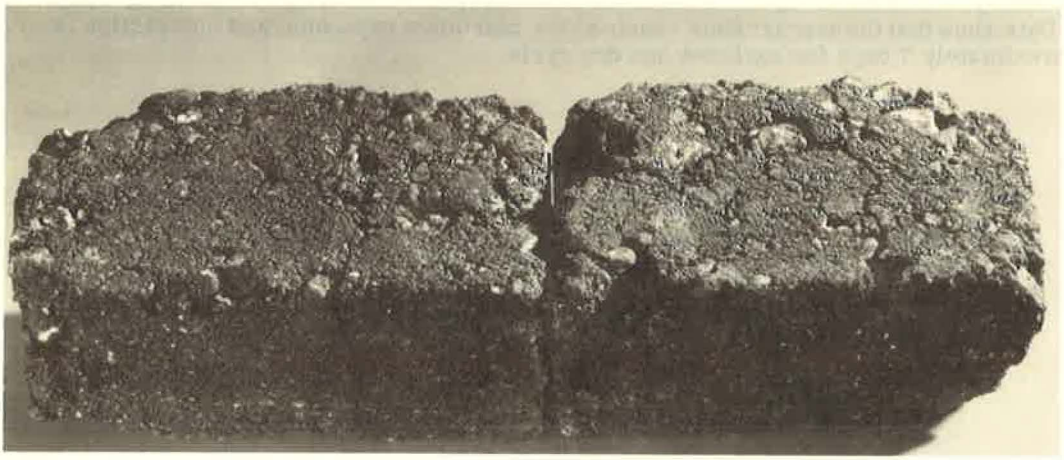

Figure 14. Test bar 62-1863, completely block-cracked at end of third cycle; $\frac{1}{2}$ in. section sawed from center of test bar for microviscosity test.

Figure 15. Transverse cracks ranging from 3/4 to 1 1/2 in. in width.

project. The pavement was constructed from aggregates obtained from a local pit.

Samples were taken from the existing pavement and from the aggregate source. Sufficient material was obtained to complete routine tests as well as expansion and contraction tests. Test results are given in Table 3.

Differential thermal analysis (DTA) of the raw aggregate indicated that the minus 200 mesh material contained nontronite (iron-rich montmorillonite) and X-ray diffraction showed montmorillonite and layered silicates.

To duplicate the field mix design, laboratory specimens were mixed in the Hobart mixer, using 6.3 percent of 85-100 paving asphalt. After mixing, the samples were compacted (see Appendix) into test bars and placed in the 100 F oven. After the specified period, the bars were placed in the moist room for the beginning of the test.

In addition, a test bar, 3 by 3 by 11.25 in., was sawed from a slab sample removed from the existing pavement. The sawed bar was dried in a 100 F oven to constant weight and then placed in the moist room for the beginning of the test.

The expansion and contraction occurring in the laboratory specimen and the AC sample bar sawed from existing pavement are shown in Fig. 16. Both AC bars show approximately the same rapid expansion in the first few hours of the dry cycle. However, the laboratory-prepared AC bar expanded more than the bar removed from

TABLE 3

TEST RESULTS—AC PAVEMENT

Samples	Agg. Class.[a]	Absorb.[b] (%)	Asph. 85-100 (%)	Stab. Value	Coh.	Sp. Gr.
From exist. pav't.	Volcanic-olivine basalt and andesite weathered, and altered feldspar montmorillonite	--	6.3	37	247	1.98
Fabricated in lab.		1.9	6.3	39	170	2.03

[a]By X-ray diffraction and DTA.
[b]By modified CKE test.

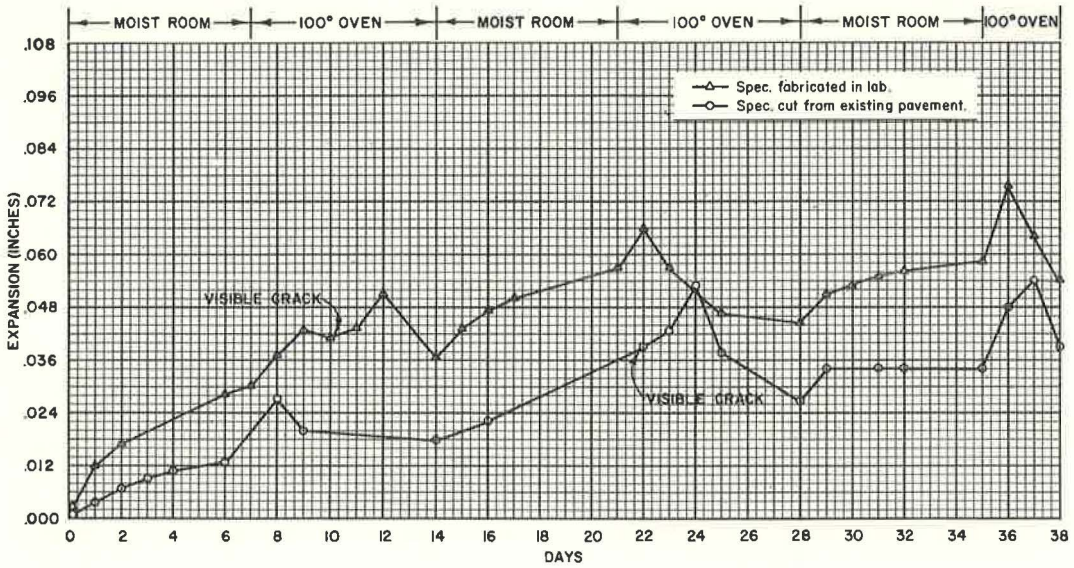

Figure 16. Test 62-5748.

the existing pavement during the wet cycle, probably because the asphalt in the latter had a longer time to be absorbed by the absorptive aggregates (both fine and course). This added depth of penetration of asphalt into the aggregates partially sealed off the pores of the aggregates and prevented it from absorbing water, thereby reducing expansion during the wet cycle.

We also felt that the expansion could be related to the type of clay (nontronite) present in the mix. To investigate this, a specimen with the clayey portion removed was fabricated. The results (Fig. 17) indicate that expansion was considerably reduced in the wet cycle. However, in the dry cycle, expansion was greater and somewhat more abrupt than it was in the regular test bar.

The smaller expansion during the wet cycle and greater expansion in the dry cycle appear to be caused by the following factors:

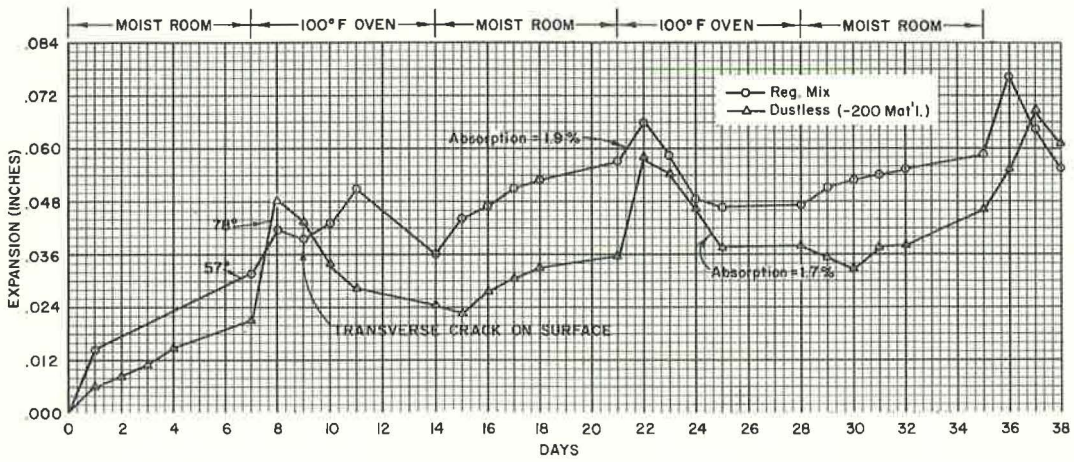

Figure 17. Test 62-5748.

1. The minus 200 material contained a considerable amount of clay (nontronite). When this expansive clay was removed from the AC mix, the total amount of expansion during the wet cycle was also reduced.

2. By wasting the minus 200 material, the natural barrier between the moisture and the larger absorptive aggregates was removed, thereby making a constant supply of water available to the larger aggregates during the wet cycle. When the dustless (minus 200 material) mix test bar was placed in the 100 F oven, the absorbed moisture entrapped in the larger aggregates attempted to escape immediately by evaporation. However, all the moisture could not escape at once through the minute interstices, and, as a result, vapor pressure rapidly built up during the first few hours of the dry cycle, causing a sharp increase in expansion.

INFLUENCE OF MINERAL FILLER ON EXPANSION

In July 1961 an experimental test section was constructed for the purpose of comparing the effectiveness of various fillers on an asphalt concrete mix. The control section was a normal AC mix conforming to our standard specifications with no commercial filler added. The results of the tests on the AC control sample, as well as on the AC sample with various fillers, are given in Table 4.

Test bars were also fabricated from the various mixtures to see whether or not expansion would occur. Two percent of three mineral fillers, A, B, and C, were used. During road construction, AC samples were taken from the paver from each section including the control section, and test bars were fabricated. Figure 18 represents the expansion and contraction behavior of the test bars.

Filler A

As shown in Figure 18, Filler A expanded excessively during the first hours of the dry cycle. This phenomenon did not occur in the AC control bar or the other AC bars with different fillers added. From results obtained, we assumed that Filler A was the contributing factor which caused this high expansion during the dry cycle. Transverse cracks appeared during the dry period of the first cycle. After cracking, the amount of expansion decreased. This usually occurs when the cracks have progressed through the test bar.

Since July 1961, five condition surveys have been made of this test section. Nine months after the completion date, transverse cracks from $\frac{1}{16}$ to $\frac{1}{8}$ in. in width were visible at about 10-ft intervals throughout this section. The amount of cracking, both transverse and longitudinal, have continued to increase with time. As indicated in Table 4, 132 lin ft of cracking per station was visible during the October 1963 survey.

This filler was also used in an experimental AC test section in another part of the state. This section also showed cracks appearing shortly after the pavement was completed. The aggregates, asphalt, and location were entirely different for these two projects.

TABLE 4

INFLUENCE OF FILLERS

Sample	Agg. Class.	Absorp.[a] (%)	85-100 Asph. (%)	Stab. Value	Coh.	Sp. Gr.	Lin Ft Cracks/100 Ft
Control	Granite, andesite and rhyolite	0.4	5.0	36	164	2.37	30
Filler	A	-	5.3	37	400	2.36	132
Filler	B	-	4.8	38	315	2.38	22
Filler	C	-	4.5	37	220	2.37	42

[a]By modified CKE test.

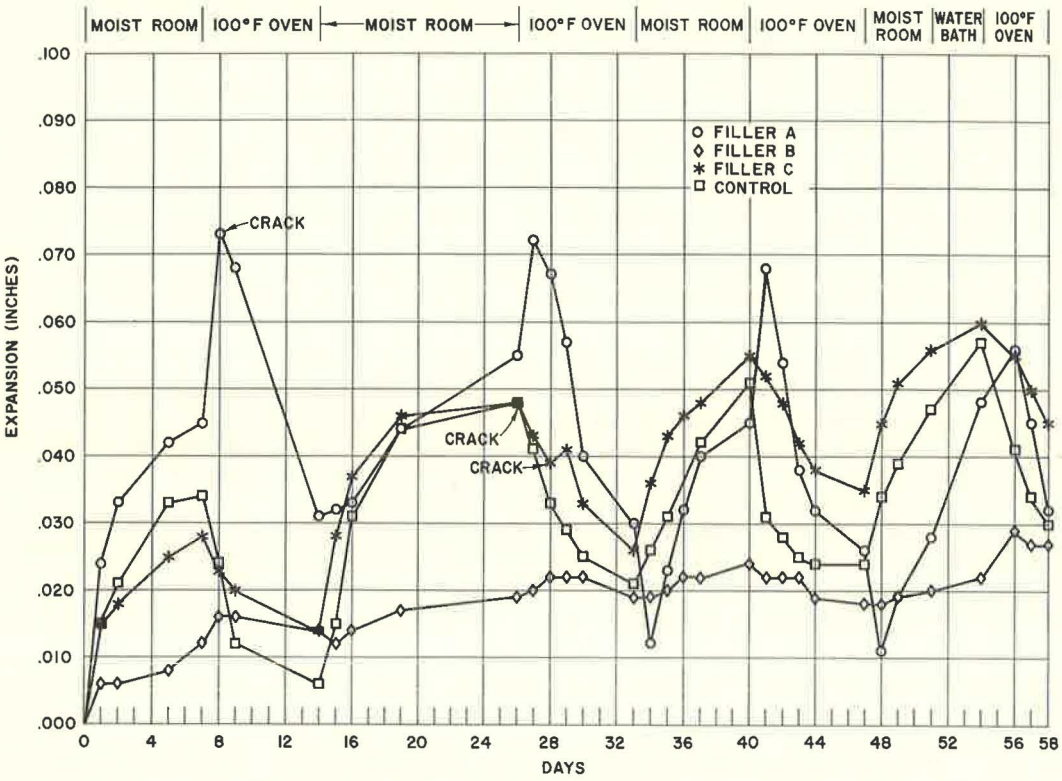

Figure 18. Effect of various fillers.

Filler B

This mineral filler reduced the maximum expansion from 0.057 to 0.029 in., or 51 percent, as compared with the control bar. No cracks were visible on the test bar after four complete cycles.

The April 1962 condition survey showed slight pitting and a few hairline transverse cracks. However, the last survey made (October 1963) showed no additional cracks or pitting since the April 1962 survey.

Filler C

This filler did suppress expansion during the first cycle but was ineffective in decreasing expansion in succeeding cycles. Cracking appeared during the drying period of the second cycle.

The pavement survey showed that excessive pitting occurred after the December 1961 survey but before the April 1962 survey. Transverse cracks were visible during the April 1962 survey, and longitudinal cracks were noticed in the October 1963 survey.

Filler B appears to be superior to the control and Filler C section, and all test sections seem to be superior to the Filler A section.

INFLUENCE OF ASPHALT CONTENT ON EXPANSION

It is the policy of the California Division of Highways to recommend the highest possible asphalt content for asphalt concrete mixes, consistent with other specification requirements such as stability. This is particularly important when using absorptive aggregates. Figure 19 shows that for a fairly absorptive aggregate, the maximum expansion was decreased from 0.049 to 0.008 in. by increasing the average asphalt

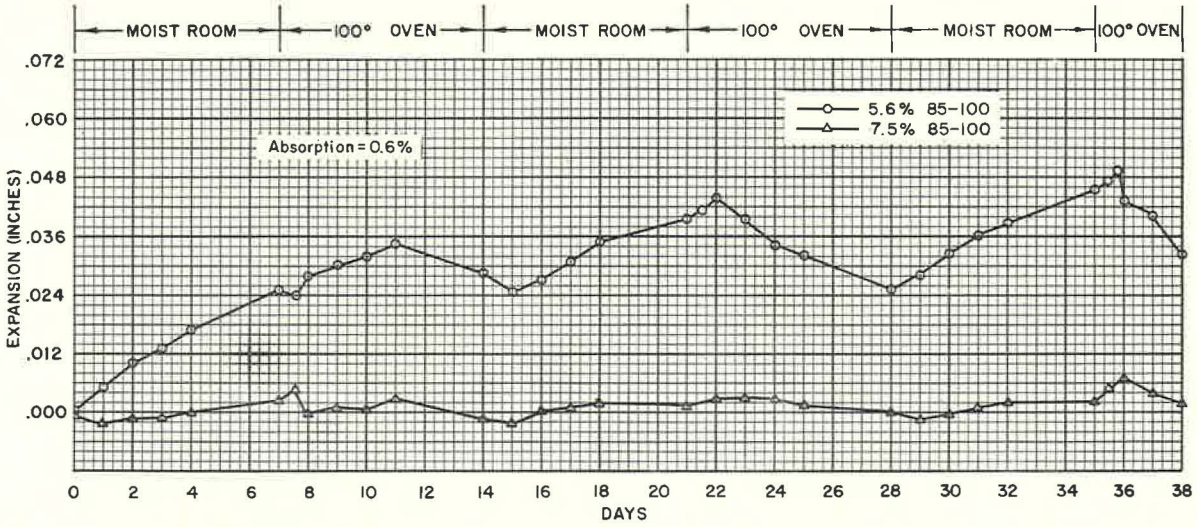

Figure 19. Test 64-1769

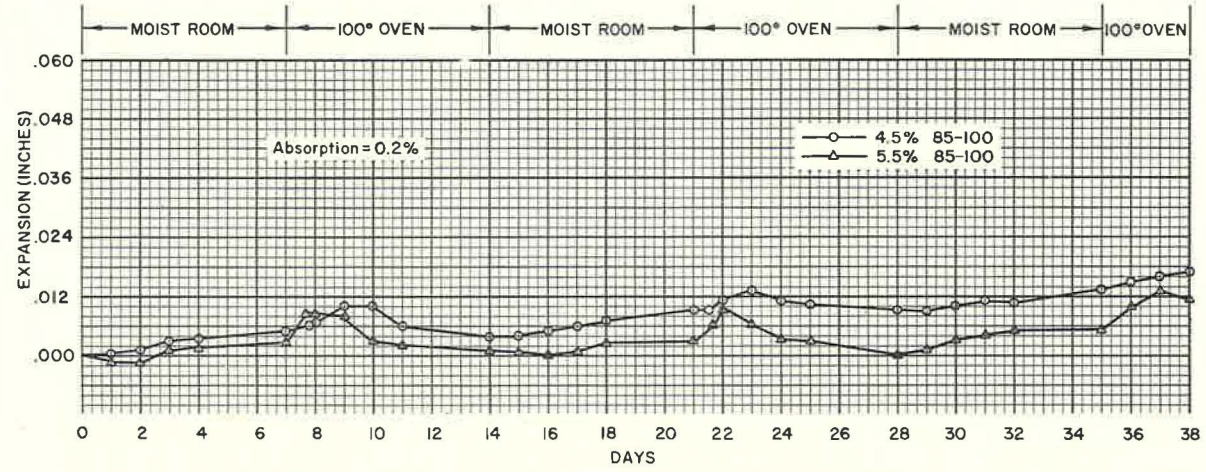

Figure 20. Test 64-1539

film thickness by 1 μ. The same increase in film thickness of a nonabsorptive or slightly absorptive aggregate will reduce the expansion only slightly, as illustrated in Figure 20.

MODIFIED CKE TEST

By modifying the CKE test, the relationship between expansion and contraction and the absorption of the aggregates used in test bars could be shown. The present CKE test is based on factors which include both surface area and absorption. Certain limits (k factors) are provided in the standard specifications to eliminate or reduce the number of highly absorptive aggregates used. This test has been used by the California Division of Highways since 1940 to indicate the amount of oil or asphalt required for a given mix and has given excellent service. The modified CKE test treats surface area and absorption of the aggregate as two distinct and separate factors. We have used this test for several years, primarily as a research tool. However, it has not officially replaced the California test method No. 303-D.

We are presently in the process of setting limiting values for absorption, and the modified CKE test will be the subject of a separate paper.

The equipment for the modified CKE test is identical to that used in the present test. Briefly, the procedure consists of placing 100 gm of the combined aggregate (up to $\frac{3}{4}$ in. maximum size) in the centrifuge cup, pouring 20 ml of kerosene over the sample, and centrifuging it immediately (within 5 sec) for a period of 2 min at 400 g. The sample is then weighed and the surface area is determined from the amount of kerosene retained. Next the sample is placed in a small pan of kerosene and is permitted to soak for 10 min. It is centrifuged again for a period of 2 min at 400 g. The sample is then reweighed and the additional amount of kerosene retained is determined. The total amount of kerosene retained minus the amount retained after first centrifuge period is equal to the absorption of the aggregate. The surface area and asphalt content are then determined from appropriate charts.

The main difference between the present and proposed CKE test procedure is that the present method involves only one centrifuging. However, the results obtained combine surface area and absorption. The modified method involves centrifuging the sample twice, thereby making it possible to obtain the true surface area and true absorption. Therefore, in future specifications, absorption can be limited and undesirable expansive aggregates can be eliminated.

FUTURE STUDIES

1. Test results have shown that some test bars fabricated from absorptive aggregates expanded as much as 2 percent longitudinally. The longitudinal and transverse pressures that these expansive mixes are capable of exerting are not known. Equipment is now being designed to measure these forces in test bars and in existing AC pavements.
2. It is proposed to determine by X-ray diffraction and DTA if there is an element, or a group of elements, which can be identified with expansive aggregates. If so, we hope to find some method to control their expansive properties.
3. To increase field-laboratory correlation studies, it is proposed that test bars be fabricated from certain preliminary AC mix designs and some construction control samples, particularly when absorptive aggregates are involved.
4. Maximum absorption values will be set on aggregates used in construction of AC mixes.

CONCLUSIONS

1. There is a relationship between the percent absorption of the aggregate as determined by the modified CKE test and the expansion and contraction of the mix. Generally, the higher the absorption, the greater is the expansion.
2. Maximum expansion usually occurs during the wet cycle. However, several figures show maximum expansion occurred during the first 24 hr of the dry cycle.

3. Maximum contraction occurs during the dry cycle.
4. AC test bars generally continue to expand during the test cycle and usually do not return to their original length.
5. Inherent strains are capable of cracking test bars without the aid of external forces.
6. Tests to date show that expansion can be reduced by removing expansive clays from the aggregate mix.
7. Tests indicate that an increase in asphalt content usually reduces expansion in the wet cycle.
8. Expansion can be reduced by some mineral fillers, but other fillers may encourage expansion.
9. An ideal expansion suppressor would be a filler, natural or manufactured, which would absorb the moisture entering into the AC pavement without increasing in volume.
10. Studies made to date show good correlation between expansion bars and actual pavement conditions.
11. A new test procedure has been presented which will aid the engineer in making a more prudent analysis of the aggregates to use in the construction of AC pavements.

There are still many unanswered questions concerning the causes and effect of expansion and contraction. We feel, however, that when this study is completed, the information gained will increase understanding of AC pavement failure. With the causes of certain types of failures known, we feel that corrective measures can be taken.

ACKNOWLEDGMENTS

Special acknowledgment is due Merle Nelson, John Skog, Kenneth Iwasaki, and J. L. Beaton.

REFERENCES

1. Hveem, F. N. Pavement Deflection and Fatigue Failures. Highway Research Board Bull. 114, pp. 43-87, 1955.
2. Monismith, C. L. Flexibility Characteristics of Asphaltic Paving Mixtures. Proc. AAPT, Vol. 27, pp. 74-106, 1958.
3. Monismith, C. L. Effect of Temperature on the Flexibility Characteristics of Asphaltic Paving Mixtures. ASTM STP No. 277, pp. 89-108, 1960.
4. Papazian, H. S., and Baker, R. A. Analysis of the Fatigue Type Properties of Bituminous Concrete. Proc. AAPT, Vol. 28, pp. 179-210, 1959.
5. Nijboer, L. W. Mechanical Properties of Asphalt Materials and Structural Design of Asphalt Roads. Highway Research Board Proc., Vol. 33, pp. 185-200, 1954.
6. Porter, O. J. Foundations for Flexible Pavements. Highway Research Board Proc., Vol. 22, pp. 100-143, 1942.
7. Franck, G. Deflection Measurements on Flexible Roads. Revue des Route, Vol. 27, No. 311, pp. 75-88, Dec. 1957.
8. Hveem, F. N. Quality Test for Asphalt—A Progress Report. Proc. AAPT, Vol. 15, 1943.
9. Hveem, F. N. Use of the Centrifuge Kerosene Equivalent as Applied to Determine the Required Oil Content for Dense Graded Bituminous Mixes. Proc. AAPT, 1942.

Appendix

PROCEDURE FOR FABRICATING 3- BY 3- BY 11.25-IN. ASPHALT CONCRETE BARS

1. Place approximately 4,000 gm asphalt concrete mixture in a 230 F oven for at least 2 hr.
2. Into a 3- by 3- by 11.25-in. steel mold (Fig. 21) preheated to 140 F, place sufficient asphalt concrete mix to fill the mold one-half full.
3. Rod the mix 20 blows with a $^{3}/_{8}$-in. diameter bullet-nosed rod (Fig. 22).
4. Add sufficient material to fill the mold.
5. Rod second lift 20 blows. (Be sure mix is well rodded around end pins.)
6. Compact specimen for 5 min at 15-lb pressure on the dial of the kneading compactor (125 psi) (Figs. 23 and 24).
7. Continue compaction for an additional 5 min at a pressure of 31 lb on the dial of the kneading compactor (250 psi).
8. Place steel plate ($2^{7}/_{8}$ by $^{1}/_{4}$ by 11 in.) on specimen and compact for 2 min at the 31-lb pressure for leveling-off load (Fig. 25).
9. Strip mold from specimen and place compacted specimen on sheet of plywood (Fig. 26).
10. Secure steel end pins to test specimen with epoxy resin (Fig. 27).
11. Leave specimen in 100 F oven for approximately 63 hr.
12. At the start of the test, record length of AC bar and place bar in moist room. Make and record measurements.
13. After 7 days in the moist room, place the AC bars in the 100 F oven. Make measurements every 2 hr.

Figure 21. Mold and carriage which holds steel mold during compaction.

Figure 22. AC mix being rodded with $^{3}/_{8}$ in. bullet-nosed rod.

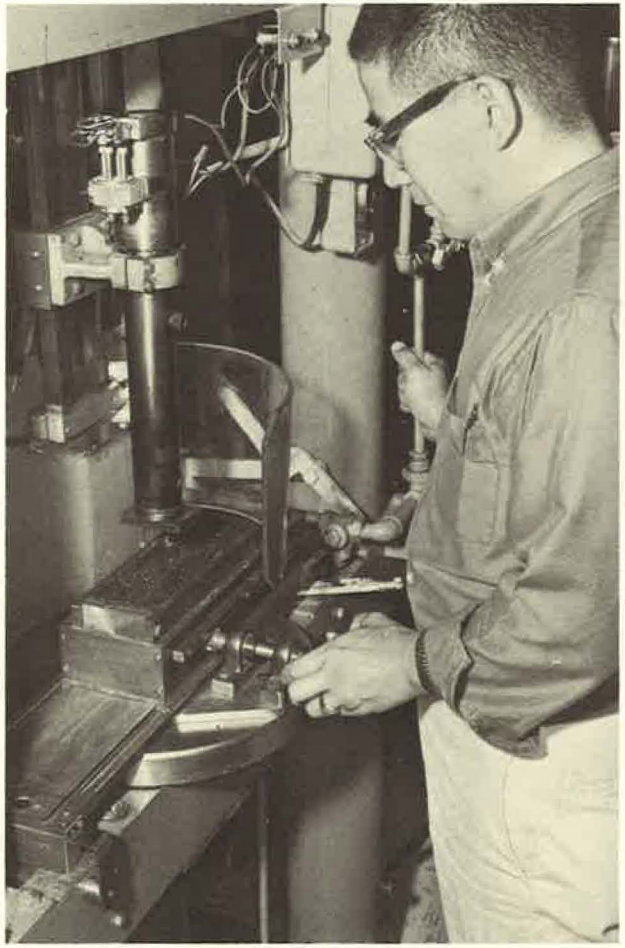

Figure 23. AC mix ready to be compacted with 2- by 3-in. rectangular compacting foot (2 by 3 in.).

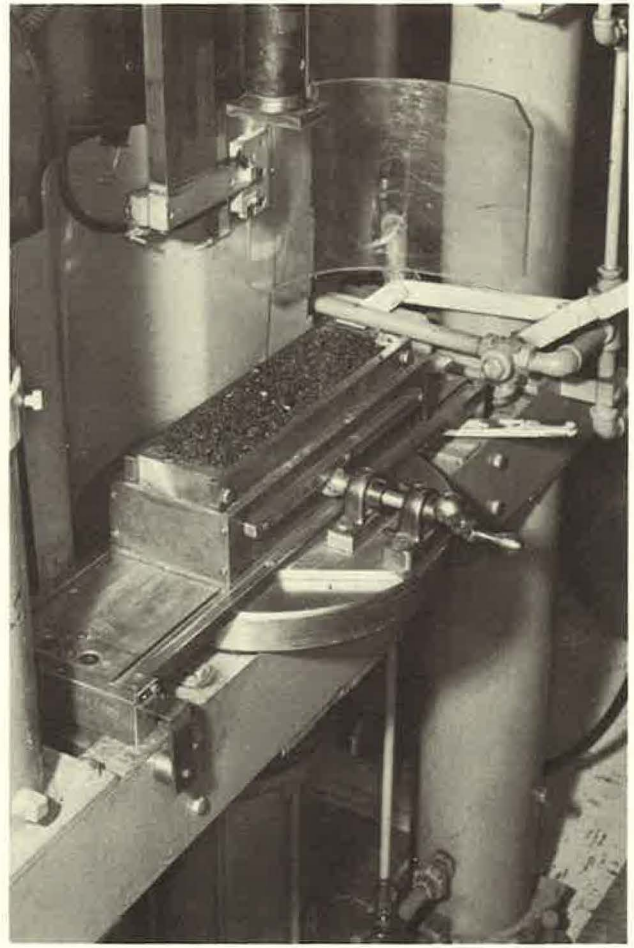

Figure 24. AC bar being fabricated; crank is turned $\frac{1}{4}$ rev after each stroke of compactor foot.

Figure 25. AC bar receiving leveling-off load.

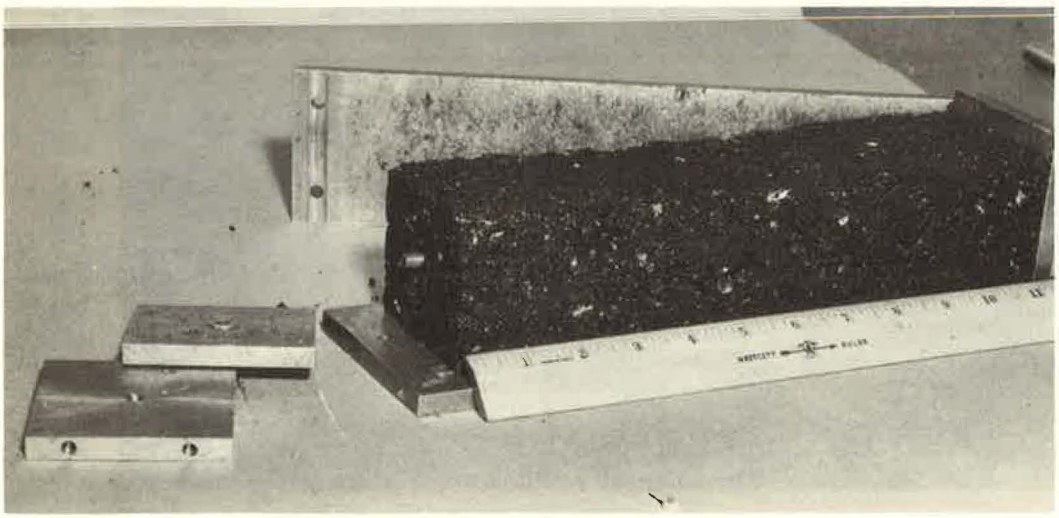

Figure 26. Metal mold being stripped from AC bar, showing steel pins used for measurement.

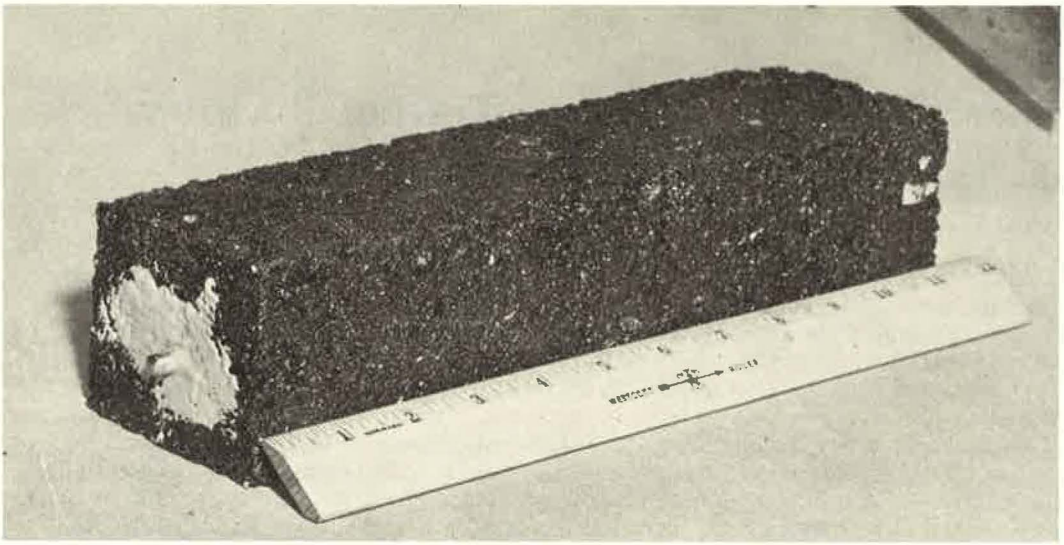

Figure 27. Finished AC bar showing steel pins secured into bar with epoxy.

14. After the first 8 hr in the 100 F oven, make measurements once a day for the remainder of the 7-day period. Then place the specimen again in the moist room and begin the second cycle. Continue this for three cycles, or in some special cases, six cycles. (One cycle equals 7 days in the moist room and 7 days in 100 F oven.)

Experiences with Gyratory Testing Machine

B. E. RUTH and J. H. SCHAUB
Respectively, Instructor and Chairman, Department of Civil Engineering, West Virginia University

•IN 1961, the Department of Civil Engineering of West Virginia University established a bituminous mixtures laboratory as a part of the facilities of the new Engineering Sciences Building. The equipment obtained for the laboratory included a Model 4-C gyratory testing machine (Engineering Development Co., Inc., Vicksburg, Miss.) to permit instruction and research with the most recently available and promising test equipment.

Late in 1961, a research contract was initiated between West Virginia University, the West Virginia State Road Commission, and the U. S. Bureau of Public Roads to develop a bituminous mixture design procedure suitable for West Virginia aggregate and gradation and to reproduce the successful experience designs developed through state experience. The general approach to the mixture design study was to utilize the gyratory testing machine for laboratory sample compaction and to measure the engineering properties of the samples using stabilometer, cohesiometer, air voids, and density techniques. As the research program progressed, it became apparent that there were numerous aspects of the gyratory testing machine that should be investigated. Initial studies dealt with uniformity of compaction as reported by several laboratories, effect of various angles of gyration, ram pressure, and number of revolutions with the fixed roller and the air roller. The latter investigations opened still other areas of interest, including the effect of air-roller pressure and the significance of results.

Very little is contained in the literature with respect to gyratory compaction and testing since the initial studies by the Texas Highway Department (7) and the development by the Corps of Engineers (1) of the present-day form of the equipment. The available literature deals primarily with fixed-roller compaction. It has also been noted that there is appreciable interest in the results obtained by the work at West Virginia University. This paper is presented in an effort (a) to define the character of the studies performed to this date at West Virginia University, (b) to present the problems encountered with the equipment, (c) to illustrate the type of results that have been obtained, (d) to discuss the tentative conclusions reached from the results, and (e) to indicate the present trend and probable future aspects of the West Virginia University research with the gyratory testing machine.

LIMITATIONS OF EXISTING BITUMINOUS MIXTURE DESIGN METHODS

There are numerous factors that limit the use of the various bituminous mixture design procedures employed today. The following discussion is not intended to consider all of these factors but has been limited to comments of particular interest to the authors' studies with the gyratory testing machine.

Present methods of bituminous mixture design consider the influence of vehicular traffic by changing the design criteria or the amount of laboratory compaction. Materials that fail to meet the design criteria are either discarded or altered by changing the aggregate gradation, mineral filler content, and/or grade of asphalt cement to attain the desirable mixture characteristics. The modification of a bituminous mixture may be desirable if it is assumed that the various test measurements are accurate and that the design criteria are applicable to existing conditions.

Paper sponsored by Committee on Mechanical Properties of Bituminous Paving Mixtures.

Variations due to materials, equipment, and the skill of the technician may result in erroneous selection of design asphalt contents. Elimination of complex and numerous test procedures would be beneficial in reducing much of this variation.

Certain aggregate types and gradations yield inadequate stability but when subjected to a slight increase in compactive effort show an appreciable increase in stability. Laboratory compaction should simulate the density and stability characteristics that are reasonably and economically attainable by field compaction of the mixture. Is it feasible to increase stability with a greater amount of compactive effort, or is it more desirable to alter the aggregate gradation without increasing compactive effort? Current design methods consider only the alteration of the grading to obtain satisfactory stability, although inadequate stability may still exist after construction (because of a low degree of field compaction) or failure of the pavement surface may develop with traffic (as a result of 100 percent or more of laboratory compaction). Certainly the existing design procedures do not define the minimum acceptable stability or the maximum density for construction to assure reasonable compaction requirements and adequate stability for the life of the pavement. Existing procedures attempt to do this by a middle-of-the-road approach.

Limitations of existing bituminous mixture design methods may be summarized as follows:

1. Design procedures do not establish a minimum field-compacted density based on a stability criterion;
2. Design procedures do not establish a maximum field-compacted density based on stability considerations for the densities developed during the life of the pavement; and
3. Design procedures do not evaluate the stability characteristics of mixtures through a wide range of density conditions.

OPERATIONAL ASPECTS OF MODEL 4-C GYRATORY TESTING MACHINE

The major operational aspects of the gyratory testing machine have been thoroughly discussed in the literature (1, 3); however, certain significant aspects of operation have been neglected. The ensuing discussion pertains to the utilization of different upper rollers and to the operational difficulties encountered in the studies performed at West Virginia University.

Fixed-strain operation may be attained by using either the fixed roller or the oil-filled roller, as shown in Figure 1. The oil-filled roller offers the advantage of direct measurement of roller pressure for constant angles of gyration. Pressure changes provide more sensitive measurements of variation in the character of the sample than may be obtained by observing changes in the width of the gyrograph and, thus, provide a direct comparison between different aggregates, gradations, and asphalt contents. If pressure readings are not utilized, the only recourse is to assume that the mixture will have adequate stability at the design asphalt content selected on the basis of the gyrograph.

Flushing, or widening of the gyrograph, results when the force exerted by the off-center weight of mold and mold chuck exceeds the resisting force of the mixture being compacted. If the angle of gyration is increased, the force exerted by the mold chuck increases so that flushing will be observed at a higher level of mixture resistance. This effect is most desirable since it provides a basis for establishing arbitrary levels of stability for different contact pressures to evaluate mixtures for a wide range of traffic conditions.

McRae states:

> The 100 ram pressure, 1 ½° angle of gyration, and 20 revolutions may be a better selection for heavy highway traffic (75 blow Marshall). In general, increasing the angle of gyration produces a lower optimum for the same density. (6)

The logical design procedure would be to utilize a ram pressure and an angle of gyration similar to actual contact pressures and strains to produce stabilities sufficient for each level of traffic service. This assumes that a criterion is available to define

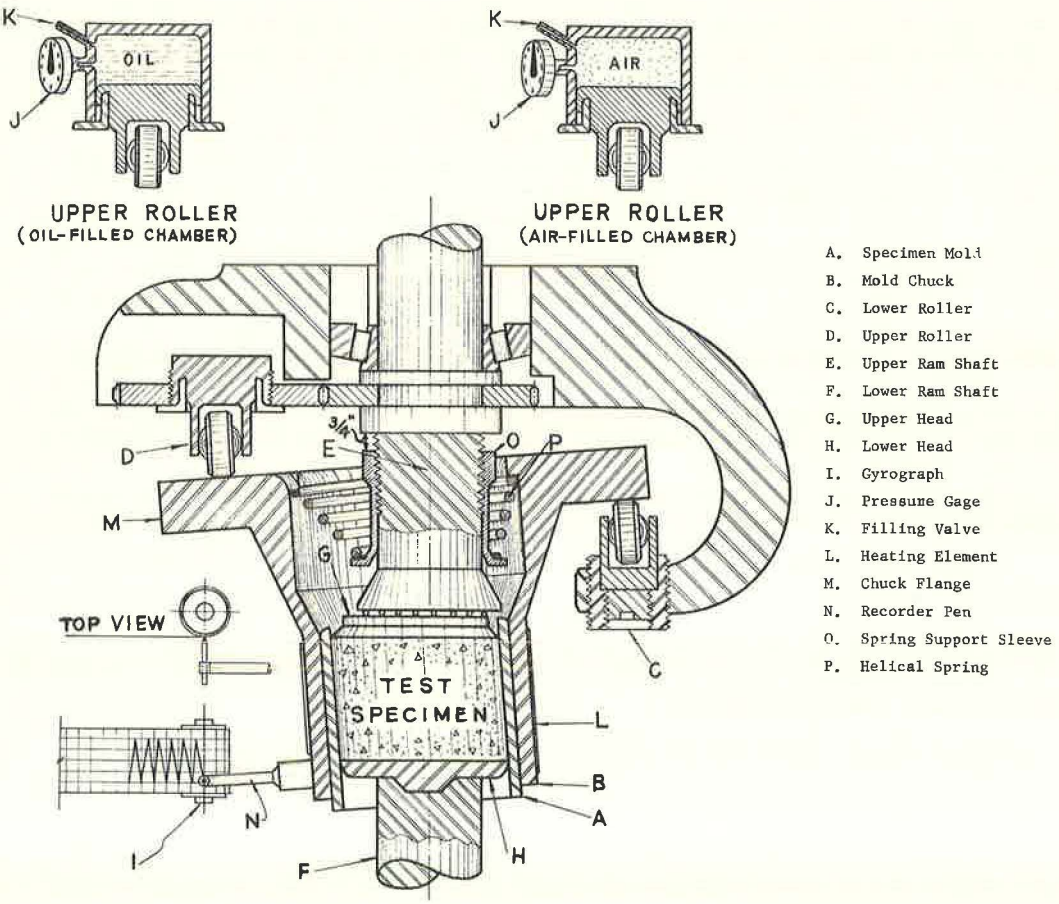

Figure 1. Schematic side view of section through gyrating mechanism (from U. S. Corps of Engineers).

the optimum number of revolutions that must be attained without reducing stability below the acceptable standard.

Normal procedure for setting the angle of gyration is to: (a) insert the sample into the mold chuck, allowing several revolutions to seat the sample; (b) place the upper and lower roller in line with the recording pen; (c) allow sufficient time to record a line on the chart; (d) rotate the rollers 180 deg; and (e) record another line on the chart. If the desired angle was 1 deg, the lower roller would be adjusted until the distance between the two lines was exactly 8 divisions. Each chart division is 7.5 min of angle. It should be remembered that the recorder chart is offset from the center of the mold. The top view of the recorder pen and chart is shown in Figure 1. If the rollers are not aligned properly, the recording pen will indicate a larger angle than actually exists.

When setting large angles of gyration, the sample must have adequate stability to accept the greater load. As previously mentioned, flushing will occur at higher stability when the angle of gyration is increased. Greater difficulty in the setting of accurate and reproducible large angles of gyration may be experienced unless this condition is recognized.

The effect of sample height on the performance of a mixture also must be considered. Kallas (2) reports that heights from 2 1/4 to 2 3/4 in. had no significant effect on the recorded angle of gyration when using a 1-deg and 200-psi setting. Although less likely,

TABLE 1

AGGREGATE GRADATION FOR COMPARATIVE COMPACTION STUDIES

Sieve Size	Passing Sieve (%)	
	1st Series	2nd Series
¾ in.	100	-
½ in.	90	100
⅜ in.	80	95
No. 4	60	65
No. 8	40	45
No. 16	32	32
No. 30	21	-
No. 50	12	14
No. 100	11	8
No. 200	8	4

this may be the case at 2 or even 3 deg. This condition further indicates the lack of sensitivity provided by the gyrograph. Consequently, it is believed that gyrograph widening should be used only as a general guide in the design of asphaltic mixtures.

Another factor of interest is the use of the gyratory testing machine air roller (Fig. 1) for variable strain compaction and testing. This method of operation provides a variable degree of angle kneading which is dependent on the nature of the material (1). Adjustment of the air-roller pressure permits the use of a wide range of strains which are dependent on the initial setting of the angle, air-roller pressure, and the resistance of the specimen. Changes in sample stability are accompanied by changes in the pressure developed in the air roller. If the air-roller pressure is initially set too high, the operation reverts to the fixed-strain condition and flushing will occur without a change in pressure. In this case, the air roller remains in a fixed position and widening of the gyrograph occurs in the same manner as with the fixed roller. The angle of gyration is set by using the fixed roller following established procedures or by using the air roller at high pressures, assuming that the roller is fully extended. The first method is more reliable, but care must be taken to assure that the dimensions of both rollers are the same. A height gage can be used to measure the distance from the roller mount plate to the bottom of the roller. Model 4-C gyratory testing machine rollers should be interchangeable without affecting the angle of gyration.

The maximum recorded angle that can be attained during operation is approximately 5 deg. The actual angle is less than 5 deg since the recorded angle value includes the effect of the recorder pen during operation. As the angle is increased, the neutral axis of the mold chuck raises and displaces the recorder pen upward with respect to the chart. At 5 deg the chuck mold will hit the spring support sleeve near point 0 and the upper portion of the gyrograph will be on the margin of the chart paper. Excessive angles are not normally encountered unless air-roller pressures are being recorded for high levels of strain. Tests of this type may, over a period of time, further restrict the angle of gyration by moving the threaded spring support sleeve downward and hitting the helical spring. The distance between the upper lock rings and the spring support sleeve should be set at ¾ in.

COMPARATIVE COMPACTION STUDIES

A comparative study of gyratory compaction was initiated in 1962 in cooperation with the Asphalt Institute and the U. S. Bureau of Public Roads. The first series of tests utilized material furnished by the Asphalt Institute. The material for the second series was furnished by West Virginia University. The aggregate gradations for these mixtures are given in Table 1. Duplicate samples for each of three different asphalt contents were prepared for each participant by the laboratory furnishing the material. These samples were compacted by the three laboratories using the fixed roller, 100-psi ram pressure, 1-deg angle, and 30 rev plus 3 for leveling. The comparison of the differences in unit weight is given in Table 2.

The first series appeared to give reasonable variation in density values except that the maximum density difference for the average of two samples for each laboratory was approximately twice as large as the difference between the samples compacted at any one laboratory. For example, the maximum density differences for the 4. 5 percent

TABLE 2

DIFFERENCES IN UNIT WEIGHT

Series	% Asphalt[a]	Max. Density Diff. (pcf)	
		Between Labs.	Between Samples[b]
1st	4.5	1.8	0.9
	5.5	1.1	0.5
	6.5	0.1	0.15
2nd	5.66	2.3	2.2
	6.54	0.4	1.2
	7.41	0.3	0.4

[a]By weight of total mix.
[b]At any one lab.

asphalt content specimens from different laboratories was 1.8 pcf, and the difference at any one laboratory was 0.9 pcf. This discrepancy was attributed to variation in the procedure used at each laboratory. The method for setting the angle of gyration and the procedure used in putting the mixture into the mold were considered the major sources of error.

A second series of samples was prepared following a detailed materials handling and compaction procedure. In the second series, the loose material was heated to 250 F for 4 hr and then was transferred into heated compaction molds using a large funnel to allow the mixture to be dumped into the mold without excessive delay. The flat side of a metal spatula was used to press the mixture into the mold so that the funnel could be removed. A 4-in. diameter metal plunger was inserted in the mold and the mix was compressed by hand to provide approximately ½ in. of clearance between the top of the mold and top of the sample. The chuck heater was not used because of the short time required for compaction and the negligible effect of temperature within the normal operating range (2).

The results as given in Table 2 indicate that the variation in density between samples from different laboratories did not exceed that obtained in samples from any one laboratory; in fact, it is considerably smaller for the samples with 7.0 percent asphalt content. Comparison of samples compacted at any one laboratory illustrates that the gradation has a pronounced effect on the uniformity of compaction. The finer grading, as used in the first test series, logically produces more uniform compaction characteristics resulting in less variation in density.

It is not intended that the results or comparisons presented in the previous discussion be considered as applicable to different materials, gradings, or laboratories. The most significant fact is that the gyratory testing machine does provide a method of compaction which will give reproducible results and that the method of sample preparation does influence the obtained results. The latter may be significant when comparing results from more than one laboratory.

FIXED-ROLLER DESIGN

Prior research appears to have been concentrated on the fixed-strain application of the gyratory testing machine using either the fixed roller or the oil-filled roller for compaction. Research by McRae and other personnel at the U. S. Army Engineer Waterways Experiment Station (1) has established gyratory compaction criteria that are essentially equivalent to 50 and 75 blow Marshall compaction, i.e. 100-psi and 200-psi ram pressure, respectively, with a 1-deg angle and 30 rev plus 3 for leveling. With this procedure, the design asphalt content is determined by selecting an asphalt content 0.5 percent below that where flushing occurs as indicated by the widening of

the gyrograph. The design asphalt content selected in this manner provides the maximum unit weight attainable for any specified compactive effort.

Design of bituminous mixtures using this generalized approach may be inadequate since the amount of gyrograph widening necessary to denote a loss in stability or flushing of the mixture is not specified. Another approach to the selection of a design asphalt content is to utilize the gyratory testing machine as a compactor and, for those cases where the gyrograph does not widen appreciably, select the design value on the basis of air voids in the compacted specimen.

Kallas (2) describes a procedure combining both of these approaches for the selection of a design asphalt content. This gyratory design procedure, using the equivalent 50 and 75 blow Marshall compaction for medium and heavy traffic, respectively, defines the design asphalt content as 1 percent less than the critical asphalt content, determined as that asphalt content causing a 14-min increase in the width of the gyrograph. Test results obtained in establishing this criterion indicate that the optimum asphalt contents are essentially the same as those determined by the Marshall and Hveem method of mix design and apparently provide desirable air void contents. Kallas reports that slag aggregate mixtures and open-graded or coarse mixtures did not perform in the same manner as the dense-graded mixtures and are, therefore, excluded from consideration in the design approach.

Studies performed at West Virginia University verify, within certain limitations, the design approach presented by Kallas. Typical results from different materials and gradations are illustrated by the comparative curves of four different mixtures shown in Figures 2 and 3. Table 3 summarizes the values of the design asphalt content selected by the Kallas procedure and by the air-roller design procedure discussed later in this paper. These design asphalt contents were readily determined from the gyrographs with the exception of the slag-sand mixture, TR-9.

An example of the gyrographs (Fig. 4) for mixture TR-1 at 7.5 percent asphalt content shows a uniform width of 13 chart divisions corresponding to a gyratory angle of 1 deg 37.5 min. At 8.5 percent asphalt content, the width of the gyrograph is 15 divisions, which is an increase of 2 divisions or 15 min. Therefore. disregarding the relatively insignificant difference between the 15-min increase and the 14-min increase design criterion, the design asphalt content is 7.5 percent. A close inspection of the three gyrographs for the 8.0 percent asphalt content samples demonstrates the variation in angle that may occur with certain mixtures with the same asphalt content and prepared by identical compaction procedures. The widths of the gyrographs are 14, 13, and 14.5 divisions, respectively. The variation is probably due to slight differences in particle orientation between samples. The density for the second sample is lower than that of the other 8.0 percent asphalt content. It may be considered that the critical asphalt content is found at the point of incipient failure where a slight change in the structural arrangement within the sample creates a notable reduction in one or more of the physical properties.

Variations in the gyrographs of most slag mixtures, especially those that yield a flat density curve throughout a wide range of asphalt content, make it difficult to apply the Kallas design criterion. For example, the gyrograph produced with mixture TR-9 under fixed-roller operation showed variable amounts of widening at sample asphalt contents of 10.0, 10.5, and 11.0 percent. This condition is a direct result of the surface texture, angularity and porosity of the slag aggregate. In addition, mixtures of this type are characterized by high mineral aggregate voids and stability with little effect on the density. Further research may explain the mechanism of slag mixture performance. At present it is logical to assume, from the standpoint of economics and design, that reduction of asphalt content by the addition of fine aggregate (sand, not necessarily slag) will improve the characteristics of the mix so that existing design procedures can be utilized.

The problems associated with the use of the fixed roller in the design of bituminous mixture may be summarized as follows:

1. The fixed-strain method of testing may not be compatible to field compaction because of the sample restraint in the mold;

SIEVE SIZE / MIXTURE NO.	PERCENT PASSING								
	1/2	3/8	4	8	16	30	50	100	200
TR-1 LIMESTONE	100	94	65	47	27	18	11	6	2
TR-7 CRUSHED GRAVEL & OHIO RIVER SAND	100	96	67	43	36	21	8	4	1.5
TR-8 LIMESTONE & L. S. ROCK DUST	100	96	69	47	40	26	14	10	6
TR-9 SLAG & OHIO RIVER SAND	100	97	66	46	37	21	8	4	1.5

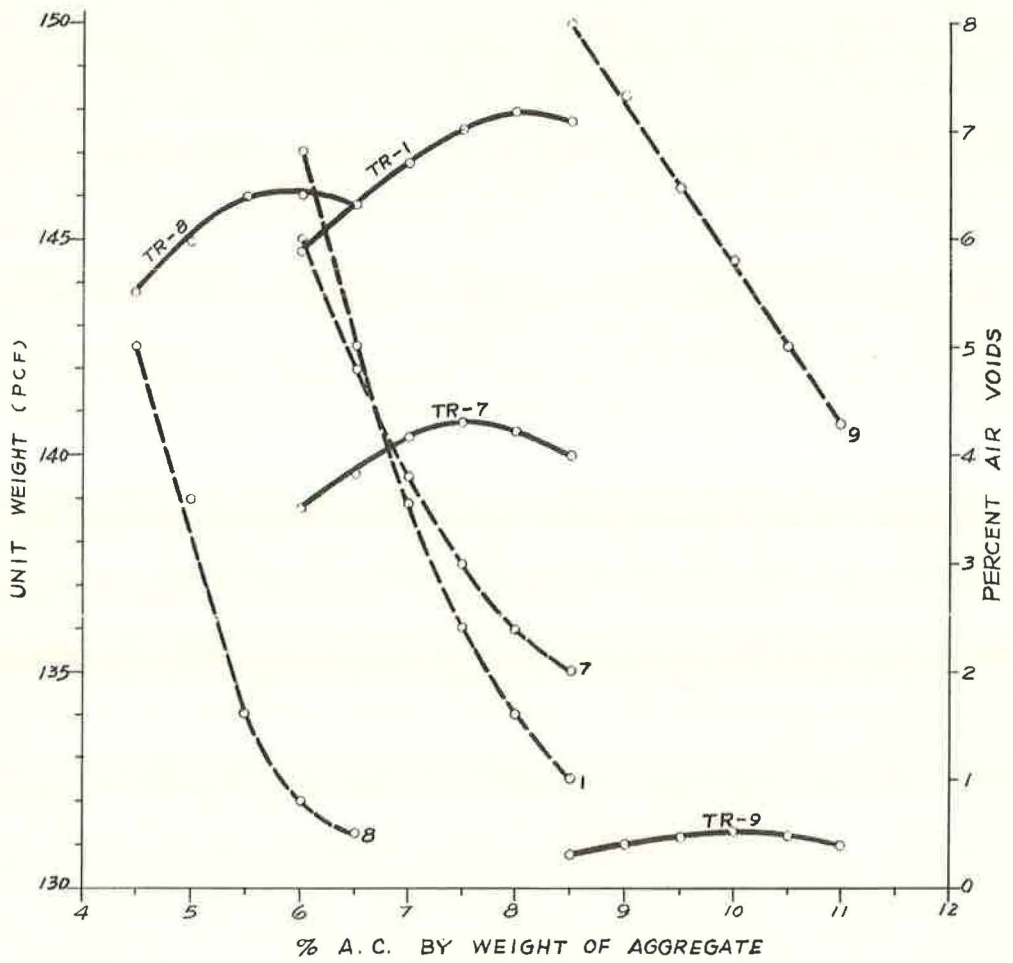

Figure 2.

2. The gyrograph does not provide adequate sensitivity;
3. Widening of the gyrograph to determine the design asphalt content is dependent on material type and gradation and, consequently, does not evaluate the relative stability of different mixtures; and

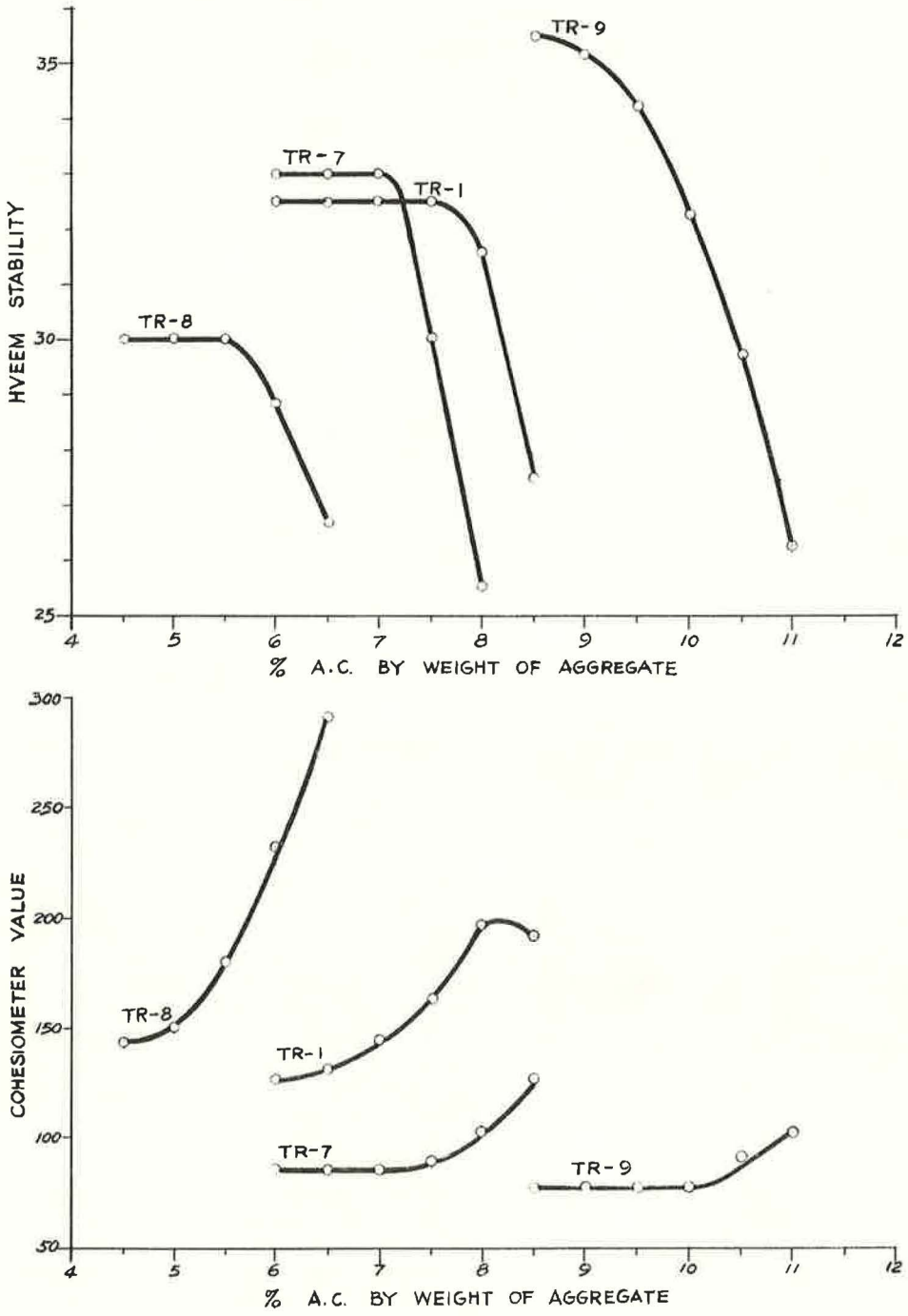

Figure 3.

4. The mechanism of flushing with fixed-strain operation is entirely dependent on the weights of the mold and mold chuck which become more critical as the angle of gyration is increased.

TABLE 3

DESIGN DATA FOR TEST MIXTURES

Mix No.	Design Procedure	Design Asphalt Content[a] (%)	Unit Weight (pcf)	Air Void Content[a] (%)	Min. Agg. Voids (%)	Hveem Stability	Cohesiometer Value
TR-1	Fixed roller	7.5	147.4	2.4	18.7	35	155
	Air roller	6.5	145.7	5.0	19.2	34	130
TR-7	Fixed roller	7.5	140.7	3.0	18.5	30	90
	Air roller	7.2	140.0	3.6	18.4	32.5	85
TR-8	Fixed roller	5.5	146.0	1.5	13.6	30	185
	Air roller	5.0	144.8	3.8	14.6	30	150
TR-9[b]	Fixed roller	11.0	131.0	4.6	25.5	26.5	100
	Air roller	10.5	131.4	5.0	25.2	30	90

[a]All mixtures using 85-100 penetration asphalt cement.

[b]Gyrograph showed 11-min increase in angle at 11.5 percent asphalt content; 12.0 percent asphalt content was not compacted so design asphalt content corresponding to 1 percent below the 14-min increase in angle may be closer to 10.5 percent than to 11.0 percent.

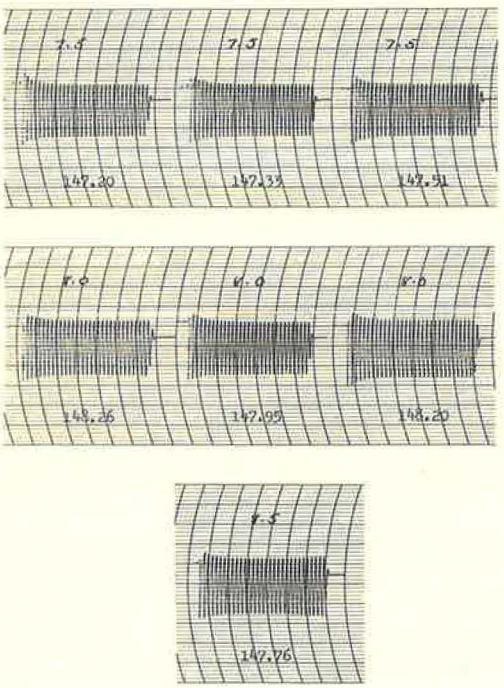

Figure 4. Mixture TR-1 gyrographs.

STUDY OF AIR-ROLLER CAPABILITIES

Application of the air roller for compaction or simulation of traffic has received very little attention in the literature, though it has been suggested that variable strain testing may be a useful tool for these purposes (1). Goode (5) investigated the effect of angle, revolutions, and initial air-roller pressure on the hot-mix compaction of two different aggregate gradations. Busching (4) used the fixed roller for initial compaction and the air roller for secondary compaction. These studies were limited in scope and, consequently, were not used to establish a design procedure.

Air-roller studies at West Virginia University were initiated in 1962. At that time, two possible approaches using the air roller appeared to warrant investigation. The first of these used the air roller to evaluate samples previously compacted by the fixed roller. It was thought that air-roller revolutions would simulate the effect of traffic on the compacted mixture and that some concept of the stability of the mixture under long-time repetitive loading might be obtained. The second approach was based on available field densification data for certain of the mixtures under laboratory study. Since construction compaction does not achieve the same density as obtained in the laboratory, it appeared to be reasonable to compact a sample in the laboratory with the fixed roller

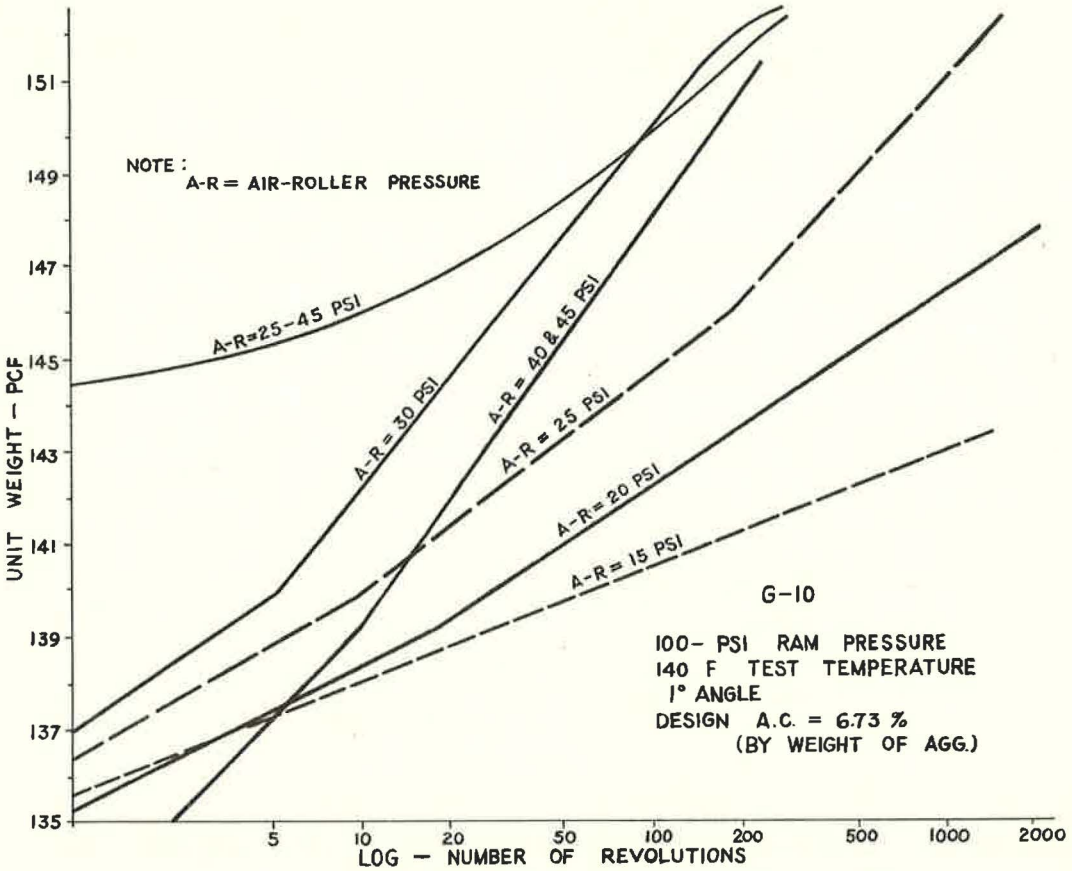

Figure 5. Effect of air-roller pressure on densification and revolutions.

to a density equal to that expected in the field and then to apply air-roller compaction until the density of the sample equaled that obtained in the field after a given length of time.

The two approaches were studied first from the standpoint of the effects of initial air-roller pressure on densification of samples for various numbers of revolutions using a 1-deg angle of gyration. Standard laboratory compacted samples were prepared using fixed-roller compaction with 1-deg angle of gyration, 100-psi ram pressure, and 30 rev plus 3 for leveling. Compaction of samples for duplicating field-compacted densities used the same procedure, except that 4 rev were used instead of 30. All samples were then densified at 140 F using different initial air-roller pressures and varied numbers of gyrations. Bulk specific gravities were obtained for each sample before and after air-roller compaction following the procedure outlined in paragraphs 4a and 4b of ASTM Designation: D 1075. Sample height values obtained during air-roller compaction were used to calculate intermediate densities. The results (Fig. 5) show increasing rates of densification for the low-density samples as the initial air-roller pressure was increased from 15 to 30 psi.

Air-roller pressures of 30 psi and greater produced similar rates of densification. The lateral shift between the 30- and 45-psi lines is attributed to the difference in initial densities. The slight difference in slope may be a direct result of difficulties encountered in measuring the bulk density of low-density samples. During the tests with 30- to 45-psi initial air-roller pressures, there was no discernible air-roller pressure change. Pressure fluctuations were readily observed in tests where the initial air-roller pressure was less than 30 psi. If there is no change in pressure

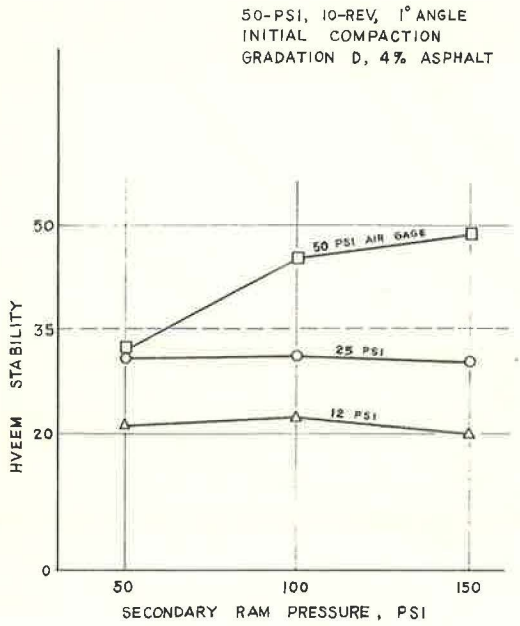

Figure 6. Hveem stability vs secondary ram pressure, air-filled upper roller, 400-rev secondary compaction (4).

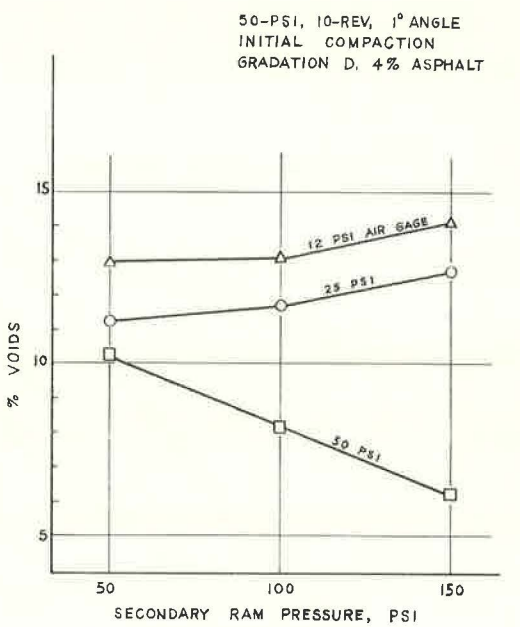

Figure 7. Percent voids vs secondary ram pressure, air-filled upper roller, 400-rev secondary compaction (4).

during air-roller densification, the test is actually a fixed-strain test instead of a variable-strain test. This condition occurs at different initial air-roller pressures, depending on the characteristics and temperature of the mixture.

One of the most significant aspects of Figure 5 is the change in rate of densification at 25-psi air-roller pressure. From 0 to 10 rev there is a tendency to parallel the 15-psi densification curve, between 10 and 200 rev to parallel the 20-psi curve, and above 200 rev to parallel the 30- to 45-psi curve. These changes are the result of the combined effects of changes in air-roller pressure which directly influence the angle of gyration and the characteristics of the mixture at different densities. At low initial air-roller pressures, the angle of gyration, as recorded on the gyrograph, was very small, indicating that the strain was also small. With this condition a great number of revolutions would be necessary to achieve any appreciable densification. At high initial air-roller pressure, the strain was so great that there were no observable air-roller pressure changes as the number of revolutions increased. With this condition, the test was essentially one of fixed strain. The 25-psi initial air-roller pressure was apparently of the right order of magnitude, for the mixtures and test conditions used, to produce increasing densification and resistance to strain with increasing numbers of revolutions and to reflect these increases with observable changes in the air-roller pressure. It was tentatively concluded, therefore, that the range of strain through which changes in the physical characteristics of the test mixture could be observed most readily could be obtained best with an initial air-roller pressure of 25 psi for initial angles of gyration of 1 deg.

Results obtained by Busching (4) further illustrate some of the effects of air-roller densification (Figs. 6 and 7). Busching concludes:

> These figures indicate that for a constant ram pressure stability is a function of the angle of gyration. It appears that densities and stabilities produced by air-filled roller compaction would be equivalent to those produced by fixed-roller compaction provided air pressures were high enough.

Tests performed on high-density samples showed similar rates of densification at air-roller pressures of 25 to 45 psi. Samples 1 and 2 (Fig. 5) illustrate the typical densification curves obtained for this range of pressures. The rate of densification above 100 rev is about the same as that obtained with low-density samples tested at 25 and 30 psi.

It should be mentioned that similar tests performed on this mixture at different asphalt contents did not show an appreciable difference in rates of densification. It is difficult to identify such changes because the initial density varies with asphalt content.

DEVELOPMENT OF TENTATIVE AIR-ROLLER DESIGN PROCEDURE

The results obtained in the study of air-roller capabilities clearly demonstrated that stability and rate of densification are dependent on the magnitude of strain for constant ram pressure, revolutions, and mixture type. If two mixtures of different stability-densification characteristics are tested at an initial angle of 1 deg and an air-roller pressure of 25 psi, for example, it would be possible for the high-stability sample to resist further densification so that no change in stability would occur. The low-stability sample may respond to air-roller densification and indicate trends in stability with increasing revolutions. Therefore, the problems associated with the air-roller testing procedure are twofold and may be stated as follows:

1. The 1-deg initial angle of gyration is not adequate to produce variable strains of sufficient magnitude to overcome the high resistance of certain mixtures without the increased use of air-roller pressure. If the air-roller pressure is increased to a satisfactory level for these mixtures, the testing of low-resistance mixtures will be essentially a fixed-roller test.
2. The change in angle, even if the angle is reduced from 1 to 0 deg, does not produce a large change in air-roller pressure. Therefore, the measurement of the angle of gyration by either air-roller pressures or gyrograph is not sufficiently sensitive for observing changes in the physical characteristics of a sample during densification.

A study was initiated for the purpose of minimizing these undesirable effects. The same mixture that was used in the previously described air-roller tests was compacted to a low density by fixed-roller compaction at a 1-deg angle of gyration. These samples were heated to 140 F and tested with initial angles of gyration of 2 and 3 deg, using air-roller pressures of 15, 20, and 30 psi for the 2-deg tests and 5 to 10, 15, and 20 psi for 3-deg tests. (The air-roller pressure gage was graduated in 5-psi increments so that precise settings or readings could not be obtained.) The results of this study showed that for the 3-deg angle of gyration, even with air-roller pressures as low as 5 to 10 psi, a minimum angle of approximately 2 deg was maintained during the initial stages of densification and an extreme increase in angle occurred within a short period of time. These tests were stopped when the mold chuck started hitting the spring support sleeve and the gyrograph indicated an angle of gyration of approximately 5 deg. At this point in the test, the top of the gyrograph was in the upper margin of the chart and the air-roller pressure for the initial setting of 5 to 10 psi was 27 psi. The undesirable aspects of the 3-deg test are as follows:

1. The air-roller pressure did not drop to the original setting before the capabilities of the gyratory testing machine were exceeded; and
2. Low-stability mixtures would be subjected to excessive strain (angle of gyration).

The first statement suggests that lower air-roller pressures at a 3-deg angle of gyration may alleviate the problem. It is not practical, however, to use an initial pressure of 0 psi since it is virtually impossible to attain a reliable setting. The frictional resistance and effectiveness of the seal in the pneumatic cell would likewise prevent the use of very low pressures. Also, it is apparent that the contact pressure on the chuck flange, for a given angle of gyration, must be adequate to prevent premature overstraining of the sample.

The second statement suggests that the angles of gyration would be in excess of 2 deg for low-stability mixtures and the samples would not exhibit normal stability or

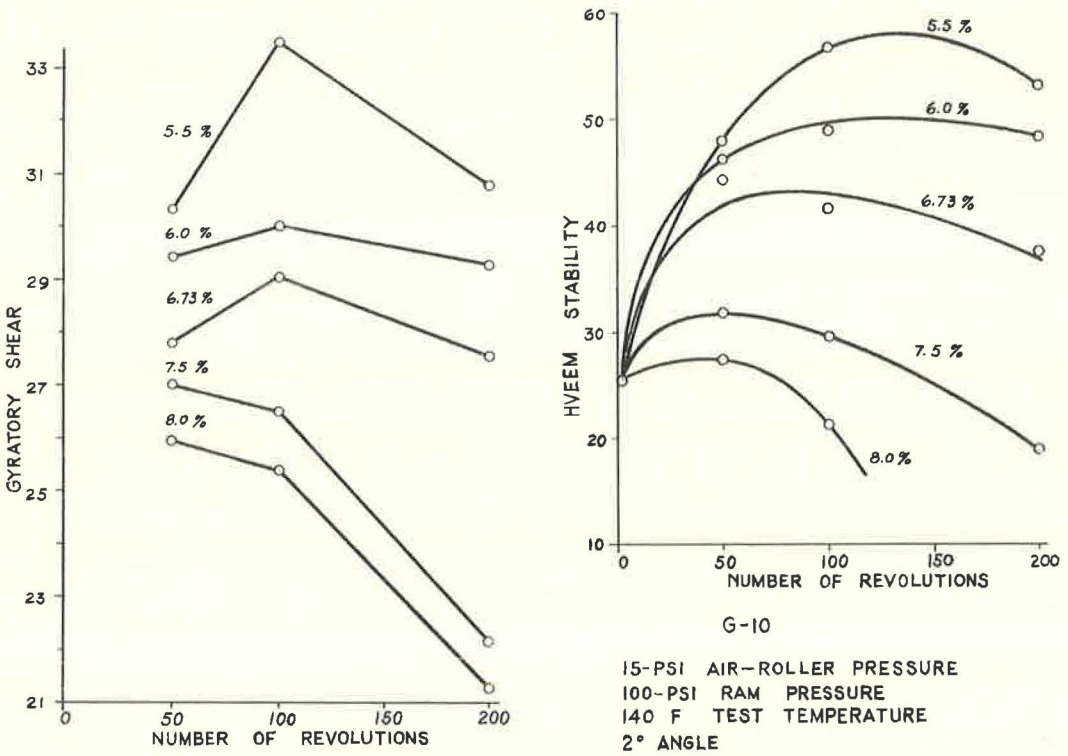

Figure 8. Stability vs revolutions for different asphalt contents.

densification characteristics. In studies performed by the U. S. Corps of Engineers (1), the following observation was made:

> Increase in gyration angle from 1 to 2 degrees causes an increase in both unit weight and stability, and an increase in angle beyond 2 degrees causes a decrease in both unit weight and stability.

This pertinent characteristic may be either a benefit or a hindrance in air-roller testing of bituminous mixtures. If, as indicated, the strain remains excessive throughout the test, the results probably are not representative of conditions existing in the field. If the strain never exceeds 2 deg, assuming a static condition where density and stability remain constant, the test is valueless because no change in mixture characteristics can be observed. Somewhere between these two extremes lies the optimum or most desirable testing procedure.

The results of the 2-deg angle of gyration tests indicated that air-roller pressures of 15 or 20 psi appeared to give the largest range in pressure variation throughout a given increase in density. It was decided to use the 2-deg angle of gyration and an air-roller pressure of 15 psi for the testing of different mixtures. It should be emphasized that the observed angle of gyration is produced by the combined effect of air-roller pressure and the force exerted by the weight of the chuck at that particular angle.

The first tests using this concept were made on mixture G-10 which was the same as used in earlier air-rolling testing. Correspondence from J. L. McRae (6) provided information that was utilized in all air-roller studies. McRae suggested the use of a gyratory shear value to indicate stability. This parameter is defined as follows:

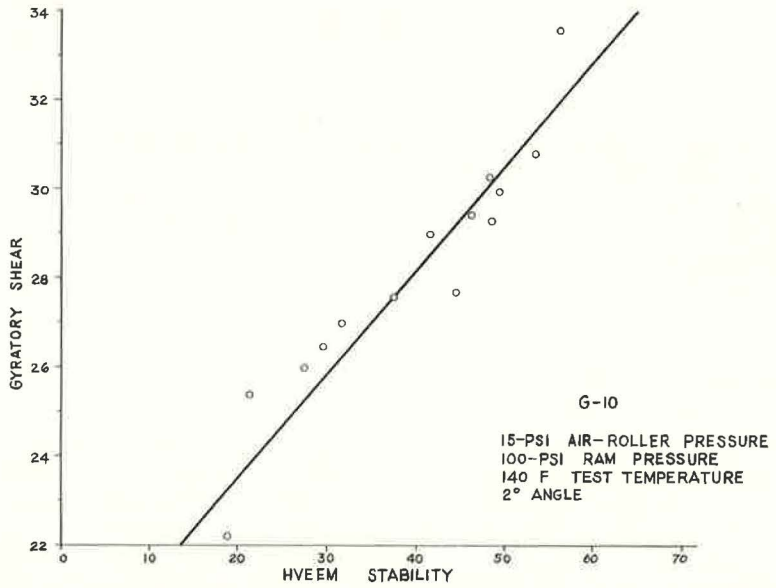

Figure 9. Gyratory shear vs Hveem stability.

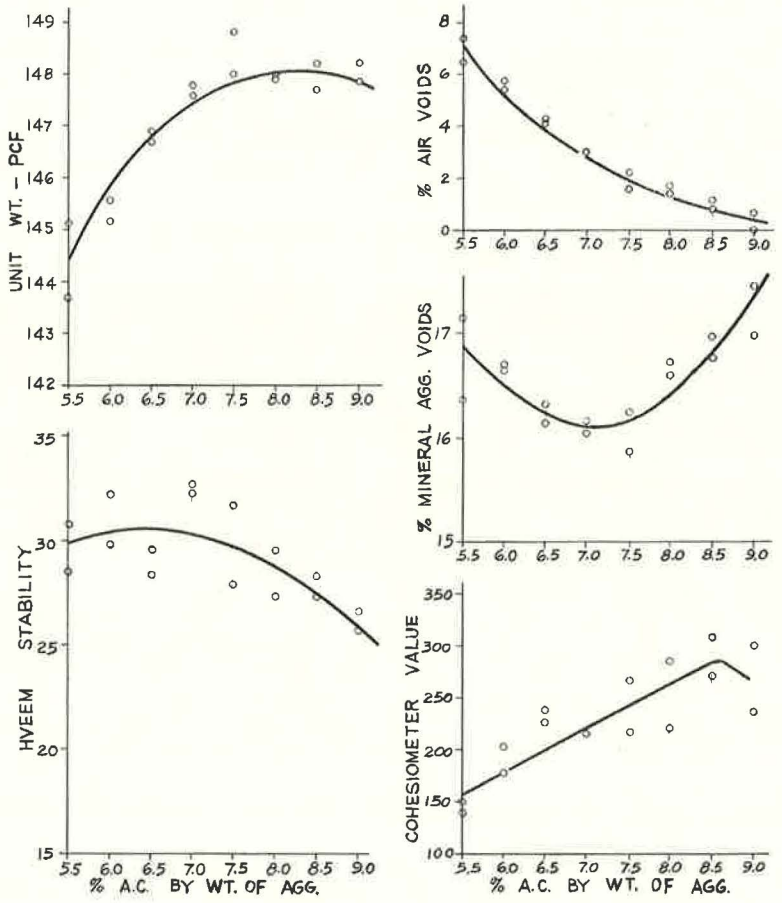

Figure 10. Mixture G-12 results.

$$G_S = \frac{P \cdot L}{V} \quad (1)$$

where

P = load in upper roller (lb) = effective area of upper roller times unit pressure, p, on upper roller = 5.28 × p;
L = distance from center of sample to center of roller = 5 in.;
V = volume of sample = area times height, H = 12.56 × H; and

$$G_S = \frac{5.28 \times p \times 5}{12.56 \times H} = \frac{2.1p}{H},$$

where

p = roller pressure (psi), and
H = height of samples (in.).

The results of the G-10 series (Fig. 8) showed a remarkable similarity between plots of gyratory shear and stability vs number of revolutions. In both cases, the relative order of magnitude of stability values is the same for the different asphalt contents. At the 7.5 percent asphalt content, gyratory shear and stability values do not exceed 27.0 and 32.0, respectively. Comparisons of G_S and stability values (Fig. 9) indicate a reasonably good correlation. Unfortunately, further tests on higher stability mixtures were not satisfactory because the strain was not sufficient to produce changes beyond a certain stability level even though the samples were run for 250 rev. This implied that a higher level of strain was needed to facilitate testing of all mixtures within a reasonable period of time.

The air-roller pressure was increased to 20 psi for all subsequent testing and appeared to yield better results throughout a wide variety of mixtures. In an effort to improve the accuracy of pressure measurements, a 3-in. pressure gage, reading directly to 0.2 psi, was installed on the air-roller cell. Pressure readings were easily estimated to 0.1 psi with this gage. The procedure used in evaluating the different mixtures is briefly outlined as follows:

1. Two or three samples were compacted at each asphalt content using the fixed roller, 1-deg angle of gyration, 100-psi ram pressure, and 30 rev plus 3 for leveling. The upper limit in asphalt content was based on flushing as indicated by the gyrograph. These samples were then evaluated for density, stability, cohesiometer value, air void content, and mineral aggregate voids. The data were plotted and the design asphalt content determined from the curves by Hveem medium traffic criteria with due consideration given to a desirable range of air void values. Mixture G-12 (Fig. 10) illustrates the typical curves obtained from the testing procedure.
2. After the compaction of samples in the first step, three or four different asphalt contents were selected and eight samples were compacted for each asphalt content using fixed-roller compaction. These samples were extruded for density determination and were reinserted into the mold for air-roller testing at 140 F. The samples were ranked from low to high density for each asphalt content.
3. The angle of gyration was adjusted for 2 deg using the fixed roller before installing the air roller. The air-roller press was set at 20 psi. The lowest density sample was densified for 10 rev and succeeding higher density samples were densified by greater numbers of revolutions to eliminate some of the variation in test results that would otherwise occur with random sample selection. Sample heights and air-roller pressures were recorded on the data sheet (Fig. 11) for each specified number of revolutions. Readings were obtained by stopping the gyratory testing machine at the desired number of revolutions. Density, stability, and cohesiometer values were determined for each sample. Average gyratory shear and stability values vs revolutions were plotted (Figs. 12 and 13) for comparison.

Six different gradations, as shown in Table 4, were compacted following this procedure. Curves of stability vs number of revolutions for the mixtures illustrate definite trends with increasing asphalt content. At low asphalt contents, stability values con-

GYRATORY AIR-ROLLER DENSIFICATION DATA SHEET

Gradation: G-12 Date 8-9-63

Angle of Gyration 2 ° Ram Pressure 100 psi

Sample Number	A.C.%		Revolutions 0	10	25	50	100	150	200	250	350		Hveem Stability
7	6.5	Press.	20	34.8									
		Ht.	2.587	2.532									
		G_s	—	28.86									34.05
2	6.5	Press	20	33.8	33.6								
		Ht.	2.576	2.519	2.487								
		G_s	—	28.18	28.35								37.76
5	6.5	Press.	20	34.0	33.4	33.6							
		Ht.	2.591	2.539	2.510	2.480							
		G_s	—	28.12	28.36	28.45							39.08
6	6.5	Press	20	33.3	33.0	32.8	32.8						
		Ht.	2.576	2.528	2.500	2.472	2.457						
		G_s	—	27.66	27.72	27.86	28.26						41.97
4	6.5	Press.	20	33.7	33.8	33.90	33.7	33.7					
		Ht.	2.566	2.519	2.490	2.463	2.431	2.410					
		G_s	—	28.09	28.51	28.46	29.11	29.37					46.84
1	6.5	Press.	20	33.8	32.5	32.3	32.0	31.8	31.3				
		Ht.	2.535	2.505	2.473	2.450	2.406	2.384	2.368				
		G_s	—	28.34	27.60	27.72	27.93	28.01	27.76				50.45
3	6.5	Press.	20	32.7	32.5	32.5	32.0	31.4	31.2	30.5			
		Ht.	2.548	2.516	2.485	2.456	2.421	2.400	2.385	2.373			
		G_s	—	27.24	27.46	27.74	27.76	27.91	27.47	26.99			51.75
8	6.5	Press.	20	32.0	31.8	31.7	31.7	31.3	30.8	30.1	28.2		
		Ht.	2.553	2.505	2.478	2448	2.414	2.394	2.379	2.369	2.353		
		G_s	—	26.83	26.45	27.19	27.59	27.96	27.19	26.68	25.17		43.96
Average G_s				27.42	27.85	28.04	28.13	28.19	27.47	26.84	25.17		

Figure 11.

tinued to increase with densification throughout the test range of number of revolutions. With increased asphalt content, the stability values increased with densification to a critical density. Additional revolutions beyond this point produced a continuous reduction in stability. In general, stability and the number of revolutions to achieve maximum stability decreased with increased asphalt content. It was assumed that the peaks defined a satisfactory condition before failure of the mixture. The number of revolutions for each peak was used to obtain the corresponding gyratory shear value. Table 5 summarizes the data obtained in this fashion. A gyratory shear value of 27.0 was considered indicative of a strain condition immediately before failure for those mixtures tested.

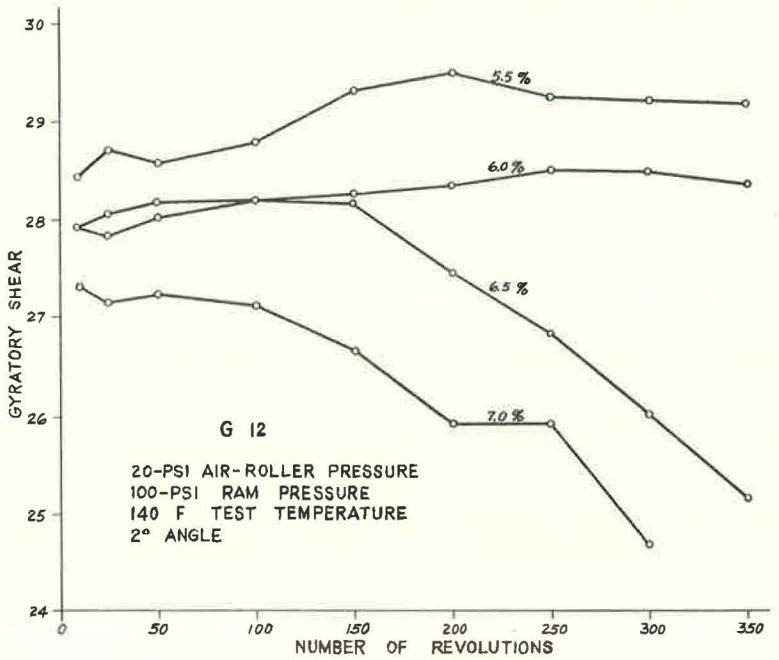

Figure 12. Gyratory shear vs revolutions.

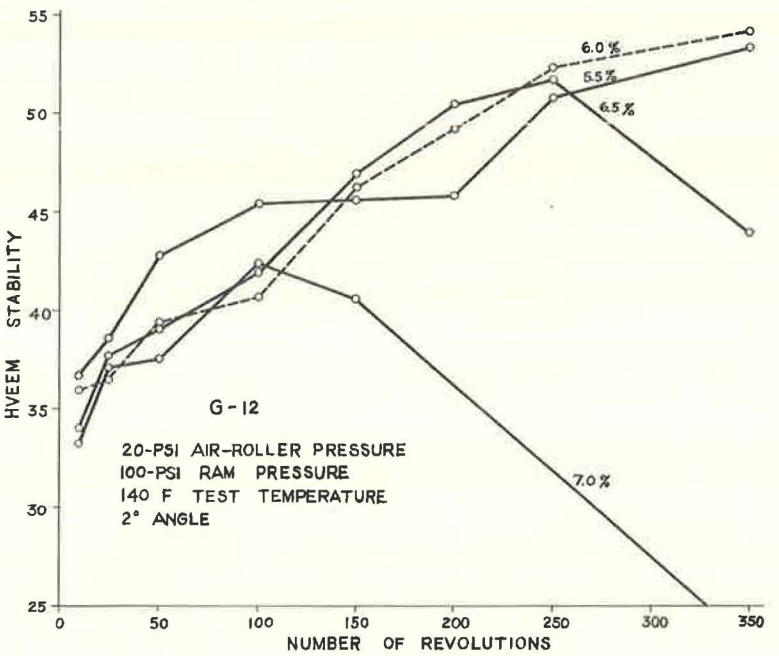

Figure 13. Hveem stability vs revolutions.

TABLE 4

Mixture	Passing Sieve (%)								
	½ In.	⅜ In.	No. 4	No. 8	No. 16	No. 30	No. 50	No. 100	No. 200
G-12	100	95	65	40	25	-	8	5.2	3
G-50	100	96	67	53	37	-	17	10.6	6
G-75	100	98	84	75	53	37	23	13.6	7
R-1	100	90	67	50	37	-	16	12.0	8
S-1	100	92	65	45	30	22	12	5.8	4
S-2	100	92	65	45	35	26	18	14.3	10

TABLE 5

Mixture	Values at Peak of Curve			Hveem Std. Gyratory Compaction			
	Asphalt Content (%)	Hveem Stability	No. Rev	Corresponding Gyratory Shear (G_S)	Design Asphalt Content	% Air Voids	No. Rev at G_S = 27.0
G-12	6.5	53	250	26.8	6.5	4.0	250
	7.0	45	100	27.2			
G-50[a]	7.5	49	150	28.5	8.0	5.8	200
	8.0	51	200	27.2			
G-75[a]	10.0	45	100	26.3	-	-	-
	11.0	43	125	27.5			
R-2	5.5	36	25	27.0	5.0	4.0	125
	6.0	28	10	27.0			
S-1	9.5	44	150	27.0	9.0	3.4	350
	10.0	44	50	26.8			
S-2	6.5	48	200	26.8	7.0	4.6	50
	7.0	38	50	26.5			
Avg.	-	-	-	27.05	-	-	195

[a]Revolutions increase with asphalt content for peak values; this phenomenon appears to be unique with the limestone-slag sand mixtures.

The next step in the analysis was to determine the number of revolutions to define the desired asphalt content corresponding to that established by Hveem design criteria using fixed-roller compaction. Numerous problems arise when one attempts to obtain design asphalt contents using gyratory rather than kneading compacted samples. Although the densities obtained by both methods of compaction may be about the same, the stability values are not similar for certain mixtures. Busching reports (4) an instance of a mixture giving inadequate stability when prepared by kneading compaction but showing a definite increase in stability when prepared by gyratory compaction and densified by 400 rev with the air roller.

Variability in data and selection of a design asphalt content further complicate the problem. Therefore, although the numbers of revolutions given in Table 5 show extreme variability, an arbitrary value of 200 rev was selected to define the point at which the sample would be evaluated. Limited studies of other mixtures indicate that this is a reasonable value for the mixtures and test conditions used in this study.

APPLICATION OF TENTATIVE AIR-ROLLER DESIGN PROCEDURE

During a period of 2 years, only limited information could be obtained on the field-compacted densities and the effect of traffic densification for typical asphaltic concrete surfacing mixtures in West Virginia. The need for test roads was apparent, but a test road program was complicated by the wide variety of aggregate types and combinations in use. The use of different construction projects for different materials was not desirable because time, location, and traffic variables would be introduced.

This problem was solved through the joint efforts of the West Virginia State Road Commission and the U. S. Bureau of Public Roads. A test road site was selected near Beckley, W. Va., on a 3-mi section of new construction of W. Va. 54. One 12-ft lane, 3 mi long, was subdivided into fourteen 1,200-ft sections with the surfacing for each section consisting of a different design mixture. Design asphalt contents for the ten sections to be used were determined by the tentative air-roller design procedure described earlier in this paper. The asphalt contents used in the remaining four sections were established by the West Virginia State Road Commission. Design asphalt contents were obtained from the gyratory shear vs numbers of revolutions curves (Figs. 14 to 23, Table 6) by interpolating between the two asphalt contents bracketing the design criterion (G_S = 27.0 at 200 rev).

The design of the slag and silica sand mixture, TR-9, did not follow the defined procedure. The TR-9 mixture (Fig. 21) maintains approximately the same value of gyratory shear for the different asphalt contents up to 200 rev. This condition is typical of slag mixtures having a low percentage of fines. The 10.5 percent design asphalt content was selected for this mixture even though the G_S value did not exceed 26.7 at 200 rev. Lower asphalt contents developed G_S values in excess of 27 and maintained this level of stability well beyond the 200-rev point.

Six of the test road mixtures were compacted at the design asphalt content and tested by the air roller as a check on the design. The results showed excellent reproducibility with the exception of mixtures TR-7 and TR-10. Time limitations prevented further investigation of these discrepancies before the test road construction. A review of G_S values for the different mixtures indicated that the variability for TR-7 and TR-10 was much larger than that for the other mixtures. Although air void content is not considered in this design procedure, it is of interest to note that it varied from 2.4 to 6 percent (Table 3) for samples compacted at the design asphalt content by standard fixed-roller procedures which provide the reference level for field compaction.

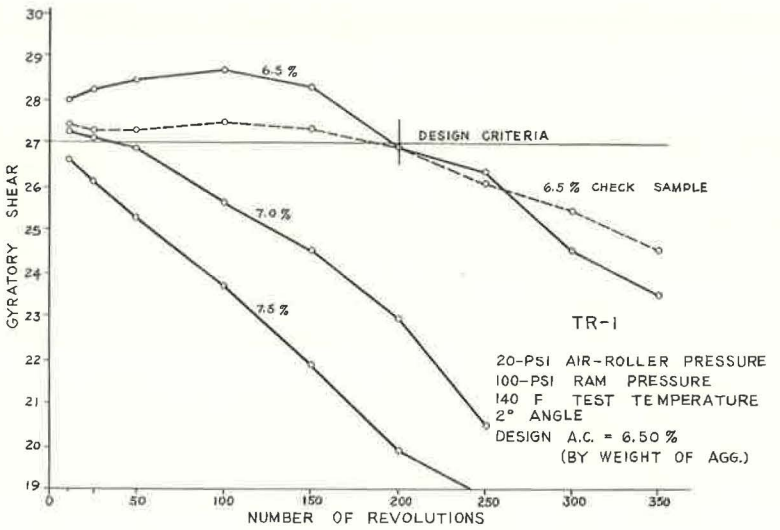

Figure 14. Gyratory shear vs revolutions.

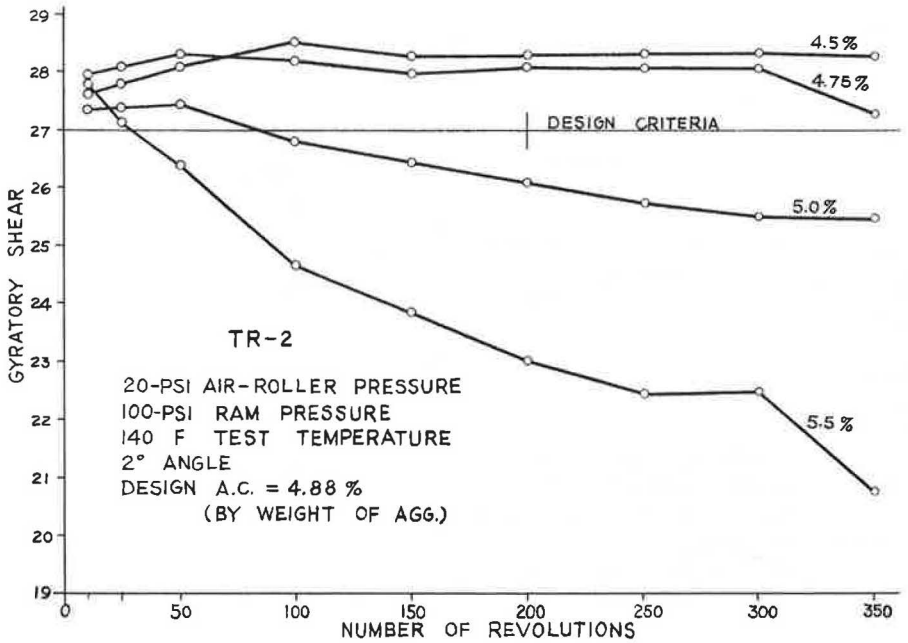

Figure 15. Gyratory shear vs revolutions.

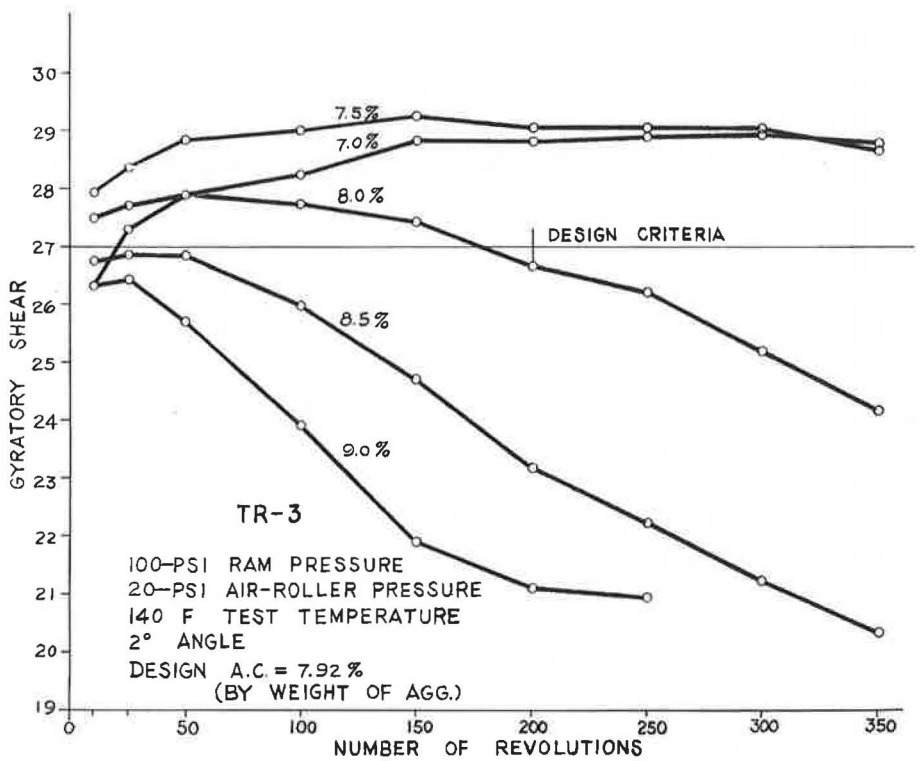

Figure 16. Gyratory shear vs revolutions.

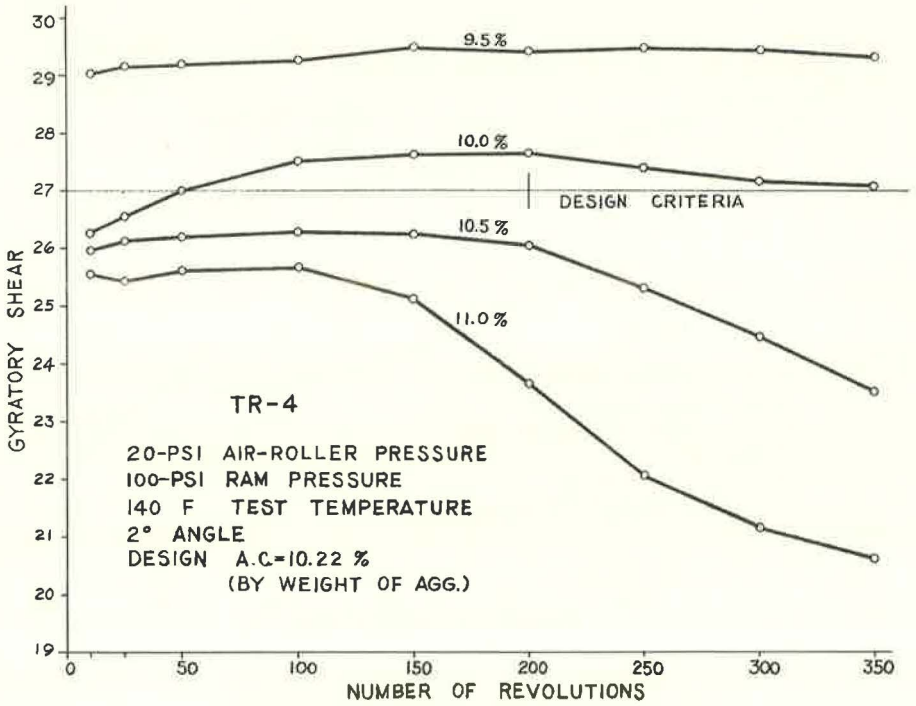

Figure 17. Gyratory shear vs revolutions.

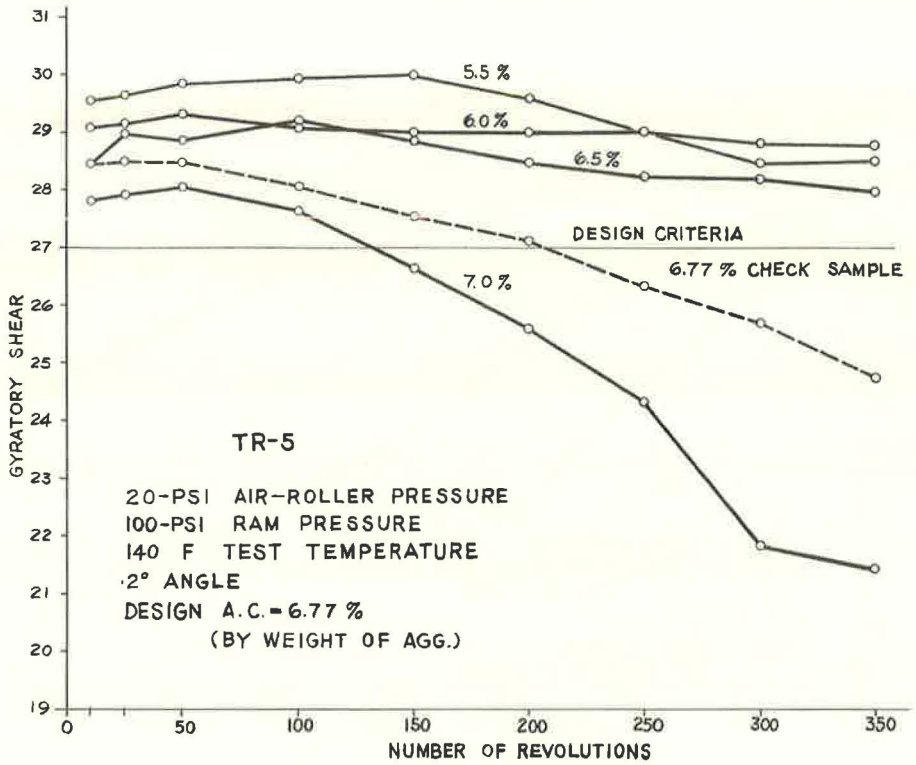

Figure 18. Gyratory shear vs revolutions.

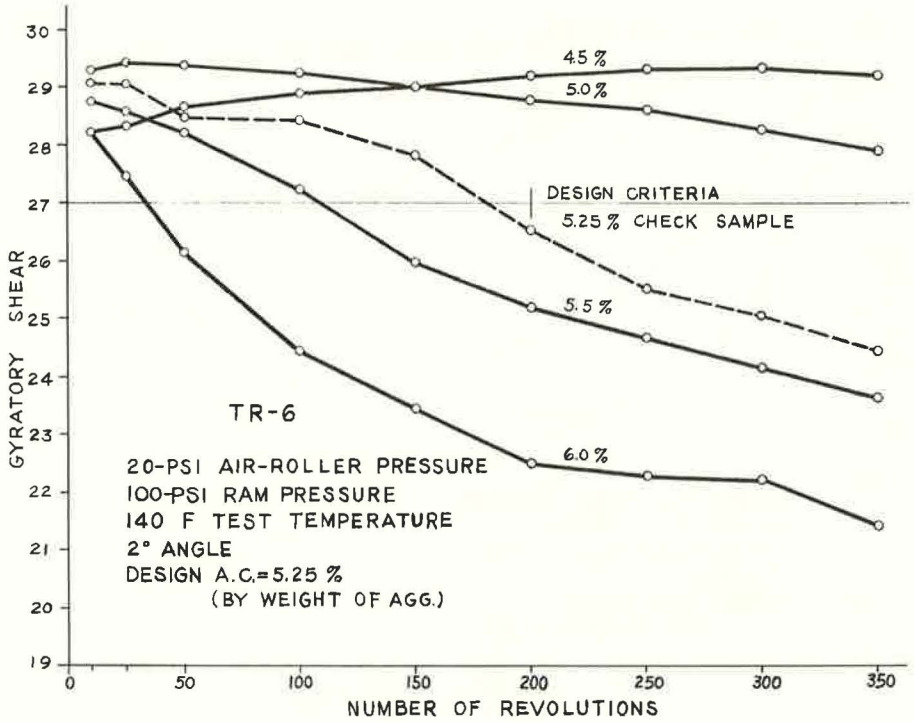

Figure 19. Gyratory shear vs revolutions.

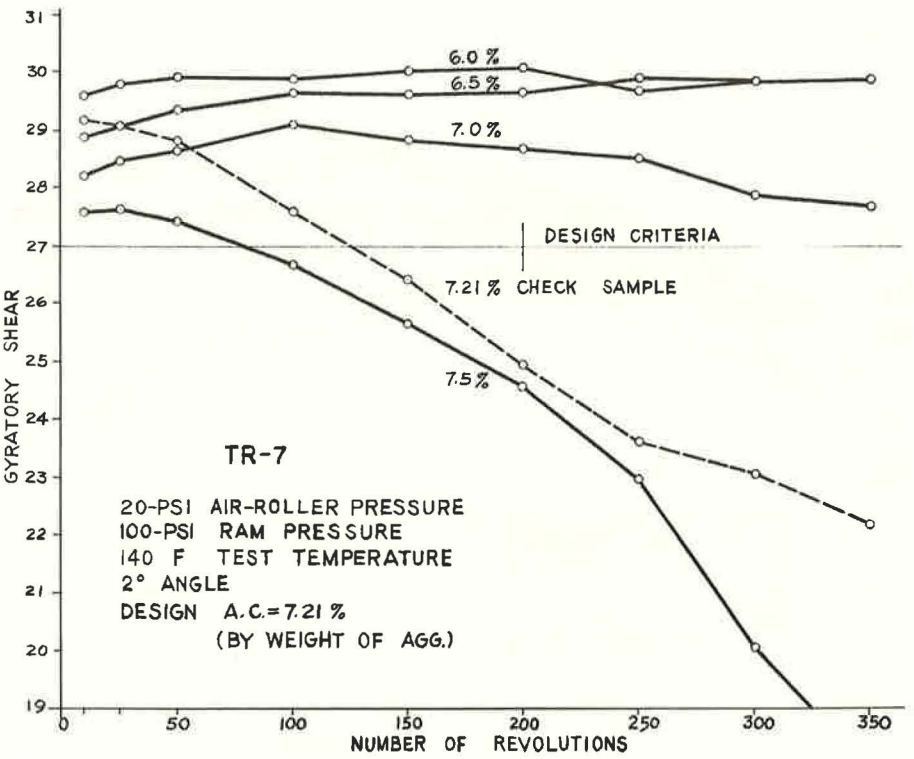

Figure 20. Gyratory shear vs revolutions.

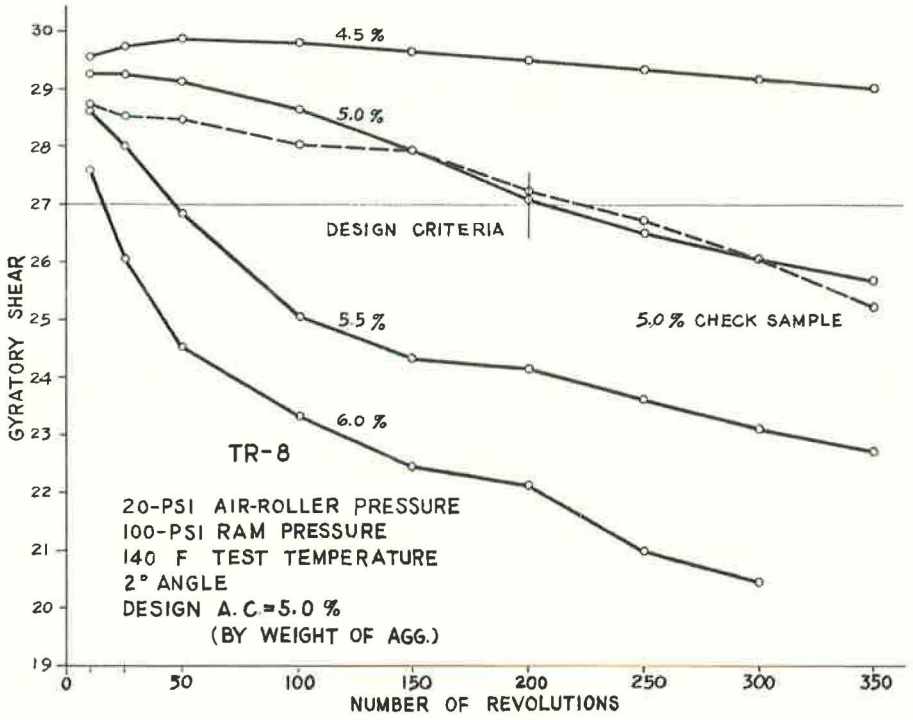

Figure 21. Gyratory shear vs revolutions.

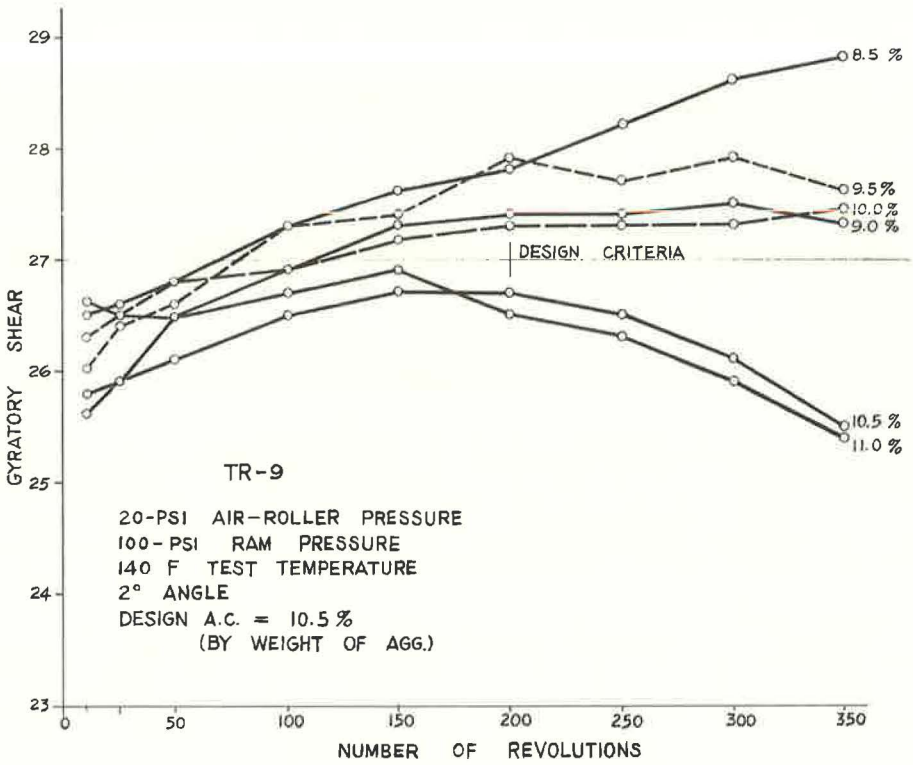

Figure 22. Gyratory shear vs revolutions.

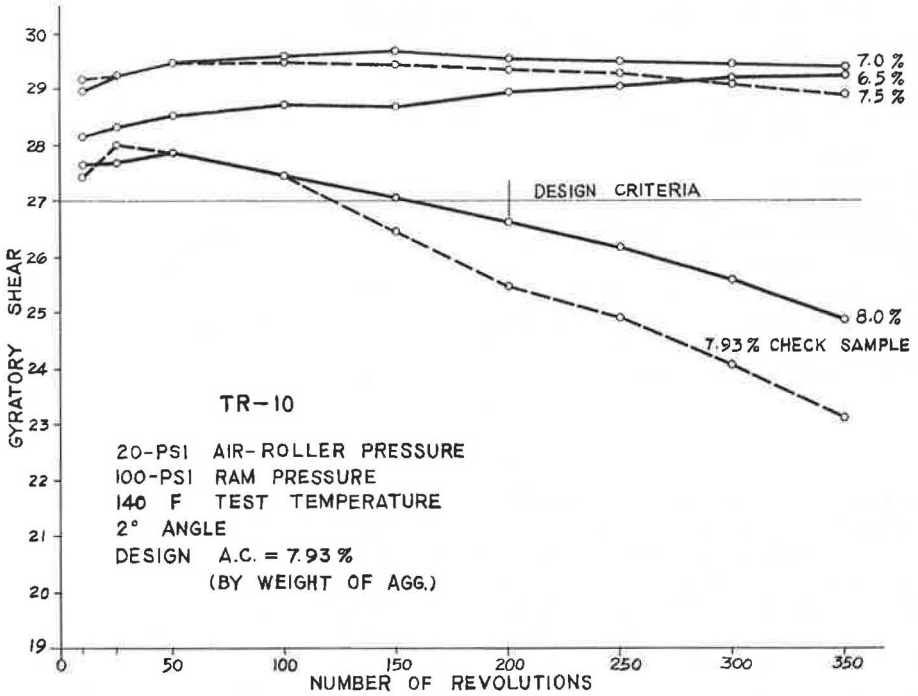

Figure 23. Gyratory shear vs revolutions.

TABLE 6
GRADATIONS FOR TEST ROAD MIXTURES

	Mixture	Passing Sieve (%)								
		½ In.	⅜ In.	No. 4	No. 8	No. 16	No. 30	No. 50	No. 100	No. 200
TR-1	No. 12 limestone, L. S. sand	100	94	65	47	27	18	11	6	2
TR-2	No. 12 limestone, L. S. sand, L. S. rock dust	100	94	67	50	31	23	16	11	6
TR-3	45% No. 12 L. S., 50% No. 13 slag, 5% L. S. rock dust	100	95	67	53	37	25	17	11	6
TR-4	20% No. 12 L. S., 75% No. 13 slag, 5% L. S. rock dust	100	98	84	75	53	37	23	14	7
TR-5	No. 12 limestone, silica sand	100	96	68	45	35	20	8	4	2
TR-6	No. 12 limestone, silica sand, L. S. rock dust	100	96	70	49	39	25	14	9.7	6
TR-7	No. 12 gravel, silica sand	100	96	67	43	36	21	8	4	1.5
TR-8	No. 12 gravel, silica sand L. S. rock dust	100	96	69	47	40	26	14	10	6
TR-9	No. 12 slag, silica sand	100	97	66	46	37	21	8	4	1.5
TR-10	No. slag, silica sand, L. S. rock dust	100	98	74	56	46	32	15	8.6	6

Little difficulty was experienced in the compaction of the test road mixtures during construction. One of the most interesting situations encountered during construction was in the hauling and compaction of mixture TR-9. This mixture was so fluid that the load shifted in the truck bed on curves and slopped over the tail gate when the trucks accelerated. The laying and rolling operations were not significantly hindered by this fluid condition.

Outwardly it appears that the designed mixtures were adequate from the standpoint of field construction, but only time will determine the suitability of these mixtures and the adequacy of the design procedure. Roller pass, air permeability, nuclear density, and temperature data were obtained for each section during construction of the road. Cores of the compacted materials and samples of the loose mixtures were obtained for laboratory testing. Laboratory studies and observation of the test road will be continued to provide data on traffic densification for future use in conjunction with air-roller testing and to evaluate the performance of the various mixtures under field conditions.

PROPOSED STUDIES

The ever-increasing need for better methods to evaluate highway materials rationally has resulted in the continual development of new equipment and procedures. Research is needed to develop the necessary methodology and equipment for identifying, both quantitatively and qualitatively, the important parameters which govern the performance of asphaltic mixtures. The gyratory testing machine is relatively new. It is felt that the potential of this equipment has not been fully realized and that it offers an excellent tool for further detailed studies of the mechanism of mixture performance.

The authors suggest that future use of the gyratory testing machine, particularly with the air roller, may include the following applications: (a) to simulate field construction compaction, (b) to simulate traffic densification, (c) to evaluate effects of binder viscosity, (d) to evaluate effects of aggregate surface texture, (e) to evaluate effects of mineral filler-asphalt ratios, (f) to evaluate effects of grading, and (g) to act as an accelerated serviceability test.

It is not intended to imply that all of these problems listed can be satisfactorily solved by the gyratory testing machine. This list is merely intended to illustrate the wide variety of problems that appear suitable for study with the gyratory equipment.

ACKNOWLEDGMENTS

The authors wish to express their appreciation for the efforts and invaluable assistance provided by personnel of the West Virginia State Road Commission. In particular, Mark Fara, former Research Coordinator and R. T. Hughes, Materials Control Engineer, should be commended for their assistance in the planning of the test road and in the control of plant production. The comments and suggestions offered by personnel of the U. S. Bureau of Public Roads were especially helpful in the research study.

REFERENCES

1. Development of the Gyratory Testing Machine and Procedures for Testing of Bituminous Paving Mixtures. U. S. Army Engineer Waterways Experiment Station, Vicksburg, Miss., Tech. Rept. No. 3-595, 1962.
2. Kallas, B. F. Gyratory Testing Machine Procedures for Selecting the Design Asphalt Content of Paving Mixtures. Paper presented at 1964 Ann. Mtg. AAPT.
3. Busching, H. W., and Goetz, W. H. Use of a Gyratory Testing Machine in Evaluating Bituminous Mixtures. Highway Research Record No. 51, pp. 19-43, 1964.
4. Busching, H. W. Stability Relationships of Gyratory-Compacted Bituminous Mixtures. M.S.C.E. thesis, Purdue Univ., 1963.

5. Goode, J. F. Unpub. report to Highway Research Board Committee on Mechanical Properties of Bituminous Paving Mixtures, Department of Materials and Construction, 1964.
6. McRae, J. L. Personal correspondence, Dec. 4, 1961.
7. Ortolani, Lawrence, and Sanberg, Harry A., Jr. The Gyratory Method of Molding Asphaltic Concrete Test Specimens; Its Development and Correlation with Field Compaction Methods, A Texas Highway Department Procedure. Proc. AAPT, Vol. 21, 1952.